CHAPTER 7 DAMAGE RESISTANCE, DURABILITY, AND DAMAGE TOLERANCE

7.1 OVERVIEW AND GENERAL GUIDELINES

7.1.1 Principles

Engineered structures must be capable of performing their function throughout a specified lifetime while meeting safety and economic objectives. These structures are exposed to a series of events that include loading, environment, and damage threats. These events, either individually or cumulatively, can cause structural degradation, which, in turn, can affect the ability of the structure to perform its function.

In many instances, uncertainties associated with existing damage as well as economic considerations necessitate a reliance on inspection and repair programs to ensure the required structural capability is maintained. The location and/or severity of manufacturing flaws and in-service damage can be difficult to anticipate for a variety of reasons. Complex loading and/or structural configurations result in secondary load paths that are not accurately predicted during the design process. Some manufacturing flaws may not be detectable until the structure is exposed to the service environment. For example, joints with contaminated surfaces during bonding may not be detectable until the weak bond further deteriorates in service. The numerous variables associated with damage threats (e.g., severity, frequency, and geometry) are rarely well defined until service data is collected. Moreover, established engineering tools for predicting damage caused by well-defined damage events often do not exist. Economic issues can include both non-recurring and recurring cost components. The large number of external events, combined with the interdependence of structural state, structural response, and external event history, can result in prohibitive non-recurring engineering or test costs associated with explicitly validating structural capability under all anticipated conditions. Moreover, large weight-related recurring costs associated with many applications rule out the use of overly conservative, but simpler approaches.

The goal in developing an inspection plan is to detect, with an acceptable level of reliability, any damage before it can reduce structural capability below the required level. To accomplish this, inspection techniques and intervals for each location in the structure must be selected with a good understanding of damage threats, how quickly damage will grow, the likelihood of detection, and the damage sizes that will threaten structural safety. To avoid costs associated with excessive repairs, inspection methods should also quantify structural degradation to support accurate residual strength assessments.

This concept of combining an inspection plan with knowledge of damage threats, damage growth rates and residual strength is referred to as “damage tolerance”. Specifically, *damage tolerance is the ability of a structure to sustain design loads in the presence of damage caused by fatigue, corrosion, environment, accidental events, and other sources until such damage is detected, through inspections or malfunctions, and repaired.*

Durability considerations are typically combined with damage tolerance to meet economic and functionality objectives. Specifically, *durability is the ability of a structural application to retain adequate properties (strength, stiffness, and environmental resistance) throughout its life to the extent that any deterioration can be controlled and repaired, if there is a need, by economically acceptable maintenance practices*. As implied by the two definitions, durability addresses largely economic issues, while damage tolerance has a focus on safety concerns. For example, durability often addresses the onset of damage from the operational environment. Under the principles of damage tolerance design, the small damages associated with initiation may be difficult to detect, but do not threaten structural integrity.

7.1.2 Composite-related issues

All structural applications should be designed to be damage tolerant and durable. In using composite materials, a typical design objective is to meet or exceed the design service and reliability objectives of the same structure made of other materials, without increasing the maintenance burden. The generally good fatigue resistance and corrosion suppression of composites, help meet such objectives. However, the unique characteristics of composite materials also provide some significant challenges in developing safe, durable structure.

The brittle nature of some polymer resins causes concern about their ability to resist damage and, if damaged, their ability to carry the required loads until the damage is detected. While the primary concerns in metal structure relate to tension crack growth and corrosion, other damages, such as delamination and fiber breakage resulting from impact events and environmental degradation are more of a concern in polymer matrix composites. In addition, composites have unique damage sensitivities for compression and shear loading, as well as tension.

In composite structure, the damage caused by an impact event is typically more severe and can be less visible than in metals. As a result of the increased threat of an immediate degradation in properties, another property, damage resistance, has been used for composite structures and material evaluation. *Damage resistance is a measure of the relationship between parameters which define an event, or envelope of events (e.g., impacts using a specified impactor and range of impact energies or forces), and the resulting damage size and type.*

Damage resistance and damage tolerance differ in that the former quantifies the damage caused by a specific damage event, while the latter addresses the ability of the structure to tolerate a specific damage condition. Damage resistance, like durability, largely addresses economic issues (e.g., how often a particular component needs repair), while damage tolerance addresses safe operation of a component.

Optimally balancing damage resistance and damage tolerance for a specific composite application involves considering a number of technical and economic issues early in the design process. Damage resistance often competes with damage tolerance during the design process, both at the material and structural level. In addition, material and fabrication costs, as well as operational costs associated with inspection, repair, and structural weight, are strongly influenced by the selected material and structural configuration. For example, toughened-resin material systems typically improve damage resistance relative to untoughened systems, which results in reduced maintenance costs associated with damage from low-severity impact events. However, these cost savings compete with the higher per-pound material costs for the toughened systems. In addition, these materials can also result in lower tensile capability of the structure with large damages or notches, which might require the addition of material to satisfy structural capability requirements at Limit Load. This extra material and associated weight results in higher material and fuel costs, respectively.

7.1.3 General guidelines

There are a large number of factors that influence damage resistance, durability and damage tolerance of composite structures. In addition, there are complex interactions between these factors which can lead to non-intuitive results, and often a change in a factor can improve one of the areas of damage resistance, durability, or damage tolerance, while degrading the other two. It is important for a developer of a composite structure to understand these factors and their interactions as appropriate to the structure's application in order to produce a balanced design that economically meets all of the design criteria. For these reasons, this chapter contains detailed discussions of influencing factors and design guidelines in each of the areas of damage resistance, durability, and damage tolerance (Sections 7.5 through 7.8). The following paragraphs outline some of the areas where significant and important interactions occur. The intent is to highlight these items that involve areas of several of the following detailed information sections.

- An important part of a structural development program is to determine the damages that the structure is capable of carrying at the various required load levels (ultimate, limit, etc.). This information can be used to develop appropriate maintenance, inspection and real-time monitoring techniques to ensure safety. The focus of damage tolerance evaluations should be on ensuring safety in the event of "rogue" and "unanticipated" events, not solely on likely scenarios of damage.

- The damage tolerance approach involves the use of inspection procedures and structural design concepts to protect safety, rather than the traditional factors of safety used for Ultimate Loads. The overall damage tolerance database for a structure should include information on residual strength characteristics, sensitivities to damage growth and environmental degradation, maintenance practices, and in-service usage parameters and damage experiences.

- Fiber and matrix materials, material forms, and fabrication processes are constantly changing. This requires a strong understanding of the durability and damage tolerance principles, the multitude of parameter interactions, and an intelligent, creative adaptation of them to achieve durability and safety goals. Also, new materials and material forms may have significantly different responses than exhibited by previous materials and structures (i.e., "surprises" will occur). Therefore, the information and guidelines based on previous developments should not be blindly followed.

  - Focusing strictly on meeting regulatory requirements will not ensure economical maintenance practices are established. For example, the Ultimate Load requirements for barely visible impact damage, BVID, in critical locations (see FAR 23.573, AC 20-107A, etc.) result in insufficient data to define allowable damage limits (ADLs) in higher-margin areas. Similarly, demonstrating compliance for discrete source damage requirements typically involves showing adequate structural capability with large notches at critical locations. Neither of these requirements ensure safe maintenance inspection practices are established to find the least detectable, yet most severe defect (i.e., those reducing structural capability to Limit Loads). As a result the supporting databases should not be limited to these conditions. An extensive residual strength database addressing the full range of damage variables and structural locations is needed to provide insights on ADLs for use in Structural Repair Manuals. For example, clearly visible damage may be acceptable (i.e., below the ADLs) away from stiffening elements and in more lightly loaded portions of the structure. A more extensive characterization of the residual strength curves for each characteristic damage type (impact, holes, etc.) will also help define damage capable of reducing strength to Limit Load.

  - Well-defined inspection procedures that (a) quantify damage sufficiently to assess compliance with Allowable Damage Limits (ADLs) and (b) reliably find damage at the Critical Damage Threshold (CDT), discussed in Section 7.2.1, will help provide maintenance practices which are as good or better than those used for metal structure. Clearly defined damage metrics facilitate quantitative inspection procedures, which can be used to define the structural response of the detected damage.

  - Currently, most initial inspections of composite structure have involved visual methods. Therefore, dent depth has evolved as a common damage metric. Development efforts should define the dent depths that correspond to the threshold of detectability for both general visual (surveillance in Boeing terminology) and detailed visual levels. The influence of dent-depth decay, which can come from viscoelastic and other material or structural behaviors, must be considered for maintenance inspection procedures and the selection of damage that will be used to demonstrate compliance.

  - Another factor motivating a more complete characterization of damage and structural variables is that the internal damage state for a specific structural detail is not a unique function of the dent depth. It is a complex function of the impact variables (i.e., impactor geometry, energy level, angle of incidence, etc.). A range of these variables should be evaluated to understand the relationship between them and to determine the combinations that result in the largest residual strength degradation.

  - Structure certified with an approach that allows for damage growth must have associated in-service inspection techniques, which are capable of adequately detecting damage before it becomes critical. These inspection methods should be demonstrated to be economical before committing to such a certification approach. In addition, the damage growth must be predictable such that inspection intervals can be reliably defined.

7.1.4 Section organization

This chapter of the handbook addresses the multitude of issues associated with the damage resistance, durability, and damage tolerance of composite materials. Discussions are heavily reliant on experience gained in the aircraft industry, since it represents the area where composites and damage tolerant philosophy have been most used. As the associated composite technologies continue to evolve, additional applications and service history should lead to future updates with a more complete understanding of: (1) potential damage threats, (2) methods to achieve the desired reliability in a composite design, and (3) improved design and maintenance practices for damage tolerance.

Section 7.2 focuses on the requirements for military and civilian aviation applications, as well as methods of compliance. Discussion of the characteristics of various types of composite damage and a list of possible sources of the damage are given in Section 7.3. Composite damage inspection methods and their limitations are discussed in Section 7.4. Sections 7.1 through 7.4 are relatively mature in their content.

Sections 7.5 through 7.8, which comprise the bulk of this section, address the major material and structural responses: damage resistance, durability, damage growth under cyclic loading, and residual strength, respectively. Each section includes detailed discussions of: (a) the major factors that affect response; (b) design-related issues and guidelines for meeting objectives and requirements; (c) testing methods and issues; and (d) analytical predictive methods, their use, and their success at predicting observed responses.

At this point in time, not all parts of Sections 7.5 through 7.8 are complete. Section 7.5, Damage Resistance, currently contains information on influencing factors and guidelines; sections on test and analysis methods will be added in the future. Section 7.6, Durability, currently contains only limited information. Future updates will complete this section. Section 7.7, Damage Growth Under Cyclic Loading, contains some limited information on the growth of impact damages. Additional parts of this section will be added in the future. Section 7.8, Residual Strength, contains extensive information on influencing factors, guidelines and analysis methods; the section on test methods will be added in the future.

Section 7.9 includes several examples of successful damage-tolerant designs from a number of composite aircraft applications. These examples illustrate how different aspects of damage tolerance come to the forefront as a function of application.

7.2 AIRCRAFT DAMAGE TOLERANCE

Damage tolerance provides a measure of the structure's ability to sustain design loads with a level of damage or defect and be able to perform its operating functions. Consequently, the concern with damage tolerance is ultimately with the damaged structure having adequate residual strength and stiffness to continue in service safely until the damage can be detected by scheduled maintenance inspection (or malfunction) and be repaired or until the life limit is reached. The extent of damage and detectability determines the required load level to be sustained. Thus, safety is the primary goal of damage tolerance.

Damage tolerance methodologies are most mature in the military and civil aircraft industry. They were initially developed and used for metallic materials, but have more recently been extended and applied to composite structure. The damage tolerance philosophy has been included in regulations since the 1970's. It evolved out of the "Safe Life" and "Fail Safe" approaches (Reference 7.2).

The safe-life approach ensures adequate fatigue life of a structural member by limiting its allowed operational life. During its application to commercial aircraft in the 1950's, this approach was found to be uneconomical in achieving acceptable safety, since a combination of material scatter and inadequate fatigue analyses resulted in the premature retirement of healthy components. The approach is still used today in such structures as high-strength steel landing gear. Due to the damage sensitivities and relatively flat fatigue curves of composite materials, a safe-life approach is not considered appropriate.

The fail-safe approach assumes members will fail, but forces the structure to contain multiple load paths by requiring specific load-carrying capability with assumed failures of one or more structural elements. This approach achieved acceptable safety levels more economically, and, due to the relative severity of the assumed failures, was generally effective at providing sufficient opportunity for timely detection of structural damage. Its redundant-load-path approach also effectively addressed accidental damage and corrosion. However, the method does not allow for explicit limits on the maximum risk of structural failure, and it does not demonstrate that all partial failures with insufficient residual strength are obvious. Moreover, structural redundancy is not always efficient in addressing fatigue damage, where similar elements under similar loading would be expected to have similar fatigue-induced damage.

7.2.1 Evolving military and civil aviation requirements

The “duration of damage or defect” factor based on degree of detectability has been the basis for establishing minimum Air Force damage tolerance residual strengths for composite structures in requirements proposed for inclusion in AFGS-87221, “General Specification for Aircraft Structures”. These strength requirements are identical to those for metal structure having critical defects or damage with a comparable degree of detectability. Requirements for cyclic loading prior to residual strength testing of test components are also identical. The non-detectable damage to be assumed includes a surface scratch, a delamination and impact damage. The impact damage includes both a definition of dent depth, i.e., detectability, and a maximum energy cutoff. Specifically, the impact damage to be assumed is that “caused by the impact of a 1.0 inch (25 mm) diameter hemispherical impactor with a 100 ft-lb (136 N-m) of kinetic energy, or that kinetic energy required to cause a dent 0.10 inch (2.54 mm) deep, whichever is least.” For relatively thin structure, the detectability, i.e., the 0.1 inch (2.5 mm) depth, requirement prevails. For thicker structure, the maximum assumed impact energy becomes the critical requirement. This will be illustrated in Section 7.5. The associated load to be assumed is the maximum load expected to occur in an extrapolated 20 lifetimes. This is a one-time static load requirement. These requirements are coupled with assumptions that the damage occurs in the most critical location and that the assumed load is coincident with the worst probable environment.

In developing the requirements, the probability of undetected or undetectable impact damage occurring above the 100 ft-lb (136 N-m) energy level was considered sufficiently remote that when coupled with other requirements a high level of safety was provided. For the detectability requirement, it is assumed that having damage greater than 0.10 inch (2.5 mm) in depth will be detected and repaired. Consequently, the load requirement is consistent with those for metal structure with damage of equivalent levels of detectability. Provisions for multiple impact damage, analogous to the continuing damage considerations for metal structure, and for the lesser susceptibility of interior structure to damage are also included.

In metal structure, a major damage tolerance concern is the growth of damage prior to the time of detection. Consequently, much development testing for metals has been focused on evaluating crack growth rates associated with defects and damage, and the time for the defect/damage size to reach residual strength criticality. Typically, the critical loading mode has been in tension. Crack growth, even at comparatively low stress amplitudes, may be significant. In general, damage growth rates for metals are consistent and, after test data has been obtained, can be predicted satisfactorily for many different aircraft structural configurations. Thus, knowing the expected stress history for the aircraft, inspection intervals have been defined that confidently ensure crack detection before failure.

By contrast, composites have unique damage sensitivities for both tension and compression loads. However, the fibers in composite laminates act to inhibit tensile crack growth, which only occurs at relatively high stress levels. Consequently, through the thickness damage growth, which progressively breaks the fibers in a composite, has generally not been a problem. In studying the effects of debonds, delaminations or impact damage, the concern becomes compression and shear loads where local instabilities may stimulate growth. Unlike cracks in metal, growth of delaminations or impact damage in composites may not be detected using economical maintenance inspection practices. In many cases, the degraded performance of composites with impact damage also cannot be predicted satisfactorily. Hence, there is a greater dependence on testing to evaluate composite residual strength and damage growth under cyclic loads. In the absence of predictive tools for growth, design values are typically established with sufficient margins to ensure that damage growth due to repeated loads will not occur. This method for avoiding the potential growth of damage in design and certification is known as the "no-growth" approach. It has been practical for most composite designs, which have proved to be fatigue insensitive at typical design stress levels.

The damage tolerance design procedures for civil/commercial aircraft are expressed more generally but with equal effectiveness. Civil aviation requirements are addressed in Federal Aviation Regulations (FAR) 23.573, 25.571, 27.571, 29.571 and Joint Airworthiness Requirements (JAR) 25.571. Advisory Circular 20-107A and ACJ 25.603 provide means of compliance with the regulations concerning composite material structure. Advisory Circular AC25.571-1 (rev. B was issued 2/18/97) provides means of compliance with provision of FAR Part 25 dealing with damage tolerance and fatigue life (25.571). Unlike military requirements, civil/commercial ones do not recommend any energy level or detectability thresholds. In fact, they do not assume the inspections will be visual. Relative to impact damage, it is stated in the FAA guidelines in AC20-107A, Paragraph 6.g. “It should be shown that impact damage that can be realistically expected from manufacturing and service, but not more than the established threshold of detectability for the selected inspection procedure, will not reduce the structural strength below Ultimate Load capability. This can be shown by analysis supported by test evidence, or by tests at the coupon, element, or subcomponent level.” This guidance is to ensure that structure with barely detectable impact damage will still meet ultimate strength requirements. A similar wording to the above has been added to FAR 23.573. In practice, visual inspections are most often used for initial detection. It is important to consider lighting conditions when determining visibility. Dent depth thresholds are typically used to quantify visibility, with typical values being 0.01 to 0.02 inches (0.25 to 0.50 mm) for tool-side impacts and 0.05 inches (1.3 mm) for bag-side impacts.

It is also stated in 7.a(2) of AC 20-107A “The extent of initially detectable damage should be established and be consistent with the inspection techniques employed during manufacture and in service. Flaw/damage growth data should be obtained by repeated load cycling of intrinsic flaws or mechanically introduced damage.” And, in 7.a.(3) of AC 20-107A, it is stated “The evaluation should demonstrate that the residual strength of the structure is equal to or greater than the strength required for the specified design loads (considered as ultimate).” This guidance is to ensure that visible impact damage (VID) will be detected in a timely manner and will be repaired before strength is reduced below Limit Load capability. Damage such as runway debris, which may not be immediately obvious, would likely be considered as VID. The difference in the Air Force specification and the FAA guideline is primarily in the residual strength value. Also, while the Air Force specification assumes visual inspection, the FAA guideline leaves the inspection method to be selected. Consequently, since specifications and guidelines differ with the type of aircraft, the manufacturer must be aware of the differences and apply those guidelines and specifications appropriate to the situation.

The FAA guidelines for discrete source damage are stated in 8.b of AC 25.571-1A. They state that “The maximum extent of immediately obvious damage from discrete sources (§ 25.571(e)) should be determined and the remaining structure shown, with an acceptable level of confidence, to have static strength for the maximum load (considered as Ultimate Load) expected during completion of the flight.” It is stated in 8.c.(2) of AC 25.571-1A “(2) Following the incident: Seventy percent (70%) limit flight maneuver loads and, separately, 40 percent of the limit gust velocity (vertical or lateral) at the specified speeds, each combined with the maximum appropriate cabin differential pressure (including the expected external aerodynamic pressure).” The discrete sources listed in 25.571(e) are as follows: (1) Impact with a 4-pound bird; (2) Uncontained fan blade impact; (3) Uncontained engine failure; or (4) Uncontained high energy rotating machinery failure. These high-energy sources are likely to penetrate structures. Damage from a discrete source that is not immediately obvious must be considered as VID with Limit Load. MIL-A-83444 has similar requirements for “in-flight” and “ground evident damage”. The design loads for these two conditions are the maximum loads expected in 100 flights.

The following summarize current aeronautical requirements for composite aircraft structures with damage:

1. Structure containing likely damage or defects that are not detectable during manufacturing inspections and service inspections must withstand Ultimate Load and not impair operation of the aircraft for its lifetime (with appropriate factor).
2. Structure containing damage that is detectable during maintenance inspections must withstand a once per lifetime load, which is applied following repeated service loads occurring during an inspection interval (with appropriate factor).
3. All damage that lowers strength below Ultimate Load must be repaired when found.
4. Structure damaged from an in-flight, discrete source that is evident to the crew must withstand loads that are consistent with continued safe flight.
5. Any damage that is repaired must withstand Ultimate Load.

Static and fatigue tests are usually conducted during design development and validation to show that composite structures satisfy certification requirements (Reference 7.2.1(a)).

The [inverse] relationship between design load levels and damage severity is shown in Figure 7.2.1(a). As is the case with metal commercial aircraft components, ultimate strength and damage tolerance design philosophies are used to help maintain the reliable and safe operation of composite structure. The load and damage requirements are balanced such that there is an extremely low probability of failure. Residual strength design requirements for relatively small damage, which are likely to occur in service, are matched with very high (unlikely) load scenarios (ultimate). The design requirement for more severe damage states, such as those caused by impact events that have a very low probability of occurrence, are evaluated for the upper end of realistic load conditions (limit). The most severe damage states considered in design are those occurring in flight (e.g., engine burst). The flight crew generally has knowledge of such events and they limit maneuvers for continued safe flight. Depending on the specific structure and an associated load case, continued safe flight load requirements may be as high as limit (e.g., pressure loads for fuselage).

Maintenance technology for composite aircraft structure benefits from a complete assessment of service damage threats on structural performance. Unfortunately, the necessary links between composite design practices and maintenance technology has not received the attention required to gain acceptance by commercial airlines and other customers. In the past, damages selected to size structure for the design load conditions shown in Figure 7.2.1(a) have not met all the needs of maintenance. A more complete database is needed to determine the effects of a full range of composite damages on residual strength. A complete characterization of the residual strength curve (i.e., residual strength versus a measurable damage metric) can help establish the Allowable Damage Limits (ADL) and Critical Damage Threshold (CDT) as a function of structural location. Well-defined ADLs can help airlines accurately determine the need for repair. Generous ADLs in areas prone to damage may help minimize maintenance costs by allowing cosmetic repairs instead of structural repairs that require more equipment and time.

The amount of damage that reduces the residual strength to the regulatory requirements of FAR 25.571 are referred to as the Critical Damage Threshold (CDT). It is desirable to design structure such that service damage falling between the ADL and CDT limits can be found and characterized using practical inspection procedures. This goal provides aircraft safety and maintenance benefits. By definition, all damage of this extent must be repaired when found. Damage approaching the CDT must be found with extremely high probability using the selected inspection scheme (i.e., it should be reliably detectable with the specified inspection scheme). A complete description of the critical damage characteristics, as related to the inspection scheme, is valuable information for maintenance planning activities. As with metals, damage tolerant design to relatively large CDTs provides the confidence for safe aircraft operations with economical inspection intervals and procedures.

The ADL and CDT definitions in Figure 7.2.1(a) both imply zero margins of safety for respective load cases. These parameters will vary over the surface of the structure as a function of the loads and other factors driving the design. As such, they have meaning to maintenance and should not be thought of as the design requirement for ultimate and Limit Loads. Design requirements and objectives are established for a given application, within general guidelines set by industry experience and the FAA. The design criteria used to meet these requirements become even more program-specific, depending on available databases for the selected structural concept.

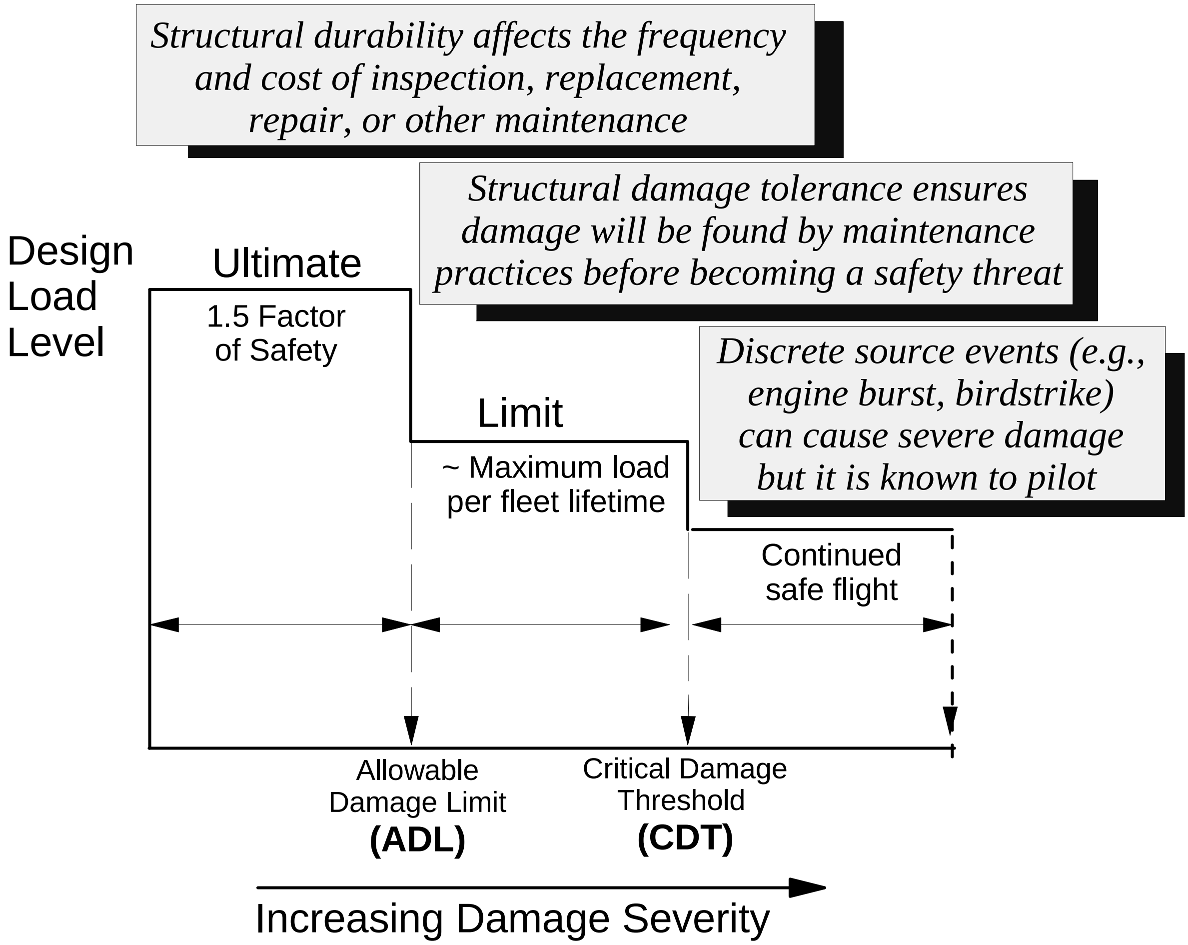

FIGURE 7.2.1(a) *Design load and damage considerations for durability & damage tolerance.*

Figure 7.2.1(b) helps illustrate the requirements for damage subjected to time in service (i.e., repeated loads and environmental cycling). For relatively small damages, which likely exist in the structure and may be undetected by either quality control at the time of manufacturing or service inspection, the structure should retain static strength for Ultimate Loads over the aircraft's life. When detailed visual inspection techniques are used for service, barely visible impact damage (BVID) is usually classified as a threshold for undetectable damage. If damage is of a size and characteristic that can be detected by selected service inspections (e.g., visible impact damage, VID), then the load requirement drops to Limit Load. Structure with such damage is only expected to sustain the service environment for a period of time related to the inspection interval. In the cases of both undetectable and detectable damages, factors are typically applied in fatigue testing, damage tolerant design and maintenance to account for the variability in material behavior under repeated loading and the reliability of inspection techniques. In certification practice for composite materials, a load enhancement factor is often used to reduce the additional test cycles needed to account for material variability (References 7.2.1(b) to 7.2.1(d)).

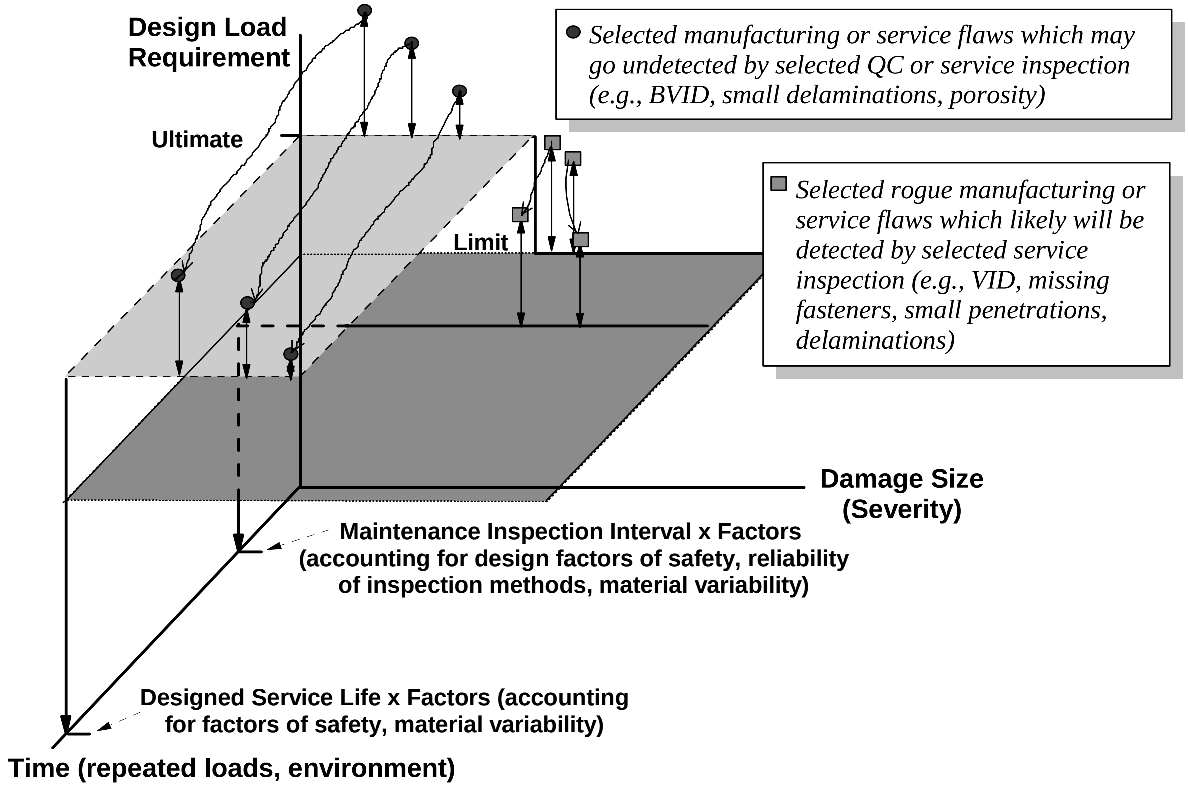

FIGURE 7.2.1(b) *Repeated load and residual strength requirements for damaged composites.*

Figure 7.2.1(c) illustrates another important aspect of damage tolerance, which is related to rare accidental damage and discrete source impact events that yield relatively large damages. Such damages are typically treated as obvious or assumed to exist when a discrete source event occurs in service that is known to the crew. In both cases, there is no repeated load requirement. The requirements for discrete source damage are defined in aeronautical regulations. There is generally no specific damage size requirements for obvious damage, but to be classified as such, it must be detectable without directed inspection (e.g., large penetrations or part malfunction). Service databases have shown that such damage does occur and may go undiscovered for a short period of time. As a result, it is good fail-safe design practice to ensure structure is capable of sustaining Limit Load with obvious damage. The analyses and test databases used to meet discrete source damage requirements typically characterize the residual strength curve, which can also be used to meet design criteria for obvious damage. For bonded structure, there are other requirements to ensure fail safety in the case of large debonds (e.g., FAR 23.573). Such requirements relate to the unreliability of secondary bonding.

The range of damages shown in Figures 7.2.1(b) and 7.2.1(c) have traditionally provided a basis for durability and damage tolerance assessments of composite structure. However, complex design details and secondary load paths can also result in damage initiation and significant growth in composites structures. Since these details and load paths are difficult to analyze, the resulting damage initiation and growth are often not identified until large-scale tests of configured structure are conducted. Alternatively, damage growth must either be arrested by design features or be predictable and stable (e.g., analogous to metal crack growth). In this case, safety is achieved through damage tolerant design and maintenance practices similar to those for metal structures.

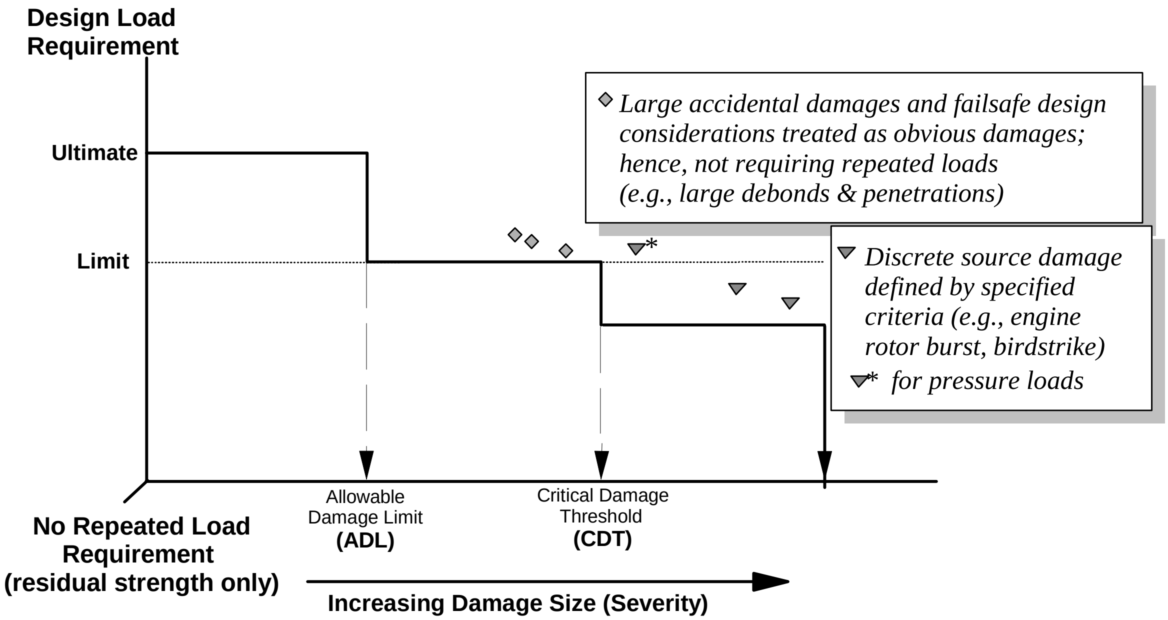

FIGURE 7.2.1(c) *Residual strength requirements for large damage in composite structure.*

7.2.2 Methods of compliance to aviation regulations

There is a notable difference between military and civil aviation methods of compliance. For military aircraft, the government defines the requirements (Military Specifications) and works with the manufacturer to establish the method of compliance. The government is also the customer in this instance. In civil aviation, the government defines the requirements through regulations (FAR's, JAR's) and accepted means of compliance through guidance material (Advisory Circulars). Compliance must be demonstrated to the agency (FAA, JAA). In this instance the government is a neutral, third party.

This difference in ultimate ownership also influences the attitude the different agencies adopt regarding durability. To the extent that durability is an economic issue, it is not generally of concern to civil aviation authorities. It is a concern to military agencies because maintainability expenses affect their cost of ownership.

The reason why visual inspection methods, rather than a special one (requiring some special techniques like ultrasonic pulse echo for instance), is preferred by the aircraft manufacturers and operators for impact damage detection is purely economic. Unlike fatigue cracks in metallic structure that can only be initiated at restricted and easily identifiable areas (where stress raisers and/or corrosion exist) impact damage may occur anywhere on large exposed surfaces, raising the cost of an inspection plan covering the entire surface of the structure.

The use of visual methods for initial damage detection results in a more conservative (i.e., heavier) design than would the use of more stringent inspection methods, since the damage level required for visibility is more severe. However, the visual approach results in improved damage tolerance capability, since the structural strength is typically less sensitive to changes in damage severity as damage severity increases. A majority of the compression strength reduction occurs for energy levels below the detectability threshold that will govern static strength requirements. Then, limited extra strength reductions should be expected for higher energies to be considered for damage tolerance evaluation.

7.2.2.1 Compliance with static strength requirements (civil aviation)

As far as impact damage is concerned, the AC 20-107A (§ 6g) proposes the following means for complying with the regulations: *It should be shown that impact damage that can be realistically expected from manufacturing and service, but no more than the established threshold of detectability for the selected inspection procedure, will not reduce the structural strength below Ultimate Load capability.*

This sentence explicitly defines energy cut-offs and detection thresholds, which are illustrated in Figure 7.2.2.1. The first cut-off threshold is the established threshold of detectability for the inspection method used. The second cut-off threshold is the maximum impact energy that the structure can be expected to tolerate during manufacturing and in service. These two thresholds are assumed to describe accidental damage for new structure representative of the minimum quality. Minimum values of these cut-offs and thresholds need to be established so that there is consistency between the detectable size and the selected NDT procedure plus consideration of realistic energy levels.

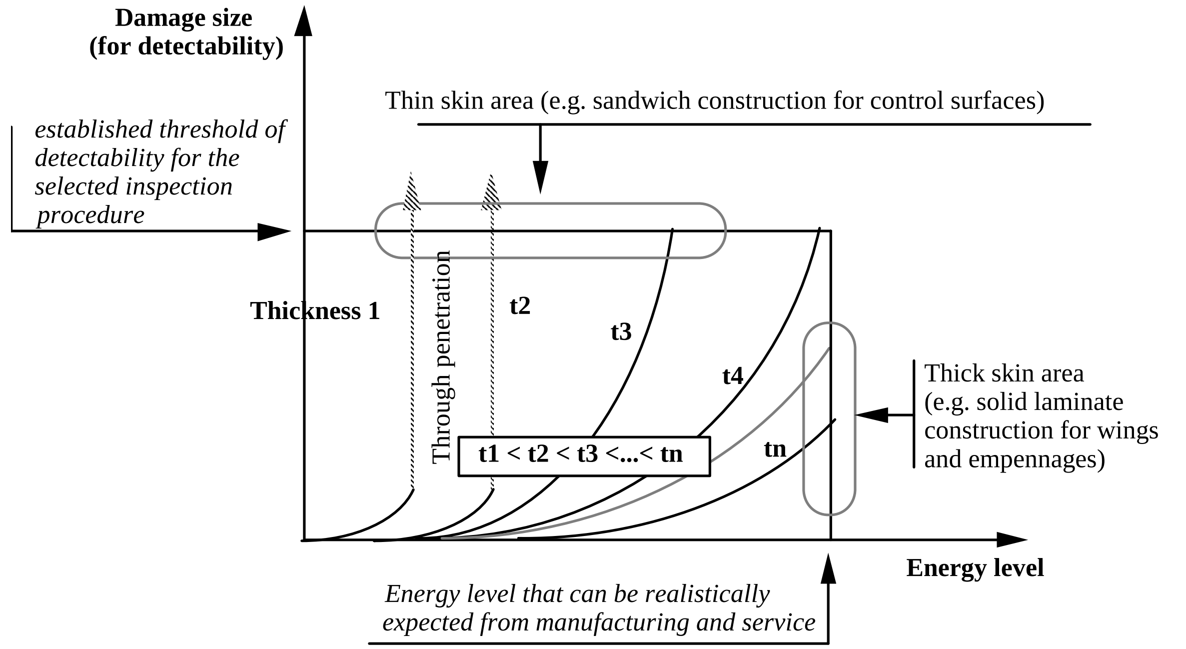

FIGURE 7.2.2.1 *Damage size as a function of impact energy for different laminate thickness.*

Establishing the energy cut-off values requires defining the energy level associated with the word *realistic.* The rectangle in Figure 7.2.2.1 represents the domain in which structure is capable of withstanding Ultimate Loads, without necessary repairs. This applies to the start of service life, when the aircraft rolls out of the manufacturer's plant, as well as at the end of lifetime when composite parts are likely to have accumulated some accidental damage below the detectability thresholds. Damages that are above the rectangle in Figure 7.2.2.1, are assumed to be detected and repaired with cosmetic or structural solutions so that the structure's residual capability to withstand Ultimate Loads is preserved or restored, respectively.

The purpose of “damage tolerance” is to address situations with only a limited occurrence; therefore, a large majority of the aircraft structure should retain Ultimate Load capability during the service life. A discussion of one method of estimating these realistic energy levels is given in Section 7.3.3.

7.2.2.2 Compliance with damage tolerance requirements (civil aviation)

Damage tolerance has to address the situation where, due to fatigue, corrosion or accidental occurrence, Ultimate Load strength capability may not exist and will have to be restored before the damage becomes critical. As far as accidental impact is concerned, two situations have to be addressed. The first case involves those damages that meet static strength requirements (as per 25.305) and that might evolve during fatigue loading, while still remaining undetectable with the selected inspection procedure. The second case involves those damages that are outside the coverage illustrated by Figure 7.2.2.1, due to higher energy levels that will produce:

- More easily detectable damages associated with additional strength reduction for thin gage laminates (detectability threshold situation),
- Additional strength reduction without visual detection capability, in case of energy cut-off (E>Eco).

Obviously, there will be an intermediate situation where damages that were not previously detectable will become detectable. The damages that have to be addressed in a damage tolerance substantiation are illustrated in Figure 7.2.2.2(a).

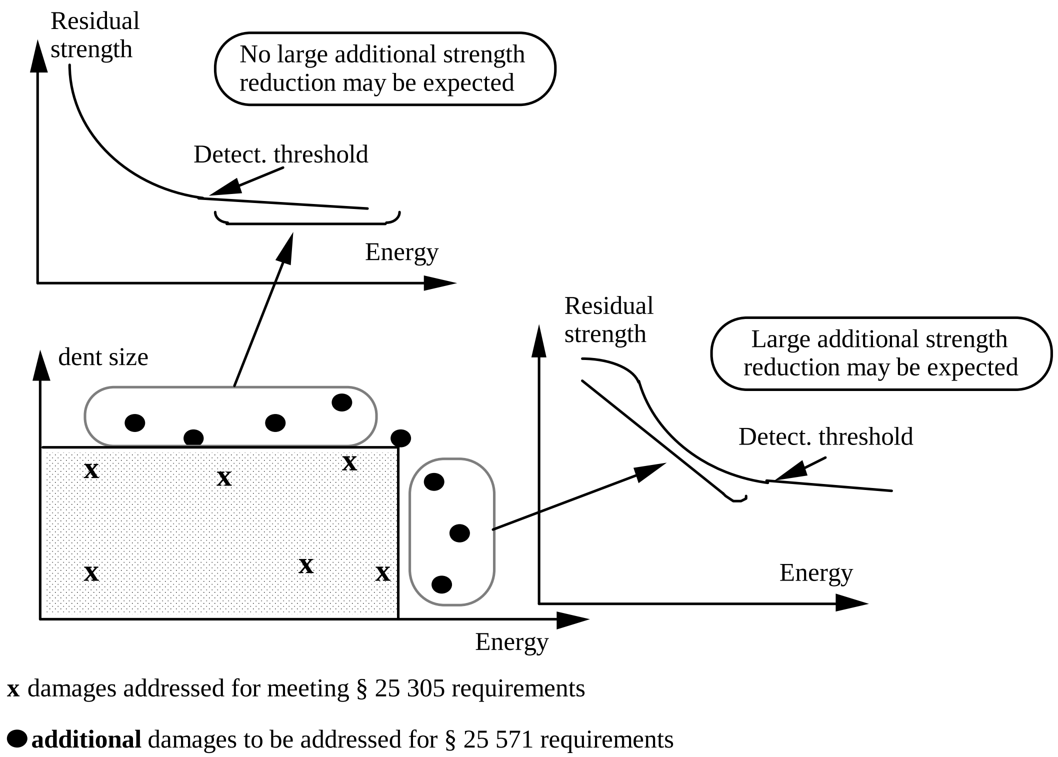

FIGURE 7.2.2.2(a) *Damages beyond those for Ultimate Load considerations.*

Depending on their detectability, different § 25 571 sub-paragraphs will apply:

- For those accidental impacts that will never be detected by the selected (visual) inspection procedure, meaning those already accounted for in the scope of static strength requirements plus those with an increased energy, damage tolerance as per 25 571 (b) is impractical. Then, demonstration will have to be made according to sub paragraph 25 571 (c), fatigue (safe-life) evaluation. In fact, due to the presence of initial damage in that fatigue demonstration, the latter is usually called “safe-life flaw tolerant” or “enhanced safe-life” demonstration.
- For those visually detectable accidental impacts, damage tolerance as per § 25 571 (b) applies.

As for § 25 305 requirements, new cut-offs and thresholds have to be defined:

- A new energy cut-off level limited to the maximum value that is to be assumed in a risk analysis and that should correspond to extremely improbable events (less than 10^{-9} per hour according to ACJ 25 1309),
- A new detectability threshold above which damage will become “obvious” (detectable within a very small number of flights by walk-around inspection).

Between the damage size detectable at detailed scheduled inspections and this new threshold, residual static strength requirements are laid down in the regulatory documents § 25 571(b). There is no residual strength requirement associated with “obvious” damage. However, aircraft take off is not allowed in such situations before assessment and restoration of Ultimate Load capability

There is a third detectability threshold which corresponds to the situation where the flight crew is at once aware of the event; then, lower loads (per § 25 571(e)) are required. This situation is referred to as “discrete source” damage. All these new thresholds are illustrated in Figure 7.2.2.2(b).

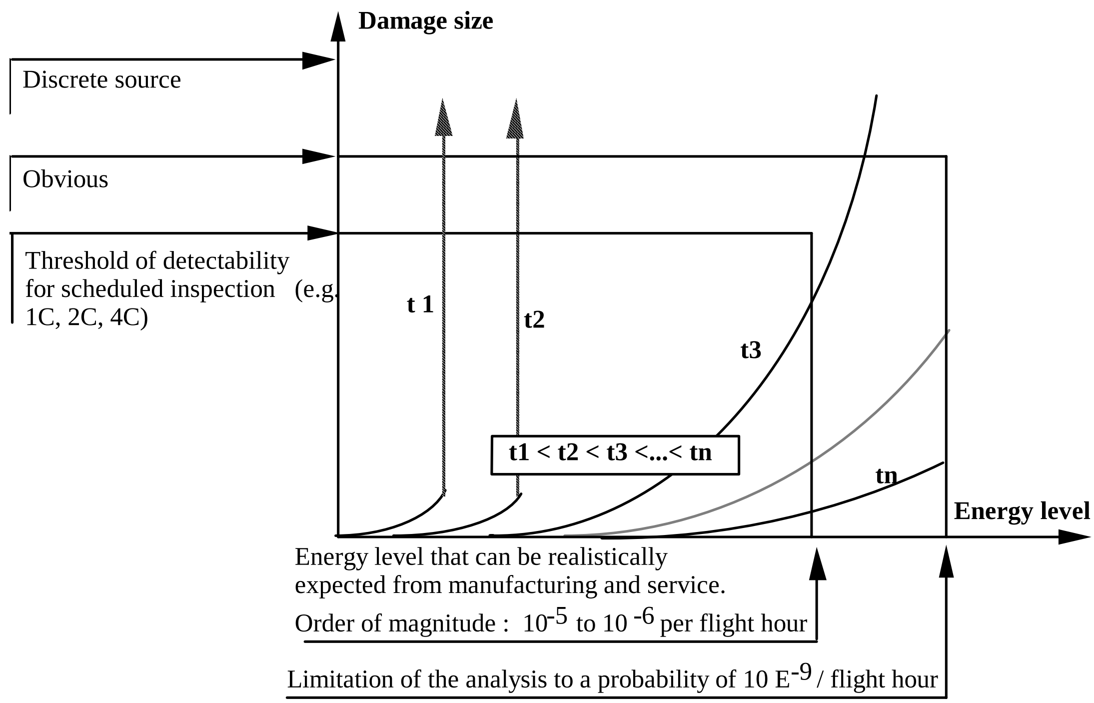

FIGURE 7.2.2.2(b) *Additional damage size and energy level thresholds.*

As discussed previously, impact damage can cause an immediate drop in composite residual strength. In most cases, such damage does not grow due to the generally good fatigue resistance of composites. The fact that an accidental impact damage in a composite structure is generally not expected to propagate in fatigue raises a specific issue for interpreting § 25 571 (b), as illustrated in Figure 7.2.2.2(c). This sketch shows the difference that can be found between non-growing impact damage in a composite structure and a, prone to grow, fatigue crack in a metallic one. Whatever the damage source is, damage tolerance per § 25 571(b) requires the following: "*The residual strength evaluation must show that the remaining structure is able to withstand loads (considered as Ultimate Loads) corresponding to the following conditions...".* As shown with the metal curve in Figure 7.2.2.2(c), an inspection interval can be rationally derived such that fatigue damage in metallic structure is safely detected and repaired before the strength drops below Limit Loads. Metal crack growth analyses and tests have matured to support such an assessment.

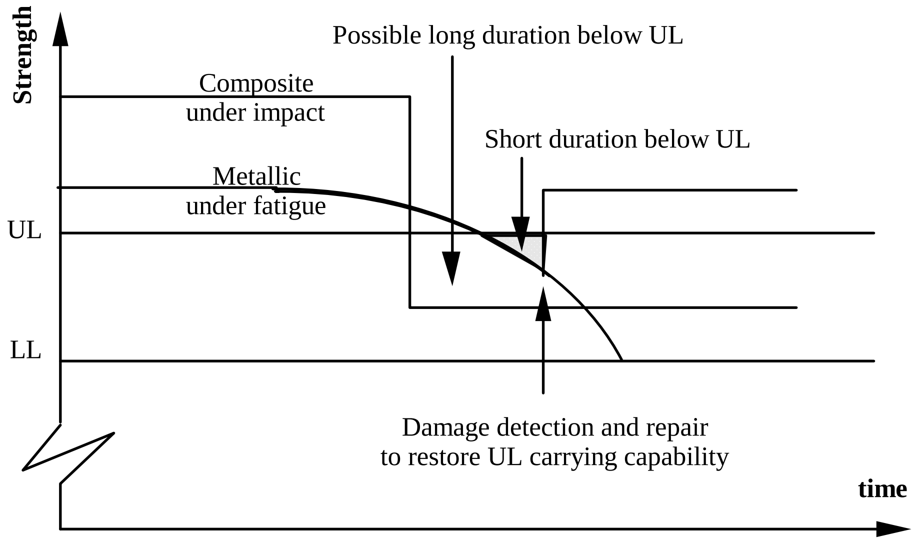

FIGURE 7.2.2.2(c) *Comparison of composite non-growing damage and metal fatigue crack damage (Ultimate Load, UL, and Limit Load, LL).*

For the case of the no-growth, composite concept, a structure with impact damage could sustain a long duration below Ultimate Load without a threat of the residual strength further dropping to the critical threshold defined by § 25 571(b) (i.e., Limit Load). This interpretation could lead to the situation of a composite structure allowed to fly a long time with residual strength just above Limit Loads, as illustrated in Figure 7.2.2.2(c). Regardless of the damage growth resistance of composite structure, damage that lowers the residual strength below Ultimate Load must be detected and repaired when found. Hence, the issue becomes one of defining a rationale inspection interval to attain equivalent or higher levels of safety than metal practice.

The advisory circular AC 20 107A, addresses the issue illustrated in Figure 7.2.2.2(c) in the paragraph 7a (4), which is related to the selection of inspection intervals: *"For the case of the no-growth concept, inspection intervals should be established as part of the maintenance program. In selecting such intervals, the residual strength associated with the assumed damages should be considered"*. In other words, the larger the strength reduction is, the sooner the damage should be detected. Also, the probability of damage occurrence plays a major role in deriving inspection intervals. For instance, more frequent inspections should normally be required for a flap, which is subjected to more damage threats, than for a vertical fin. In other words, both the capability of the composite structure and service history should be considered in defining the inspection intervals. Although metal structure has similar considerations for accidental damage, an inherent resistance to foreign object impact makes fatigue damage growth a dominant factor in defining inspection intervals for metal parts.

In considering the issues of damage severity and probability of occurrence for a composite structure, damage reducing residual strength to Limit Load should be extremely unlikely. The residual strength curve, damage growth resistance, service databases and user maintenance practices should all be considered in establishing the inspection intervals. In addition, the design criteria and certification approach used to substantiate the composite structure for damage tolerance should be coupled with subsequent maintenance practices. In the end, the composite structure should be sufficiently tolerant to damage such that economical maintenance practices can be safely implemented (e.g., detailed damage inspections and repair at scheduled maintenance intervals).

7.2.2.3 Deterministic compliance method (civil aviation example)

This section describes an analysis and testing methodology to support certification and maintenance of composite structures based on: (a) establishing residual-strength-versus-damage-size relationships; (b) establishing methods of damage detection and minimum detectable damage sizes; and (c) determining damage sizes that reduce capability to both to Ultimate Load and Limit Load. Flow charts outlining an approach for achieving damage tolerant and fail-safe designs are presented.

Several composite primary structures, such as the Boeing 777 empennage and NASA-ACEE/Boeing 737 horizontal stabilizers, have been certified per FAR 25 and JAR 25. The 737 stabilizers have demonstrated excellent service performance (Reference 7.2.2.3(a)). This service experience, as well as component testing (References 7.2.2.3(b) through 7.2.2.3(e)), has shown that current composite primary aircraft structure has excellent resistance to environmental deterioration and fatigue damage. This leaves accidental damage as the primary consideration for damage tolerance design and maintenance planning for the relatively thicker-gage composites associated with primary structure.

In-service damage resistance and repair of thin gage composite structure has become a major issue for the commercial airlines. In order to make composites cost effective for the airlines, allowable damage limits (ADLs) must be as large as possible while still meeting regulatory Ultimate Load requirements. To achieve this goal, test data and analytical methods encompassing the complete range of potential damage sizes and types are required.

This discussion presents a design approach to ensure that composite structures have low in-service maintenance costs as well as adequate damage tolerance. Several damage sizes based on detectability levels are described, and requirements for each damage size relative to FAA and JAA regulations are discussed. Suggestions are made for developing appropriate databases to satisfy regulatory damage tolerance requirements and achieve low maintenance costs.

Several methods for improving the performance of impacted composite panels and components have been proposed (References 7.2.2.3(f) and (g)). One approach is to increase the inherent toughness of the composite by using tougher resin matrices; this is only appropriate for medium to thick gage laminates as increased toughness has little benefit for thin laminates or sandwich facesheets. Although this method improves damage resistance and reduces maintenance costs, increased material costs, reductions in matrix stiffness at elevated temperatures, and potential reductions in large notch residual strengths must be considered in the final selection.

In metallic structures, damage tolerance has been demonstrated using fracture mechanics to characterize crack growth under cyclic loading, predict the rate of crack growth in the structure under anticipated service loads, and establish inspection intervals based on realistic damage detection reliability considerations (Reference 7.2.2.3(h)). Since typical CFRP composites have relatively flat S-N curves, and because these damages do not propagate under aircraft wing/empennage operational loading spectra, the above method normally cannot be used to establish inspection plans. Instead, a *no-growth approach* has been used to demonstrate compliance with damage tolerance requirements for composite primary structures on commercial aircraft for current composite structures.

The types and sizes of damages that are barely detectable or larger are classified into several groups based on the likelihood of damage detection, as shown in Figure 7.2.2.3(a). The selection of damage sizes must be consistent with the established inspection program and with the corresponding reduction in static strength. The following paragraphs describe the different damage types and sizes:

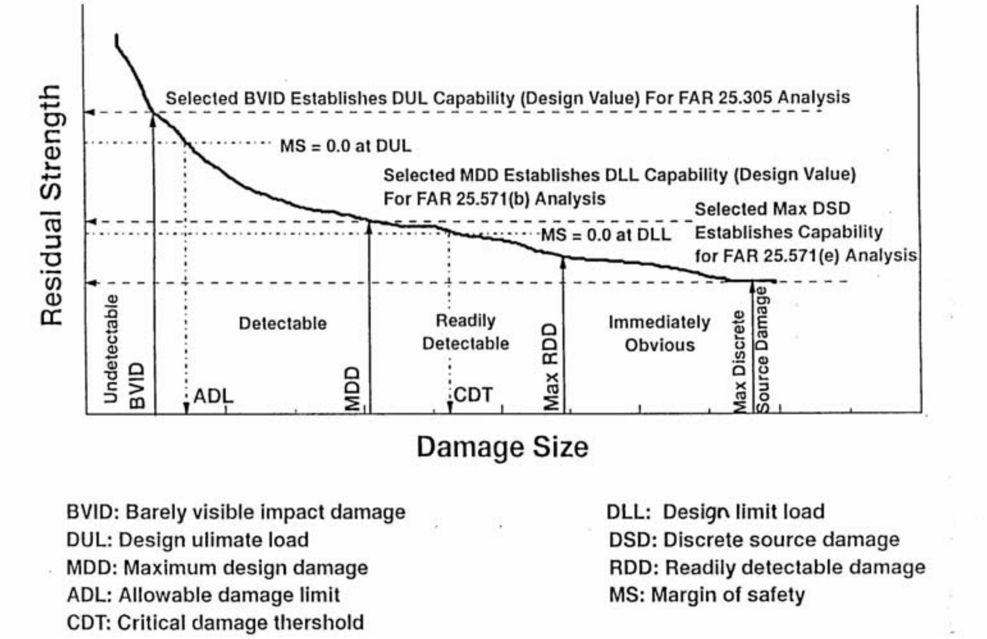

FIGURE 7.2.2.3(a) *Residual strength requirements versus damage size.*

1. Barely visible impact damage (BVID) establishes the strength design values to be used in analyses demonstrating compliance with the regulatory Ultimate Load requirements of FAR 25.305. For small aircraft and different classes of rotorcraft the corresponding requirements are 23.305, 27.305 and 29.305. In the case of small aircraft, the BVID static strength requirement has been added to the regulation for composite damage tolerance, FAR 23.573. The extent of such damage needs to be established as part of criteria defined prior to the design phase. The term visible is used since the primary inspection method in current use involves visual observation. An upper limit of 100 ft-lb (140 Joules) on the BVID impact energy level is applied based on this value being at the upper limit of what could be realistically expected.

2. Allowable damage limits (ADL), defined as damage that reduces the residual strength to the regulatory Ultimate Load requirements of FAR 25.305, are determined to support maintenance documents. Given that the structure's strength with BVID damage will result in positive margins at design Ultimate Load (DUL), the corresponding ADL will generally be larger than the BVID (see Figure 7.2.2.3(a)). Characteristics describing the detectability of the ADL as well as the type and extent of the damage are documented to support maintenance programs.

3. Maximum design damage (MDD) establishes the strength design values to be used in analyses demonstrating compliance with the regulatory damage tolerance requirements of FAR 25.571(b). In the case of small aircraft, the regulation for composite damage tolerance, FAR 23.573, while analogous rotorcraft rules can be found in 27.571 and 29.571. Current efforts are underway to develop a unique composite damage tolerance rule for rotorcraft, which will be given the numbers 27.573 and 29.573, depending on the class of rotorcraft. The extent of such damage needs to be established as part of criteria defined prior to the design phase.

4. Critical damage thresholds (CDT) are defined as damages that reduce the residual strength to the regulatory requirements of FAR 25.571(b) (or the equivalent for other types of aircraft). Given that the structure's strength with MDD-sized damage will result in positive margins at design Limit Load (DLL), the corresponding CDT will be larger than the MDD. Characteristics describing the detectability of the CDT as well as the type and extent of the damage are documented to support the establishment of required inspection methods and intervals. Using the selected inspection

technique, realistic damages smaller than the corresponding CDT are shown to be detectable with high probability before any growth causes it to exceed the CDT.

5. Readily detectable damage (RDD) can be detected within a small number of flights during routine aircraft servicing. For damage that is not readily detectable, the structure should be evaluated for all possible damage growth mechanisms. The maximum extent of damage that is considered readily detectable, but which is not immediately obvious, should be established. The advisory circular for damage tolerance, ACJ 25.571(a), allows the residual strength of RDD to be confirmed at load levels less than the regulatory loads specified in FAR/JAR 25.571(b) (Reference 7.2.2.3(i)).

6. Damages larger than the maximum RDD are considered to be immediately obvious. Except for damage resulting from in-flight discrete sources (rotor burst, bird strike, etc.), no residual strength analysis is required for obvious damage.

The residual strength curve shown in Figure 7.2.2.3(a) starts near ultimate strength and spans the range to discrete source damage sizes. This range encompasses damage conditions critical to meeting all requirements such as:

1. Damage sizes and states which support the ADL (Ultimate Load levels) and repairable damage sizes to be placed into the Structural Repair Manual;
2. CDT damages for Limit Load design values;
3. RDD for less than Limit Load but greater than continued safe flight load design values; and
4. “Discrete source” damage for continued safe flight load design values.

Test data and analysis methods developed by the Boeing-NASA/ACT program (References 7.2.2.3(j) through 7.2.2.3(l)) show that the inspection methodologies and damage growth mechanisms should be established to ensure accidental damage occurring in service can be found and repaired before compromising limit strength capabilities. Visual inspection is the preferred damage detection method, and the no-growth approach for damages less than Limit Load size has been the basis for certification. For new composite primary structure application, these approaches will require revalidation.

Figures 7.2.2.3(b) and 7.2.2.3(c) identify the inspection decision points, requirements, development tasks, analyses and actions required to meet the damage tolerance requirements of a principal structural element (PSE). Figure 7.2.2.3(b) outlines the levels of damage tolerance requirements and can be used for test, analysis and maintenance planning. Figure 7.2.2.3(c) defines the flow of events and actions to be used to develop the data required for damage tolerance certification.

The deterministic compliance method is based on a minimum of two sets of testing and analysis. The first set is designed to show positive margins of safety at design Ultimate Load with BVID size damages. This testing includes mostly coupons and subcomponents containing BVID. The second set of testing is designed to show positive margins of safety with large damage at design Limit Load. This testing includes subcomponent (e.g., five-stringer panels) and component structures with through the thickness damage, skin-stiffener debonds, large impact damages, etc. These types of damage are considered to be maximum design damage (MDD). Tests are used to show MDD-sized damage is easily detectable. Tests are also used to show MDD-sized damage and smaller will not grow under operational loads.

Although this method meets FAA requirements for damage tolerance, it may not provide enough data to support the definition of accurate ADLs in structural repair manuals. Consequently, allowable damage sizes are conservatively set to smaller values. This has had the effect of increasing in-service repair costs of thin composite honeycomb sandwich panels in commercial aircraft.

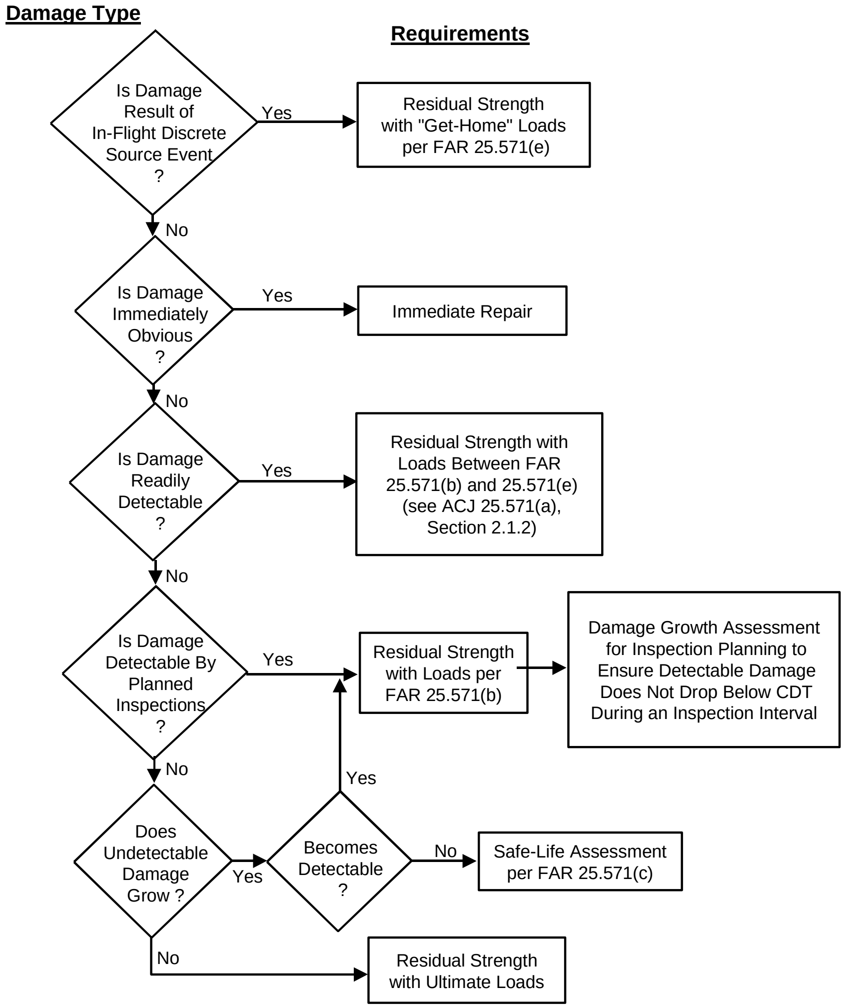

FIGURE 7.2.2.3(b) *Levels of damage tolerance assessments.*

The following are recommended approaches for developing data to support certification and to allow for reduced maintenance costs of composite aircraft structures:

1. The residual strength curve for each significant type of potential damage on each principal structural element should be determined by analysis and/or test.
2. Characteristics describing the inspectability of the CDT as well as the type and extent of the damage should be documented to support maintenance planning activities.
3. For readily detectable damage, the magnitude of the threats that should be considered, similar to those in FAR 25.571(e), should include impact damage by ground vehicles and ground handing equipment, impact with jet gates, runway debris and thrown tire treads. Service experience has shown that damage associated with such events may persist for a few flights before the damage is detected and the structure repaired. The extent of damage that should be considered must be established by taking into account susceptibility to each type of accident.

Structural damage design should be coupled with development of the aircraft maintenance plan in order to reduce in-service damage occurrences and repair costs. Test validation and analyses should address design ultimate strength, damage growth, residual strength, and maintenance issues for composite structures. Independent studies of design Ultimate Load or Limit Load strength without data and analyses at intermediate load levels will not provide a balanced design that supports cost-effective maintenance. For example, damage considered for ultimate strength analyses is more likely to occur in-service while the associated loads are very unlikely. The reverse is true for limit strength analyses. A database that covers a range of damage scenarios increasing in severity will allow for more cost-effective use of composite structures in commercial aircraft service.

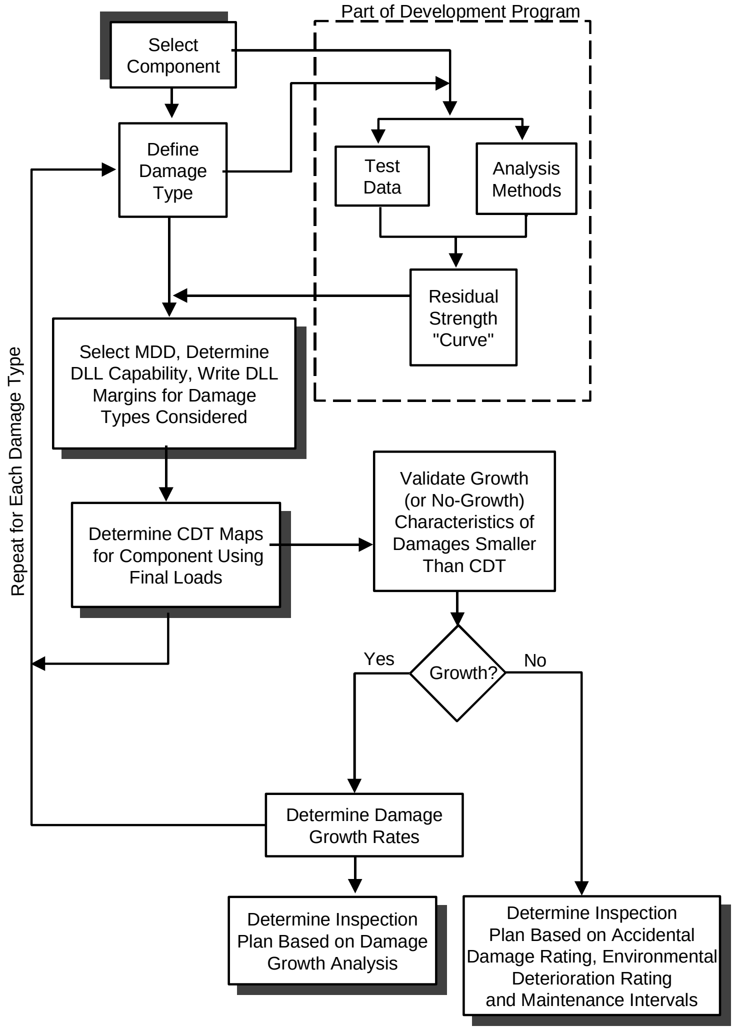

FIGURE 7.2.2.3(c) *Damage tolerance assessment flowchart for fail-safe loads.*

7.2.2.4 Probabilistic or semi-probabilistic compliance methods (civil aviation)

Probabilistic or semi-probabilistic methods consider first that the scheduled inspection program must account for damage severity. The use of these methods are acceptable for civil aviation as they comply with paragraph 7a (4) of the FAA Advisory Circular AC20 107A: *"For the case of the no-growth concept, inspection intervals should be established as part of the maintenance program. In selecting such intervals, the residual strength associated with the assumed damages should be considered.*"

In other words the larger the strength reduction is, the sooner the damage should be detected. Furthermore, these methods also consider that the need for inspection cannot disregard the likelihood of damage occurrence. The more likely the damage is, the sooner it should be detected. As a result, these methods depend on service data. Figure 7.2.2.4(a) illustrates how this *"residual strength associated with the assumed damage"* is governed by both the inspection interval and the damage probability.

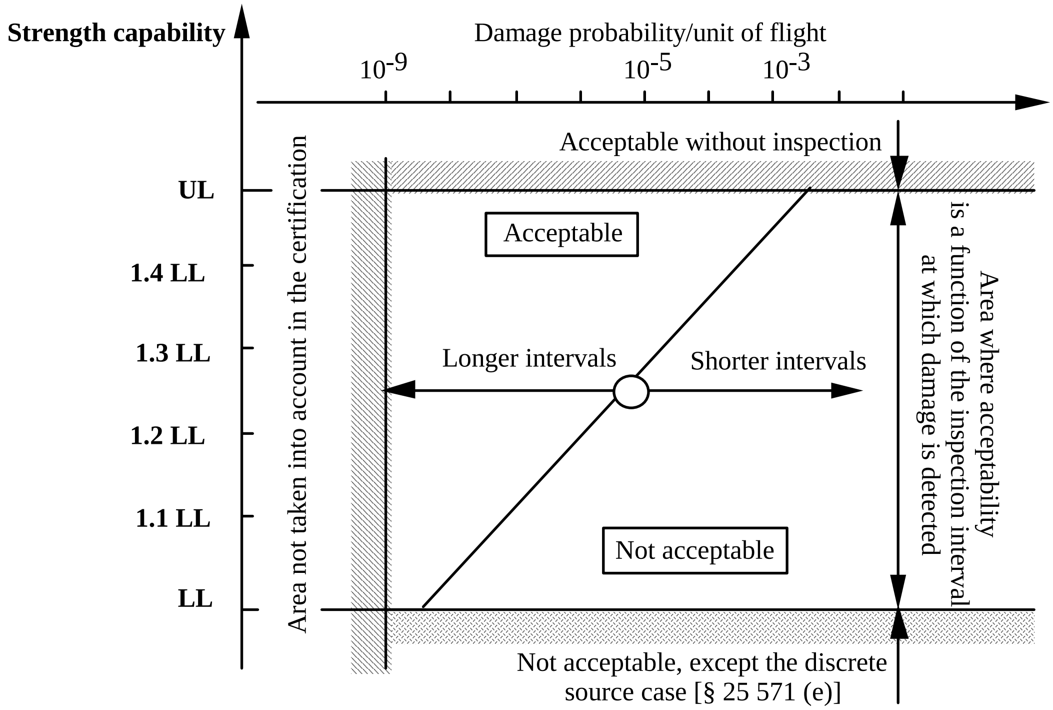

FIGURE 7.2.2.4(a) *Illustration of probabilistic determination of acceptable residual strength levels.*

Since these methods require some probabilistic input data, they are referred to as probabilistic or semi-probabilistic approaches. They were initially developed by Aerospatiale for certification of the ATR 72 outer wing, and later for the A330/340 ailerons. Subsequently a probabilistic approach was implemented by ALENIA for the ATR carbon tail.

The basis of a probabilistic approach is to demonstrate that the inspection program will ensure that the combination of an occurrence of a load having "k x LL" intensity, with the presence of a "missed" accidental impact damage reducing the structure strength to "k x LL" load level, remains acceptable. The term "k x LL" refers to a factor times Limit Load. For primary structure catastrophic failure, this combination must be extremely remote (probability $\leq 10^{-9}$ per flight hour according to ACJ 25 1309). Higher probabilities can be accepted for less critical parts.

Except for the case of hailstone impacts, load and damage occurrences can be considered as independent phenomena. Then it should be demonstrated that:

$$\text{Probability}_{\text{load (k.LL)}} \ * \ \text{Probability}_{\text{missed damage (k.LL)}} \ \leq \ 10^{-9} \qquad \text{7.2.2.4(a)}$$

The following elements are contained in all probabilistic methodologies:

1. Perform a building block approach for deriving strength versus energy curves for all critical parts of the structure.
2. Investigate impact damage scenarios in order to derive the impact threat probability laws.
3. Demonstrate the no-growth concept of all damages up to VID threshold, in general through a full-scale fatigue test.

4. Perform residual static tests for checking the assumed strength of the damaged structures.

General Method

The first step of a probabilistic damage tolerance evaluation is the identification of each critical part of the structure with respect to low-velocity, impact damage tolerance. External skins of the aircraft, subjected to high compression stresses, which are exposed to in-service accidental impacts, are of prime concern. The following steps are applied to each critical zone:

1. Derive the entire residual static strength versus impact energy curve from analysis supported by test.
2. Determine accidental impact threats in terms of energy versus probability curves.
3. Calculate, within each scheduled inspection interval, the probability to have such accidental damages on the structure.
4. Determine load (or stress, or strain) occurrences versus probability curves.
5. Check that the scheduled inspection program will make damage detection highly probable before the probability target is exceeded.

Such probabilistic or more exactly semi-probabilistic approaches are detailed in References 7.2.2.3(e), 7.2.2.4(a) and (b). Since not all of the input parameters used in these referenced methods are expressed through a probability law, for instance the residual static strength versus impact energy, the methods are semi-probabilistic.

The input parameters for the method are defined as follows (Reference 7.2.2.3(e)):

The Impact Threat. The method takes into account a complex threat consisting of miscellaneous damage sources, including occasional sources that may occur only during maintenance operations between two scheduled detailed inspections, and continuous sources for which damage may occur at each flight. Each source of damage is described by a probability function to model the impact energies involved (log-normal law).

The typical impact sources, which are taken into account in the analysis, are:

- Continuous impact sources: Tool drop, foot traffic, collision with service vehicles, projection of runway debris.
- Occasional impact sources: Fall of a removable component during a maintenance operation.

The Inspection Program. The method takes into account a complex maintenance program composed of several types of inspections (see Section 7.4) with a different periodicity. The efficiency of each type of inspection is described by a probability distribution to model the detection probability as a function of the damage dent depth. This means that damages that have to be taken into consideration are not only those naturally omitted by the inspection level (damages up to "visible" impact damage (VID) are to be assumed between two detailed inspections), but also those existing and not noticed by the inspector during the procedure. The latter still have to be accounted for during the next inspection intervals.

For commercial aircraft composite structures, complex non-destructive methods are typically not used to find damage. Once the damage is found, other methods (e.g., ultrasonic) may be used to better characterize its extent. The three methods of inspection considered to initially find damage include general visual inspection, external detailed visual inspection and internal detailed visual inspection. The mathematical modeling of the detection probability is based on statistical studies, which allow for each type of inspection to derive a probability distribution (log-normal law).

The Occurrence of Static Loads. The probability of occurrence of static loads (between limit and ultimate Load) is described by a log-linear probability distribution. The probability of occurrence of static loads varies uniformly (on a log-linear basis) from the range of 10^{-5} per flight hour for a static load equal to Limit Load up to 10^{-9} per flight hour for a static load equal to Ultimate Load.

The Residual Strength of the Impacted Structure. A B-basis curve is assumed for the residual static strength versus impact energy. The effects of environment are taken into account by the use of residual strength values obtained under worst environmental conditions.

The Relationships Between Energy, Damage Size, and Indentation. Two empirical deterministic relationships are taken into account in the analysis. The first one links impact energy to the associated damage size (delaminated area), and the second one relates the damage size (and thus the impact energy) to an associated indentation parameter (this latter being the relevant parameter for the visual detectability of the damage).

The analysis enabling the assessment of the probability of failure (calculated at its maximum, i.e., during the last flight hour of the aircraft's life) is then based on a partition of the energy range involved in the description of the impact sources.

The two main steps of the method are:

1. The calculation of the probability of existence of a damage of a given size at the beginning of the last hour of the aircraft life. This calculation takes into account the different damage sources (continuous and occasional in-service sources) as well as the complex maintenance program (date and type of each inspection).
2. The calculation of the probability of failure during the last flight hour, which must be less than 10^{-9} per flight hour (see Figure 7.2.2.4(b)).

A special use of this probabilistic method also enables the determination of the load level k×LL to be sustained by a structure damaged by a VID, in such a way that the static test at k×LL implies an acceptable in-service risk level for the structure with its inspection program.

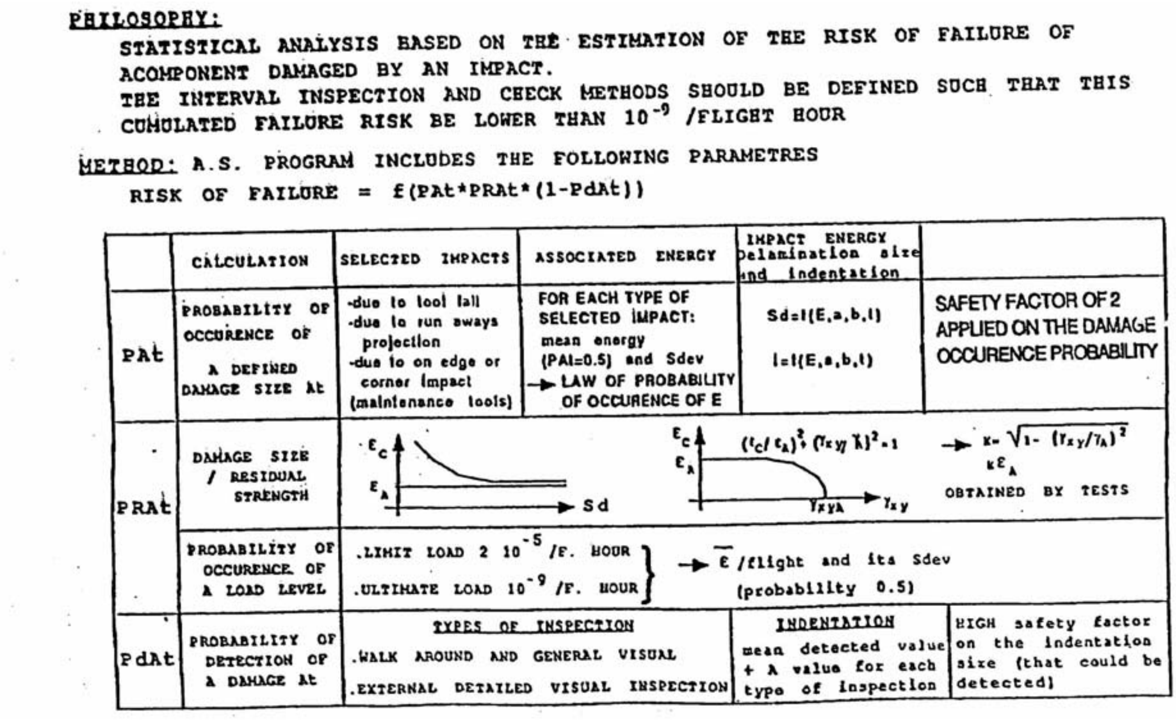
PHILOSOPHY:

STATISTICAL ANALYSIS BASED ON THE ESTIMATION OF THE RISK OF FAILURE OF A COMPONENT DAMAGED BY AN IMPACT.
THE INTERVAL INSPECTION AND CHECK METHODS SHOULD BE DEFINED SUCH THAT THIS CUMULATED FAILURE RISK BE LOWER THAN 10^{-9} /FLIGHT HOUR

METHOD: A.S. PROGRAM INCLUDES THE FOLLOWING PARAMETRES
RISK OF FAILURE = f(PAt*PRAt*(1-PdAt))

	CALCULATION	SELECTED IMPACTS	ASSOCIATED ENERGY	IMPACT ENERGY Delamination size and indentation	
PAt	PROBABILITY OF OCCURENCE OF A DEFINED DAMAGE SIZE At	-due to tool fall -due to run aways projection -due to on edge or corner impact (maintenance tools)	FOR EACH TYPE OF SELECTED IMPACT: mean energy (PAI=0.5) and Sdev → LAW OF PROBABILITY OF OCCURENCE OF E	Sd=f(E,a,b,I) I=f(E,a,b,I)	SAFETY FACTOR OF 2 APPLIED ON THE DAMAGE OCCURENCE PROBABILITY
PRAt	DAMAGE SIZE / RESIDUAL STRENGTH	ε_c, ε_A, Sd	ε_c, ε_A, $(\varepsilon_c/\varepsilon_A)^2 + (\gamma_{xy}/\gamma_A)^2 = 1$, γ_{xyA}, γ_{xy}		→ $k = \sqrt{1-(\gamma_{xy}/\gamma_A)^2}$ $k\varepsilon_A$ OBTAINED BY TESTS
	PROBABILITY OF OCCURENCE OF A LOAD LEVEL	.LIMIT LOAD 2 10^{-5} /F. HOUR .ULTIMATE LOAD 10^{-9} /F. HOUR	→ $\overline{\varepsilon}$ /flight and its Sdev (probability 0.5)		
PdAt	PROBABILITY OF DETECTION OF A DAMAGE At	TYPES OF INSPECTION .WALK AROUND AND GENERAL VISUAL .EXTERNAL DETAILED VISUAL INSPECTION		INDENTATION mean detected value + A value for each type of inspection	HIGH safety factor on the indentation size (that could be detected)

FIGURE 7.2.2.4(b) *Probabilistic methodology for determining inspection intervals.*

Simplified Method

In References 7.2.2.4(a) and (b) there is, first, no differentiation between discrete and continuous damage sources. Therefore, all damage threats are equally shared throughout the inspection interval. Secondly, this method does not include any probability law for detecting the dent - the BVID energy or dent depth must be selected high enough to prevent any oversight.

Both assumptions allow calculations to be simplified in the following way:

Let pa = probability of accidental damage at the end of unit aircraft utilization (e.g., one flight hour, one flight ....).

n = inspection interval expressed in terms of unit aircraft utilization (n flights, n hours)

Pr = probability of occurrence of the flight load (e.g., gust), the intensity of which combined with the accidental damage of probability pa would lead to a catastrophic failure.

The probability to have at least one accidental damage at the last flight preceding the inspection (where the likelihood of a damaged structure is higher) is then equal to:

$$1-(1-pa)^n \cong (n)(pa) \qquad 7.2.2.4(b)$$

The relationship 7.2.2.4(a) then takes the following simple formulation:

$$(Pr)(n)(pa) < 10^{-9} \qquad 7.2.2.4(c)$$

The following steps of the damage tolerance evaluation are illustrated in Figure 7.2.2.4(c) taken from Reference 7.2.2.4(b):

1. The residual static strength versus energy curve is evident as the first quadrant of the diagram. A “B” basis value curve is recommended.

2. The damaged state of the structure after n flights is represented in the fourth quadrant. This is a probability law assumed here to be log-linear in order to simplify the sketch. Actually this law is close to log-linear. From equation 7.2.2.4(b) this curve can be easily obtained through a simple translation of the damage threat per flight. For this illustration, “n” has been assumed to be a thousand flights.

3. The probability law for load (or stresses, or strain) occurrences is represented in the second quadrant. This law is assumed to be log-linear in the interval between limit and Ultimate Loads. Figures reported on the horizontal axis are typical of a commercial aircraft.

4. Each point on the strength versus energy curve (quadrant 1) corresponds to:

   a. One energy level with its associated probability to have at least one damage of such severity (or higher) on the structure at the last flight before inspection.
   b. One residual static strength with the associated probability to encounter a load of the same magnitude per flight.

5. The product of these two probabilities is plotted in the third quadrant where a picture of the whole first quadrant curve can be drawn. In the same quadrant, a line representative of equation 7.2.2.4(c) splits the diagram into two domains:

a. Acceptable values (probabilities lower than 10^{-9}), top right
b. Not acceptable values (probabilities higher than 10^{-9}), bottom left

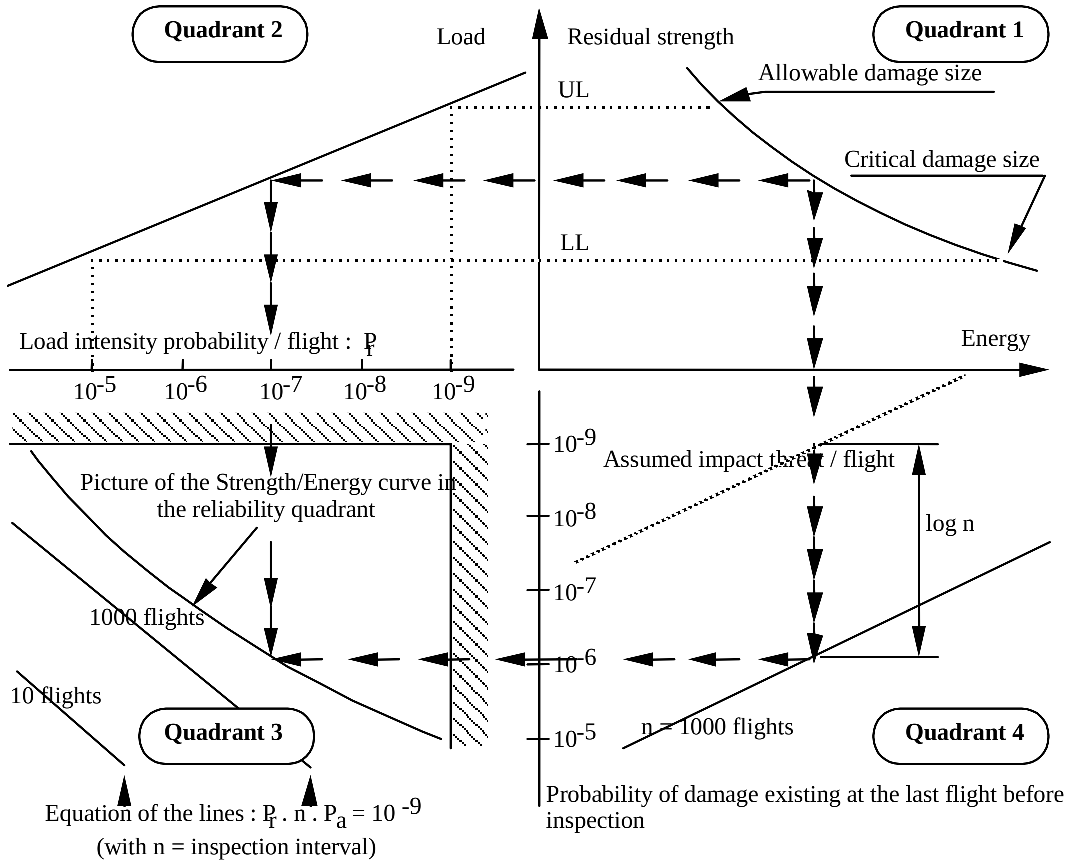

FIGURE 7.2.2.4(c) *Simplified probabilistic methodology for determining inspection intervals.*

Acceptable damage tolerance is demonstrated for an inspection interval equal to n if the whole curve is located above the border line. This illustration shows that when the inspection interval (n) increases, the strength-energy picture curve moves downward while the straight line delimiting the 10^{-9}, probability target moves upward. Acceptable damage tolerance is not achieved when both curves cross.

For very thick laminates where VID is extremely improbable, the calculation is performed with n equal to the whole aircraft lifetime. For thinner laminates where VID can be expected, the maximum acceptable inspection interval is the highest one, among those of the scheduled inspection program, containing the whole strength-energy picture curve above it.

7.2.2.5 Comparison of deterministic and probabilistic methods

The following paragraphs briefly summarize the major differences between the deterministic compliance method and the semi-probabilistic method given in the previous two sections. Both of these methods have been used to successfully certify composite primary structure on commercial transport aircraft. Other probabilistic approaches, covering various aspects of composite design and certification, are reviewed (Reference 7.2.2.5). In the same reference, Northrop Grumman Commercial Aircraft Division (NGCAD) proposes a quite comprehensive method covering both static and damage tolerance requirements, with an application exercise to the Lear Fan. Nevertheless, none of these methods have so far been implemented in an aircraft certification program.

In the deterministic method, an upper limit of 100 ft-lb (140 Joules) is used for ultimate strength impact damage, whereas in the probabilistic method, lower levels have been used based on the assessments discussed in Section 7.3.3.

In the deterministic method there is no upper limit on the energy level for impact damages to be considered for Limit Load analyses; damage is considered up to the point of being readily detectable. In the probabilistic method, the upper limit on impact energy for Limit Load analyses is set at a probability of 10^{-9}.

In the deterministic method, inspection intervals have been set based on a qualitative rating system, which is derived based on structural capability and aircraft service experience for the effects of accidental damage and environmental degradation. In the probabilistic method, the maximum inspection intervals are derived using the probabilities of damage and load occurrence, with a reliability of at least 10^{-9}.

7.2.2.6 Full-scale tests for proof of structure (civil aviation)

Compliance with the requirements is built, step by step, through what is usually called a “building block approach” (see Volume 3, Chapter 4). Tests carried out to support the analysis are arranged like a pyramid, where a full-scale test culminates at the top, the bottom referring to generic tests dedicated to the derivation of a statistical basis for allowable values. Low velocity impacts, with their relevant thresholds, should be addressed throughout this pyramid of tests, from the “allowable” level to the full-scale demonstration.

When introducing a low velocity impact damage in a test article, it is important that the selected detectability threshold captures the worst possible situation in terms of internal damage, hence the need to use blunt impactors. Hemispherical impactor geometry, with the smallest size at least 0.5 inch (12.5 mm) diameter, are recommended.

Due to the absence of interaction between high static stresses and fatigue behavior, it is current practice of transport aircraft manufacturers to conduct tests on only one full-scale test article, for both static and fatigue/damage tolerance demonstration. A typical arrangement of tests for this purpose (from various Airbus applications), is illustrated Figure 7.2.2.6.

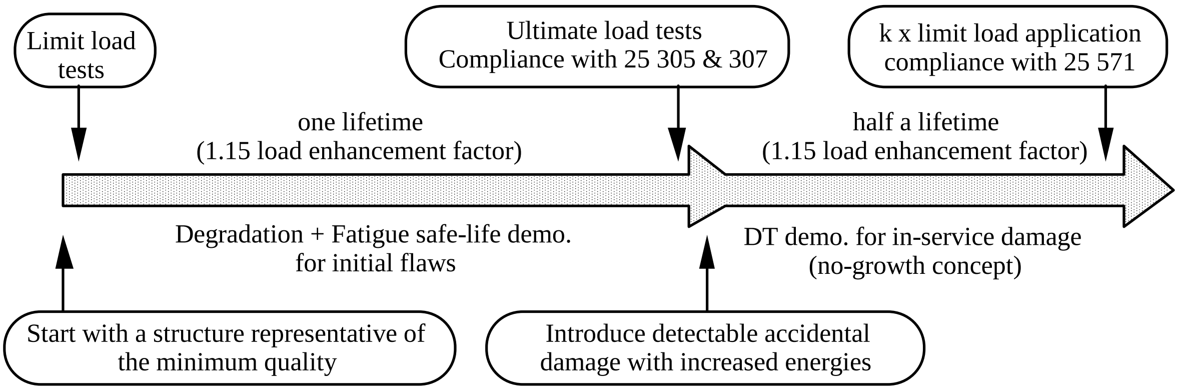

FIGURE 7.2.2.6 *Test sequence for the full-scale aircraft, proof of structure test.*

Proof of structure, full-scale static test. The test program starts with an article provided with simulated low velocity impact damages, limited by the selected energy cut-off levels and deliberately inflicted at the most stressed areas of the structure. The Ultimate Load capability is demonstrated after fatigue, allowing for environmental adverse conditions. This is in line with the means of compliance provided by the AC 20 107A § 6 Proof of structure-static, sub § (a) : *The effects of repeated loading and environmental exposure which may result in material property degradation should be addressed in the static evaluation.*

Proof of structure, full-scale fatigue/damage tolerance test. When considering the effects of material variability on the repeated load behavior of composite structures, a factor on loads is preferred to a factor on life. The rationale of such approach and the recommended load enhancement factors can be found in References 7.2.1(a) to 7.2.1(d). The demonstration has two parts.

First, an enhanced safe life (flaw tolerant) demonstration, to show that no damage will initiate and grow in a structure representative of the minimum quality allowed by the quality control specification (considering not only impact damage but also various manufacturing flaws). This phase is in line with AC 20 107A § 7 Proof of structure - Fatigue/Damage tolerance, (b) fatigue (safe life) evaluation: *Fatigue substantiation should be accomplished by component fatigue tests or by analysis supported by test evidence, accounting for the effects of the appropriate environment. The test articles should be fabricated and assembled in accordance with production specifications and processes so that the test articles are representative of production structure, etc.*

Second, a no-growth demonstration for more severe impact damages, some of which may become detectable at the scheduled inspection intervals. This phase is in line with AC 20 107A § 7 Proof of structure - Fatigue/Damage tolerance, sub § (a): *Structural details, elements, and subcomponents of critical structural areas should be tested under repeated loads to define the sensitivity of the structure to damage growth. This testing can form the basis for validating a no growth approach to damage tolerance requirements.*

A demonstration of the regulatory static load capability is needed to complete this second phase. A “k” value higher than 1.0 can be required depending on the result of a probabilistic approach, if used for certification. It is the second phase of the full-scale test that brings most to the demonstration of the structural safety. At this stage, a precise definition of damage growth is required. For instance, there may be a possibility where an impact damage will grow under the first service loads following the occurrence and, then reach a definite size after a certain time. This is still to be assumed as a “no-growth” situation, since the "growth" is not detrimental to the structural capability. On another hand, a damage can be definitely arrested by a design precaution (a bolt row for instance). Provided regulatory load capability exists after this size extension, the result is comparable to a no-growth situation.

7.3 TYPES, CHARACTERISTICS, AND SOURCES OF DAMAGE

Damages are generally discussed in two frames of reference - by stage of occurrence and by physical anomaly. Stage of occurrence is separated into manufacturing and in-service categories. Damages occurring during manufacturing are more accurately classified as “flaws” rather than “damages”. They are not distinguished as such in this write-up.

Composite aircraft parts can be damaged during manufacturing, shipping, and service. A primary focus in composites is low velocity impacts that can cause significant damage that may not be clearly visible. Sources of such impact damage include falling tools and equipment, runway debris, hail, birds, and collision with other airplanes or ground vehicles. Airplanes can also be damaged by high velocity impacts from discrete source events (e.g., parts of rotating machinery that fail in turbofan engines and penetrate the engine containment system, the aircraft skin, and supporting structure). All of the above damages can occur to either military or commercial aircraft. Military aircraft may also suffer ballistic damage, as may occur in battle.

Concerns about the effects of impact damage can be quite different, depending on the specific design and application. Compressive residual strength of laminated composite material forms is known to depend on the extent of delaminations and fiber failure caused by transverse impacts. Tensile residual strength is affected by fiber failure. Impact damage can also affect the environmental resistance of a composite structural component or the integrity of associated aircraft systems. For example, impact damage may allow moisture to penetrate into the sandwich core in light-gauge fairing panels or provide a path for fuel leaks in stiffened wing panels. These effects must be understood for safe and economic composite applications.

7.3.1 Damages characterized by stage of occurrence

7.3.1.1 Manufacturing

Manufacturing damage includes anomalies such as porosity, microcracking, and delaminations resulting from processing discrepancies and also such items as inadvertent edge cuts, surface gouges and scratches, damaged fastener holes, and impact damage. The inadvertent (non-process) damage can occur in detail parts or components during assembly or transport or during operation. A list of sources of manufacturing defects is given below:

Improper cure or processing
Improper machining
Mishandling
Improper drilling
Tool drops
Contamination
Improper sanding
Substandard material
Inadequate tooling
Mislocation of holes or details

Most manufacturing damage, if beyond acceptance limits, will be detected by routine quality inspection. For every composite part, there should be acceptance/rejection criteria to be used during inspection of the part. Damage that is acceptable will be incorporated in the substantiation analysis and test program to demonstrate ultimate strength in the presence of this damage. Some “rogue” defects or damage beyond specification limits may go undetected and consequently, their existence must be assumed as part of damage tolerant design. Establishing the size of the “rogue” or missed flaw is part of the design criteria development process.

Examples of rogue flaws occurring in manufacturing include a contaminated bondline surface, or inclusions such as prepreg backing paper or separation film that is inadvertently left between plies during lay-up. Current inspection methods may not detect these types of defects. As a result, current design practices include the effect of large debonds in damage tolerance criteria which may impose severe weight penalties. In the future, advanced inspection techniques and in-process quality control may lead to less severe criteria. Without adequate inspection techniques, in-process quality controls must be sufficiently rigid to preclude this type of defect.

7.3.1.2 Service

The main characteristic of in-service damage is that it occurs during service in a random manner. Damage characteristics, location, size, and frequency of occurrence can only be predicted statistically, which involves a large amount of data accumulation. In-service damage is typically classified as non-detectable and detectable (often referred to as non-visible and visible). A part has to be designed in such a way that likely, non-detectable damage (per the selected inspection method) can be tolerated under Ultimate Loads and for the life of the structure. The most common in-service damage is due to an impact event. A list of sources of in-service damage threats is given below:

Hailstones
Runway debris
Ground vehicles, equipment, and structures
Lightning strike
Tool drops
Birdstrike
Turbine blade separation
Fire
Wear
Ballistic damage (Military)
Rain erosion
Ultraviolet exposure
Hygrothermal cycling
Oxidative degradation
Repeated loads
Chemical exposure

7.3.2 Damages characterized by physical imperfection

Damage can occur at several scales within the composite material and structural configuration. This ranges from damage in the matrix and fiber to broken elements and failure of bonded or bolted attachments. The extent of damage controls repeated load life and residual strength, and is, therefore, critical to damage tolerance.

Fiber Breakage. This defect can be critical because structures are typically designed to be fiber dominant (i.e., fibers carry most of the loads). Fortunately, fiber failure is typically limited to a zone near the point of impact, and is constrained by the impact object size and energy. Only a few of the service related events listed in the previous section could lead to large areas of fiber damage.

Matrix Imperfections. (Cracks, porosity, blisters, etc.) These usually occur on the matrix-fiber interface, or in the matrix parallel to the fibers. These imperfections can slightly reduce some of the material properties but will seldom be critical to the structure, unless the matrix degradation is widespread. Accumulation of matrix cracks can cause the degradation of matrix-dominated properties. For laminates designed to transmit loads with their fibers (fiber dominant), only a slight reduction of properties is observed when the matrix is severely damaged. Matrix cracks, a.k.a. micro-cracks, can significantly reduce properties dependent on the resin or the fiber/resin interface, such as interlaminar shear and compression strength. For high temperature resins, micro-cracking can have a very negative effect on properties. A discussion of the effects of matrix damage on the tensile strength can be found in Reference 7.3.2(a). Matrix imperfections may develop into delaminations, which are a more critical type of damage.

Delamination and debonds. Delaminations form on the interface between the layers in the laminate. Delaminations may form from matrix cracks that grow into the interlaminar layer or from low energy impact. Debonds can also form from production non-adhesion along the bondline between two elements and initiate delamination in adjacent laminate layers. Under certain conditions, delaminations or debonds can grow when subjected to repeated loading and can cause catastrophic failure when the laminate is loaded in compression. The criticality of delaminations or debonds depend on:

- Dimensions
- Number of delaminations at a given location.
- Location - in the thickness of laminate, in the structure, proximity to free edges, stress concentration region, geometrical discontinuities, etc.
- Loads - behavior of delaminations and debonds depend on loading type. They have little affect on the response of laminates loaded in tension. Under compression or shear loading, however, the sublaminates adjacent to the delaminations or debonded elements may buckle and cause a load redistribution mechanism, which leads to structural failure. Methods to estimate the criticality of delamination and debonds are presented in Section 7.8.4.2.

Combinations of Damages. In general, impact events cause combinations of damages. High-energy impacts by large objects (i.e., turbine blades) may lead to broken elements and failed attachments. The resulting damage may include significant fiber failure, matrix cracking, delamination, broken fasteners, and debonded elements. Damage caused by low-energy impact is more contained, but may also include a combination of broken fibers, matrix cracks and multiple delaminations. There is some experimental evidence that, for relatively small damage sizes, impact damage is more critical than other defects (see Figures 7.3.2(a) and (b), References 7.3.2(b) and (c)). Note that all of the data shown in these figures are for damage sizes less than 2 inches (50 mm). Some results for damages greater than 2 inches (50 mm) suggest large holes or penetrations are at least as severe as equivalent sizes of impact damage.

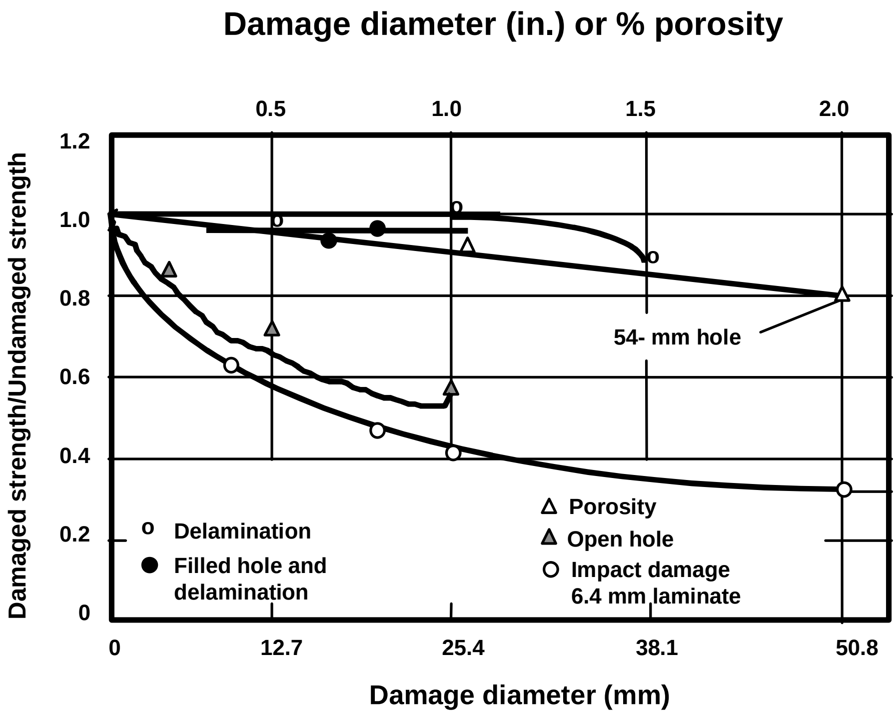

FIGURE 7.3.2(a) *Relative severity of defect damage on static compression strength.*

Flawed Fastener Holes. Improper hole drilling, poor fastener installation, and missing fasteners may occur in manufacturing. Hole elongation can occur due to repeated load cycling in service. Such issues can effectively extend the size of the hole and lead to assumptions that the hole is open (or filled, depending on which leads to the greater notch sensitivity). The notch sensitivity of a composite has generally been dealt with by using semi-empirical analyses.

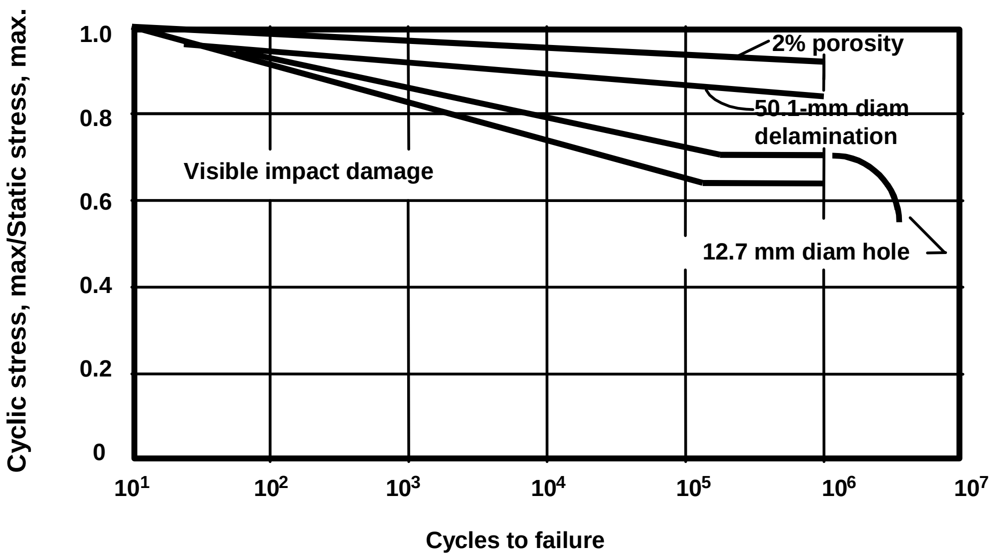

FIGURE 7.3.2(b) *Relative severity of defect damage on compression fatigue strength, $R=10$.*

7.3.3 Realistic impact energy threats to aircraft

As discussed in Section 7.2.2, certification of aircraft composite structure requires the establishment of realistic impact energy level cut-offs for Ultimate Load considerations. A conservative assumption is to set the energy level at a 90% probability, analogous with the concept of a B-basis strength value. This then means that the *realistic* energy cut-off has been selected in such a way that, at the end of lifetime of the aircraft, no more than 10% of them will have been impacted with an energy value equal to this cut-off level or higher. For these 10% corresponding to a more damaged situation, and then possibly not being able to comply with the Ultimate Load requirements, damage tolerance considerations will demonstrate the regulatory safety level.

Letting Eco = energy cut-off value, and with Pa the probability, per flight, to encounter one impact with an energy $E \geq Eco$, then, $(1\text{-}Pa)$ is the probability for an aircraft to have encountered either no impact or impacts of a lower energy on that flight. In fact the risk of low velocity impact damage is not likely to occur during the actual flight, but during the various operations associated with this flight, e.g., aircraft servicing and a shared part of the risk associated with the scheduled inspections.

Then it follows that:

$(1\text{-}Pa)^n$ is the probability to have never encountered any impact with an energy of $E \geq Eco$ after n flights, and then the probability to have encountered at least one damage created by an impact with an energy of $E \geq Eco$ after n flights is given by:

$$P = 1 - (1\text{-}Pa)^n$$

Assuming that:

n = 50,000 flights for a short/medium range commercial aircraft,
P = 0.1

Then $Pa = 2.1 \times 10^{-6}$

In this case, the realistic energy level to be allowed for is the one corresponding to a probability of occurrence of 2.10^{-6} per flight. Should the target of P be 0.01, Pa would then be equal to $2.1\ 10^{-7}$, which obviously corresponds to a higher energy level, though not very far from it since the probability versus energy relationship is assumed to be log-linear.

In the case of FAR 25 fixed wing structures, both values for Pa are lower than the probability commonly associated with Limit Loads occurrences, which can be assumed in the range of 10^{-5} per flight hour. It may be unreasonable to state that such so-called “realistic” energy level occurrence is more “realistic” than a limit Loads event. Then, clipping this probability figure at the 10^{-5} per flight value should also be acceptable where the average duration of one flight is around one hour.

At this stage, one must unfortunately admit that there is very little data for quantifying energy levels in relation to these probability values. Just for the purpose of an exercise to illustrate this approach, some figures drawn from the literature are given hereafter.

In reality, Pa is the product of two probabilities since associated events are assumed as independent:

$$Pa = \text{Probability (impact damage occurrence) x Probability (damage energy} \geq \text{Eco)}$$

As far as the second term is concerned, the only results known from a field survey are reported in Reference 7.3.3(a). With the analysis of 1644 impacts, this survey can be considered as quite comprehensive. Although, these records are representative of military aircraft from the US Navy Forces (F-4, F-111, A-10 and F-18), they can be extended to transport category aircraft investigations since maintenance tools and operations should not be very different. In this study, all the 1644 impact dents observed on the metallic structures have been converted into energy levels through a calibration curve obtained on a F-15 wing, shown in Figure 7.3.3(a). According to this reference, the upper limit impact energy for the aircraft surveyed is approximately 35 ft-lb (48 joules).

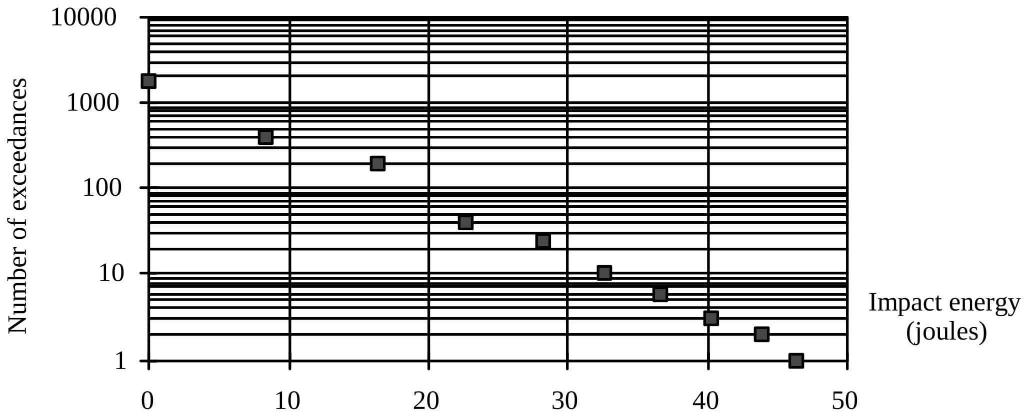

FIGURE 7.3.3(a) *Number of exceedences versus impact energy level for an aircraft lifetime.*

Since this report does not mention the aircraft lifetime in relation to each identified damage and the impact location, it is impossible to derive an impact hazard per flight hour. Nevertheless, this survey provides: 1) the order of magnitude of the expected energy, should an impact occur, and 2) the shape of the curve of exceedence (Ne) versus energy. The latter can be assumed as log-linear in this range of energy, with a slope of about -11 ft-lb/Log Ne (-15 joules/Log Ne).

The probability (Pe) of exceeding a given level of energy, should an accidental impact occur, can be then easily drawn from this curve through the relationship:

$$\text{Log } Pe = - x(j) / 15$$

More rigorously, a two-parameter, Weibull distribution has been established from this field survey (Reference 7.3.3(a)), with shape and scale parameters equal to 1.147 and 8.2 (5.98 for ft-lb energy units), respectively.

In regards to the probability of damage occurrence, useful data are published in Reference 7.3.3(b). Data collected from visits to American Airlines, Delta Airlines, United Airlines, the North Island Naval Aviation Depot and from communications with De Havilland Aircraft Inc. are summarized in this report. Records concerning 2100 aircraft shared by 19 operators have been analyzed. For a total number of 3,814,805 flight hours, 1484 maintenance induced damages - which correspond to low velocity impact damages - have been noticed. Statistics on hail storms, lightning strikes and bird strikes are also reported in this reference. Unfortunately, the energy level associated with these maintenance-induced and service damages have not been investigated.

From these data, the low velocity impact damage probability of occurrence can be estimated at 3.9 10^4 per Flight Hour. This figure obviously concerns the whole aircraft and the probability associated to a dedicated part - e.g. a rudder skin - should be lower. Given that “Murphy's law” should not be ignored, impact damage probabilities of the same order of magnitude should be assumed. With a figure ranging between 10^{-3} and 10^{-5} per hour, the event should be assumed as reasonably probable, according to the definitions provided by the ACJ 25 1309.

Now combining all these field survey data, Figure 7.3.3(b) shows the value of Pa versus impact energy for various damage occurrence probabilities (per hour) in the reasonably probable domain. With the objective that the “realistic” energy level encompasses 90% of the aircraft population at the end of lifetime (Pa = 2.1 10^{-6}), assuming a damage occurrence probability at the upper bound of the reasonably probable domain and one flight times one hour, the result of this application exercise is:

FIGURE 7.3.3(b) *Probability of different levels of impact events.*

Eco should not be below 30 ft-lbs (40 joules). Assuming now Pa = 10^{-5}, the associated energy level is 22 ft-lbs (30 joules).

The energy cut-off threshold selected for Airbus programs (since the A320 type certification and after) is 37 ft-lb (50 joules), except for the inboard part of the horizontal tailplane, where the cut-off is 103 ft-lb (140 joules). Reflecting USAF requirements and company design criteria, Boeing has used an impact energy cut-off threshold of 100 ft-lb (136 joules) for commercial aircraft certification programs.

With the view to implement a probabilistic approach in the damage tolerance demonstration of the ATR 72 CFRP outer wing, Aerospatiale investigated accidental impact scenarios for deriving the figures needed by their method (Reference 7.3.3(c)) . After these investigations, a 27 ft-lb (36 joules) cut-off threshold for structural substantiations was used.

7.4 INSPECTION FOR DAMAGE

The ability to detect damage is the cornerstone of any maintenance program employed to ensure the damage tolerance of a specific structure. Such a program must combine one or more inspection methods with an appropriate schedule to reliably detect damage prior to unacceptable performance degradation. Inspection methods are also relied upon to quantify such damage in support of residual strength assessments. Accessibility for inspection must be accounted for in the design and in maintenance plans.

To achieve economic goals, in-service inspection programs often rely on combinations of frequent, relatively simple inspections (usually of broad areas) and less frequent, but more intense, examinations (typically of more localized areas). The capabilities of each inspection method (i.e., detectability threshold, detection reliability) must be well understood as a function of damage state for each structural location. Since the impact variables (i.e., impactor geometry, velocity, angle of incidence, etc.) strongly influence the damage state at a specific location, the detectability thresholds and reliabilities should be quantified considering the ranges of these variables expected in service.

Inspection procedures can be divided into two main classes. The first, which is most general, includes both destructive and nondestructive methods used for concept development, detailed design, production, and maintenance. The second class includes only those nondestructive evaluation (NDE) methods that can be practically used in service to locate and quantify the effects of impact damage. The second class is a subset of the first and depends on a technology database suitable for relating key damage characteristics to structural integrity.

7.4.1 Aircraft inspection programs

In aircraft applications, scheduled inspections are the basis for initially detecting damage that does not result in an obvious malfunction. Aircraft structures have historically relied heavily on visual methods in this process. Typical scheduled inspections for these applications are:

- Walk around – long distance visual inspection to detect punctures and large areas of indentation or fiber breakage, i.e., readily detectable damage.

- General visual inspection – careful visual examination of relatively large areas of internal and/or external structure for indications of impact damage (e.g., dents, fiber breakout) or other structural anomaly. Adequate lighting and appropriate access to gain proximity (e.g., removal of fairings and access doors, use of ladders and work stands) are required. Inspection aids (e.g., mirrors) and surface cleaning may also be necessary.

- Detailed visual inspection – close-proximity, intense visual examination of relatively localized areas of internal and/or external structure for indications of impact damage or other structural anomaly. Like general visual inspections, adequate lighting and appropriate access to gain proximity are required. Inspection aids and techniques may be more sophisticated (e.g., lenses, grazing light on a clean element) and surface cleaning may also be necessary.

- Special detailed inspection – inspections of specific locations for non-visible damage using non-destructive procedures (e.g., ultrasonics, x-ray, and shearography).

The use of visual inspection methods for initial damage detection is likely to continue due to the cost and time associated with applying other NDE procedures over the full surface of a structure. Advances in optical techniques, for example, allow large areas of a structure to be quickly inspected for local defects; however, the high cost of equipment needed for such procedures remains as a barrier to implementation of the technology by aircraft operators.

The widespread use of visual inspection procedures for finding service damage in composite structure has led to the use of barely visible impact damage (BVID) thresholds in design sizing (Reference 7.4.1(a)). The FAA has recommended such design practice for composite structure to account for damage that may never be found in service. Past interpretations of the threshold for visibility have been somewhat subjective, with different commercial and military applications defining minimum visible dent depths between 0.01 in. (0.25 mm) and 0.10 in. (2.5 mm).

When damage is initially detected, more detailed visual measurements and various types of ultrasound are used in directed inspections to quantify its extent. Surface damage measurements (e.g., location, dent depth, or crack length) can be quantified with gages and scales commonly used in maintenance. "Coin tapping," which is based on principles similar to lamb wave propagation, provide a rough measure of the extent of sub-surface damage. Pulse-echo ultrasound, which requires equipment and some training, has also been applied in service to get a more accurate measurement of the extent of sub-surface damage with single-side access. These procedures are simple to apply without having to disassemble the structure, but tend to yield very subjective results. More repeatable measurements are conceivable when the structural repair manual (SRM) provides instructions on how they should be applied to specific structure.

Aerospatiale (Reference 7.4.1(b)) has shown that a dent depth between 0.01 and 0.02 in. (0.3 and 0.5 mm) is detectable, through a detailed visual inspection, with a probability better than 0.90. However, the use of dent depth as a damage metric has several shortcomings. First, dent depths depend on a number of impact variables, including the impactor geometry, and may not be a good indication of the extent of underlying damage. Also, in Reference 7.4.1(c) it was shown that the impact dent could decay with time under the combination of fatigue and aging due to viscoelastic phenomena. In some cases, the initial impact indentation dent depth (δ_1) may be as much as 3 times that of the decayed dent depth. This was also confirmed by Canadian investigations reported in Reference 7.4.1(d). Dent decay versus time is probably material dependent. When using maintenance damage detection schemes based on visibility, it is thus necessary that damages used to demonstrate tolerance to BVID have decayed dent depths greater than or equal to the detectability thresholds (δ_d). Therefore, in the absence of data, an initial dent depth of at least .04 in. (1 mm) should be selected to remain detectable at the end of the longest scheduled inspection interval.

7.4.2 Recommendations for damage inspection data development

Aircraft manufacturers apply a range of inspection procedures to help meet development and application goals. These goals include identifying: (a) critical damage types and design criteria for specific structural details, (b) process and quality controls for production parts, and (c) reliable procedures for maintenance in the field. Impact surveys, which involve applying a range of impact damage to representative structure, are recommended to support the development of enabling inspection technologies. They should result in definition of visual damage characteristics for routine inspections, and more rigorous, but reliable, NDE procedures that may be used to quantify residual strength. These efforts should include quantification of the impact event, and application of both nondestructive (e.g., through-transmission ultrasound) and destructive (e.g., microscopic cross-sections) measurements of the resulting damage. Note that, as discussed in Section 7.5 (Damage Resistance), impact surveys provide the most meaningful results when applied to specific structural configurations and design details.

7.4.2.1 Goals

The most obvious goal of the impact survey inspection results is the definition of detectability limits and detection probabilities for the recommended in-service inspection methods. Comparison of results from the in-service techniques with more sophisticated laboratory methods provides a strong basis for quantifying both parameters. The range of impact variables and structural configurations included in the impact survey allow variations in the detectability limits and detection probabilities with these variables to be addressed.

A less apparent, but equally important goal of the impact survey inspection results is the development of techniques for quantifying structural degradation. Reductions in structural performance parameters (i.e., stiffness, strength) must be defined to avoid overly conservative assumptions in residual strength assessments, which lead to excessive repair requirements. The impact survey results provide the opportunity to accomplish this through the development of relationships between field-measurable damage parameters and the actual degradation determined from destructive evaluation. Note that there is little relevance to relationships between impact *event* metrics and the resulting structural degradation since, generally, little or nothing is known about the event that caused the damage (e.g., impactor geometry, energy levels, time since occurrence).

7.4.2.2 Inspection techniques

Both destructive and NDE methods should be applied to maximize the information gained from impact surveys. All of the NDE methods recommended for field maintenance should be included in the survey. Correlation between field NDE techniques and more rigorous laboratory evaluations, including destructive mechanical tests (to be discussed in Section 7.8.3) and microscopy of cross-sections, should help establish key characteristics of impact damage.

Inspection methods which are generally only suitable for impact surveys conducted in the laboratory include through transmission ultrasound (TTU), microscopy, thermal deply, local reduced stiffness measurements, and residual strength tests. The last one will be presented in Section 7.8.3. The use of TTU requires access to both sides of a structure, special equipment (e.g., ultrasonic signal generators and transducers capable of frequencies between 1 and 10 MHz) and a grease or fluid media to couple probes with the damaged structure. Microscopic cross-sections are best used to see matrix cracks and delamination. A polished cylindrical-section highlighted by dye penetrant may help define how such matrix damage combines to form sublaminates (which will be discussed further in Sections 7.8.2 and 7.8.3). Destructive methods which burn away resin (referred to as thermal deply for laminates) are the most efficient laboratory procedures for characterizing the extent of fiber damage. Although such methods were first applied to laminates made from unidirectional tape, they also work for other material forms, such as textiles.

Pulse-echo ultrasound (PEU) and X-ray, which both require special equipment, can be used in either laboratory or field applications. Only one-side access is needed for PEU. It has been used to provide some measure of the extent of delamination at different levels. As was the case with TTU, some fluid media is normally required to couple the PEU transducer with a damaged structure's surface. More advanced ultrasonic methods using laser pulses and optical data reduction (one-sided, no contact access) are expected to emerge as NDE technology progresses. X-ray typically requires the penetration of special fluids to highlight the damaged substructure.

The reduced stiffness resulting from damage may be quantified in a test laboratory, without generating further damage, by applying an out-of-plane load at the impact site and measuring the local deflection. This technique, which applies load in a manner similar to quasi-static impact tests, provides a measure of local load carrying capability. Local reduced stiffness measurements help to quantify effective mechanical properties rather than discrete damage characteristics and, therefore, can result in simpler residual strength analyses. An ultrasonic method, which (with more development) may be suitable for field applications, uses lamb wave dispersion measurements to quantify axial and flexural stiffness (Reference 7.2.2.3(j) and 7.4.2.2). Lamb waves propagate in a flexural mode at wavelengths on the order of structural thickness. Relatively low frequencies (less than 1 MHz) are required to generate such waves. Changes in velocity as a function of frequency (i.e., wave dispersion) relate to structural bending and extensional stiffness through analysis. This method has been successfully applied to quantify the reduced stiffness of impact damage created by a wide range of sources. Figure 7.4.2.2 shows a plot correlating a mechanical measurement of local reduced bending stiffness with that obtained from flexural wave propagation. Note that neither dent depth nor ultrasonic C-scan area had as good a correlation with mechanical measurements of reduced stiffness.

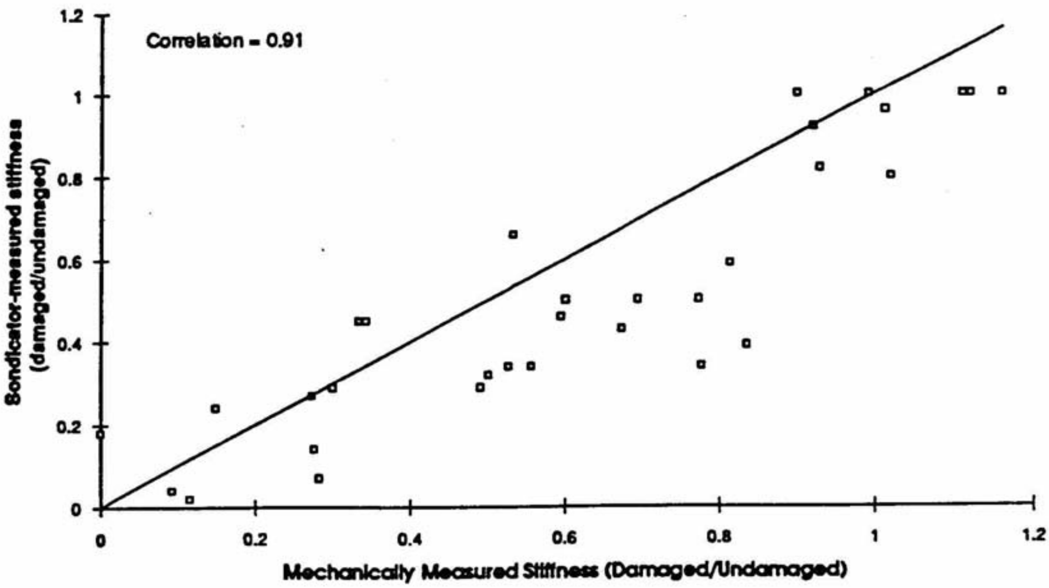

FIGURE 7.4.2.2 *Mechanical and ultrasonic experimental measures of local reduced stiffness at impact damage (References 7.2.2.3(j) and 7.4.2.2).*

7.5 DAMAGE RESISTANCE

Damage resistance, as used in the context of this discussion, relates to a structure's resistance to various forms of damage occurring from specific events. It is generally an issue of structural weight for the designer, and of economics for the operator. Considering potential threats for commercial and military aircraft, this covers a large range of damage states. Based on the specific structural configuration and design details, some damage types pose a more serious threat to structural performance than others. The ensuing discussion will highlight known damage resistance mechanisms and the trade in properties one can expect in selecting a particular material type or design configuration for different applications.

7.5.1 Influencing factors

The composite impact damage characteristic that has been given the most attention to date is delamination and/or element disbond resistance. Numerous attempts at improving this property through material developments were pursued during the 1980s and into the 1990s. These included toughened resin systems, stitching, z-pinning, and textile material forms (with varying degrees of through the thickness reinforcement). Fiber stress versus strain properties were also found to be important to the resistance of impact damage dominated by fiber failure. The high tensile strain-to-failure of fiberglass and aramid fibers make them significantly more resistant to failure under impact loads than carbon. Finally, impact damage resistance has been found to depend on both the structural configuration and local design detail. Examples of the former have been noted in differing impact damage characteristics for composite structures stiffened by sandwich core materials and discrete elements. Laminate stacking sequence, local thickness buildups at bonded elements, adhesive layer inserts, proximity of discrete structural elements, and redundant mechanical fasteners are some typical examples of structural details crucial to impact damage resistance.

7.5.1.1 Summary of results from previous impact studies

The majority of composite damage studies performed to date have pursued the fundamentals of composite material response. Reviews of studies addressing the fundamentals of composite material response, as related to damage resistance, can be found in References 7.5.1.1(a) through 7.5.1.1(d).

Many impact studies performed in the past concentrated on relatively thick wing-type structures (References 7.5.1.1(e) through 7.5.1.1(i)). Impact testing was performed on both coupons and subcomponents using simulated impact threats, usually with a hemispherical impactor tip (typically referred to as a “tup”). These tests correlated well with industry studies involving various shop tools dropped onto test articles. Documented studies for tests performed at the structural level generally evaluated damage by visibility and residual strength, although planar ultrasonic C-scans have also been used in some cases. More detailed evaluations of impact usually occurred only at the coupon level. For example, results shown in Figure 7.5.1.3 are characteristic of those obtained with standard test coupons developed by NASA (impact specimen size = 7 in. X 12 in. (180 mm x 300 mm) and machined CAI specimen size = 5 in. X 10 in. (130 mm x 250 mm)) and Boeing (impact and CAI specimen size = 4 in. X 6 in. (100 mm x 150 mm)).

The damage states and resulting residual strengths observed in these early tests were found to be a strong function of impact energy and relatively independent of the impactor shape. Transverse cracks and delaminations were found to be the primary failure mechanism for the “brittle” epoxy laminates under study at that time, with the areal extent of damage being a strong function of the impact energy. Local fiber failures were suppressed, until penetration was achieved, by the formation of large delaminations which reduced contact forces by locally softening the laminate. Matrix damage was primarily responsible for reduced CAI strength, while fiber failure, which would be influenced by impactor geometry, was not found to be a strong contributor to the observed compression strength degradation. These findings, along with ease of analytical modeling, led to the use of spherical shaped impactors with diameters between 0.5 in. (13 mm) and 1.0 in. (25 mm) for the majority of impact studies on fibrous composites to date.

Towards the end of the 1980s, an extensive evaluation of impact in wing-gage structure was performed by Northrop and Boeing under contract with the U.S. Air Force (Reference 7.5.1.1(j)). The focus of this study was on the impact damage resistance of material, laminate, and structural geometry. A building-block test approach was used, including coupons, 3- and 5-stringer stiffened panels, and wing boxes (multi-spar and multi-rib). Those variables that were found to have a significant effect on the test results included laminate thickness, laminate lay-up, material toughness (as quantified by interlaminar G_{Ic}), stiffener type, impact location, and panel boundary conditions. Tests and analyses were documented on the impact structural response, characteristics of the resulting damage, and CAI strength. Figure 7.5.1.1 shows typical results from this extensive study. Note the effects of laminate thickness and impact energy on the resulting damage, as measured by visible dent depth. As shown in Figure 7.5.1.1, an energy cut-off, rather than visibility limits, has been used to bound Ultimate Load design requirements for thick structure. Also worthy of note for stiffened structure is the importance of local fiber failure in the flange and webs of stiffeners subjected to impact. This effect is not shown in Figure 7.5.1.1 although the high levels of impact energy required to create such damage may also lead to an energy cut-off for ultimate design considerations. Realistic impact threat levels should also be considered when establishing Limit Load requirements; however, an energy cut-off is not appropriate since aircraft safety is dependent on detecting any damage occurring in a multitude of real-world scenarios.

More recently, the impact damage resistance of relatively thin-gage stiffened fuselage and sandwich structures were studied by Boeing under contract with NASA (References 7.5.1.1(l) through 7.5.1.1(n)). Several material, laminate and structural variables were evaluated in a designed experiment which also included a wide range of extrinsic variables related to the impact event. The extent and type of impact damage to the matrix and fibers was measured using several different destructive and nondestructive methods. Some of the thicker-gage fuselage panels included in this study were on the order of outboard wing or empennage panels (skin gages ≈ 0.18 in. (4.6 mm)).

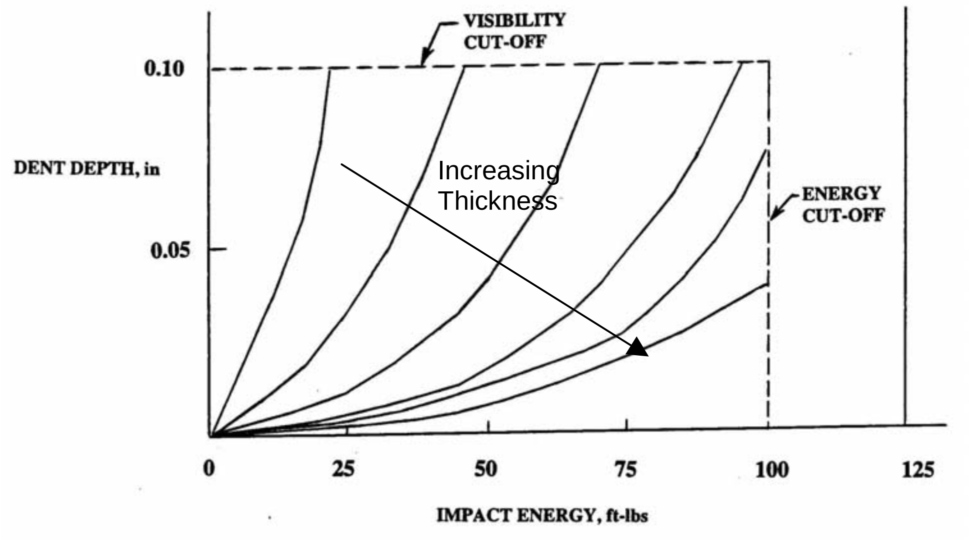

FIGURE 7.5.1.1 *Test results for the effects of laminate thickness on dent depth for a range of impact energies (Reference 7.5.1.1(k)).*

As was the case with previous studies, impact energy and laminate thickness were found to have a strong effect on the resulting damage in fuselage gage structure (Reference 7.5.1.1(l)). Of the extrinsic variables found to be important, impactor diameter and shape had the most important implications to damage resistance, inspectability and post-impact residual strength. At high impact energies, impactors with relatively large diameter created more extensive damage and less surface indication (i.e., dent depth) than smaller impactors which typically penetrated the laminate. Unlike the relatively thick laminates (0.2 to 0.5 in. (5.1 mm to 13 mm)) considered for wing structures, matrix toughness had little effect on the damage area of minimum gage fuselage structure (i.e., 0.09 in. (2.3 mm) thick). Other design variables affecting impact damage resistance included stiffener geometry, addition of adhesive layers at skin/stiffener interfaces, carbon fiber type, and matrix toughness for the thicker laminates. Several interactions between these variables were found to be as strong as the individual variable main effects. Test correlation with analytical simulations showed that the fixture used to support the stiffened panel had a significant effect on the structure's dynamic response during impact. This shows the need to test panels with boundary conditions as close to those of the configured structure as feasible or use static indentation tests.

7.5.1.2 Through-penetration impacts

Few investigations have addressed resistance to high-energy impact events that penetrate the entire laminate. Reference 7.5.1.2 performed limited through-penetration impacts of all-CFRP and GFRP/CFRP hybrid laminates using a blade-like impactor, shown in Figure 7.5.1.2(a). Impact energies were selected to be at least sufficient to result in penetration. Comparison of the instrumented force-displacement results for through-penetration impacts revealed significant differences between material types.

Curves for several CFRP materials are shown in Figure 7.5.1.2(b). The AS4/938 tow has a higher load than the AS4/938 tape, resulting in an approximately 60% higher event energy. This difference may be attributed to the larger damage formed adjacent to the penetration in the tow-placed laminate, as observed in ultrasonic scans.

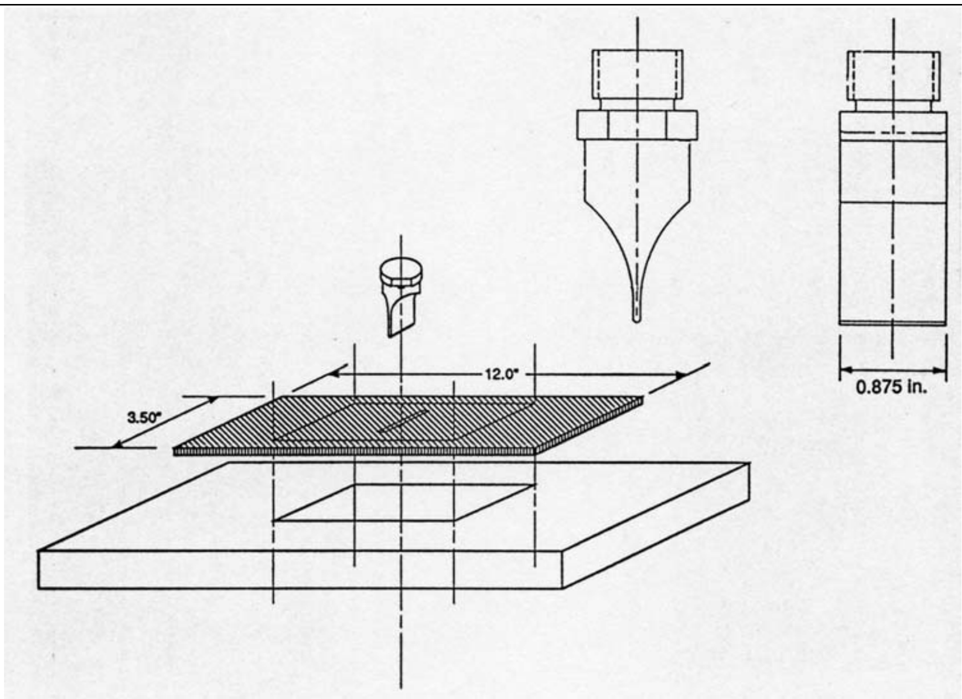

FIGURE 7.5.1.2(a) *Penetrating impact support fixture.*

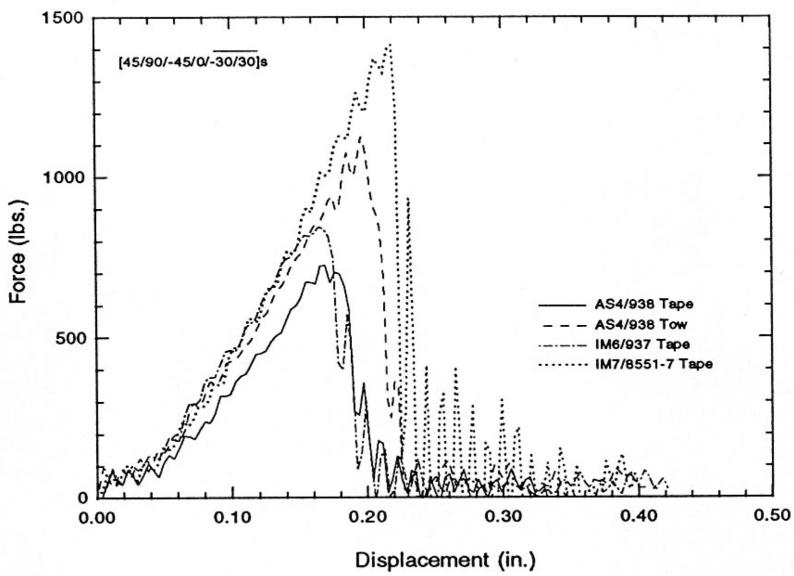

FIGURE 7.5.1.2(b) *Instrumented impact results for through-penetration of AS4/938 tow and tape, IM6/3501-6, and IM7/8551-7.*

The IM6/937A tape results showed a peak load and total event energy that were 20-25% above that of the AS4/938 tape. The amount of damage area created was similar for the two materials, as might be expected for equivalent resin systems. The energy differences, therefore, might be due to the slightly higher laminate bending stiffness and fiber strengths, both a result of the higher stiffness of the IM6 fiber.

Penetration of IM7/8551-7 tape resulted in a 40% higher maximum load and a 65% higher total event energy than IM6/937A tape. Ultrasonic scans indicated that damage created adjacent to the penetration was significantly smaller in IM7/8551-7 than in any of the other materials. Possible causes for the energy difference include: (a) the slightly higher bending stiffness and fiber strength with the IM7 fiber, and (b) the increased energy absorbed per unit damage due to the higher toughness of 8551-7. Neither of these, though, appear likely to account for a majority of the energy increase. Extension of the crack beyond the net impactor length, however, would require additional fiber failure and associated energy. This scenario is plausible since 8551-7 resin is resistant to matrix damage that would reduce the stress concentration near the corners of the penetrator. Note that the ultrasonic methods used for the current study are unable to distinguish fiber failure zones.

Force-displacement curves are presented in Figure 7.5.1.2(c) for tow-placed laminates of 100% AS4/938, 100% S2/938, and an intraply hybrid consisting of 50% AS4 / 50% S2 / 938 with a 12 tow repeat unit width. As expected from the fiber stiffness difference, the slope of the 100% S2/938 curve is less than that of the 100% AS4/938, and that of the intraply hybrid falls midway between. The total event energy of the S2/938 was over twice as large as that of the AS4/938, and the intraply hybrid energy was midway between. Another conspicuous feature of the intraply hybrid curve is the relative ductility of the failure, as compared to either the AS4/938 or S2/938.

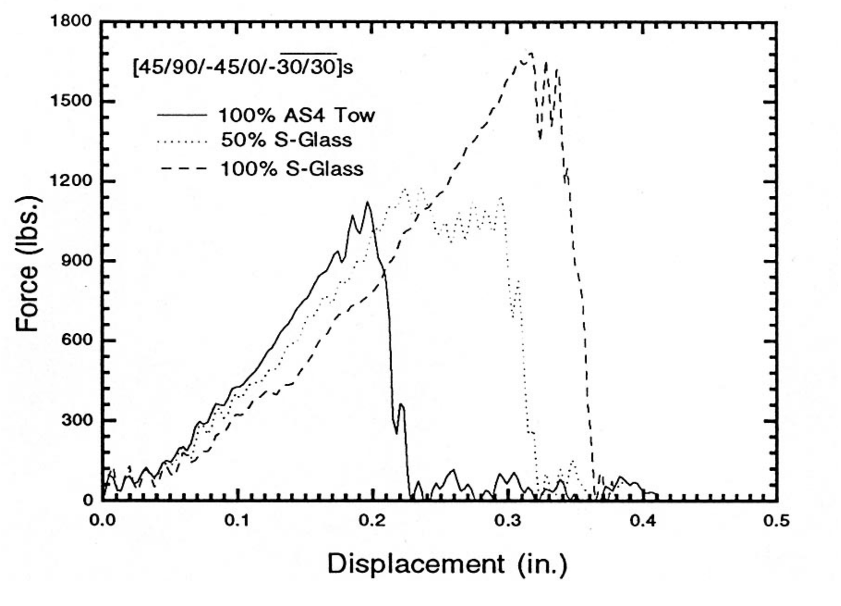

FIGURE 7.5.1.2(c) *Instrumented impact results for through-penetration of tow-placed laminates consisting of various percentages of AS4 and S2.*

Lay-up and/or thickness effects were also observed to significantly affect the resulting damage state. Figure 7.5.1.2(d) compares the delamination extent for the 10-ply laminate with that of the 16-ply laminate. The relatively high bending stiffness of the 16-ply laminate may result in the formation of larger matrix splits and delaminations near the crack tip.

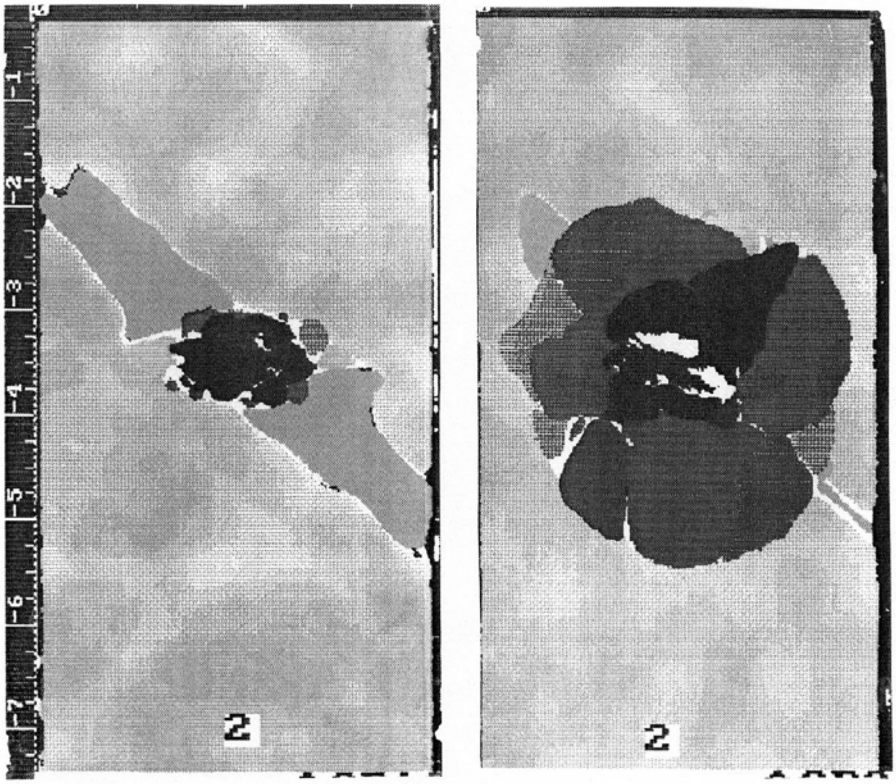

FIGURE 7.5.1.2(d) *Ultrasonic C-scans of AS4/938 tape 10-ply and 16-ply through-penetration specimens.*

7.5.1.3 Material type and form effects

The ability of composite structures to resist or tolerate damage is strongly dependent on the constituent resin and fiber material properties and the material form. The properties of the resin matrix are most significant and include its ability to elongate and to deform plastically. The area under a resin's stress-strain curve indicates the material's energy absorption capability. Damage resistance or tolerance is also related to the material's interlaminar fracture toughness, G, as indicated by energy release rate properties. Depending on the application G_I, G_{II}, or G_{III} may dominate the total G calculation. These parameters represent the ability of the resin to resist delamination, and hence damage, in the three modes of fracture. The beneficial influence of resin toughness on impact damage resistance has been demonstrated by tests on newer toughened thermoset laminates and with the tougher thermoplastic material systems.

Investigations have been conducted on the effect of fiber properties on impact resistance. In general, laminates made with fabric reinforcement have better resistance to damage than laminates with unidirectional tape construction. Differences among the carbon fiber tape laminates, however, are small. Some studies have been made of composites with hybrid fiber construction, that is, composites in which two or more types of fibers are mixed in the lay-up. For example, a percentage of the carbon fibers are replaced with fibers with higher elongation capability, such as fiberglass or aramid. Results (References 7.5.1.3(a) through 7.5.1.3(d)) in both cases have shown improvement in damage resistance and residual compression strength after impact. Basic undamaged properties, however, were usually reduced.

Figure 7.5.1.3 shows typical standard flat specimen test results which distinguish the impact damage resistance of a toughened composite (IM7/8551-7) and an untoughened material system (AS4/3501-6).

The toughened material resists delamination growth under transverse loading, resulting in smaller damage diameter per given level of impact force. Studies have shown that mode II interlaminar fracture toughness (G_{IIc}) is the critical property for resisting delamination growth under transverse load conditions (References 7.5.1.3(e) and (f)). The G_{IIC} of a laminate can be enhanced by toughening the matrix. The value of G_{IIC} has also been found to be a strong function of the thickness of toughened resin interlayers existing between plies in the laminate. Composite laminates with this microstructure have improved delamination resistance. However, systems that use toughened resins throughout the laminate may have a significant loss of hot/wet compressive strength, reduced large notched tensile strength, and other drawbacks.

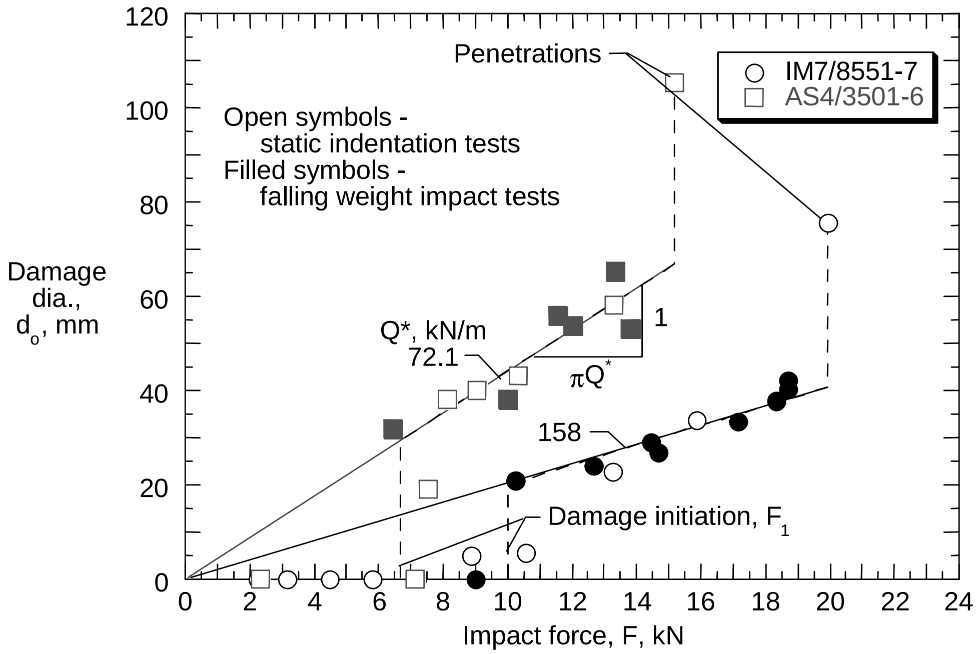

FIGURE 7.5.1.3 *Impact test results for untoughened and toughened, interlayered carbon/epoxy laminate made from prepreg tape (Reference 7.5.1.3(i)).*

It should be noted that the test results in Figure 7.5.1.3 are a strong function of the laminate thickness, stacking sequence, and specimen geometry. All of these structural variables were held constant for both materials in the figure. Although the relationship between damage size and impact force may differ somewhat, test trends shown in Figure 7.5.1.3 are similar to those obtained from impacts occurring midbay (centered between longitudinal and transverse stiffening elements) in stiffened skin panels which have similar laminate thickness. Figure 7.5.1.3 also shows static indentation tests produced similar damage sizes to those obtained in falling-weight impact events.

Some textile material forms offset the effects of matrix damage through delamination growth resistance and/or other mechanisms (Reference 7.5.1.3(g)). Stitching, which can be achieved by a number of different fabrication processes, does not completely suppress the formation and growth of matrix damage when a structure is subjected to impact. However, stitching improves sublaminate buckling resistance; and hence, helps to minimize reductions in compression-after-impact (CAI) strength related to matrix damage (Reference 7.5.1.3(h)).

7.5.1.4 Depth of damage

Impacts to thin composites cause damage throughout the thickness even for relatively small impact forces and energies. In the contact region, the damage consists of fiber and matrix damage; beyond the contact region, the damage consists only of matrix damage. The diameter of the contact region is only a small fraction of the impactor radius and of the same order of magnitude as the thickness. For example, the contact diameters for the impact tests in Figure 7.5.1.3 are only a few millimeters compared to damage diameters from 0.4 to 2.8 in. (10 to 70 mm). (The impacts were conducted using 0.5 in. (12.7 mm) diameter tups.) Because the damage extends far beyond the contact region, the shape of the impactor has little effect on the extent of the damage. Impacts to thick composites, on the other hand, will not cause damage throughout the thickness except for very large impact forces and energies.

Damage depth measured in radiographs is plotted against impact force in Figure 7.5.1.4 for a 1.4 in. (36-mm) thick, AS4/epoxy composite (Reference 7.5.1.4). (The radiographs were made from the sides of the specimens, which were only 1.5 in. (38 mm) wide.) This material represented the Filament Wound Case (FWC) made for the solid motors of the Space Shuttle. The FWC was composed of 0^{o} (hoop) and $\pm$56.5° (helical) layers. The impacts were made with the following indenters: a 0.25 in. (6.35 mm) diameter rod, a 90° corner, and 0.5 and 1 in. (12.7 and 25.4 mm) diameter hemispheres. The mass of the impactor was 11 lb (5.0 kg) and each symbol is the mean value for several specimens. The diameters of the contact region were much smaller than the thickness. The rod made the deepest damage, followed by the corner, the small hemisphere, and large hemisphere. The rod acted like a punch and, after a critical force was exceeded, plunged through the composite with only a small increase in force. The data for the corner and hemispheres had similar slopes, and impact force to cause damage of a given depth was greater for the more blunt indenter. The filled and open symbols indicate visible and non-visible damage, respectively, as viewed on the impacted surface. All the damage for the rod, corner, and most of that for the small hemisphere was visible. But damage as deep as 0.2 in. (4 mm) was not visible for the 1.0 in. (25.4 mm) hemisphere. Thus, impactor shape has a significant effect on the depth and visibility of damage for thick composites. Also, notice that the impact forces in Figure 7.5.1.4 are much greater than those in Figure 7.5.1.3.

7.5.1.5 Laminate thickness effects

Low velocity impact damage is potentially more of a problem for thin laminates than for thick laminates, see Figures 7.5.1.5(a) and (b). Figure 7.5.1.5(a) contains a graph of kinetic energy versus thickness for two different dent depths for the tests. For the range of thicknesses shown, kinetic energy required to produce a given level of damage (as characterized by indentation depth) increases with increasing thickness to approximately the 3/2 power. Figure 7.5.1.5(b) contains a graph of damage diameter versus force for static indentation tests of the same composites in Figure 7.8.1.2.7(a). The force to initiate damage also increases with increasing thickness to approximately the 3/2 power. The 16-ply composite was penetrated with a force of 700 lb_f. Composites of 24, 32, and 48 piles were not penetrated with even larger forces. Thus, the force to penetrate likewise increases with increasing thickness.

For very thick composites, damage does not develop throughout the thickness, as shown in Figure 7.5.1.4, and the damaged layers may fail under in-plane tension loading and disbond from the remaining layers. Residual tension strengths for the 1.4 in. (36 mm) thick specimens in Figure 7.5.1.4 are plotted against damage depth in Figure 7.5.1.5(c). The strengths were normalized by the undamaged strength, and each symbol is the mean value for several specimens. The filled symbols indicate the stress when the damaged layers failed, and the open symbols indicate the stress when the remaining layers failed (maximum load). (All stresses were calculated using the total area.) The damaged layers disbonded from the remaining layers when they failed. For very shallow damage, the initial failure was catastrophic; but for deeper damage additional load was required to fail the remaining layers. The decrease in strength with increasing damage depth was greater for the damaged layers than the remaining layers. The damaged layers were shown to fail according to a surface crack analysis (Reference 7.5.1.4), that is strength varies inversely with square root of damage depth. The remaining layers were shown to fail approximately as an unnotched laminate.

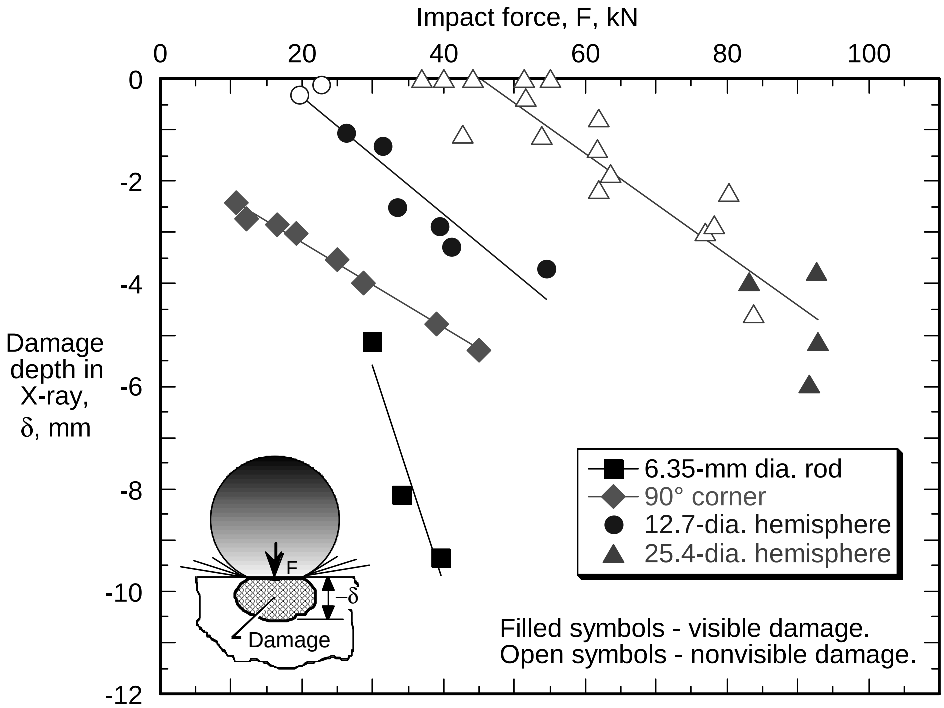

FIGURE 7.5.1.4 *Impact damage for 1.4 in. (36 mm) thick AS4/epoxy filament wound case (FWC) with impactors of various shapes (Reference 7.5.1.4).*

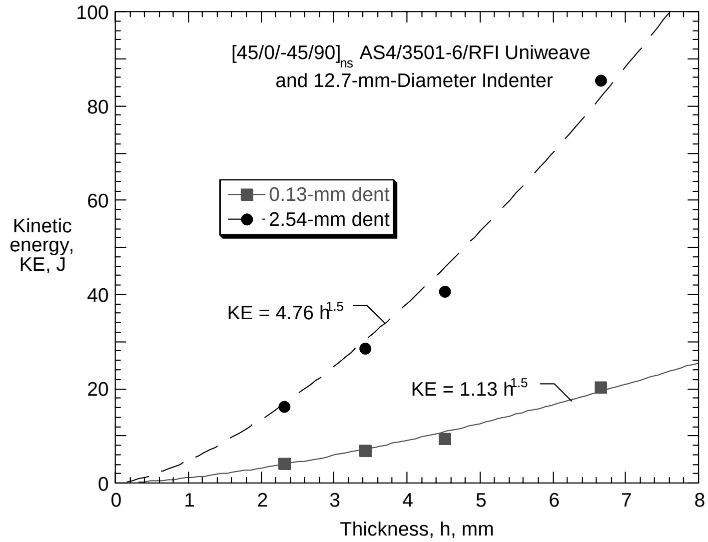

FIGURE 7.5.1.5(a) *Impact response for a given dent depth.*

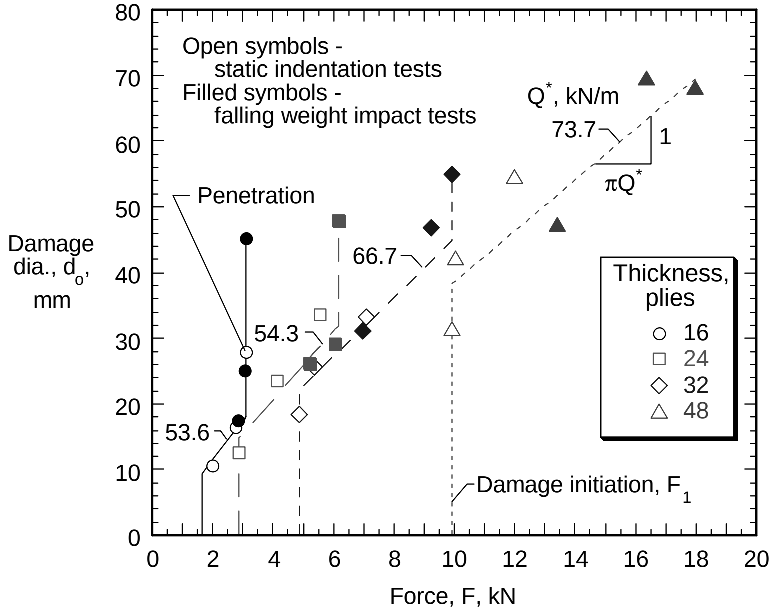

FIGURE 7.5.1.5(b) *Damage resistance of [45/0/-45/90]$_{ns}$ AS4/3501-6/RFI uniweave using 0.5 in. (12.7 mm) diameter indenter.*

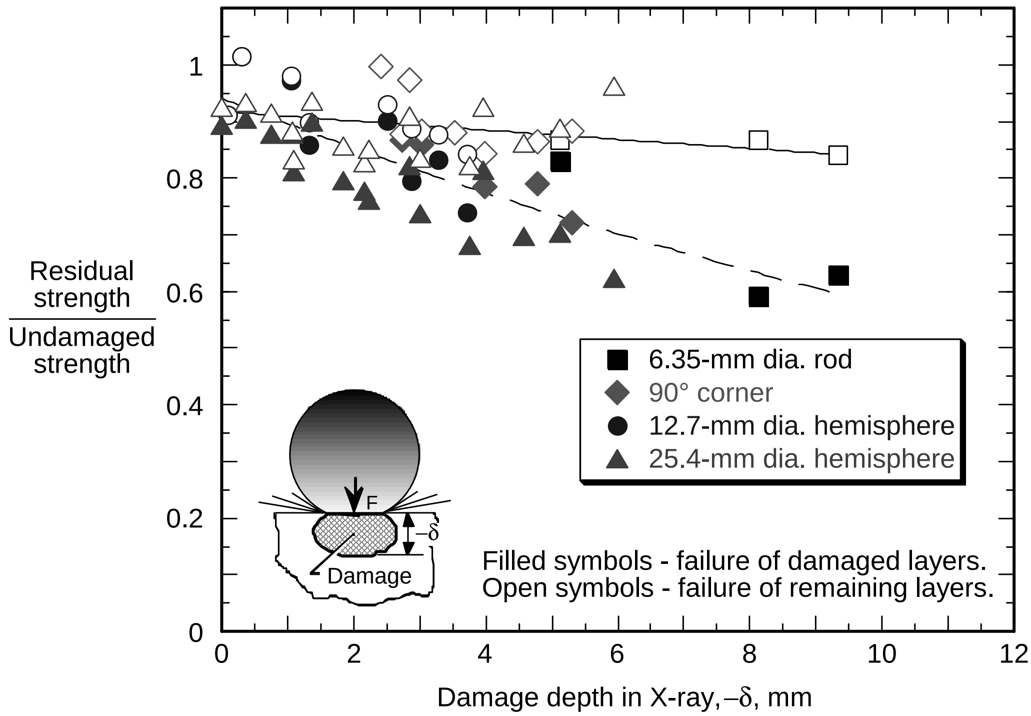

FIGURE 7.5.1.5(c) *Residual tensile strengths for 1.4 in. (36 mm) thick AS4/epoxy filament wound case (FWC) with impactors of various shapes.*

7.5.1.6 Structural size effects

Impact response for coupons and structures can be quite different. Consider a plate with transverse force and flexural stiffness k and natural frequency ω impacted by a mass m_i. When the ratio of $\omega^2/(k/m_i)$ is greater than 100, the impact response is essentially quasi-static (Reference 7.5.1.3(i)). That is, the force displacement relationships for an impact and for quasi-static loading are the same. Moreover, from energy balance considerations, the impact force F_{max} is given by:

$$\frac{1}{2} m_i v_i^2 = \frac{1}{2} \frac{F^2 \max}{k} + \frac{2}{5} \frac{F_{max}^{5/3}}{n^{2/3}} \qquad 7.5.1.6(a)$$

where

$$n = \frac{4}{3} E_2 \sqrt{R_i} \qquad 7.5.1.6(b)$$

V_i is the velocity of the impactor, R_i is the radius of the spherical impactor, and E_2 is the modulus in the thickness direction. The second term on the right hand side of equation 7.5.1.6(a) accounts for local indentation. Thus, when k is small compared to n, the impact force increases in proportion to the square root of the product of kinetic energy and flexural stiffness. Thus, impact force increases with decreasing size, increasing thickness, and the addition of stiffeners. Also, damage resistance increases with increasing thickness, and stiffeners can increase strength by arresting a fracture.

It should also be noted that when the ratio of $\omega^2/(k/m_i)$ is less than 100, the impact response is transient (Reference 7.5.1.3(i)). That is, the plate behaves as though it were smaller, resulting in larger impact forces than those given by Equation 7.5.1.6(a). On the other hand, the development of damage has the effect of reducing impact force. In Equation 7.5.1.6(a), both k and n decrease with increasing damage, thereby reducing $F_{max.}$ The maximum value of impact force is limited by the resistance of the plate to penetration. Thus, the effect of plate size can be counteracted by damage.

The effects of size are illustrated in Figures 7.5.1.6(a) through 7.5.1.6(c). Figure 7.5.1.6(a) contains a bar graph of minimum kinetic energy to reduce burst pressure for two filament-wound cylinders with the same membrane material and lay-up but with different sizes (Reference 7.5.1.6(a)) . The minimum kinetic energy to reduce burst pressure for the 18.0 in. (45.7 cm) diameter was almost ten times that for the 5.7 in. (14.6 cm) diameter.

Figures 7.5.1.6(b) and (c) contain graphs of impact force and resulting damage diameter, respectively, versus kinetic energy for .25 in. (6.3 mm) - thick, quasi-isotropic plates of various sizes (Reference 7.5.1.6(b)). For a given kinetic energy, the impact force and accompanying damage size decrease with increasing plate size - no damage at all was discernible in the 8.2 in.-square (53 cm-square) plates for energies less than 30 ft-lb (41 J). Thus, the energy threshold for causing damage increases with increasing size in a manner consistent with the energy threshold for burst strength in Figure 7.5.16.(a). It should be noted that damage reduces impact force by reducing the flexural stiffness, more so for a small plate than a large plate. Thus, the impact forces for the two smallest plates in Figure 7.5.1.6(b) were similar in magnitude due to damage.

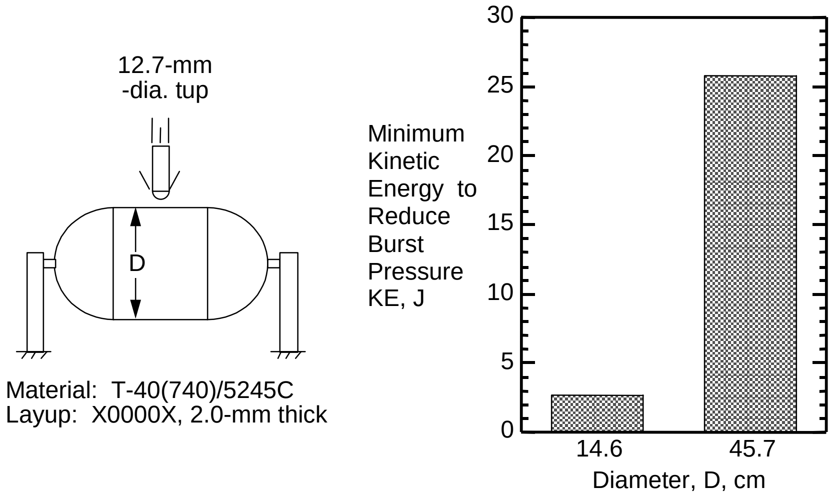

FIGURE 7.5.1.6(a) *Impact response of small and large pressure vessels (Reference 7.5.1.6(a)).*

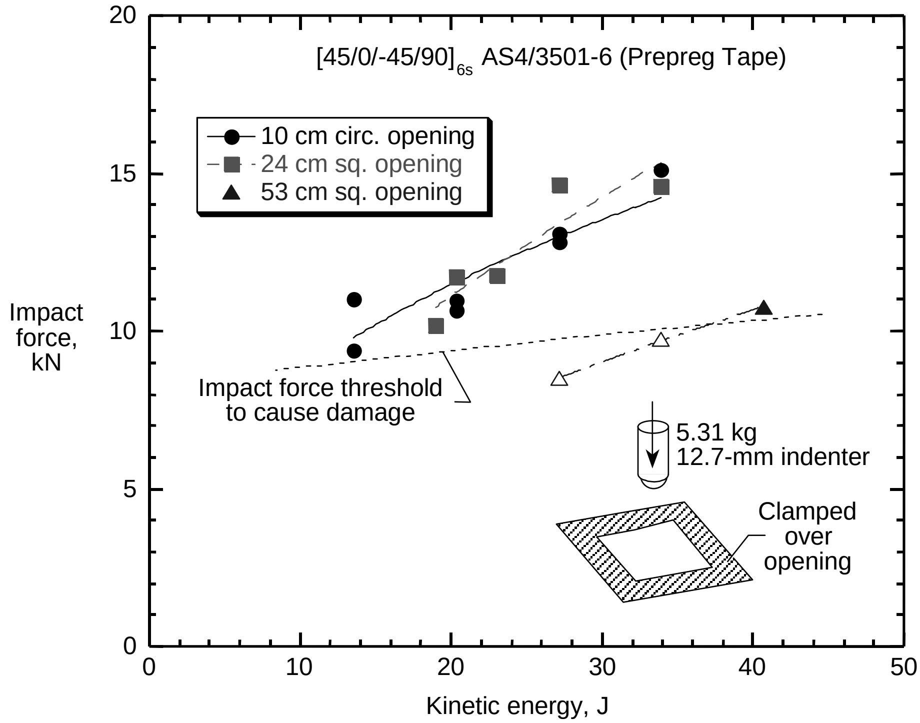

FIGURE 7.5.1.6(b) *Impact force for plates of various sizes (Reference 7.5.1.6(b)).*

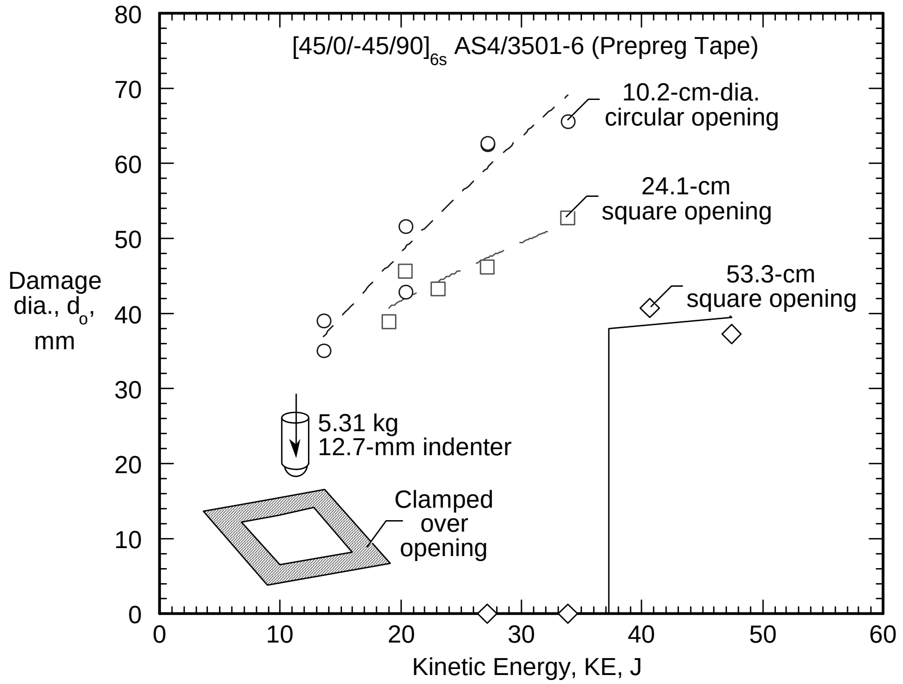

FIGURE 7.5.1.6(c) *Impact damage for small plates of various sizes (Reference 7.5.1.6(b)).*

7.5.1.7 Sandwich structure

The core and facesheet thickness in sandwich stiffened designs play an important role in impact damage resistance. Critical core variables include density, fiber type, matrix type, cell geometry, and fiber orientation. Most of the impact test and analysis evaluations performed to date were with sandwich panels having a facesheet thickness between 0.03 in. and 0.15 in (0.8 mm and 3.8 mm). The extent of damage in the core and outer impacted facesheet has been found to approach an asymptote. For example, the database collected by Boeing in the early 1990's under contract with NASA found this asymptote to be somewhat larger than the impactor diameter and dependent on the specific combination of composite core and laminate materials for panels with facesheets on the order of 0.08 in. (2.0 mm) thick (Reference 7.5.1.1(n)). Such inherent resistance to the development of large impact damage areas can have significant benefits in minimizing the effects on residual strength.

Thin-gauge honeycomb panels (facesheets less than 0.02 in. (0.5 mm) thick) have been found to damage at very low levels of impact and allow environmental degradation of the core (e.g., moisture ingression), leading to significant durability problems. Also, limited testing suggests that, for thick-facesheet sandwich panels (i.e., t > 0.20 in. (5.1 mm)), that a damage diameter much larger than the impactor diameter is possible with less surface visibility; however, residual strength tests suggest that this damage was asymmetric because the CAI strength was large and not commensurate with extensive through-thickness damage of the size noted.

Some sandwich core materials have failure mechanisms which are not limited to the local area of the impact event. Instead, core damage propagates, allowing the composite facesheet to absorb energy in deflection without failure. Damage created for such combinations of material become a threat to sandwich panel integrity when significant compression or shear loads exist because the failed core does not stabilize the facesheet over a large area. In addition, an undamaged facesheet springs back after impact, reducing visible indications of massive core failure. This phenomenon was observed in previous NASA-funded contract work performed at Boeing in the mid-1980s (Reference 7.5.1.7). The honeycomb core material used in these studies (a bias weave glass fabric impregnated with a heat resistant resin) propagated a failure that was much larger than the local “core crush region,” which typically occurs below the impactor. Figure 7.5.1.7 shows measurements of the extent of this damage. The compressive residual strength with such damage was found to be very low. As a result, the particular honeycomb core material used in these studies would not be a good candidate for primary structure applications.

For sandwich materials with thin faces, impact can result in visible core damage which has been shown to reduce the compressive and shear strengths. Impact damage which causes a break in the facesheet of the sandwich (as well as porosity, a manufacturing defect) also presents a long term durability problem in that it can allow water intrusion into the core.

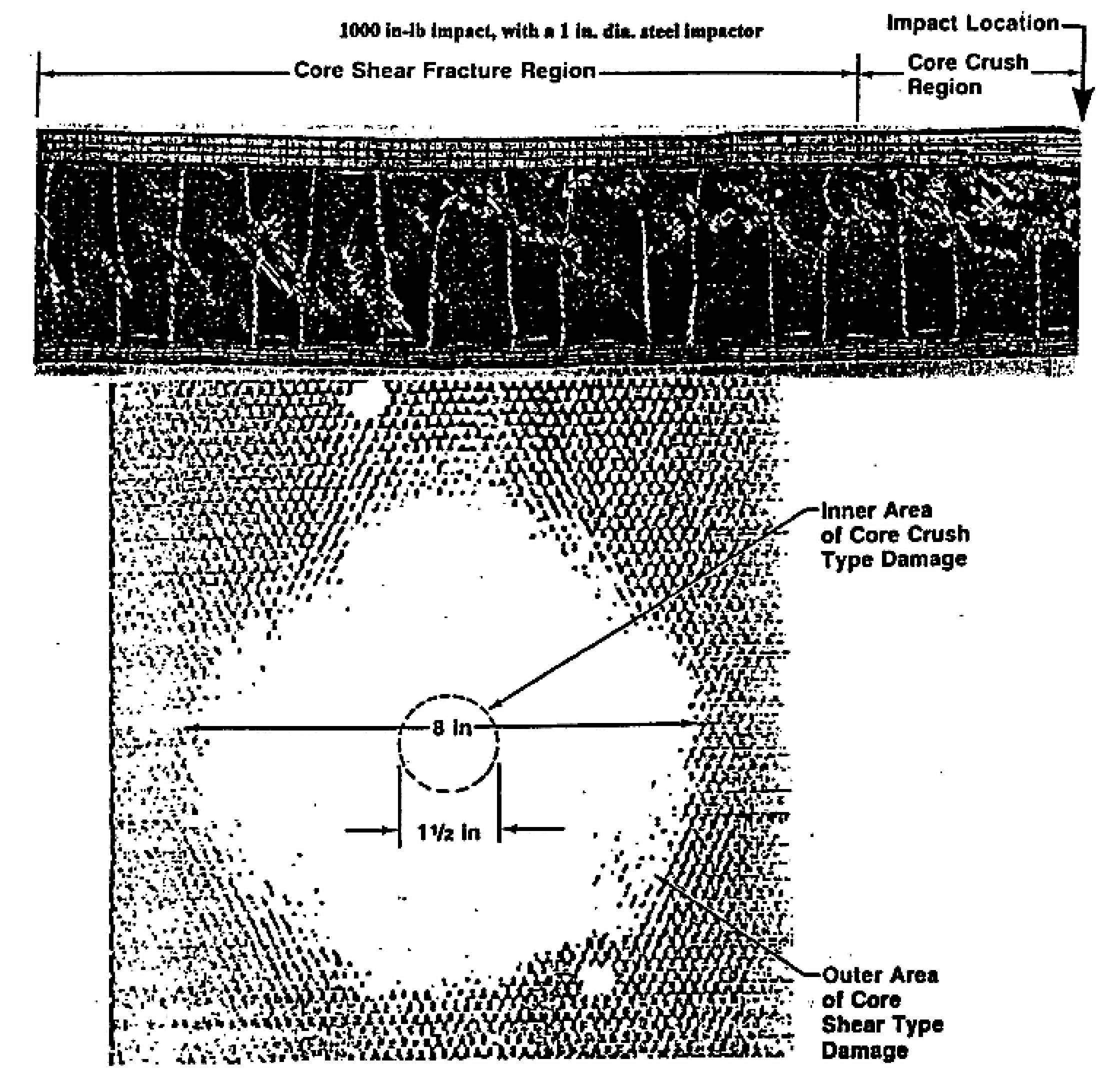

FIGURE 7.5.1.7 *Micrograph and through-transmission ultrasound data for an undesirable core impact failure mode (Reference 7.5.1.7).*

7.5.2 Design issues and guidelines

In normal operation, aircraft are subjected to potential damage from a variety of sources, including maintenance personnel and tools, runway debris, service equipment, hail, and lightning. Even during initial manufacturing and assembly, parts are subject to dropped tools, bumps during transportation to assembly locations, etc. The aircraft structure must be able to endure a reasonable level of such incidents without requiring costly rework or downtime. Providing this necessary damage resistance is an important design function. Unfortunately for the designer, providing adequate damage resistance may not always be the most popular task. Resistance to damage requires robustness, and commonly necessitates the addition of extra material above that necessary to carry the structural loads. It also influences the choice of materials, lay-up, design details, etc. As a result, there are many pressures to compromise because of competing goals for minimum weight and cost.

In order to establish minimum levels of damage resistance, various requirements for aircraft structure have been identified in the past. For example, the Air Force requirements are defined in their General Specification for Aircraft Structures, AFGS-87221A (Reference 7.5.2). In general, the Specification defines the type and level of low energy impact that must be sustained without structural impairment, moisture ingestion or a requirement for repair. It provides provision for such incidents as dropped tools, hail, and impact from runway debris. The aircraft may be zoned depending on whether the region has high or low susceptibility to damage. In some cases, commercial airline operators have requested specific levels of damage resistance, or particular material selections for components in high impact threat areas.

7.5.2.1 Use of impact surveys for establishing critical damages

Impact surveys with configured structure are required to establish critical damage scenarios for particular design and inspection procedures suitable for field maintenance. These surveys can help establish design features crucial to structural integrity. A range of impact scenarios and structural locations are included in an impact survey. Critical damage can be identified based on post-impact evaluations of: (1) damage visibility, (2) extent of delamination and fiber failure, (3) reduced local stiffness (i.e., loss of load path) and (4) residual strength. Due to the large number of material, structural, and extrinsic variables affecting damage, impact surveys have been found to provide the most meaningful results when applied to specific built-up structure. As a result, surveys using large structural configurations with representative design detail and boundary conditions are recommended. Such studies are practical because numerous impacts can be applied to a single test article. Smaller "building block" panels (e.g., 3-and 5-stringer panels) with representative impact damage are also generally required to quantify residual strength.

7.5.2.2 Structural arrangement and design details

An impact survey consists of a series of impacts applied at varying impact energies and locations to a structure. The goal of an impact survey is usually to define the relationships between impact energy, damage detectability and damage characteristics. The results of the survey are often used to establish the impact variables (energy, location, etc.) to be applied to structural test articles used to determine post-impact residual strength.

Impact at design details. The damage resistance of composite structure is strongly dependent on design detail (e.g., material form, constituents, lay-up, thicknesses, and structural configuration). It is crucial to get early design development data from structural element and subcomponent tests in order to meet goals for damage resistance. For example, impact damage in bonded or bolted structure accumulates differently than it does in flat plates. Design development data should consider a range of damage scenarios, from those known to cause durability or maintenance problems in service to those having a significant effect on residual strength requirements for ultimate and Limit Loads.

In defining the requirements for damage resistance, the type of structure is pertinent. For example, the level of impact energy which typically must be sustained by honeycomb sandwich control surfaces without requiring repair or allowing moisture ingestion is quite low, e.g., 4 to 6 in-lb (0.5 to 0.7 J). One reason these parts have been kept very light is to minimize weight and mass balancing, consequently, damage resistance is minimal. Repair is facilitated somewhat because these parts can usually be readily replaced with spares while repairs are being accomplished in the shop. Because of their light construction, however, they must be handled carefully to prevent further damage during processing or transport. By contrast, the damage resistance requirement for primary laminate structure, which is not normally readily removable from the aircraft, is typically much higher, e.g., 48 in-lb (5.4 J).

Damage-susceptible regions and details. There are certain damage-susceptible regions of the airplane that require special attention. Examples of these are the lower fuselage and adjacent fairings, lower surfaces of the inboard flaps and areas around doors. These need to be reinforced with heavier structure and perhaps glass fiber reinforcement, instead of carbon. In addition to the above, structure in the wheel well area needs special attention because of damage susceptibility from tire disintegration. Similarly, structure in the vicinity of the thrust reversers is damage prone due to ice or other debris thrown up from the runway.

Minimum weight structure, such as that used for fairings, can cause excess maintenance problems if designed too light. Sandwich structure with low density honeycomb core is an example. Also, face sheets must have a minimum thickness to prevent moisture entrance to the core. The design should not rely on the paint to provide the moisture barrier. Experience has shown that the paint often erodes or is abraded and then moisture enters.

Honeycomb sandwich areas with thin skins adjacent to supporting fittings are particularly vulnerable to damage during component installation and removal. Consequently, solid laminate construction is commonly used within a reasonable working distance of fittings.

Trailing edges of control panels are highly vulnerable to damage. The aft 4 inches (102 mm) are especially subject to ground collision and handling, as well as to lightning strike. Repairs in this region can be difficult because both the skins and the trailing edge reinforcement may be involved. A desirable approach for the design is to provide a load carrying member to react loads forward of the trailing edge, and material for the trailing edge, itself, that will be easily repairable and whose damage will not compromise the structural integrity of the component. Close out details should avoid the use of potting compounds due to the tendency to crack and cause sealing problems.

7.5.2.3 Ground hail

It may also be desirable to design composite aircraft structure to be resistant to typical hail strike energies to minimize the amount of repair required after a hailstorm. Such damage typically only occurs when the aircraft is on the ground, except for leading edges, which can experience in-flight hail damage.

7.5.2.4 Lightning

High-energy lightning strikes can cause substantial damage to composite surface structure. For civil aircraft and rotorcraft, the FAA regulations for lightning protection are FAR 25.581, 23.867, 27.601, and 29.610. Fuel system lightning protection requirements are in 25.954 and 23.954. System lightning protection requirements are in 25.1316. Advisory circulars AC20-53 and AC20-136 provide means of compliance with the regulations. Military requirements are defined in Mil-STD-1795 - Lightning Protection of Aerospace Vehicles and Hardware, Mil-Std-1757 - Qualification Test Techniques for Lightning Protection and Mil-B-5087 - Bonding, Grounding and Lightning Protection for Aerospace Systems.

There are zones on the airplane with high probability of lightning strike occurrence. These zones are called lightning strike zones. Protection of composite structure by conductive materials is required on lightning strike zones and beyond them to enable conductivity of induced currents away from attachment zones. An all-composite wing may have to be completely covered by a conductive layer, even if the attachment zone is located near the wing tip.

At fasteners and connections, electrical resistance to current flow generated by lightning produces heat that causes burning and delaminations. Minor lightning attachment also can cause significant damage, particularly to the tips and trailing edges. The following are guidelines to reduce the repair requirement:

- Provide easily replaceable conductive material with adequate conductive properties.
- Provide protection at tips and along trailing edge spans.
- Make all conductive path attachments easily accessible.

7.5.2.5 Handling and step loads

In addition to impact induced loads, there also needs to be requirements of resistance to damage from normal handling and step loads that might be encountered in manufacturing and operational environments. The following are suggested considerations:

Handling loads:
Difficult access - interpreted as finger tips only.
Overhead easy access - the ability to grip and hang by one hand.

Step loads:
Difficult access - interpreted as allowing, with difficulty, a foothold on a structure.
Easy access from above - interpreted as allowing a 2g step or “hop” onto the structure.

Note that contact areas, locations, and weights associated with each of these conditions must be defined.

7.5.2.6 Exposed edges

Laminate edges should not be positioned so they are directly exposed to the air stream since they are then subject to delamination. Options include:

1. Provide non-erosive edge protection such as a co-cured metal edge member.
2. Provide an easily replaceable sacrificial material to wrap the edges.
3. Locate the forward edge below the level of the aft edge of the next panel forward.

7.5.3 Test issues

This section is reserved for future use.

7.5.4 Analysis methods - description and assessment

This section is reserved for future use.

7.6 DURABILITY (DAMAGE INITIATION)

7.6.1 Introduction

In general, composite materials exhibit superior fatigue properties relative to that of metals. Their corrosion resistance also provides better durability for aircraft structures. Composite structural designers can usually utilize the high fatigue threshold that has been observed for commonly applied materials to simplify the fatigue design processes.

However, special considerations must be applied in fatigue/durability design of composites due to increased scatter in both strength and fatigue life due to the presence of multiple constituents. The fatigue life scatter in composites and metals are compared in Figure 7.6.1 (Reference 7.6.1) in terms of Weibull shape parameters (α). As it may be noted, a higher value of Weibull shape parameter signifies lower data variation. As shown in the figure, the modal Weibull shape parameter for commonly used composites is approximately 1.25, compared with approximately 7.0 for metals.

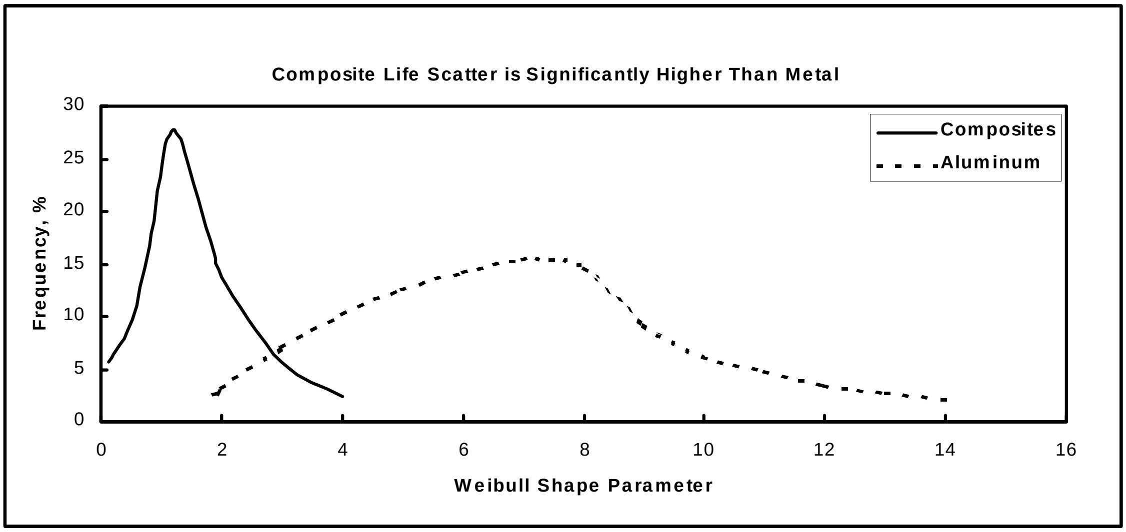

FIGURE 7.6.1 *Fatigue life scatter comparison, composites vs. metals.*

In addition to the higher scatter, two other factors significantly affect damage initiation and damage progression of composites: (1) multiple damage modes, and (2) no dominant strain energy release mechanisms.

Because composites consist of more than one constituent material, fatigue damage can initiate and propagate in any one material and/or along any material interface. Possible damage modes include fiber breakage, matrix cracking, fiber pull-out, and multi-mode delamination. Depending on the type of structural loading and the laminate construction, different modes of fatigue damage can occur at rather random locations in the composite during the process of damage initiation. Once a damage is initiated, its progression is driven by strain energy release to create new surfaces. However, because of the many modes of damage and because there is no dominate energy release mechanism, there is no clear path for damage progression. It has been observed that damage in composites often advances as a progressive damage zone that includes multiple damage types.

Unlike metallic structure, where single mode damage is propagated in a self-similar manner, the complex damage initiation and progression in composite makes analytical modeling extremely difficult. Therefore, durability of composite structures is mostly assured by performing adequate fatigue tests. Several fatigue test schemes have been proposed to overcome the scatter issue and to take advantage of the superior fatigue behavior of composites. These test schemes are discussed below.

7.6.2 Life factor approach

The life factor test approach has been successfully used for metal to assure structural durability. In this approach, the structure is tested for additional fatigue life to achieve the desired level of reliability. The test duration is determined based on the material fatigue life scatter, the number of test specimens, and the required reliability. For example, for B-basis reliability (i.e., 90% probability that the structural life exceeds the design lifetime, with 95% confidence), the required test life for typical composites and aluminum alloys are shown in Figure 7.6.2(a). As shown, the conventional two-lifetime test for aluminum structure is sufficient to assure B-basis life reliability. However, 14 lifetimes would be required for composites to assure equal reliability. The required test lives for the typical range of Weibull shape parameters for composites is tabulated in Figure 7.6.2(b) and plotted in Figure 7.6.2(c).

	n = 1	n = 5	n = 15
Composites Alpha = 1.25	**13.558**	**9.143**	**7.625**
Metals Alpha = 4.0	**2.093**	**1.851**	**1.749**

FIGURE 7.6.2(a) *Comparison of B-basis life factors, composites vs. metals.*

ALPHA	Mean/B-basis		
	n = 15	n = 5	n=1
0.50	383.569	603.823	1616.895
0.75	39.596	53.584	103.327
1.00	13.849	17.376	28.433
1.25	7.625	9.143	13.558
1.50	5.206	6.056	8.410
1.75	3.999	4.552	6.032
2.00	3.298	3.694	4.726
2.25	2.848	3.151	3.921
2.50	2.539	2.780	3.385
2.75	2.314	2.513	3.006
3.00	2.144	2.313	2.726
3.50	1.906	2.034	2.342
4.00	1.749	1.851	2.093
5.00	1.553	1.625	1.793

FIGURE 7.6.2(b) *Values of B-basis life factor as a function of Weibull shape parameter.*

The Weibull shape parameter for fatigue life distribution of commonly used composites has a modal value of 1.25, as observed in Reference 7.6.1. That is, the fatigue life variability has a coefficient of approximately 0.805. The required test life for a sample size of between 5 to 15 is from 9.2 to 7.6. For a single test article, such as a full-scale component test, the required life factor is 13.6. Such a test would cause significant cost and schedule impact in an engineering program. In addition, a prolonged fatigue test would cause fatigue failure in the metal parts of a mixed metal-composite structure, precluding the verification of the composite's reliability.

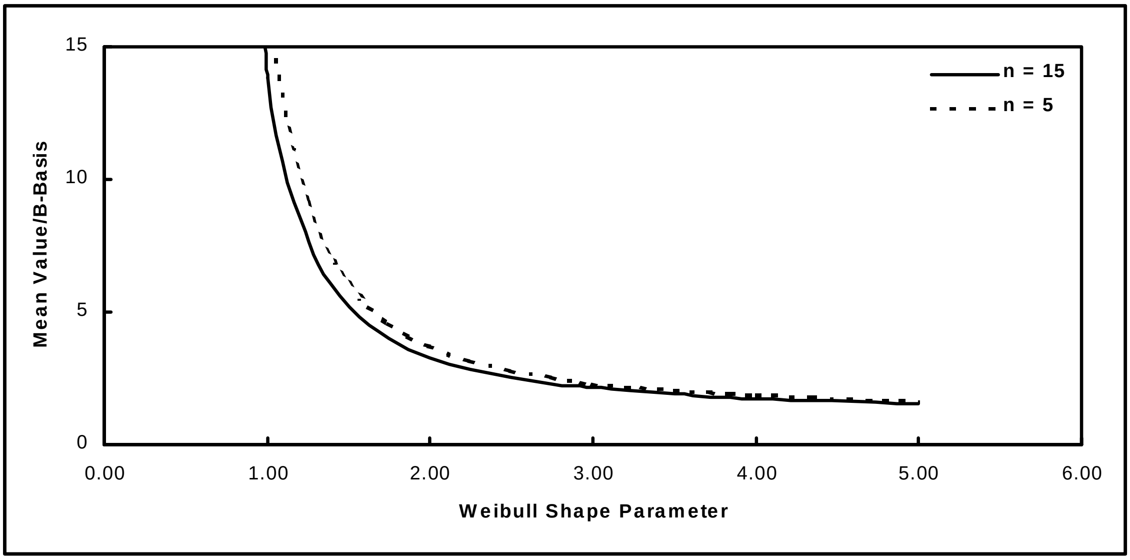

FIGURE 7.6.2(c) *Life factor for commonly used composites.*

7.6.3 Load enhancement factor approach

In order to relieve the cost and schedule impacts of composite structural fatigue tests, a combined load factor and life factor approach is developed in References 7.6.1 and 7.6.3. The objective of this approach is to increase the applied loads in the fatigue tests so that the same level of reliability can be achieved with a shorter-duration test. The required load enhancement and test life depend on the statistical distributions of both the baseline fatigue life and the residual strength.

Assuming that both the fatigue life and residual strength distributions can be described by two-parameter Weibull distribution, then the Load Enhancement Factor (LEF) in terms of test duration, N, can be written as (Reference 7.6.1):

$$\mathrm{LEF} = \frac{\left[\Gamma\left(1+\frac{1}{\alpha_L}\right)\right]^{\alpha_L/\alpha_R}}{\left[\dfrac{-\ln(l)\cdot N^{\alpha_L}}{\chi^2_\gamma(2n)/2n}\right]^{1/\alpha_R}} \qquad 7.6.3$$

where αR is the Weibull shape parameter of the residual strength distribution,

αL is the Weibull shape parameter of the fatigue life distribution,

l is the reliability, 0.9 for B-basis, 0.99 for A-basis,

γ is the level of confidence,

N is the test duration,

n is the sample size,

Γ is the Gamma function,

$\chi 2$ is the Chi-square value.

Equation (7.6.3) indicates that the LEF also depends on the sample size and the required reliability. For αL = 1.25 and αR = 20.0, the A-basis and B-basis LEF in terms of test duration, N, are plotted in Figure 7.6.3(a). Required LEF for one-lifetime and two-lifetime tests are shown in Figure 7.6.3(b). Depending upon the number of specimens tested, Figure 7.6.3(b) shows that for B-basis reliability, the required load enhancement is less than 18%.

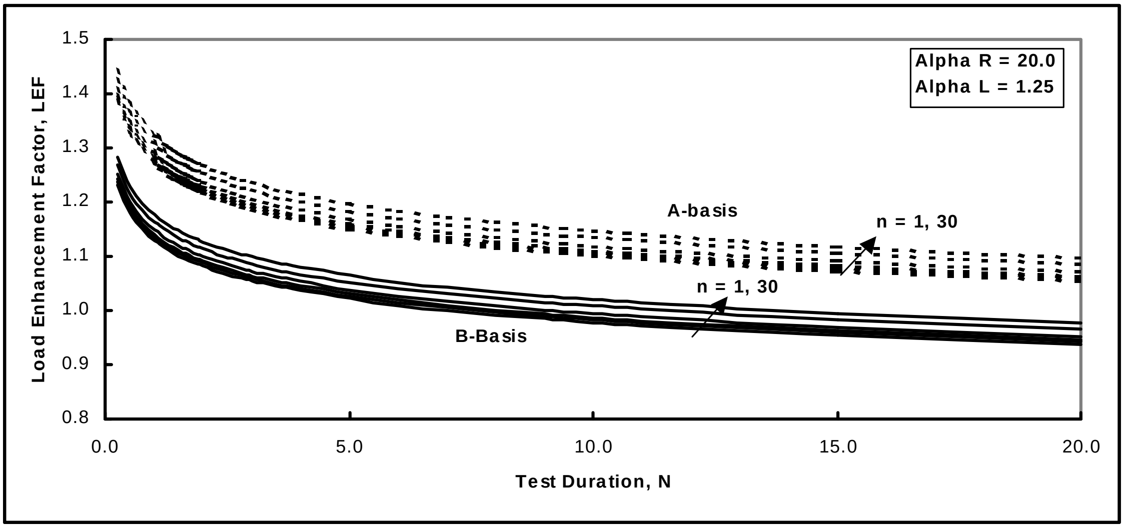

FIGURE 7.6.3(a) *LEF for commonly used composites.*

The LEF approach provides an efficient way to assure the structural life reliability. However, other effects may also require a load enhancement and resulted in an undesirably high load factor. For example, an environmental compensation factor is usually applied in order to account for service environment effects, and a spectrum severity factor is usually applied for military aircraft. Thus, an LEF of 1.18, an environmental compensation factor of 1.06, and a spectrum severity factor of 1.20 would result in an overall fatigue test factor of 1.50. This would either change the fatigue failure mode or reach the static strength of the structure. Therefore, in the application of the LEF approach, it is very important to ensure that the fatigue failure mode is preserved.

Sample Size	One Lifetime Test		Two Lifetime Test	
	A-Basis	B-Basis	A-Basis	B-Basis
1	1.324	1.177	1.268	1.127
2	1.308	1.163	1.253	1.114
5	1.291	1.148	1.237	1.100
10	1.282	1.140	1.227	1.091
15	1.277	1.135	1.223	1.087
30	1.270	1.130	1.217	1.082

FIGURE 7.6.3(b) *Typical LEF for one-lifetime and two-lifetime tests.*

7.6.4 Ultimate strength approach

The Ultimate Strength Approach uses an increased static strength margin in conjunction with the fatigue threshold to demonstrate adequate fatigue life. This approach is discussed in detail in References

7.6.1 and 7.6.4. This is a conservative approach, but, if it is satisfied, no structural fatigue test is necessary. This approach assumes that a fatigue threshold exists at a relatively high proportion of the static strength. In order to apply the ultimate static strength approach, it is necessary to design structures such that the maximum spectrum design load is no greater than the B-basis fatigue threshold.

The ultimate strength approach has seen limited application in rotorcraft design since the number of fatigue load cycles in rotorcraft fatigue spectra are approximately two orders of magnitude higher than for fixed-wing aircraft. Fatigue thresholds are not fully established at such high load cycles. Further research is needed to develop a database in order to apply this approach.

7.6.5 Spectrum truncation

In addition to the Load Enhancement Approach and Ultimate Strength Approach, spectrum truncation also utilizes the high fatigue threshold behavior to reduce composite fatigue test time. This is because the composite fatigue process, unlike that of metals, is relatively insensitive to the low stress (strain) cycles and fatigue life is dominate by the high stress (strain) cycles. It has also been observed that composite behavior is not affected by fatigue load sequence, possibly due to the brittleness of the material. In fact, the results of References 7.6.5(a) and (b) indicated that under certain types of fatigue load spectra, most of the fatigue failures were “quasi-static failure”. That is, damage initiation and progression only take place under a limited number of high stress (strain) load cycles. Removing the low stress (strain) cycles will not affect the fatigue life nor the damage evolution processes. An extensive database was developed in Reference 7.6.5(c) to demonstrate the validity of the spectrum truncation technique. References 7.6.5(d) and (e) also successfully applied this technique to modify the fatigue load spectrum.

Although there are no general guidelines for spectrum truncation for composite fatigue tests, the fatigue threshold of the material is usually used to determine the cycles to be truncated. Stress (strain) levels below the fatigue threshold are considered to cause no fatigue damage (initiation or progression) and theoretically can be removed from the spectrum without changing the test results. However, in practice, the truncation level is usually a certain percentage of the A- or B-basis fatigue threshold (e.g. 60% to 70%).

7.6.6 Durability certification

Because of the unique fatigue behavior of composites (high threshold, high data scatter and multiple fatigue damage mechanisms) durability certification of composite structures should be addressed differently from that of metallic structures. Also because of their particular fatigue behavior, durability of composite structures is assured mostly by testing instead of analysis. The building block approach is recommended for durability certification testing of composite structures. The emphasis in planning the building block test plan should be in the design development testing, which include coupons, elements, element combinations, and subcomponents. Durability and fatigue life should be verified at these lower levels of testing. The environmental effects on structural durability should also be considered in the test planning. At the full-scale level, fatigue tests should be used to verify the life of the metallic parts only. The time and cost of the durability testing can be significantly reduced by proper combination of the load enhancement factor approach and the spectrum truncation techniques. The ultimate strength approach is conservative, in general, and an extended database must be developed for application to high cycle fatigue structures, such as rotorcraft components.

7.6.7 Influencing factors

This section is reserved for future use.

7.6.8 Design issues and guidelines

This section is reserved for future use.

7.6.9 Test issues

This section is reserved for future use.

7.6.10 Analysis methods - description and assessment

This section is reserved for future use.

7.7 DAMAGE GROWTH UNDER CYCLIC LOADING

7.7.1 Influencing factors

Just after compression strength reduction due to low velocity impact was recognized in the late 1970's, many composite research teams then took up investigating the fatigue behavior of impacted CFRP specimens. Among all available results, those shown in this section are drawn from a French-German collaborative program (Reference 7.7.1(a)) involving CEAT, Aerospatiale, DASA Munich and the WIM (in Erding).

In this program, specimens representative of real world stacking sequences were impacted with various energy levels but not higher than those corresponding to the creation of visible impact damages. Usually impact damages that are to be assumed for fatigue (safe-life) investigations are those not sufficiently visible for being readily detectable. Those more severe, easily detectable, should not have to prove their capability to sustain a large number of fatigue cycles in service.

These specimens were then tested in compression-compression fatigue (R = 10) in order to :

- Plot Wöhler curves for several energy levels,
- Monitor damage growth and residual static strength versus time.

Wöhler curves for the IM7/977-2 and the T800H/F-655-2 material references are reported in Figure 7.7.1(a) for various energy levels. The ratio between the endurance limit at 10^6 cycles and the initial static strength turned out to be between 0.50 and 0.75. This means that sizing a structure (with these materials) using Ultimate Loads should push fatigue loads down to a level likely to limit fatigue problems with low energy impact damages.

Figure 7.7.1(b) illustrates damage growth, measured by C-SCAN, versus fatigue cycles for the T800H/F655-2 material. Unrealistic fatigue stresses (above 75% of the static strength) were needed to allow such measurement. This illustration shows that, despite the log axis, damage growth starts very close to the end of the specimen lifetime (between 85% and 95% for all cases investigated in this program), with a very high slope.

From these results it is apparent that, as far as low velocity impact damages are concerned, assuming the possibility of a stable (or slow) growth approach for certification purposes may not be possible. This conclusion is also supported by other laboratory results such as, for example, those presented in Reference 7.7.1(b) where very high slopes have also been shown for da/dN versus ΔG curves. These data were obtained on Double Cantilever Beam specimens made of two composite materials - the IM7/8552 and the HTA/6376 - and are representative of a mode I delamination growth phenomenon.

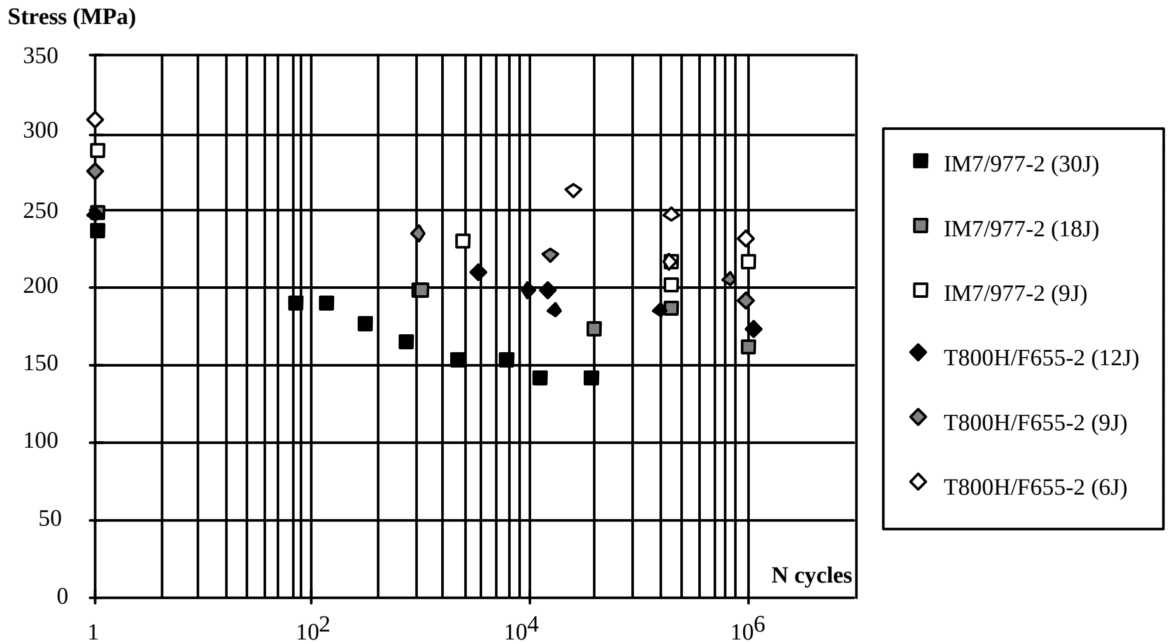

FIGURE 7.7.1(a) *Failure stress versus cycles for impact damaged laminates.*

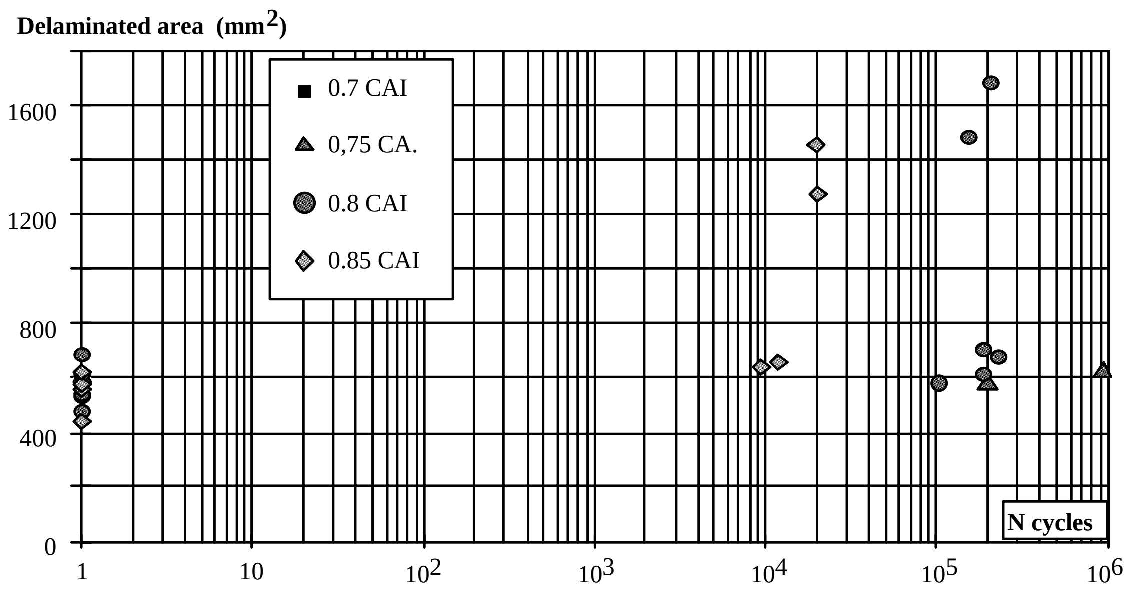

FIGURE 7.7.1(b) *Post-impact delamination size versus load cycles.*

Aside from this intrinsic material behavior, another reason for avoiding the use of a slow growth concept in certification is that the composite community is still short of analytical tools for predicting impact damage growth in fatigue. Single delaminations for which tools have been developed are not representative of the complex damage state induced by an impact.

In summary, impact damage growth under fatigue should not be used as an aircraft certification approach except in the cases of:

- Readily detectable damage
- Situations where the structural design provides a damage arrest capability

The use of a no-growth approach is then recommended for aircraft certification purposes. Due to the low fatigue sensitivity of impacted composites, this no-growth approach should be able to cover most situations.

7.7.2 Design issues and guidelines

This section is reserved for future use.

7.7.3 Test issues

This section is reserved for future use.

7.7.4 Analysis methods - description and assessment

7.7.4.1 Large through-penetration damage

This section is reserved for future use.

7.7.4.2 Single delaminations and disbonds

This section is reserved for future use.

7.7.4.2.1 Delamination growth

Under certain conditions delaminations subject to out-of-plane displacements or loading can grow and reach critical dimensions. The growth of delaminations can be treated according to the principles of fracture mechanics, using the Fracture Energy Criterion. The general procedure is as developed in Reference 7.7.4.2.1.

1. Stress field around the delaminated area is calculated (in most cases numerically).
2. A growth direction is assumed. This requires experience, otherwise several directions have to be checked.
3. The crack is expanded by da, as small as possible.
4. The energy dissipated between the two stages, G, is calculated and compared to the experimentally obtained G_c. If $G > G_c$ the delamination grows.

It should be noted that delamination growth is a competing failure mechanism with the in-plane stress concentration described in Section 7.8.3.2.1. As a result, some stable delamination growth may occur prior to an increase in stress concentration and fiber kink failure.

7.7.4.3 Impact damages

This section is reserved for future use.

7.7.4.4 Cuts and gouges

This section is reserved for future use.

7.8 RESIDUAL STRENGTH

One of the key aspects of the damage tolerance design approach involves ensuring that damaged structure has adequate residual strength and stiffness to continue safely in service until the damage can be detected by scheduled maintenance inspection and be repaired, or until the life limit is reached. The potential damage threats, the extent of damage to be considered, the structural configuration and the detectability of the damage using the selected inspection methods determine the required damage sizes to be evaluated for the regulatory load levels to be sustained. This section discusses influencing factors on the residual strength characteristics of damaged composite structure, guidelines for testing of damaged structure, and analytical methods for predicting residual strength.

7.8.1 Influencing Factors

This section discusses the varied factors that influence the residual strength of a damaged composite structure. These factors include material properties, structural configuration, loading conditions and characteristics of the damage state within the structure. Analysis methods and test programs must be configured to account for the range of these variables appropriate for the design in order to establish a set of residual strength versus damage curves.

7.8.1.1 Relationships between damage resistance and residual strength

The characteristics of the response of a material/structure to an impact event (damage resistance) and the strength of a structure with a given damage state (residual strength) are often confused. While these two items are somewhat interrelated, the following should be understood. The damage tolerance design approach uses the capabilities of a selected inspection method to establish the damage sizes to be considered for residual strength analysis. This means that the required damage sizes are functions of the detectability of the damage for the selected inspection method, and are not typically functions of a specific energy level. Practically, this means that a "tougher" structure that is more resistant to a given damage threat (impact energy level) may require more impact energy to achieve the same level of damage detectability as a "brittle" structure. Given the same level of damage detectability, the residual strength of the tougher structure may or may not be greater than the brittle structure.

Some of the material and structural characteristics that improve damage resistance tend to degrade residual strength, especially for large damage sizes, while other characteristics have a beneficial effect on both damage resistance and residual strength. The effects of these characteristics on damage resistance are discussed in Section 7.5, while the effects on residual strength are discussed in the following subsections. As is the case in other material and structural property tradeoffs, several technical and economic issues must be considered in balancing the damage resistance and residual strength of a given composite design. It should be kept in mind that a highly-damage-resistant structure may not be very damage tolerant and vice versa.

7.8.1.2 Structure with impact damage

7.8.1.2.1 Material effects

Material parameters, including matrix toughness, form (tape or fabric), and stacking sequence, mostly influence the damage pattern, thus the damage resistance. Material properties may, however, influence both damage propagation under repeated loads and residual strength. The response of a given damage will be influenced by a combination of structural parameters, like strength and stiffness of sublaminates, or fiber fracture and matrix cracking at notch tips.

Some studies have been made of composites with hybrid fiber construction, that is, composites in which two or more types of fibers are mixed in the lay-up. For example, a percentage of the carbon fibers are replaced with fibers with higher elongation capability, such as fiberglass or aramid. Results (References 7.8.1.2.1(a) through 7.8.1.2.1(d)) in both cases have shown improvement in damage resistance and residual compression strength after impact. Basic undamaged properties, however, were usually reduced.

In thin gage structures, such as a two-or three-ply fabric facesheet sandwich construction, materials can have a significant effect on damage resistance and residual strength. Investigations have generally shown that compression strength (both before and after impact) increases with the fiber-strain-to-failure capability within a particular class of materials. Higher strain capability aramid or glass fiber structures tend to be more impact resistant than high-strength carbon fiber structure. However, the compressive strengths of the undamaged and damaged aramid and glass structures are lower than that of carbon. Structure incorporating high-modulus, intermediate-strength carbon fibers, with higher strain-to-failures offer significant impact resistance while retaining higher strength.

7.8.1.2.2 Interlaminar toughness effects

In thermoset material systems, the nominal matrix toughness variations influence the impact resistance of thin gage structures but generally to a lesser extent than in thicker structures. For thermoplastic material systems, however, the generally much larger increase in the fracture toughness (G_{IC}, G_{IIC}, etc.) of the resins do translate into significant impact resistance and residual strength improvements.

Although interlaminar toughness is crucial to the extent of damage created in a given impact event, the CAI of laminates with equivalent damage states (size and type) was found to be independent of material toughness (References 7.8.1.2.2(a) through 7.8.1.2.2(c)). The model from Reference 7.8.1.2.2(b) (see also Section 7.8.4.3.1), which accounts for the in-plane stress redistribution due to sublaminate buckling, has worked equally well for tough and brittle resin systems studied. Since delamination growth may be possible with some materials and laminate stacking sequences (LSS), a more general model would also account for out-of-plane stresses.

A comparison of results from Figures 7.5.1.3 and 7.8.1.2.2 show that the toughened material has greater impact damage resistance, but essentially the same CAI strength for damages greater than 0.8 in. (20 mm) in diameter. Although the curves shown in Figure 7.8.1.2.2 are best-fit to the data, similar accuracy has been achieved for these materials and stacking sequences using the engineering analysis described in Section 7.8.4.3.1 (References 7.8.1.2.2(a) through 7.8.1.2.2(d)).

7.8.1.2.3 Stacking sequence effects

The laminate stacking sequence (LSS) can affect compression after impact strength (CAI) in several ways. First, the bending stiffness of a laminate, and failure mechanisms that occur during an impact event, are strongly dependent on the LSS. Load redistribution near the impact site is dependent on the distribution of damage through the laminate thickness (e.g., the LSS of sublaminates affects their stability). Finally, damage propagation leading to final failure also depends on the LSS. Additional discussion of LSS effects is contained in Section 7.8.4.3.1.

Many of the impact damage states studied in the past have been dominated by matrix failures. The creation of matrix cracks and delaminations which combine to form sublaminates depends strongly on LSS (References 7.8.1.2.2(a) and 7.8.1.2.2(d)). Homogeneous stacking sequences have been found to lead to characteristic damage states which repeat through the laminate thickness. Alternatively, plies can be stacked in a sequence which concentrates damage in specific zones on the laminate. Figure 7.8.1.2.3 shows experimental data indicating that LSS has a strong effect on CAI strength.

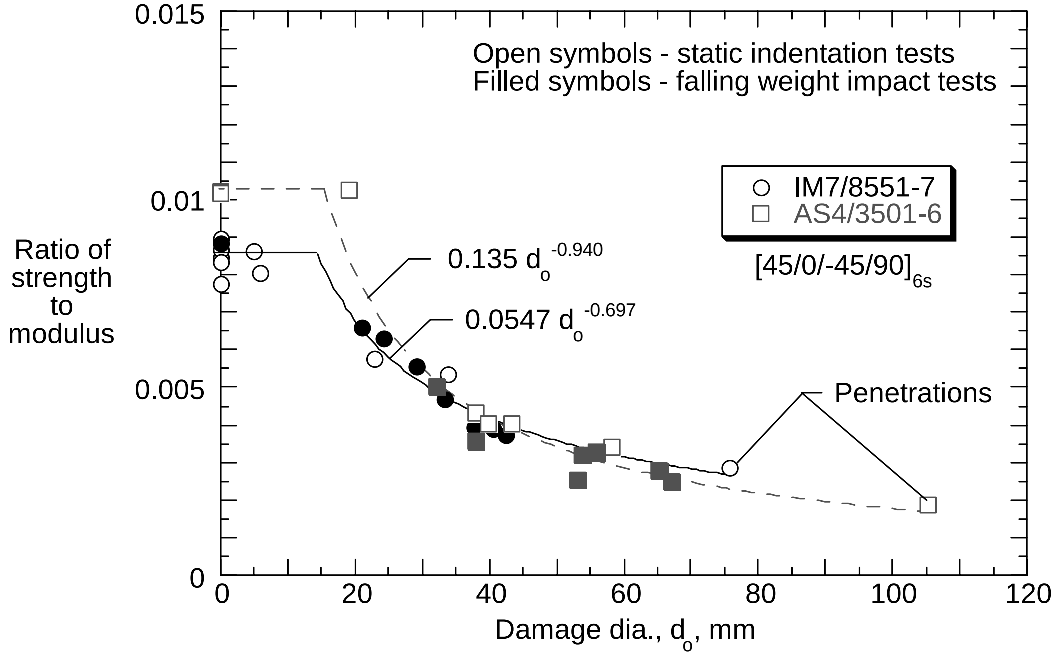

FIGURE 7.8.1.2.2 *CAI test results for untoughened and toughened, interlayered carbon/epoxy laminates made from prepreg tape (lines were fit to the data).*

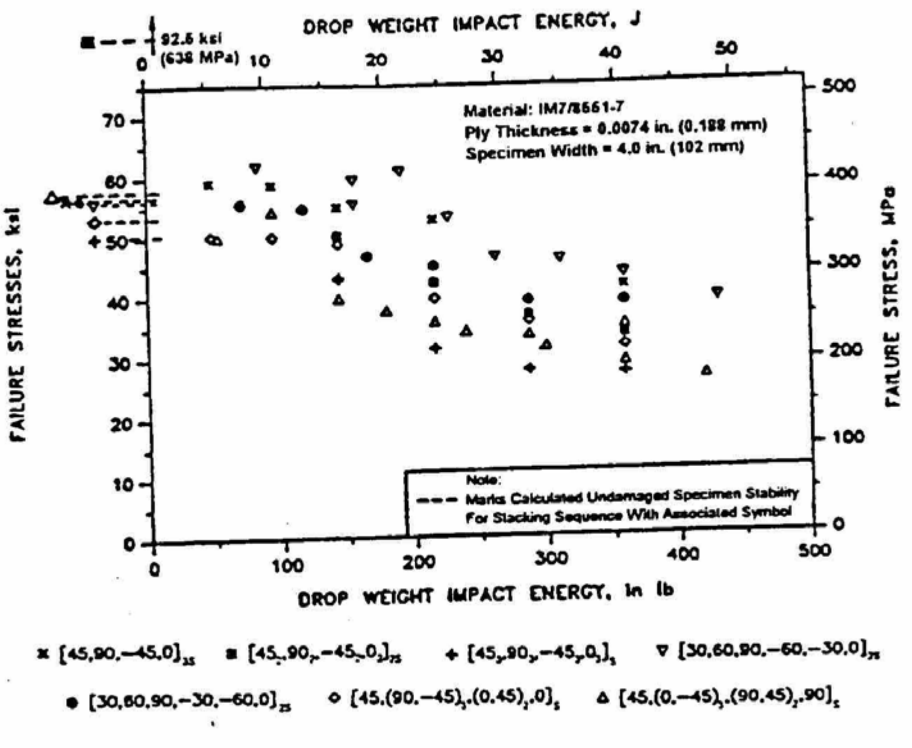

FIGURE 7.8.1.2.3 *Test data for CAI performance as a function of LSS (from Reference 7.8.1.2.3).*

7.8.1.2.4 Laminate thickness effects

Some data exists which indicates thicker laminates have higher compressive residual strength for a given damage size. This has been observed for both laminated plates and sandwich panels (Reference 7.8.1.2.4(a) and (b)). Most of this strength data was collected for open holes and notch-like large penetrations. However, based on failure due to the local compressive stress concentration next to buckled sublaminates, such an understanding of this behavior would also be crucial to accurately predicting CAI.

7.8.1.2.5 Through-thickness stitching

Methods such as through-thickness stitching have also been used to improve damage resistance and residual strength. The effect of stitching has been to reduce the size of internal delaminations due to impact and arrest damage growth. Tests involving conventional carbon/epoxies have shown increases in the residual strength of up to 15% for comparative impact energy levels (however, when comparing on a equivalent damage "detectability" criteria, the increase in residual strength may be lower). The stitching process is quite expensive, however, and probably should be considered for applications in selected critical areas only. Additionally, the stitches tend to cause stress concentrations and the tensile strength, transverse to the stitching row, is usually reduced.

7.8.1.2.6 Sandwich structure

Core density and material type has been found to have a significant influence on the damage resistance of sandwich panels. Lightweight, weak core materials allow for through-penetration damage of the facesheet under the impacting object. Damage in this case is typically localized to the rough size of the impactor. Also, lightweight core materials have a tendency to fracture under even small impact energies; if the energy is low then the facesheet may be undamaged and may spring back leaving non-visible damage to the core material. Conversely, dense, high-strength cores are less likely to fracture under the impact load, and the resulting damage is typically a dented area somewhat larger than the impacting object.

The residual strength of an impact damaged sandwich facesheet is not significantly dependent on core density if the failure mode is predominately controlled by the resulting in-plane stress concentration. However, core density can have a significant effect on the residual strength of the sandwich if the failure mode is an instability type (e.g., face wrinkling).

Although the inherent bending stiffness of a sandwich design will minimize the effect of impact location, the characteristic damage state (CDS) will have some relationship with internal stiffening elements (e.g., frames, ribs, edge closeouts, and bulkheads). For impact occurring away from stiffening elements, the CDS is expected to be similar to that observed when impacting sandwich test panels. As discussed in Section 7.4, the extent of planar impact damage in the core and impacted facesheet were found to be nearly the same for many combinations of materials and a facesheet thickness on the order of 0.08 in. (2.03 mm) (Reference 7.8.1.2.4(a)). Figure 7.8.1.2.6 shows a correlation between the extent of measured core and facesheet damage. The relationship shown in the figure may relate to mechanisms whereby the core first fails under the impactor, and then facesheet damage develops directly above the planar area where core damage has greatly reduced the local shear stiffness of the sandwich panel.

7.8.1.2.7 Impact characteristic damage states

Low velocity impacts, e.g., impacts from dropped tools as opposed to ballistic impacts, present a special problem. Impacts on the laminate surface, especially those made by a blunt object, may cause considerable internal damage without producing visible indications on the surface. Damage to the resin may be particularly severe as evidenced by transverse shear cracks and delaminations. Consequently, the resin loses its ability to stabilize the fibers in compression and the local failure may initiate total structural collapse. Similarly, the impact may damage fibers and cause local stress concentrations, which could result in significant loss of tensile, shear, or compressive strength. With conventional graphite/epoxy systems, which are quite brittle, losses in tensile and compressive strength for non-detectable impact may approach 50% and 60%, respectively. Post-impact failing strains from Reference 7.8.1.2.7 are plotted against dent depth in Figure 7.8.1.2.7(a). The AS4/3501-6 plates, which were made by resin film infusion of uniweave fabric, were 16, 24, 32, and 48 plies thick. The post-impact failing strains were lower for compression than tension. The failing strains for tension were larger than those for compression because the size of the region with damaged fibers was much smaller than that with damaged matrix.

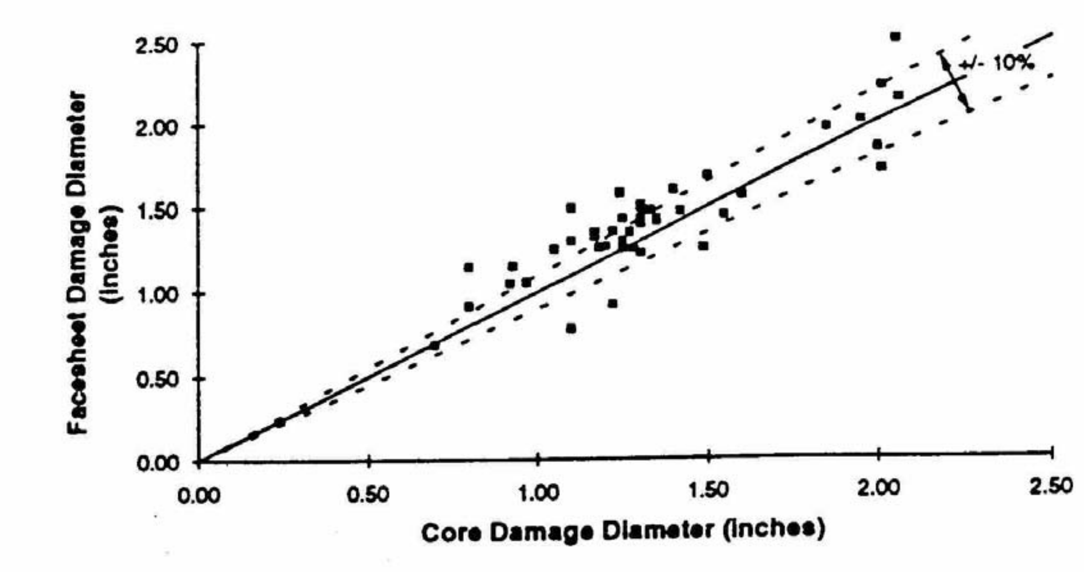

FIGURE 7.8.1.2.6 *Comparison of the planar extent of impact damage in sandwich facesheet and core materials (Reference 7.8.1.2.4).*

Much of the work documented to date on specific characteristics of impact damage has focused on impact normal to the surface of a flat plate. Figure 7.8.1.2.7(b) shows a schematic diagram classifying planar and cross-sectional views of damage observed in flat laminates following low-velocity impact by spherical objects. Three main classes of damage are shown. These include fiber failure, matrix damage, and combined fiber and matrix damage. As shown at the bottom of Figure 7.8.1.2.7(b), symmetric or unsymmetric cross-sections further distinguish each class of damage. As discussed in Section 7.4, numerous material, structural, and extrinsic variables affect damage size and type.

The most general classification of impact damage involves both fiber and matrix failures. The importance of each type of damage to structural integrity depends on the loads, part function, and further service exposure. Fiber damage, when present, tends to concentrate at an impact site. Typical matrix damage includes both matrix cracking and delamination. Matrix damage is also centered at the impact site but tends to radiate away from this point to a size dependent on the impact event and delamination resistance. Impacted laminates tend to develop a characteristic damage state (CDS) or pattern of through the thickness fiber and matrix failures. This CDS has been found to depend on the laminate stacking sequence (References 7.8.1.2.2(a), 7.8.1.2.2(b), and 7.8.1.2.2(d)).

Many factors can affect the symmetry of a CDS. Test observations indicate that thin laminates, particularly those with heterogeneous stacking sequences, tend to have asymmetric CDS, with damage initiated towards the side opposite the impacted surface (such as that shown in the bottom of Figure 7.8.1.2.7(b)). Very thick laminates also have asymmetric damage, but with the damage initiating close to the impacted surface. Work with laminates consisting of materials that have high delamination resistance, also have a greater tendency for asymmetric CDS than brittle materials tested with the same impact variables. This probably relates to the specific damage initiation and growth mechanisms.

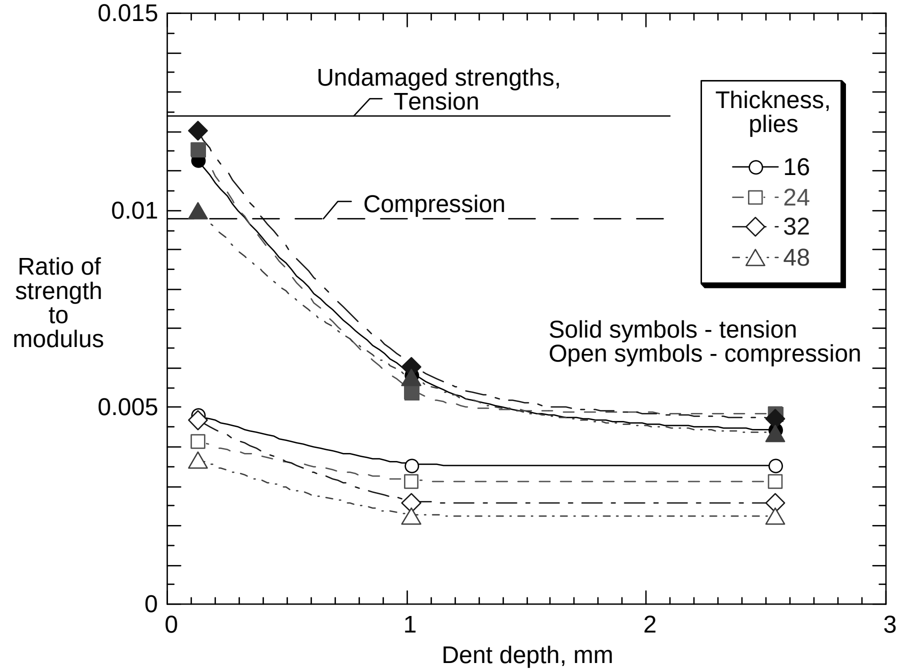

FIGURE 7.8.1.2.7(a) *Post-impact tension and compression strengths for [45/0/-45/90]$_{ns}$ AS4/3501-6/RFI uniweave (0.5 in. (12.7 mm-diameter tup)) (Reference 7.8.1.2.7).*

The tendency for CDS to develop in a composite material subjected to an impact event is very important to subsequent inspection and residual strength assessments. The extent of impact damage grows with the magnitude of a given impact event but the basic CDS tends to remain the same. The CDS of a specific configuration can be defined, prior to service exposure, during impact surveys that support detailed design. During such studies, the correlation between destructive laboratory measurements of the CDS and those obtained using NDE methods that are suitable for service can help establish a link to the residual strength prediction. For example, microscopy and TTU may be used to define the full extent of matrix and fiber failure in a CDS, while dent depth and coin tapping may be used to define the damage periphery. The combination of this information can then be used to predict residual strength. In practice, NDE data from service will yield a metric on the size of damage, while existing databases that define the CDS provide a link to residual strength prediction.

Compression and shear loaded structure are sensitive to both fiber and matrix damage that exist in the CDS. Matrix cracks and delaminations can link to locally break the base laminate into multiple “sub-laminates” that can become unstable under compression or shear loads. Figure 7.8.1.2.7(c) shows a schematic diagram of one CDS which was defined for a quasi-isotropic laminate lay-up with repeating stacking sequence (References 7.8.1.2.2(a), 7.8.1.2.2(b), and 7.8.1.2.2(d)). This is the same laminate stacking sequence that is commonly used for impact material screening tests with standard specimens (Reference 7.8.1.2.2(c)).

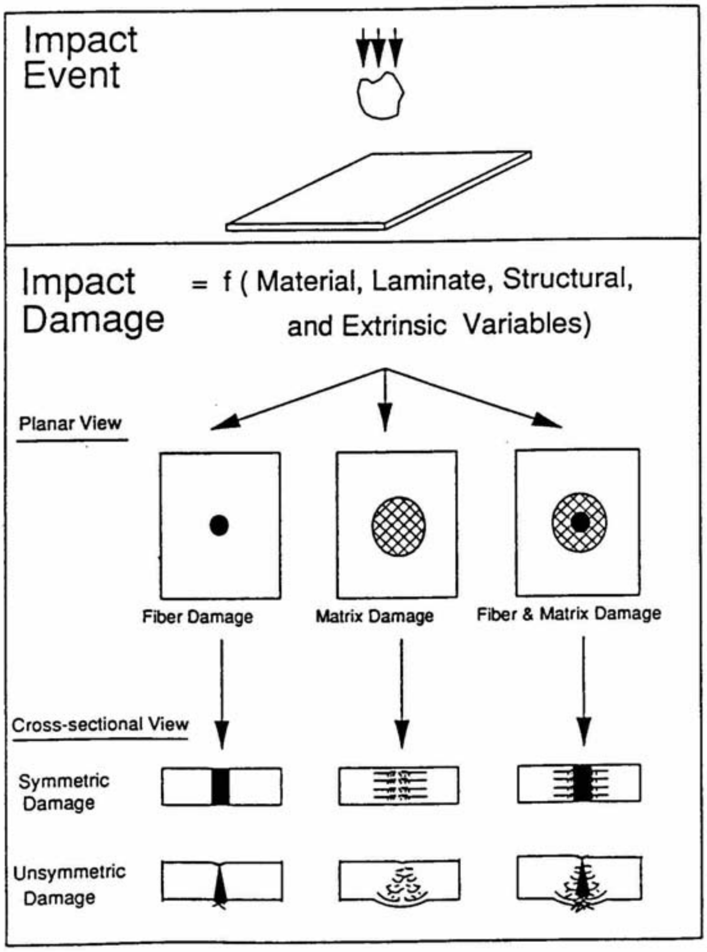

FIGURE 7.8.1.2.7(b) *Potential impact damage states for laminated composites (Reference 7.8.1.2.2(a)).*

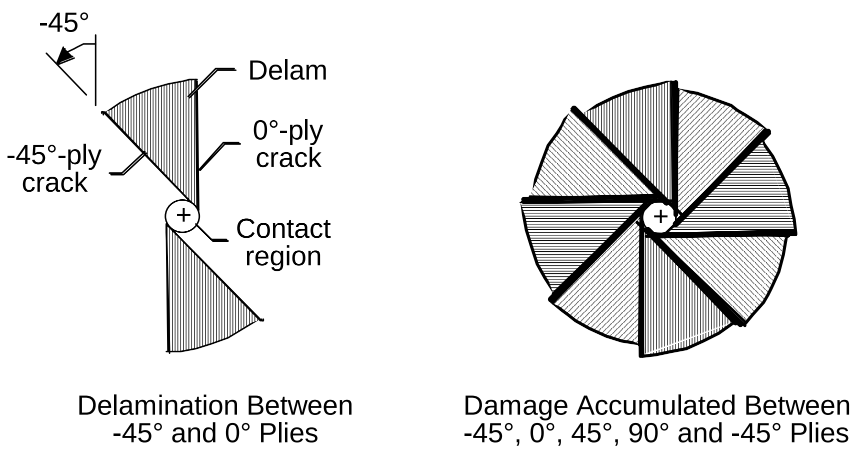

FIGURE 7.8.1.2.7(c) *Matrix cracks and delaminations for a quasi-isotropic stacking sequence combine to form distinct sublaminates (References 7.8.1.2.2(a), 7.8.1.2.2(b), and 7.8.1.2.2(d)).*

Transverse cracks bridge wedge shaped delaminations between adjacent plies in the CDS shown in Figure 7.8.1.2.7(c). This pattern continues through the laminate thickness, with interconnected delaminations spiraling toward the center, reversing direction, and proceeding out toward the back side. Depending on the specific stacking sequence, the sublaminates in a particular CDS are likely to change. Procedures that provide a circular cross-section for microscopic evaluation may be best for identifying the internal structure of sublaminates (See Reference 7.5.1.1(l)). Application of dye penetrant to the circular section's edge help to highlight the sublaminate structure.

7.8.1.2.8 Residual strength - compressive/shear loads

Experimental data using 1.0 in. (25.4 mm) diameter impactors with rounded tups show that compressive strength is reduced with damage size, see Figure 7.3.2(a), but levels off at the so-called "damage tolerance strain" (3000 to 3500 microstrain for brittle carbon epoxy systems (Reference 7.3.2(a)). This is a conservative but powerful and frequently used preliminary design strength value for Ultimate Load considerations.

Compressive failure prediction depends on the observed failure characteristics of a laminate with buckled sublaminates. Results obtained to date for a limited number of material types and laminate stacking sequences have shown that the dominant failure mode is associated with local in-plane compressive stress concentration. As a result, similar compressive residual strength curves are observed for laminates having either a toughened or untoughened matrix. Figure 7.8.1.2.2 shows normalized CAI curves for the interlayer-toughened (IM7/8551-7) and untoughened (AS4/3501-6) materials used as examples in Section 7.3.1 (note that Figure 7.5.1.3 shows transverse impact test results for the same specimens).

Delamination growth may be a critical failure mechanism for compression after impact (CAI) strength, depending on the specific damage size, laminate lay-up, and delamination growth resistance of a material (References 7.8.1.2.8(a) and (b)). Analysis of such failure modes show that damage growth tends to be stable, requiring larger compressive strains to grow larger damage. As a result, the local compressive failure due to in-plane stress redistribution remains the dominant mode, particularly for larger damage sizes. This can be explained physically by considering how much load is carried by large diameter sublaminates, which buckle at very low compressive strains. When little load is required to buckle the sublaminate, its effect on the adjacent structure is like that of a large open hole. In a sufficiently large structure, the material adjacent to the buckled impact damage may fail in compression before enough out-of-plane displacement occurs in the buckled sublaminates for significant growth. This occurs because large buckling displacements require sufficient compressive strain in adjacent undamaged material. Nevertheless, the delamination growth of buckled sublaminates should be evaluated as a potential failure mode since it has been observed in some very brittle matrix materials. Note the future development of materials with higher in-plane compression strength (i.e., greater fiber microbuckling strength) may also lead to the potential for competing failure modes.

When the CDS is dominated by fiber failure, both tension and compression residual strength will be affected. Although sublaminate buckling is not an issue, prediction of the residual strength of composites with local fiber failure still requires an estimate of the effective reduced stiffness. Once a measure of the effective reduced stiffness is known, methods which predict the stress concentration for a soft inclusion (References 7.8.1.2.8(c) and (d), 7.8.1.2.2(b)) and notched strength failure criteria can be applied (References 7.8.1.2.8(e) through 7.8.1.2.8(g) and 7.8.1.2.2(b)). Recent efforts have shown that a strain softening analysis provides an alternative to semi-empirical criteria traditionally used for the latter (References 7.8.1.2.8(h) and (i), 7.8.1.2.4(a)).

When the CDS includes both fiber failure and matrix damage (e.g., sublaminates), it is likely that a combination of methods will be needed to predict compressive strength. Fiber damage at the center of the damage may only affect the strength for relatively small damage sizes in which sublaminates buckle at relatively high strains. When the damage is larger, sublaminates buckle at much lower strains, effectively masking the effects of local fiber failure in the center of the CDS. Note that CAI results with small damage for the toughened material in Figure 7.8.1.2.2 are affected by local fiber failure (Reference 7.8.1.2.2(a)).

Figure 7.8.1.2.2 shows post-impact compressive strength results that are similar to those observed for holes or penetrations. Such behavior is recognized by the shape of the residual strength curve that initially drops steeply as a function of increasing damage size, and then flattens out for large damage. Based on the sublaminate residual strength analysis described above, impact damage larger than 2 in. (50 mm) diameter would tend to collapse onto the compressive residual strength curve for open holes. Whether this trend can be expected for all laminates and other composite material forms loaded in compression or shear remains to be demonstrated.

The compressive residual strength behavior of a given material form and laminate should be determined in support of detailed design. As mentioned earlier, the thickness of laminated composites has been shown to effectively increase the compressive residual strength. Some stitched and textile composites have been found to have very flat residual strength curves, implying reduced notch sensitivity. These examples highlight the importance of studying specific design detail (laminate, thickness, lay-up, and material form). There are currently no theories to reliably predict the compressive residual strength of composite materials without some notched strength data. A limited amount of test data indicates some dependence of compressive residual strength on notch geometry with ellipse-shaped damage having a high aspect ratio resulting in the lowest strength.

7.8.1.2.9 Residual strength - tensile loads

Degradation in the residual strength of tensile-loaded structure is most sensitive to fiber failure. As discussed earlier, fiber failure localizes within a zone that is roughly the size of the impactor. As a result, the size and shape of an impactor are crucial to the extent of fiber failure. Although impact by large diameter objects pose the most severe threats, rare impact events of significant magnitude (e.g., service vehicle collision) would be required to cause extensive fiber damage over a large area of an aircraft structure's surface. Delamination and matrix cracks do not generally decrease the integrity of tensile-loaded structure. However, the combined effect of matrix damage surrounding fiber failure should not be ignored because the former may actually increase tensile residual strength by softening the stress concentration.

In the case of tensile-loaded structure, delamination growth is generally not an alternate failure mode (Reference 7.8.1.2.9(a)). It seems reasonable to expect that the tensile residual strength of a structure with through-penetrations will be lower than one with similar sized impact damage (i.e., a softened impact damage zone carries some load). Penetrations caused by impact events may be more or less severe than those obtained by machining the same sized notch. In some materials, the penetration may include an extended zone of fiber failure beyond visible penetration. This tends to further reduce residual strength. Other materials have a large zone of matrix failure surrounding the penetration, helping to soften the stress concentration and provide higher residual strength. Many factors have been found to affect the tensile residual strength of composite materials, including fiber, matrix, manufacturing process, hybridization, and lay-up (References 7.8.1.2.9(b), 7.8.1.2.8(e) through 7.8.1.2.8(g), and 7.8.1.2.8(i)). As is the case for compression, some notched strength testing is required to establish reliable failure criteria.

7.8.1.2.10 Stiffened panels

Characteristics of impact damage in structural configurations are strongly dependent on the impact location. The CDS of panels stiffened by discrete elements will also depend on whether the element is bonded or mechanically fastened. Skin impacts spaced sufficiently far from the stiffening elements will have a CDS similar to those obtained in tests with plates. Impacts occurring near an element will experience a much stiffer structural response, with potential failures occurring within the element and its attachment with the skin. Bondline and/or delamination failures are common between bonded elements and skin. The extent of such failure will depend on the impact event and design variables (e.g., the use of adhesive layers, doubler plies, and material delamination resistance). Delaminations may originate at the interface between skin and stiffener, and then penetrate to grow delaminations between base laminate plies having lower toughness than the adhesive. Fiber failures typically occur in blade, I- or J-stiffeners when impacts occur on the outer skin's surface, directly over the stiffener's web. Figure 7.8.1.2.10(a) shows an example of this type of local failure. The distribution of fiber failure for this type of damage is an important component of the CDS since it affects the section bending properties (see Reference 7.5.1.1(l)).

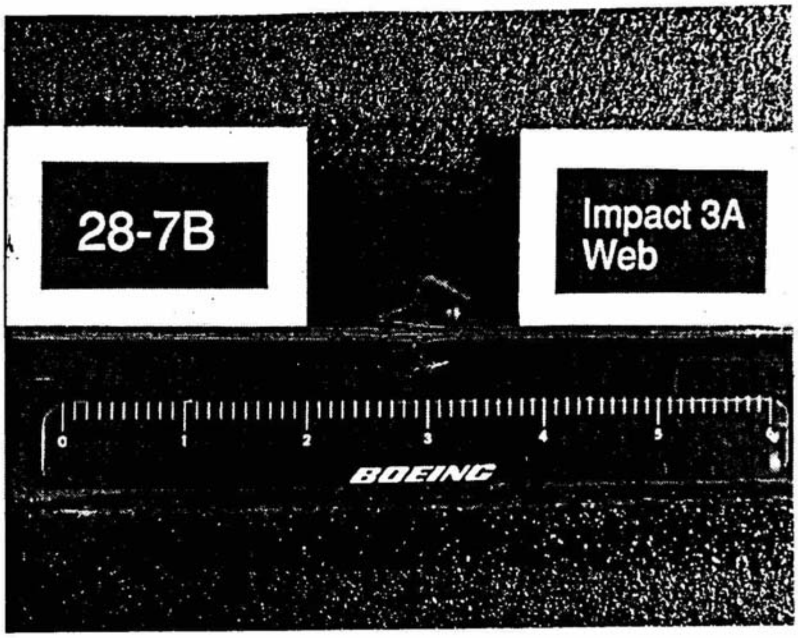

FIGURE 7.8.1.2.10(a) *Stiffener web damage in blade-stiffened skin panels (Reference 7.5.1.1(l)).*

The difference between impact responses of coupons and three-spar stiffened panels is illustrated in Figure 7.8.1.2.10(b). Post-impact compressive failing strains are plotted against kinetic energy for "hard" wing skins. The skins were nominally ¼ inch (6.35 mm) thick and were made with [38/50/12] and [42/50/8] lay-ups for coupons and panels, respectively. (The notation [38/50/12] indicates the percentage of 0° plies, ±45° plies, and 90° plies, respectively.) The spacing of the bolted titanium stiffeners was 5.5 inches (139.7 mm). A ½ inch (12.7 mm) diameter tup and 10-lbm (5 kg) impactor was used for the coupons, and, a 1 inch (25.4 mm) diameter tup and 25 lbm (11 kg) impactor was used for the panels. The two panels impacted with 40 and 60 ft-lbf (54 and 81 N-m) energies were impacted two times on the transverse centerline (over skin only), once midbay of the center spar and left-most spar and once midbay of the center spar and right-most spar. The panel impacted with 20 ft-lbf (27 N-m) energy was impacted at only one midbay location. The three panels impacted with 100 ft-lbf (135 N-m) energy were impacted three times each: once midbay (between stiffeners - over skin only), once over the skin only but near the edge of a stiffener, and once over a stiffener. A curve was fit to the coupon results. Failures were catastrophic for coupons and for panels with mid-bay impacts and failing strains were essentially equal. Failures of the panels with multiple 100 ft-lbf (135 N-m) impacts were not catastrophic. After fracture arrest by the stiffeners, the loads were increased 36% and 61% to cause complete failure. The initial failing strains for the panels with multiple 100 ft-lbf (135 N-m) impacts agreed with an extrapolation of the coupon data. Thus, the stiffeners reduced the effective size of the panel by increasing flexural stiffness and increased strength by arresting fractures.

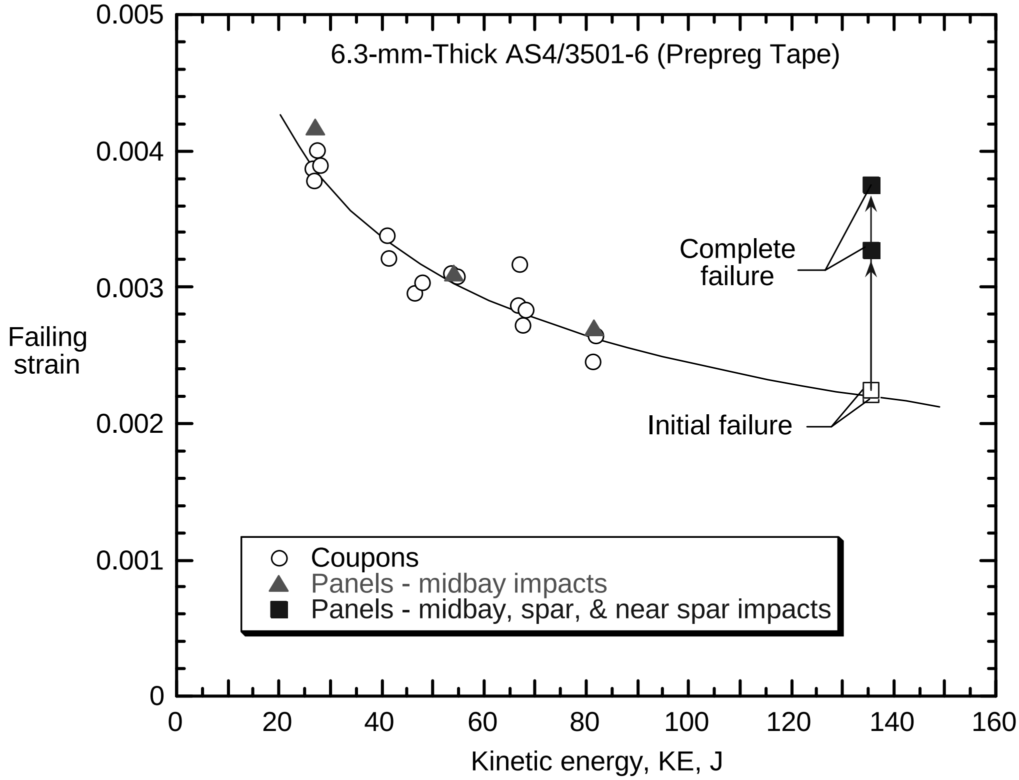

FIGURE 7.8.1.2.10(b) *Impact response of coupons and panels with three bolted spars (Reference 7.8.1.2.3)*

Structural panel level residual strength prediction involves more analysis steps than that for flat composite plates. As a result, additional structural building block tests are required. The analysis still starts with a quantitative metric which provides effective properties of the CDS for loads of interest. This measure is used to estimate the local stress or strain concentration. The effects of a given structural configuration on this stress concentration must be analyzed to predict the onset of damage growth. In redundant structural configurations, growth and load redistribution simulations may be needed for final failure prediction. Damage growth has often not been observed in composite structure because relatively small damage has typically been tested. For example, severe impact damage localized at a stiffener will require significant panel loads before gross damage propagation initiates (e.g., panel strains on the order of 0.004 in/in). Since the damage was small to start, a dynamic growth phenomena is observed, whereby the adjacent stiffening elements are unable to arrest damage growth. When the initial damage is significantly larger (e.g., a penetration which completely severs the stiffener and adjacent skin material), growth to the adjacent stiffening elements is more stable and arrest has been observed. (Reference 7.8.1.2.10).

7.8.1.3 Structure with through-penetration damage

A significant database addressing through-thickness notches was generated on a NASA/Boeing contract during the early 1990’s. This activity addressed the response for a range of materials, notch sizes and structural complexity. The following discussion, except where noted, is based on those findings (References 7.8.1.3(a) through 7.8.1.3(e), 7.8.1.2.4(a), 7.8.1.2.8(g), 7.8.1.2.8(i), and 7.8.1.2.10).

A major component of that activity was the use of tow placement (a.k.a. fiber placement) for lay-up of the skin materials. The tow placement process uses preimpregnated tow as the raw material form, and lays down multiple tows in a single pass of the tow-placement head, as illustrated in Figure 7.8.1.3(a). This technique allows the cost-effective use of intraply hybrid materials, which are materials with tows of more than one fiber type combined in a repeating pattern within each individual ply (e.g., S2-glass), as shown in Figure 7.8.1.3(b). In this program, such intraply hybrids were explored, primarily with the hybridization occurring in all plies.

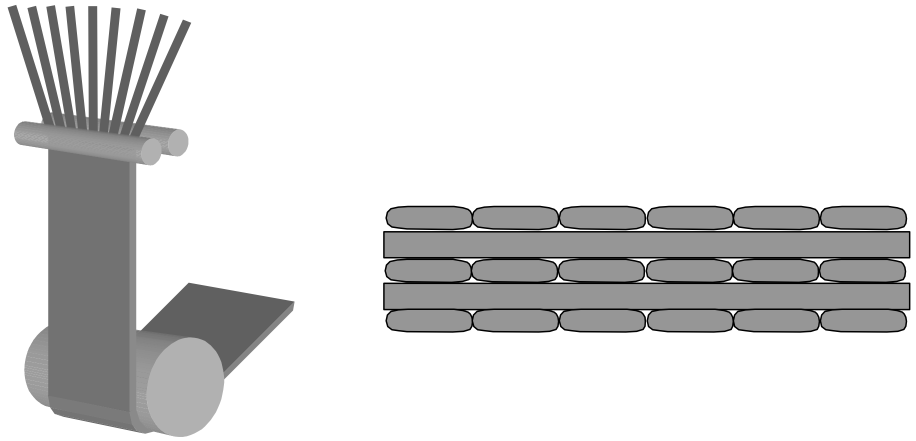

FIGURE 7.8.1.3(a) *Automated tow placement.*

Tension.

A number of variables strongly affect tensile residual strength response in the presence of through-thickness notches. In general, there is a trade-off between small-notch strength (i.e., "strength") and large-notch strength (i.e., "toughness"); high strengths are typically accompanied by low toughnesses, and visa versa. Low-strength, high-toughness behavior is characterized by lower sensitivity to changes in notch length, resulting in flatter residual strength curves.

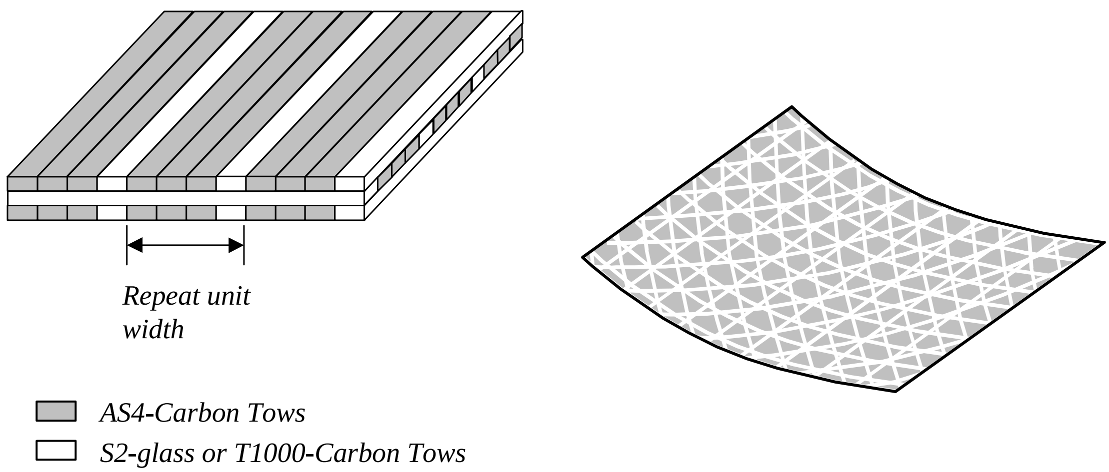

FIGURE 7.8.1.3(b) *Intraply hybrid materials.*

The effect of material for a single laminate is illustrated in Figure 7.8.1.3(c). The toughened-matrix materials (IM7/8551-7) demonstrate high strength and low toughnesses, while brittle-matrix materials

(AS4/938) exhibit lower strengths but higher toughness. An intraply hybrid of 75% AS4/938 and 25% S2/938 demonstrated the highest toughness through a very low sensitivity to changes in notch length. Note that this increased strength occurs despite a lower stiffness (i.e., higher stiffness carbon fibers were replaced with lower-stiffness glass fibers), indicating that the increase in failure strain was even higher. As shown in the figure, strengths of different materials can vary 30 to 50% for large notch lengths of interest to damage tolerance assessments (e.g., greater than 10 in. (250 mm)).

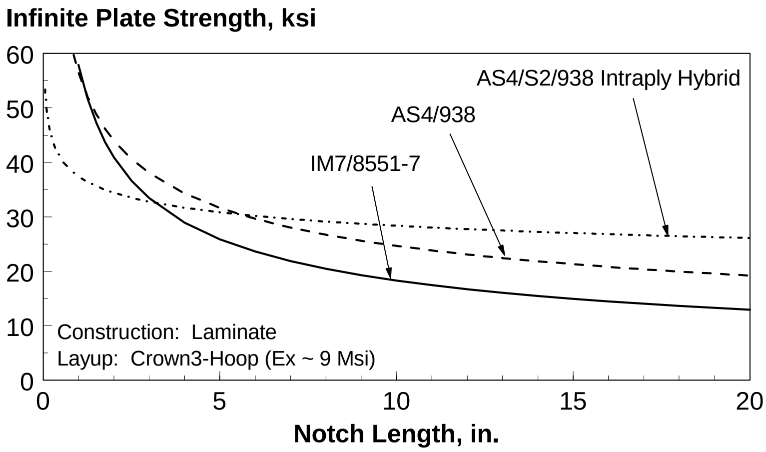

FIGURE 7.8.1.3(c) *Material effects on tension-fracture strength.*

The effects of hybridizing variables on tensile fracture strength for notch lengths of 2.5 in. (63 mm)and less were reported in Reference 7.8.1.3(c). High-strain glass (S2) and carbon (T1000) fibers were used to hybridize the baseline carbon fiber (AS4) laminate. Results for 2.5 in. (63 mm)notches are shown in Figure 7.8.1.3(d). The hybrids exhibited reduced notch sensitivities and large amounts of matrix splitting and delamination prior to failure, as shown in Figure 7.8.1.3(e). The AS4/S2-glass hybrids also had significant post-failure load carrying capability.

Lay-up was found to have a similar effect on tensile fracture strengths as does material, with higher-modulus laminates exhibiting higher strengths and lower toughnesses relative to lower-modulus laminates. High-modulus laminates of toughened-resin materials tend to have notch-length sensitivities similar to those predicted by linear elastic fracture mechanics (LEFM), while the sensitivities of other material/laminate combinations are lower. Figure 7.8.1.3(f) illustrates a representative magnitude of this effect.

A ply of plain-weave fabric included on each surface of each facesheet for manufacturing reasons resulted in significant tensile fracture improvements over tow-only laminates for most lay-ups, as shown in Figure 7.8.1.3(g). While a direct comparison of identical laminates was not available in the test results, the trend is convincing. The improvement is likely due to the added energy absorption of the fabric plies during the failure process and/or to a decreased stress concentration resulting from an increased repeatable inhomogeneity created by the fabric.

A comparison of AS4/8552 sandwich panel test results with those of AS4/938, AS4/S2/938 hybrid, and IM7/8551-7, all of which include notch sizes of 8 to 12 in. (200 to 300 mm), are shown in Figure 7.8.1.3(h). Lay-up differences are present within and between materials, confounding comparisons. The AS4/8552 results appear closest to a less-stiff AS4/938 laminate. This indicates that the impact-damage-resistance advantages of toughened-resin materials may be attainable without the loss of the tension-fracture advantages of the brittle-resin materials by incorporating fabric surface plies.

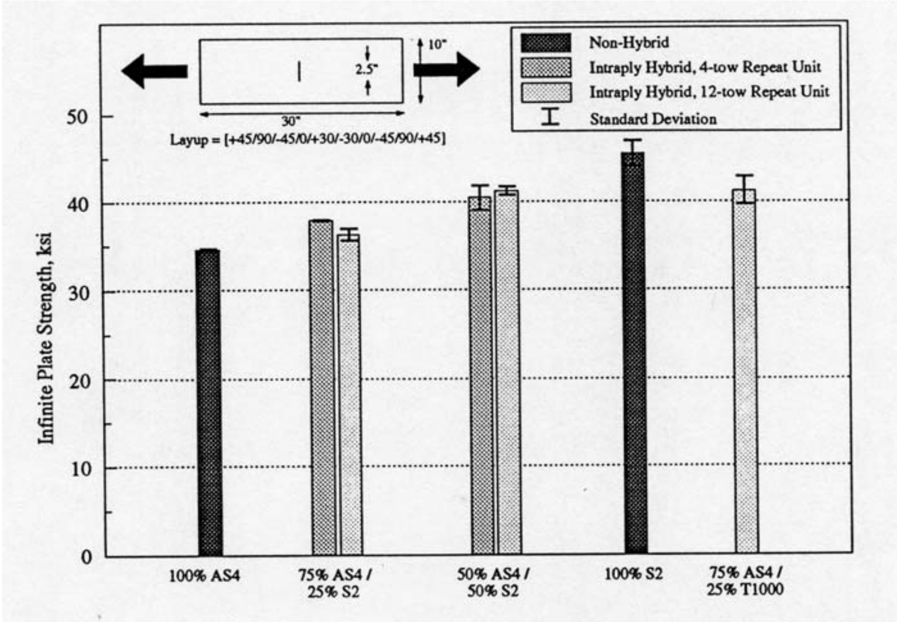

FIGURE 7.8.1.3(d) *Tension fracture strength of intraply hybrids for 2.5 inch (63 mm) crack.*

Material form and processing variables also were found to have a significant influence on tensile fracture performance. Tests from the AS4/3501-6 tape laminate are compared with results for AS4/938 tow and AS4/938 tape in Figure 7.8.1.3(i). These data indicate significantly reduced tensile fracture performance of tape when compared to tow (i.e., approximately 44% for a 9 in. (230 mm) notch). It was hypothesized that the most significant contributor to this difference was the larger scale of repeatable inhomogeneity in the fiber-placed laminates, resulting from geometrical nonuniformities in the band cross-section. This characteristic can be observed in ultrasonic scans, as shown in Figure 7.8.1.3(j). In tape, a more uniform thickness, and offset of the course-to-course splices for similarly oriented plies results in much smaller, and non-repeatable, inhomogeneities. It should be noted that the AS4/3501-6 tape panel had a resin content significantly below the process specification.

The improved tow performance, however, did not appear to be robust relative to processing parameters. Results from a series of panels are compared in Figure 7.8.1.3(k). The two 32-tow band panels both demonstrated lower tensile fracture strengths than the 12-tow band panels throughout the full range of notch sizes tested, eliminating a large portion of the tow's performance advantage over tape. The slightly reduced sensitivity to notch size of the 32-tow band panels, however, may result in superior performance for notches above 30 to 40 in. (760 to 1000 mm). Their lower strengths for notch sizes below that range are likely due to a combination of

- Differing tow-placement heads and the resulting band cross-sectional geometry changes,

- Reduced panel thickness and the associated reductions in resin content and/or fiber areal weight (likely caused by different bagging procedures), and

- Reduced prepreg tow unidirectional strength.

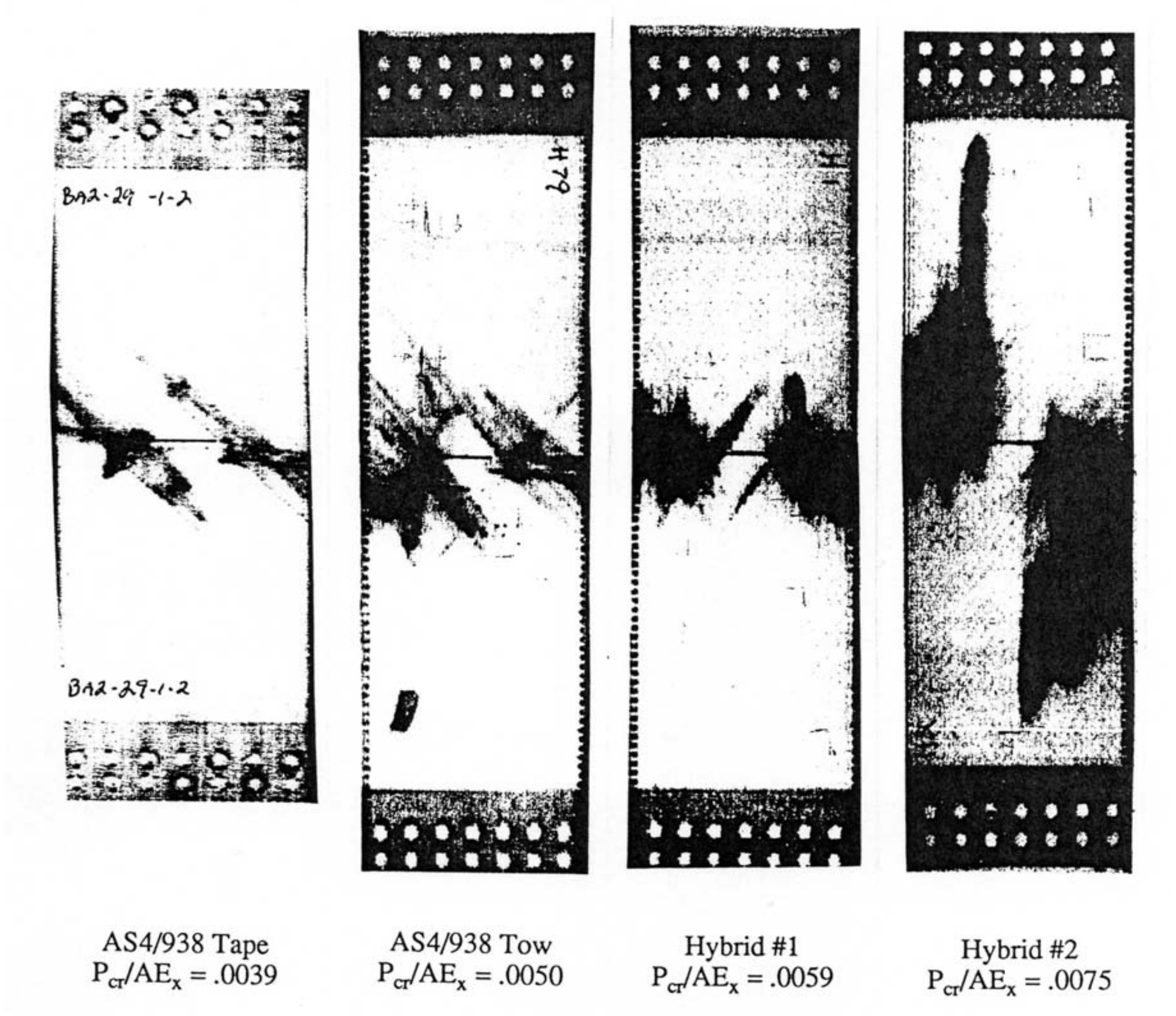

FIGURE 7.8.1.3(e) *Ultrasonic scans of failed fracture specimens.*

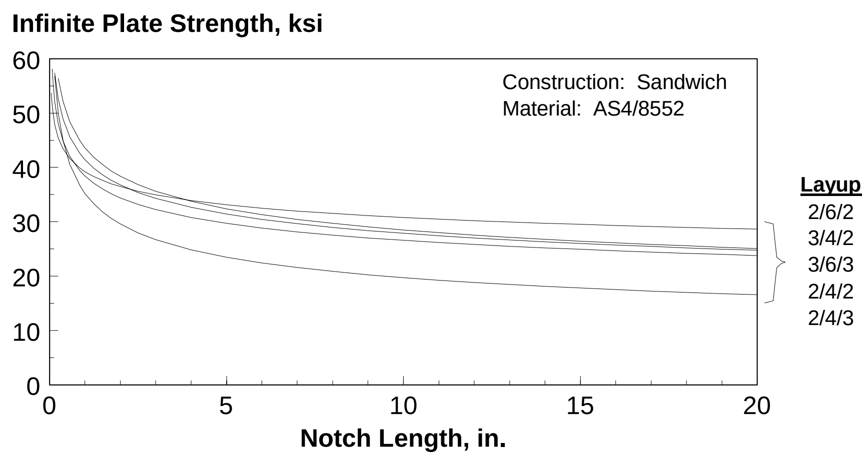

FIGURE 7.8.1.3(f) *Effect of lay-up on tension fracture strength.*

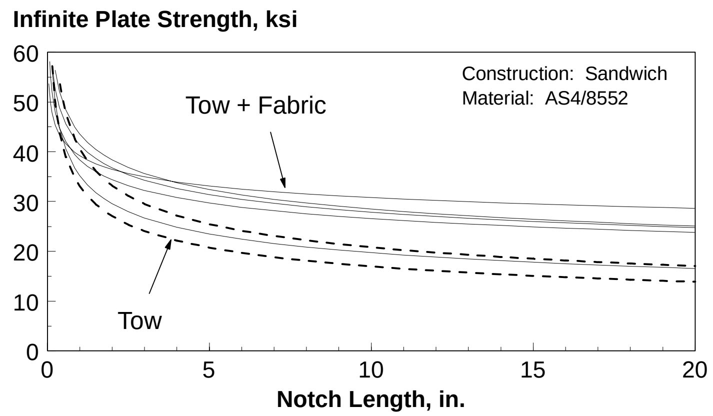

FIGURE 7.8.1.3(g) *Effect of fabric surface plies on tensile fracture strength of AS4/8552.*

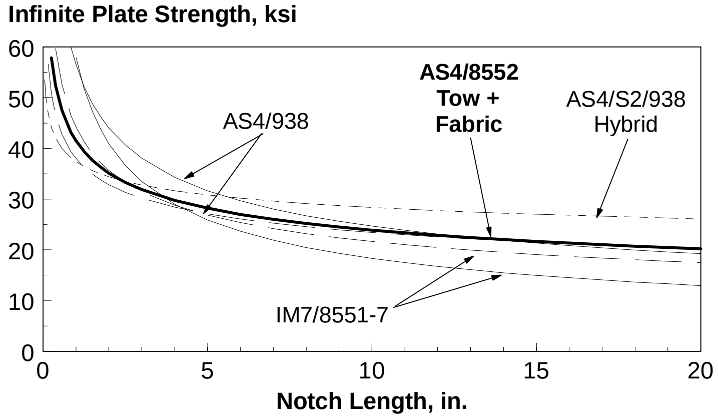

FIGURE 7.8.1.3(h) *Comparison of AS4/8552 (tow/fabric) sandwich tensile fracture results with those of AS4/938 (tow), AS4/S2/938 intraply hybrid (tow) and IM7-8551-7 (tape) laminates.*

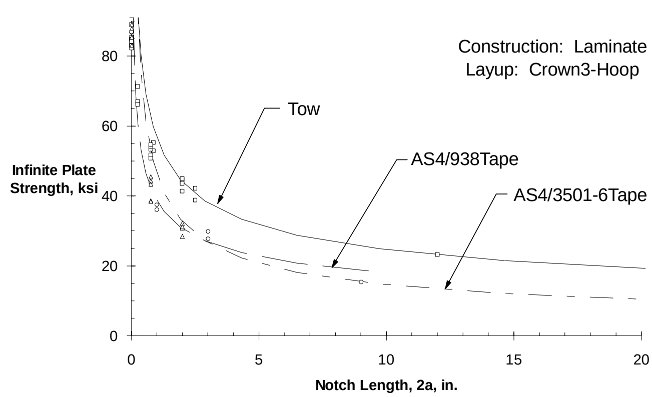

FIGURE 7.8.1.3(i) *Comparison of tow and tape tensile fracture strengths.*

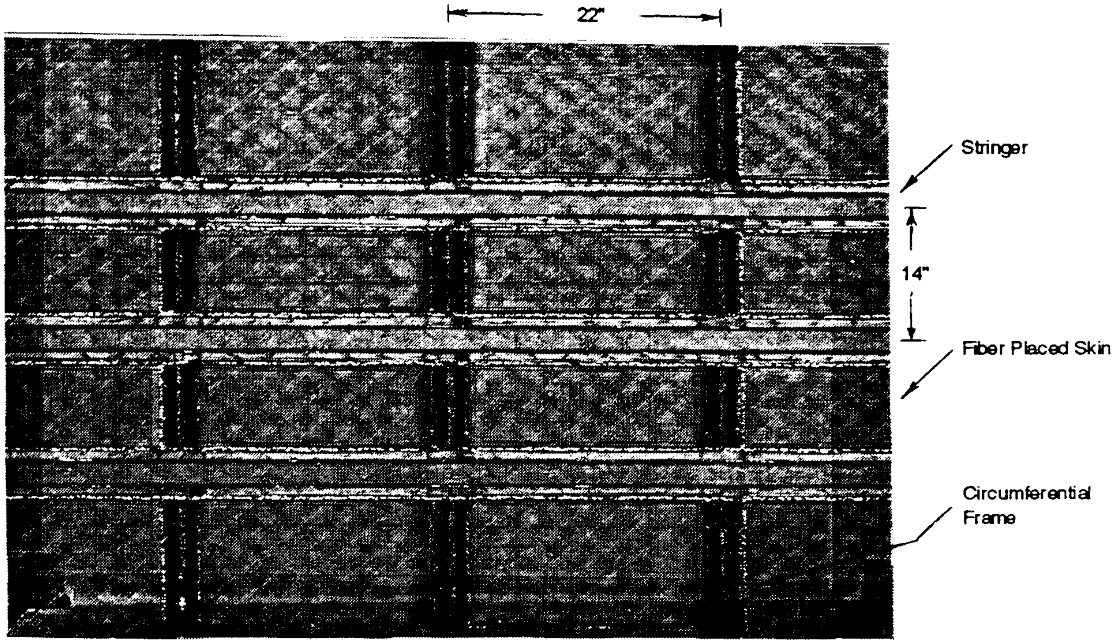

FIGURE 7.8.1.3(j) *Ultrasonic scan showing repeatable inhomogeneities.*

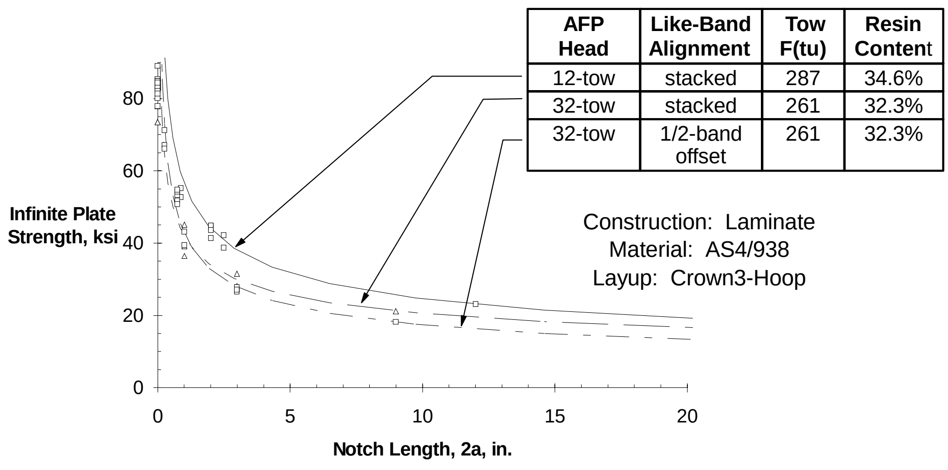

AFP Head	Like-Band Alignment	Tow F(tu)	Resin Content
12-tow	stacked	287	34.6%
32-tow	stacked	261	32.3%
32-tow	1/2-band offset	261	32.3%

FIGURE 7.8.1.3(k) *Effect of AFP processing parameters on tensile fracture strength.*

An additional contributor may have been the age of the material for the 32-tow band panels (approximately 2 years), which could have affected the AFP processing characteristics.

This strength-toughness trade is not unlike that observed in metallic structure. Figure 7.8.1.3(l) compares the response of a brittle-resin (AS4/938) and a toughened-resin (IM7/8551-7) composite material with that of a brittle (7075-T651) and a ductile (2024-T3) aluminum.

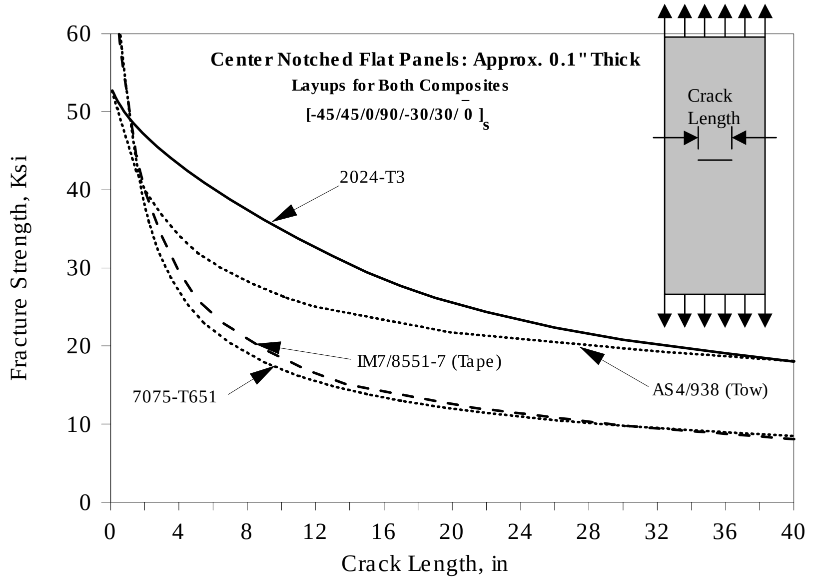

FIGURE 7.8.1.3(l) *Comparison of composite and metallic tensile response.*

Figure 7.8.1.3(m) summarizes the influencing factors on the strength-toughness trade in composite tension fracture. Higher strength but lower toughness resulted from toughened-resin materials and hard (0°-dominated) laminates. Lower strength and higher toughness resulted from brittle-resin materials, soft laminates and intraply hybridization with S2-Glass. Larger scales of repeatable material inhomogeneity appeared to result in improved toughness with little effect on strength. Matrix toughness appeared to have a larger influence on the behavior than laminate type.

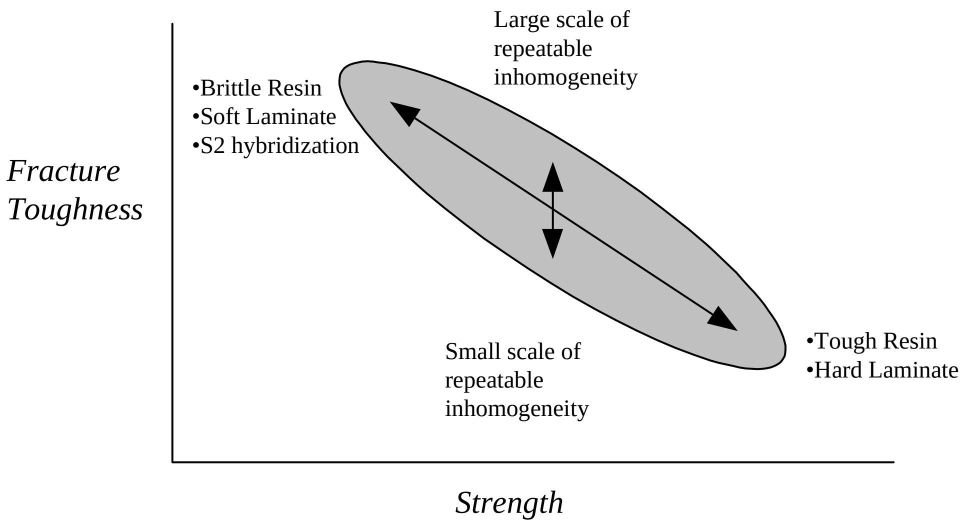

FIGURE 7.8.1.3(m) *Strength-toughness trade-off in tension.*

In addition to the strong strength-toughness trade-offs, non-classical material responses were observed. Notch-tip strain distributions prior to any damage formation were seen to be less severe, and more gradual, than classical theoretical predictions, as shown in Figure 7.8.1.3(n). Similar distributions are predicted by non-local material models, suggesting that such behavior may be active. Large specimen finite-width effects were also found to occur, particularly with those laminate/material combinations that exhibited reduced notch-length sensitivity. As shown in Figure 7.8.1.3(o), isotropic finite-width correction factors, which have been found to differ only slightly from similar orthotropic factors, were unable to account for the differences in the two notch-to-specimen-width data sets. This has been attributed to the significant damage zones created prior to failure, and the resulting interaction with the specimen boundaries.

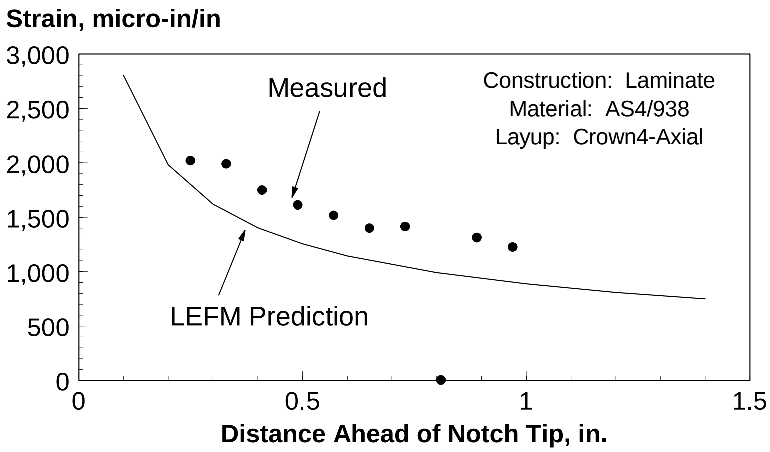

FIGURE 7.8.1.3(n) *Non-classical notch tip strains observed in large-notch tensile fracture tests.*

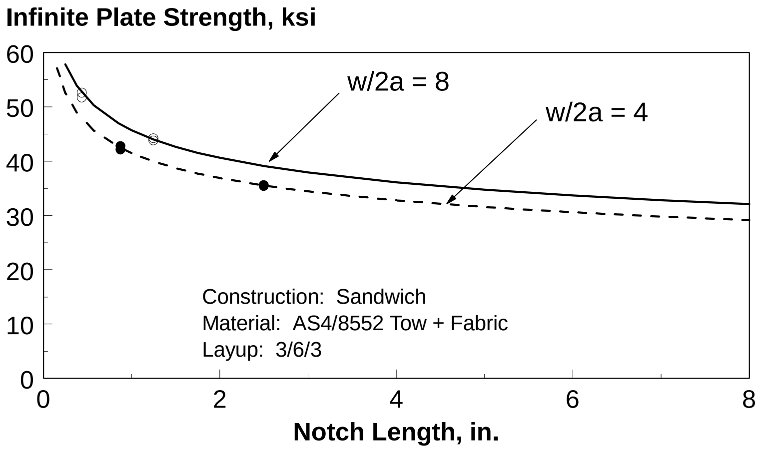

FIGURE 7.8.1.3(o) *Specimen finite width effects for quasi-isotropic AS4/8552 sandwich.*

Most efforts addressing through-penetration damage have used machined notches to represent the damage state created by a penetrating event. Reference 7.8.1.3(c) conducted limited tensile fracture comparisons of 0.875 in. (22.2 mm) through-penetrations and machined cracks. Creation of the penetrations and the resulting damage are discussed in Section 7.5.1.2. The strength results are shown in Figure 7.8.1.3(p). For the thinner specimens (t = .059 - .074 in. (1.50 - 1.80 mm)), penetration strengths were within 10% of the machined-crack strengths. One notable exception was for a toughed resin material (IM7/8551-7), which had post-impact tensile fracture strengths that were 20% lower than those for specimens with machined cracks. Evidence suggests that impact penetration of these laminates may result in effective crack extension via fiber breakage. In the case of the thickest laminates tested (t = 0.118 in. (3.00 mm)), the tensile fracture strengths of specimens with impact penetrations were up to 20% higher than those for specimens with machined cracks. This difference in response from the thinner laminates was attributed to the formation of larger delaminations near the crack tip, which reduced the stress concentration.

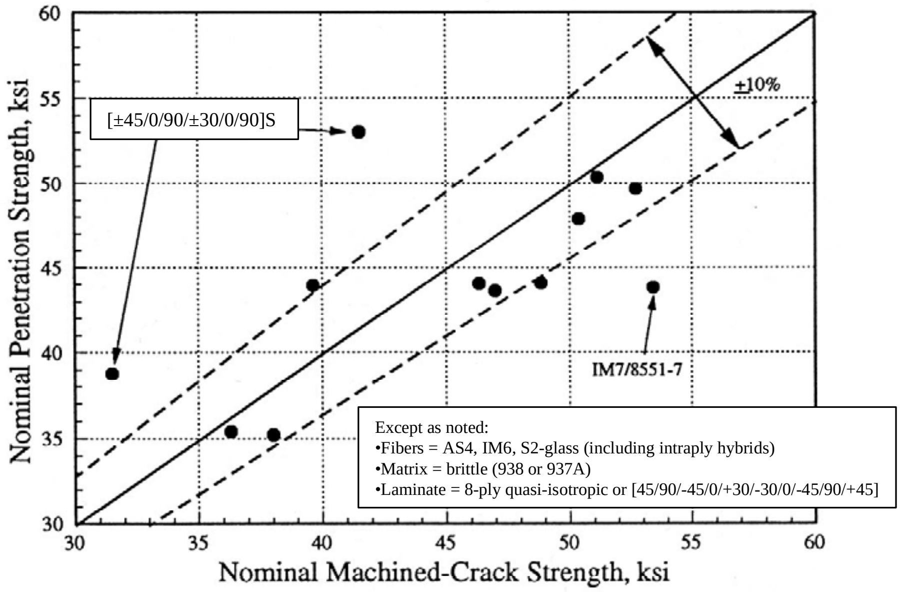

FIGURE 7.8.1.3(p) *Comparison of penetration and machined-crack strengths.*

Compression. The compressive fracture results showed significantly lower strengths than for tension, as illustrated in Figure 7.8.1.3(q). The effect of lay-up appears somewhat smaller than that for tension. The compression results also exhibit a reduced notch-length sensitivity relative to LEFM.

Unlike the tensile fracture case, where strong specimen finite-width effects accompanied reduced notch-length sensitivities, the finite-width effects in compressive fracture did not differ significantly from those predicted by isotropic correction factors, as shown in Figure 7.8.1.3(r). This suggests that large damage zones are not present prior to specimen failure, which is consistent with experimental observations.

The strongest effect observed in the compression testing was that of thickness. As shown in Figure 7.8.1.3(s), notched strengths of a wide range of materials, lay-ups, cores, and construction all with total laminate/facesheet thicknesses between 0.11 and 0.20 in. (2.80 and 5.1 mm) are within approximately ±10% of an average curve The several tests of sandwich laminates with total facesheet thicknesses of 0.44 in. (11 mm) resulted in strengths approximately 25% higher than those of the thinner laminates. This behavior was also seen in a subsequent study; the results are shown in Figure 7.8.1.3(t) (Reference 7.8.1.2.4(b)). This insensitivity to material and lay-up variables and the strong sensitivity to thickness suggest that local instability may be controlling failure.

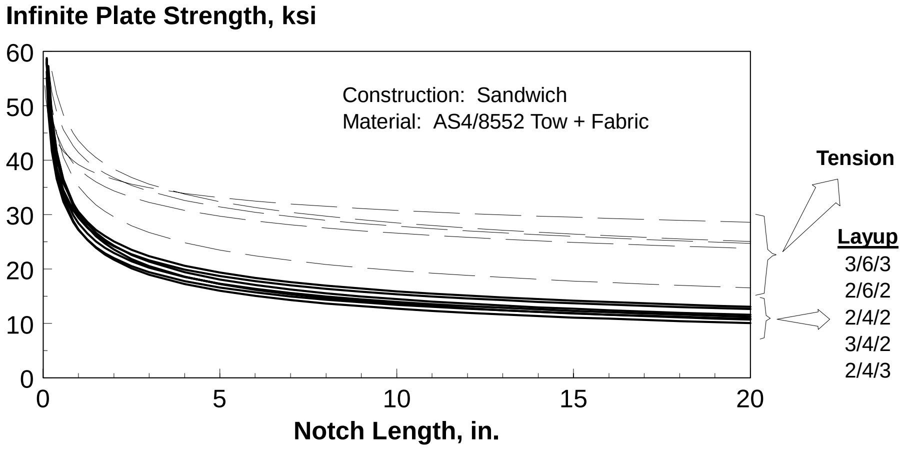

FIGURE 7.8.1.3(q) *Comparison of compressive and tensile fracture results.*

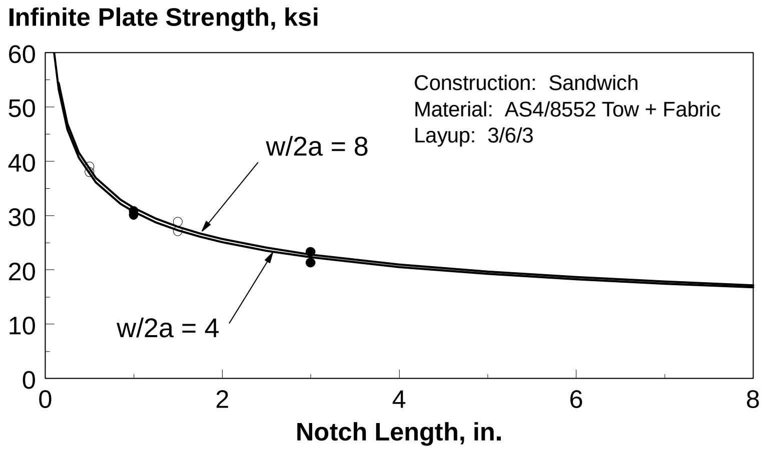

FIGURE 7.8.1.3(r) *Specimen finite width effects in compression.*

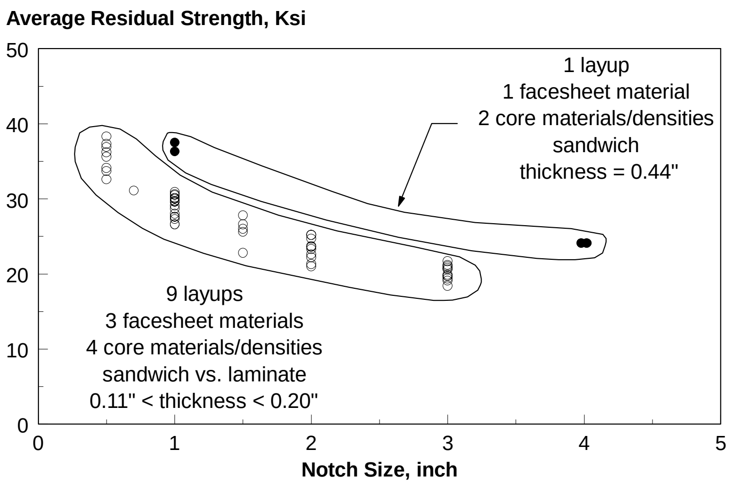

FIGURE 7.8.1.3(s) *Thickness effects on compressive fracture strength.*

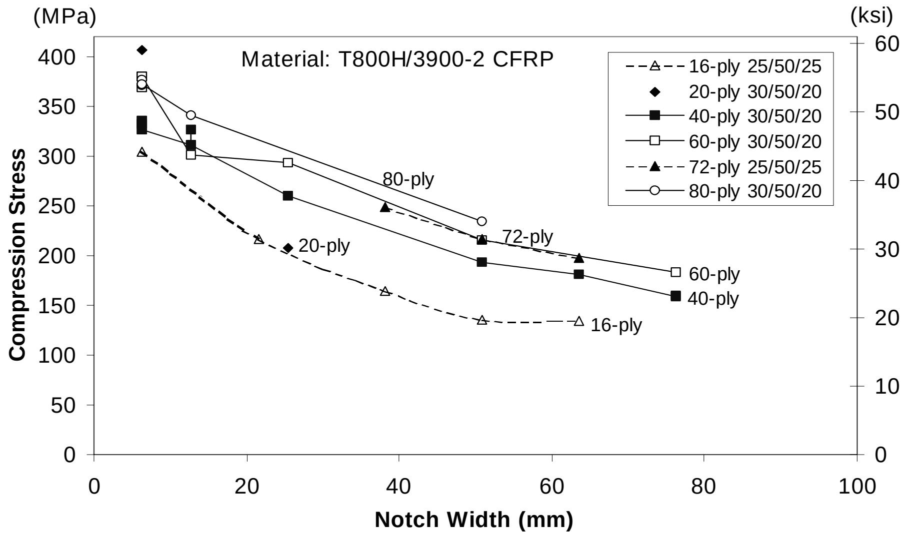

FIGURE 7.8.1.3(t) *Thickness effects on compression-fracture strength.*

7.8.1.3.1 Stitched skin/stiffener panels

A large flat wing panel with blade stiffeners containing an 8.0 in. (20.3 cm) long cut that also severed the central stiffener was testing in tension (References 7.8.1.3.1(a) and (b)). The skin material was made from 54 layers of dry uniweave fabric that were stitched together using Kevlar 29 thread. The lay-up of the skin was $[0/45/0/-45/90/-45/0/45/0]_{3S}$. The stiffener material was made from 36 layers of the dry uniweave fabric with a lay-up $[0/45/0/-45/90/-45/0/45/0]_{2S}$. The T-section stiffeners were made by stitching together dry angle-section stiffeners that were formed from the dry skin fabric. The flanges of the T-section stiffeners were stitched to the skin, and the panel was then infiltrated with 3501-6 resin. The skin fractured at a strain of 0.0023 in/in, the fracture propagated to the edge of the stiffener and was arrested. With increasing load, the fracture turned and grew parallel to the stiffener. At a strain of 0.0034 in/in, failure occurred at the loading grips. Thus, the stitched stiffeners resulted in considerable increase in failure strain.

7.8.2 Design issues and guidelines

7.8.2.1 Stacking sequences

When impact damage is dominated by fiber failure (e.g., Reference 7.8.1.2.8(c)), it is desirable to stack primary load carrying plies in locations that minimize fiber failure. Since fiber failure typically occurs first near outer surfaces, primary load carrying plies should be concentrated towards the center of the LSS. Experience to date suggests that a homogeneous LSS might be best for overall CAI performance dominated by matrix damage (Reference 7.8.2.1).

7.8.2.2 Sandwich structure

Caution should be applied when using sandwich material combinations where significant impact damage can occur within the core, without visible surface indications in the facesheet. (This type of impact critical damage state (CDS) has been identified for certain types of honeycomb (Reference 7.8.1.2.2(d)) and foam cores.) This is particularly true for compressive or shear loaded structures in which such damage may grow undetected to critical sizes. Simple impact screening tests can be used to identify this failure mechanism and the related drops in residual strength.

7.8.3 Test issues

Structural residual strength tests are typically performed to support impact surveys, detailed design development and provide structural substantiation data. Figure 7.8.3 shows the results from such a test performed with a stiffened skin panel design. Multiple impacts, spaced far enough to avoid interactions, may be used in such studies to identify the critical impact location. A range of impact damage sizes in smaller test panels and elements can help to establish the shape of the residual strength curve. This should provide the necessary building blocks to analytically determine ADL and CDT as a function of structural load paths. Tests supporting the analysis of structural configurations should be large enough to allow load redistribution and the associated damage accumulation/arrest. As a further word of caution, residual strength tests with very wide but short panels should be avoided because the effects of damage may be masked by an insufficient length for proper load introduction. The results from such tests may be unconservative. Also, the skin buckling pattern of the test panel should match that of the full-scale structure, otherwise the local stresses in the vicinity of the impact damages may not be representative and thereby produce an invalid failure result.

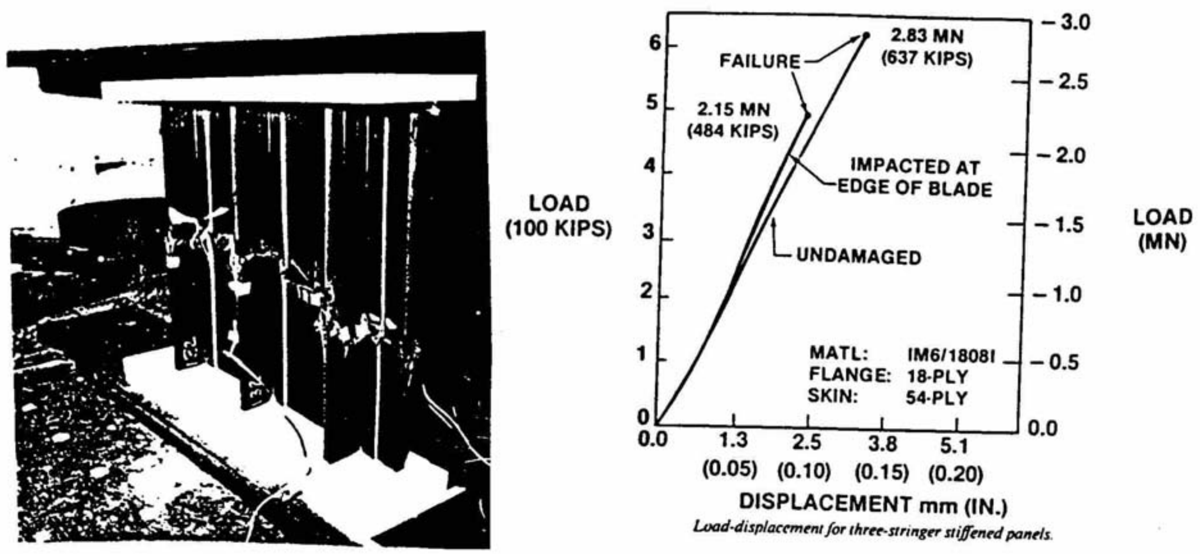

FIGURE 7.8.3 *Post-impact compressive strength test results for a stiffened structural configuration (Reference 7.8.1.2.9(b)).*

7.8.3.1 Impact tests on coupons

This section is reserved for future use.

7.8.3.2 Impact tests on stiffened panels

This section is reserved for future use.

7.8.3.3 Impact tests on sandwich panels

This section is reserved for future use.

7.8.3.4 Tests for large through-penetration damage to stiffened panels

This section is reserved for future use.

7.8.3.5 Tests for large through-penetration damage to sandwich panels

This section is reserved for future use.

7.8.4 Analysis methods - description and assessment

7.8.4.1 Large through-penetration damage

In many instances, damage tolerance assessments require the consideration of residual strength in the presence of large notches (i.e., greater than 6 inches (150 mm)). Analysis methods that can extrapolate from small notch strengths, determined from relatively small tests, to large notch sizes are highly desirable.

This section focuses on analytical methods for large through-penetration type damage in unstiffened and stiffened panels resulting from severe accidental or "discrete source" damage. For metal skins of commercial transport structures, discrete source damage is usually represented by a cut. The length of cut has traditionally been two bays of skin including one severed stiffener or frame (see Figure 7.8.4.1(a)). Similar configurations are cited in MIL-A-83444 for “fail safe crack arrest structure.” For composite laminates, cuts also give a lower bound to tension strengths. See the results in Figure 7.8.4.1(b) for cuts, impact damage, and holes (References 7.8.4.1(a), 7.8.1.2.8(c), and 7.8.2.1).

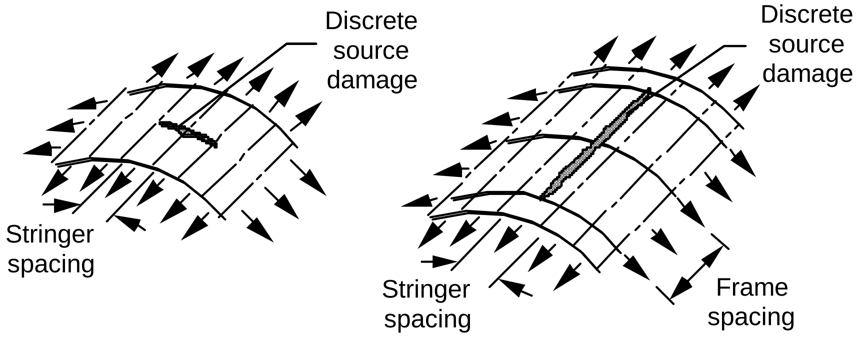

FIGURE 7.8.4.1(a) *Schematics of discrete source damage.*

Numerous models and methods have been developed for fracture of composites with crack-like cuts and tension loads. The following is a list of the methods discussed in the following sections. All of these methods represent a composite structure as an anisotropic continuum amenable to classical lamination theory.

1. Mar-Lin model.
2. Strain softening method.
3. Linear elastic fracture mechanics (LEFM)
4. R-curve method.

The primary purpose of fracture analysis methods is to provide failure predictions beyond the notch sizes and structural geometries tested during material characterization. To ensure this extrapolation capability, suitable models must revolve around theories with a basis in the physics of the problem. It is also desirable to minimize the number of degrees-of-freedom in a model to reduce material testing requirements. The following is a discussion of various analysis methods, and a brief evaluation of how well they predict the test data.

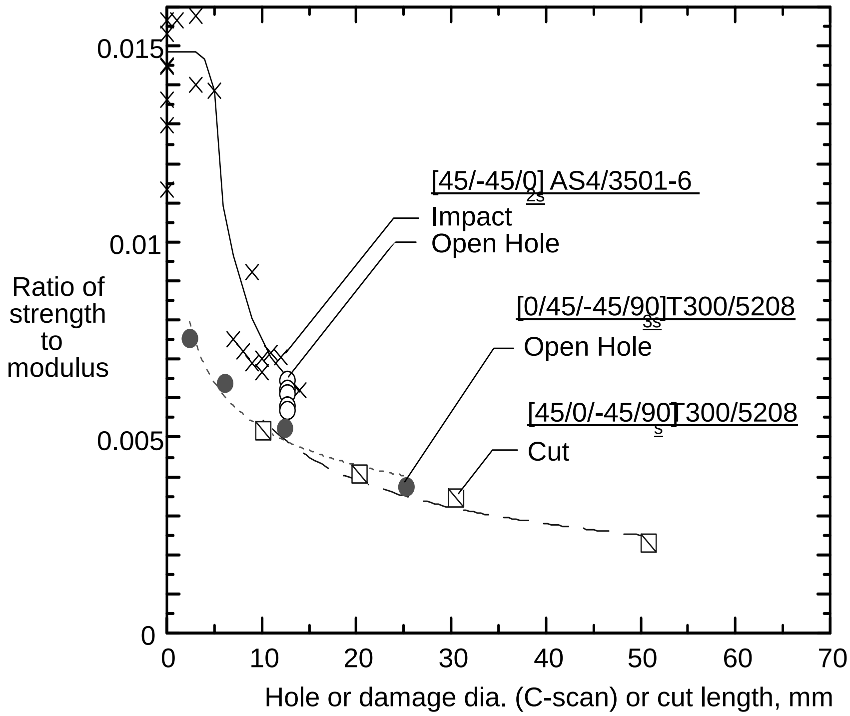

FIGURE 7.8.4.1(b) *Tension strengths of laminates (prepreg tape) with impact damage, open holes, and cuts. (References 7.8.4.1(a), 7.8.1.2.8(c), and 7.8.2.1).*

Summary of Tensile Failure Criteria. Several failure criteria have been proposed for tensile fracture. In the following discussion of the criteria, σ_n^∞ and σ_o are the notched and unnotched strengths of an infinite plate, respectively, and a is the half-crack length (Reference 7.8.1.2.8(e)).

The stress distribution at a crack tip is singular for classical continuum theories. In linear elastic fracture mechanics (LEFM) for homogeneous materials, a square-root singularity exists, and failure is predicted by

$$\sigma_n^\infty = \frac{K_{IC}}{\sqrt{\pi a}} \qquad 7.8.4.1(a)$$

where K_{Ic} is the critical stress intensity factor. This approach suffers from the physically unacceptable situation of infinite stresses at the crack tip. As a consequence, σ_n^∞ increases rapidly with decreasing a and σ_o becomes infinite, in the limit, as a approaches 0.

In composites, this has been addressed by several theories through the use of a characteristic dimension, inherent flaw size or critical damage zone length. The Whitney-Nuismer (WN) point-stress criteria (References 7.8.4.1(b) and (c)), for example, predicts failure when the stress at a characteristic dimension, d_1, ahead of the crack tip equals or exceeds σ_o. The notched strength, then, is given by

$$\sigma_n^\infty = \sigma_0 \sqrt{(1 - \left(\frac{a}{a + d_1}\right)^2} \qquad 7.8.4.1(b)$$

The two parameters in this model that must be determined are σ_o and d_1.

The Pipes-Wetherhold-Gillespie (PWG) model (References 7.8.4.1(d) and (e)) extends the WN point-stress model to include an exponential variation of d_1 with crack length. This provides added flexibility in predicting small crack data, but requires an additional parameter to be determined.

Another multi-parameter model, proposed by Tan (Reference 7.8.4.1(f)), uses a characteristic dimension to predict failure of a plate with an elliptical opening subjected to uniaxial loading. In this model, a high-aspect-ratio ellipse is used to simulate a crack. Notched strengths are predicted by factoring the actual unnotched laminate strength by the ratio of predicted notched to predicted unnotched strengths. Both of these predicted strengths are obtained using a quadratic failure criterion in conjunction with the first-ply-failure technique. The predicted notch strength is determined by applying the failure criterion at a characteristic dimension away from the crack. The coefficients in this criterion are the additional parameters that must be determined.

The Poe-Sova (PS) model (References 7.8.4.1(g) and (h)) may also be formulated with a characteristic dimension, d_2, but predicts failure when the strain at that distance ahead of the crack tip equals or exceeds the fiber failure strain. The notched failure stress is given by

$$\sigma_n^\infty = \frac{\sigma_0}{\sqrt{1 + \frac{a\xi^2}{2d_2}}} \qquad 7.8.4.1(c)$$

where ξ is a functional that depends on elastic constants and the orientation of the principal load carrying plies. The characteristic dimension relates to a material toughness parameter, which was found to be relatively independent of lay-up. The two parameters that must be determined for this model are the fiber failure strain and d_2.

Two other frequently-used models, Waddoups-Eisenmann-Kaminski (WEK) and WN average stress, each have undamaged strength as the first parameter. The second parameters for WEK and WN average stress models are referred to as critical damage size and average stress characteristic dimension, respectively. The WEK model (Reference 7.8.4.1(i)) applies LEFM to an effective crack that extends beyond the actual crack by the inherent flaw size. The WN average stress model (References 7.8.4.1(b) and (c)) assumes failure when the average stress across the characteristic dimension equals or exceeds σ_o. Both the WEK and WN average stress models were found to be functionally equivalent to the PS model if a linear strain-to-failure is assumed.

The approaches described above which use a length parameter (e.g., characteristic dimension) were formulated to account for observed experimental trends for composites. In practice, these length parameters are determined from notched strength data and given limited physical meaning in relationship to any micro-structural dimension of the material. They are often thought of as classical analysis correction factors, which enable the user to account for apparent changes in the stress distribution or fracture toughness with increasing crack size. It should be noted that the length parameter calculated for the WN point stress, WN average stress, PS, WEK, and Tan models will generally take on different values for the same set of data.

A more physically acceptable approach to predicting composite fracture may involve changes in the crack tip stress distribution as a function of material length parameters that define levels of inhomogeneity. Simplified analysis performed to evaluate the effect of inhomogeneities at the fiber/matrix scale indicated that the crack size should be at least three orders of magnitude larger than the fiber diameter to vindicate the classical continuum homogeneity assumption (Reference 7.8.4.1(j)). The results of Reference 7.8.4.1(j) show that inhomogeneity tends to reduce stress intensity factors for a range of crack lengths that is related to the level of inhomogeneity. Considering the fiber/matrix dimensional scale, the crack length range affected by inhomogeneity is smaller than that for which characteristic lengths are needed to correct classical fracture analyses for graphite/epoxy composites. However, higher levels of inhomogeneity exist in tape and tow-placed laminates due to manufacturing processes. These characteristics of composite materials may be responsible for the reduced stress concentrations traditionally found for small cracks.

Solutions to fracture problems using generalized continuum theories have also yielded results consistent with experimental trends in composites, without a semi-empirical formulation. Generalized continuum theories are formulated to have additional degrees of freedom which characterize micro-structural influence. The stress concentrations for such theories change as a function of relationships between notch geometry and material characteristic lengths (e.g., References 7.8.4.1(k) through 7.8.4.1(m)). Note that the characteristic lengths of generalized continuum models are different than those in models described earlier because they are fundamentally based on moduli from the theory. As a result, the moduli have relationships with other material behavior (e.g., wave propagation) and their values can be confirmed from a number of independent experimental measurements. Ultrasonic wave dispersion measurements have been used to predict the moduli and notched stress concentration for wood composite materials (Reference 7.8.4.1(l)). Unfortunately, considerably more work is needed to develop generalized continuum theories for applications with laminated composite plates.

For inhomogeneous materials, the stress distribution at the crack tip is also not limited to a square-root singularity. The Mar-Lin (ML) model (References 7.8.4.1(e) and 7.8.4.1(n)) allows the singularity, n, to be other than square-root. The notched failure stress is given by

$$\sigma_n^\infty = \frac{H_c}{(2a)^n} \tag{7.8.4.1(d)}$$

where H_c is the composite fracture toughness. In general, H_c and the exponent n are the two parameters that must be determined. In the Reference 7.8.4.1(e) and 7.8.4.1(n) studies, the exponent, n, was related to the theoretical singularity of a crack in the matrix, with the tip at the fiber/matrix interface. For this case, the singularity is a function of the ratio of fiber and matrix shear moduli and Poisson's ratios. Using this method, the singularities for a range of typical fiber/matrix combinations were determined to be between 0.25 and 0.35.

The Tsai-Arocho (TA) model (Reference 7.8.4.1(o)) combines the non-square-root singularity of the ML model with the inherent flaw concept of the WEK method. At the expense of another parameter, additional flexibility in predicting small-crack strengths is gained, although this effect lessens as the order of the singularity is reduced.

Other theoretical approaches which have been applied to predict tension fracture in composites include damage zone models, DZM (e.g., References 7.8.4.1(p) and (q)), and progressive damage analysis, PDA (e.g., References 7.8.4.1(r) and (s)). Both methods use finite elements to account for notch tip stress redistribution as damage progresses. The DZM utilized a Dugdale/Barenblatt type analysis for cohesive stresses acting on the surface of an effective crack extension over the damage zone length. As was the case for characteristic-length-based failure criteria described above, a Barenblatt analysis (Reference 7.8.4.1(t)) resolves the stress singularity associated with cracks. The PDA methods account for the reduced stress concentration associated with mechanisms of damage growth at a notch tip by reducing local laminate stiffness. From a practical viewpoint, both DZM and PDA methods may be more suitable in determining finite width effects and for predicting the performance of final design concepts.

Failure Criteria Functionality. This subsection reviews the degrees of freedom in curves from two parameter models which have been used extensively to predict tensile fracture for composite laminates (Reference 7.8.1.3(c)). This background will help to interpret discussions that compare theory with experimental databases. Predictions for both small crack (2a ~ 1.2 in. (30.5 mm)) and large crack (2a up to 20 in. (510 mm)) sizes will be compared. The former crack sizes are characteristic of much of the data collected for composites to date. Four theories are covered in detail; classical LEFM, WN (point stress), PS (point strain), and Mar-Lin. As a baseline for comparing changes in crack length predicted by the four theories, curves will be generated based on average experimental results (finite width corrected) for the IM6/937A tape material with W/2a = 4 and a lay-up of [+45/90/-45/0/+30/-30/0/-45/90/+45]. This will ensure that all theories agree for at least one crack length.

Figure 7.8.4.1(c) shows a comparison of the four theories for small crack sizes. Only a small difference is seen between PS and WN criteria. A close examination of the LEFM and ML curves indicates that the singularity has a significant effect on curve shape. For crack lengths less than the baseline point, ML predictions are less than those of LEFM. For crack lengths greater than the baseline point, the opposite is true, and theories tend to segregate based on singularity (i.e., WN, PS, and LEFM yield nearly the same predictions).

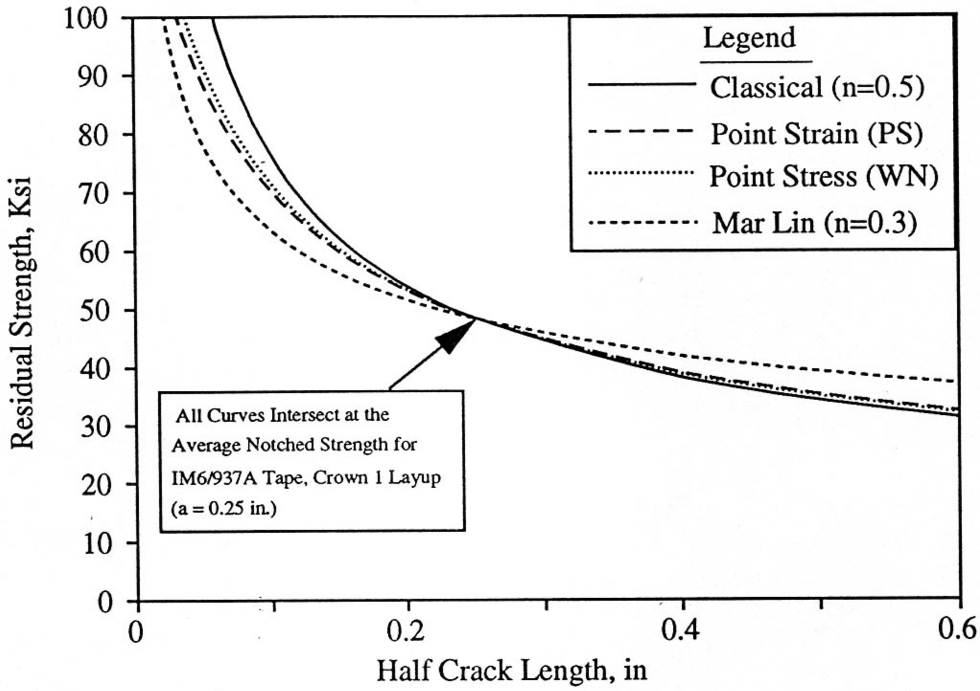

FIGURE 7.8.4.1(c) *Comparison of curve shapes for notched strength prediction theories in small crack range.*

Figure 7.8.4.1(d) shows that singularity dramatically affects differences between predictions in the large crack length range. The ratio of notched strength predictions for theories with the same order of singularity becomes a constant. For example, WN and LEFM become functionally equivalent and the relationship

$$K_{IC} = \sigma_0 \sqrt{2\pi d_1} \qquad 7.8.4.1(e)$$

will yield a value for K_{Ic} such that the two theories compare exactly for large cracks.

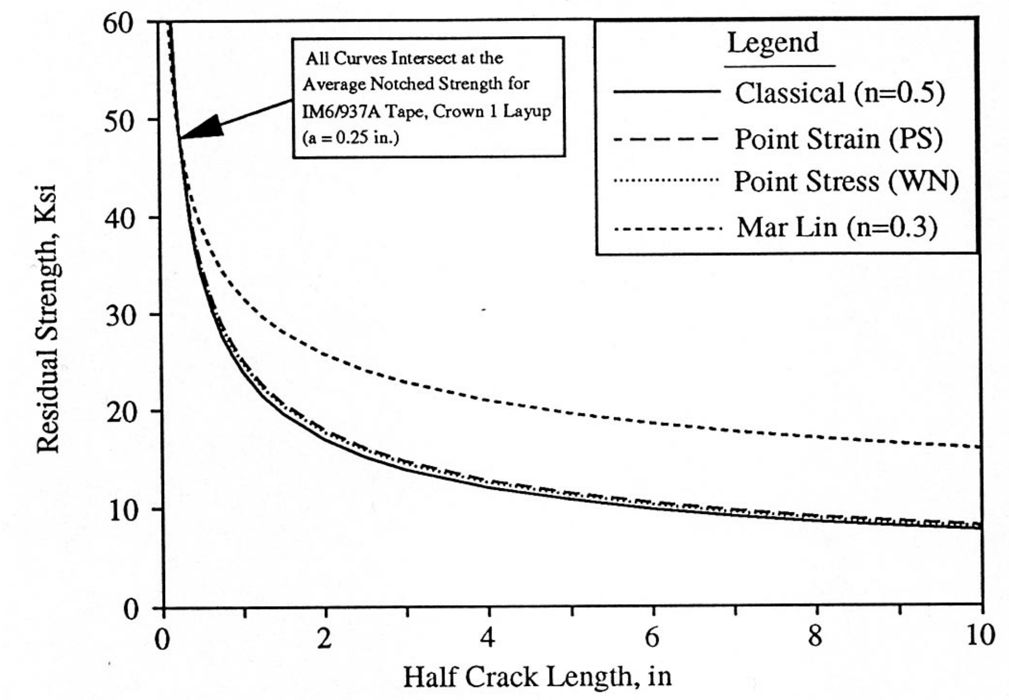

FIGURE 7.8.4.1(d) *Comparison of curve shapes for notched strength prediction theories in large crack range.*

In order to compare the effect of a range of singularities on notched strength predictions, curves in Figures 7.8.4.1(e) and (f) vary the value of n from 0.1 to 0.5. All curves in Figure 7.8.4.1(e) cross at the baseline point used to determine the corresponding fracture toughness values. By allowing both variations in fracture toughness and order of singularity, the ML criterion could statistically fit a wide range of notched strength data trends for small crack sizes. Extreme caution should be used in implementing such an approach however, since, as shown in Figure 7.8.4.1(f), projections to large crack sizes are strongly dependent on the assumed singularity.

Figures 7.8.4.1(g) and (h) show how the two parameters in the WN point stress criteria, σ_o and d_1, affect both the shape and relative positions of notched strength curves. Again comparisons are made with classical LEFM equations passing through common points. The lower set of curves corresponds to the baseline data point. Unlike the LEFM curves which rise sharply with decreasing crack length, the point stress theory has a finite strength, σ_o, at a = 0. For a given value of σ_o, increasing d_1 tends to increase the predicted notched strength and, hence, has an effect similar to increasing K_{Ic} in LEFM (see upper curves in Figures 7.8.4.1(g) and (h).

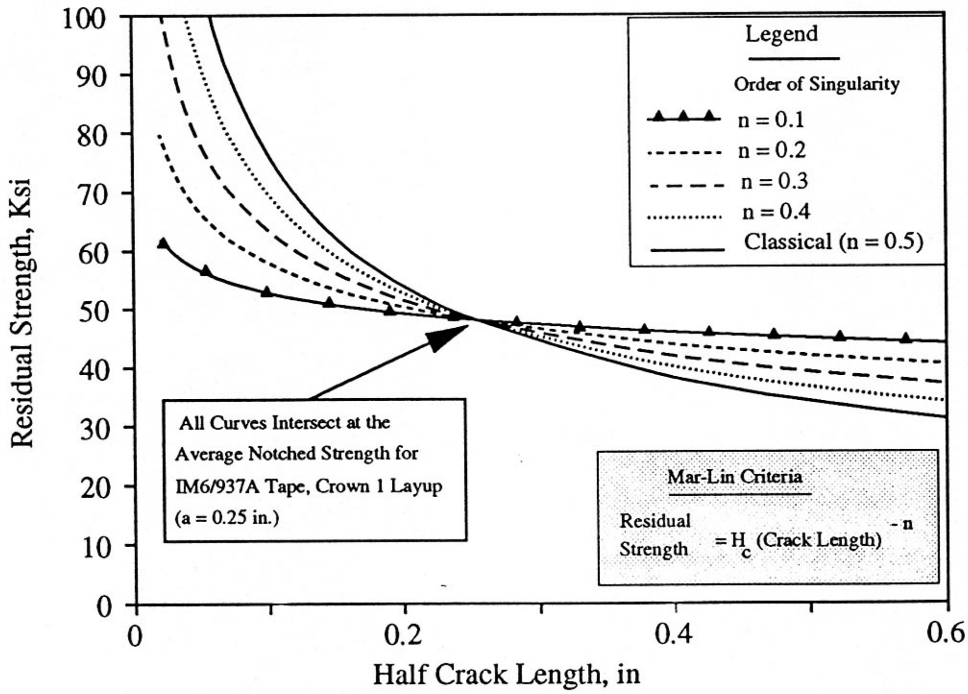

FIGURE 7.8.4.1(e) *Effect of singularity on curve shapes for notch strength prediction theories in small crack range.*

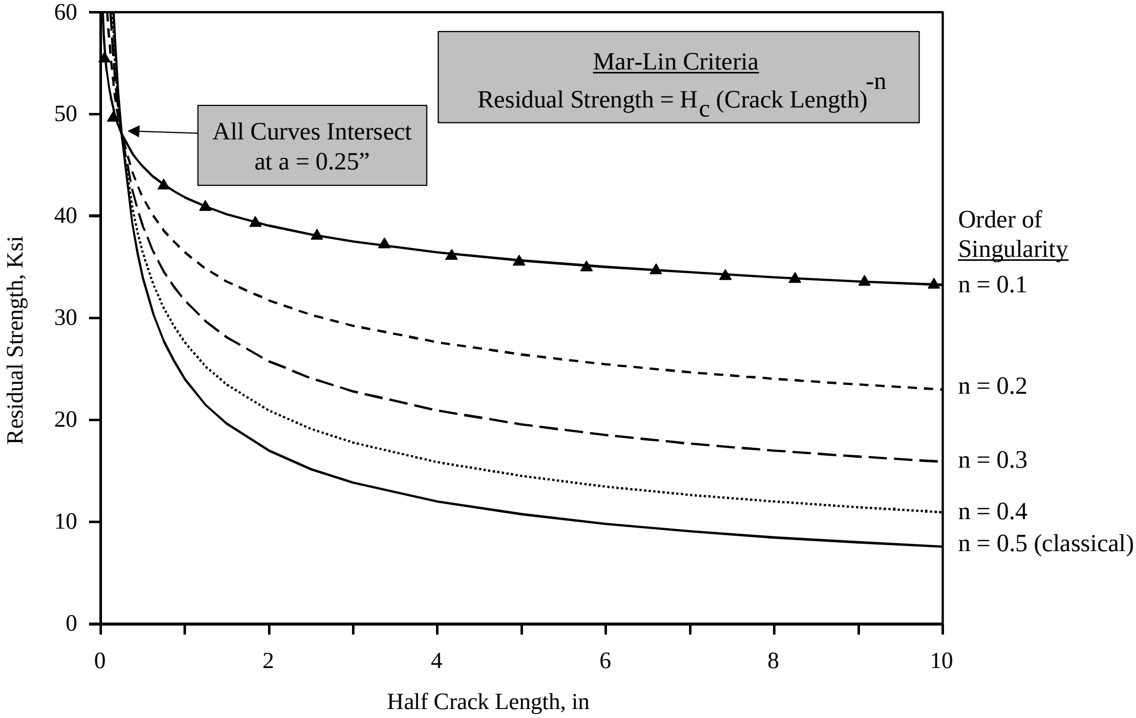

FIGURE 7.8.4.1(f) *Effect of singularity on curve shapes for notch strength prediction theories in large crack range.*

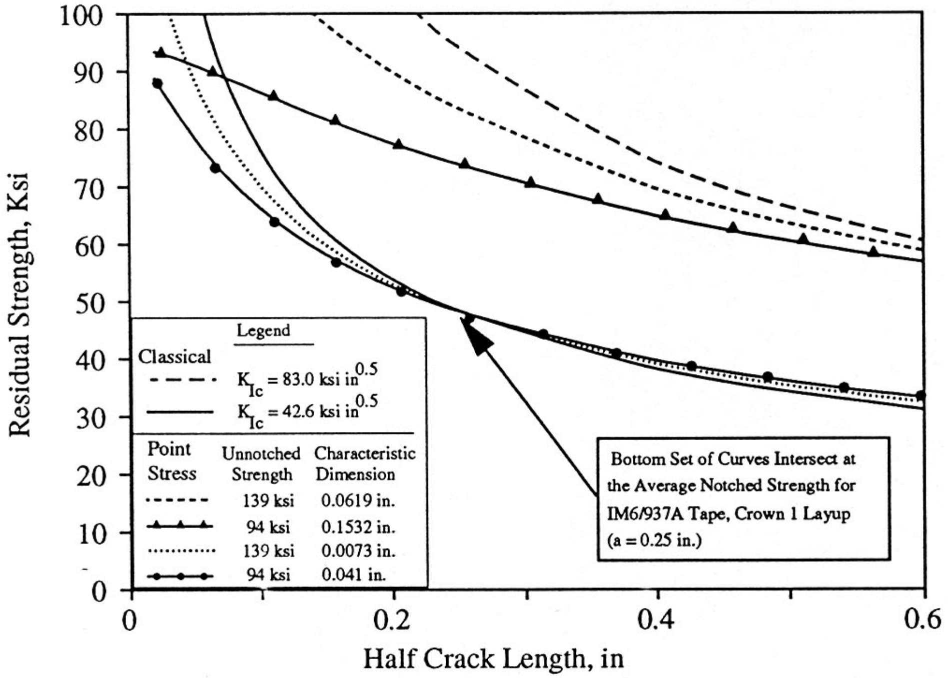

FIGURE 7.8.4.1(g) *Effects of characteristic dimension and unnotched strength on curve shapes for notch strength prediction theories in small crack range.*

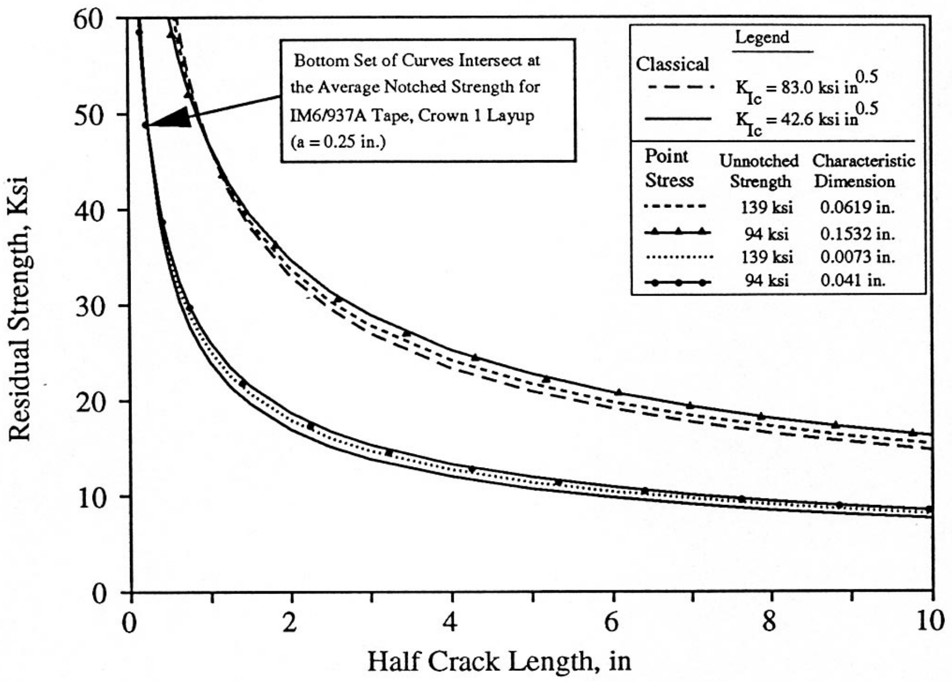

FIGURE 7.8.4.1(h) *Effects of characteristic dimension and unnotched strength on curve shapes for notch strength prediction theories in large crack range.*

In the small crack length range, a reduced value of σ_o can have the appearance of reducing the singularity. The curve shapes for lower curves in Figure 7.8.4.1(g) indicate that various combinations of σ_o and d_1 could be selected to represent data trends that follow any of the singularities shown in Figure 7.8.4.1(e) (particularly for a $\leq$ 0.25). For small crack sizes characteristic of past databases, the curve-fits for WN and ML theories are nearly indistinguishable (Reference 7.8.1.2.8(e)). This inability to distinguish lower orders of singularity in past composite data may relate to measured values of σ_o that were low due to edge delamination phenomena in finite width specimens. For large crack lengths, Figure 7.8.4.1(h) shows that the magnitude of σ_o and d_1 determine residual strength, but curve shape is dominated by the order of singularity. As discussed in reference to Figure 7.8.4.1(f), the proper order of singularity is best judged at large crack lengths.

Modified analysis methods that include "characteristic dimensions" are better at predicting small crack experimental trends than LEFM with the classical singularity of 0.5. This suggests the classical crack stress intensity is inaccurate for composites and that the actual distribution has characteristics that have an effect similar to the point stress and point strain formulations (i.e., stress intensity that is generally lower and a function of notch size). A hypothesis was posed based on evidence from analysis and experiments that suggest small crack stress distribution is strongly influenced by material inhomogeneity. Reductions in stress concentration occur for cracks having a length within several orders of magnitude of the material inhomogeneity scale. For a given crack size, therefore, notched strength increases with increasing scale of inhomogeneity. Possible scales of inhomogeneity include fiber diameter, tow width, and hybrid repeat unit width.

Each fracture theory converges to a curve dominated by the order of singularity at large crack sizes. Larger crack data (i.e., up to 2.5 in. (63 mm) long) for several materials and laminate lay-ups tended to converge with failure criteria having a singularity of 0.3. One notable exception was a toughened material, IM7/8551-7, that tended to converge to the classical curve for singularity of 0.5. This and other evidence suggested that the effective singularity was dependent on matrix splitting. The ability to split and relieve the notch stress concentration relates to characteristics of the material and laminate lay-up.

The finite element method provides the flexibility and accuracy for the multitude of configurations encountered in aircraft structure. Two methods exist to account for the effects of damage progression on load redistribution in finite element models. Progressive damage methods that degrade various stiffness properties of individual elements as specified failure criteria are met (e.g., Reference 7.8.4.1(s)) have shown some successes in modeling damage growth in specimen configurations. The magnitude of the calculations, however, provides a significant obstacle to incorporating them into the complex models required for stiffened structure.

Strain-softening models (e.g., References 7.8.4.1(d) and 7.8.4.1(u)), however, appear to have the required simplicity. Such models have been successfully used in the reinforced concrete industry, and provide the ability to capture the global load redistribution that occurs as the crack-tip region is softened by damage formation, without the computational concerns of detailed progressive damage models. These strain-softening models use a nonlinear stress-strain law that allows for a decreasing load-carrying capability of the material as strains increase beyond a critical value. A range of softening laws has been proposed. In finite element models, nonlinear springs can be used to simulate this behavior. The models can be calibrated using small-notch test results, then extended to large-notch configurations. Issues associated with modeling and calibrating bending stiffness reductions are being evaluated. These reductions are of concern for most structural configurations, where out-of-plane loading, load eccentricities, and bending loads are common. A more detailed discussion of strain-softening methods is given in Section 7.8.4.1.2

7.8.4.1.1 Reduced singularity (Mar-Lin) model

References 7.8.1.3(c) and (d) demonstrated that many material/laminate combinations have significantly lower sensitivities to large changes in notch size than predicted by classical fracture mechanics. The Mar-Lin model (References 7.8.4.1(e) and 7.8.4.1(n)) allows for non-square-root singularities that capture these reduced sensitivities by having a variable exponent, n. Specifically, the notched failure stress is given by

$$\sigma_N^\infty = \frac{H_c}{(2a)^n} \qquad 7.8.4.1.1(a)$$

where σ_N^∞ is the infinite plate notched strength, and H_c is the composite fracture toughness. In the Reference 7.8.4.1(e) and 7.8.4.1(n) studies, the exponent, n, was related to the theoretical singularity of a crack in the matrix, with the tip at the fiber/matrix interface. For this case, the singularity is a function of the ratio of fiber and matrix shear moduli and Poisson's ratios. Using this method, the singularities for a range of typical fiber/matrix combinations were determined to be between 0.25 and 0.35.

However, this idealization is overly simplistic for a notch through a multi-directional composite laminate. Alternatively, the functional form can be used, but both H_c and the exponent, n, can be considered simply as two degrees-of-freedom in the model. This approach maintains the advantages of the functional form, without requiring the exponent to depend on the simplistic idealization. Figure 7.8.4.1(f) illustrates the effect of the exponent, n, on residual strength, as n varies from 0.5 (classical) to 0.1. Each curve in the figure goes through the same point for a 0.25 in. (6.3 mm) notch. Decreases in the exponent, n, result in large increases in large-notch strength.

This functional form was successfully used (e.g., References 7.8.1.2.4(a) and 7.8.1.3(d)) to predict unconfigured large notch strength (i.e., 8 to 12 in. (200 to 300 mm)) from smaller notch data (i.e., ≤ 2.5 in. (63 mm)). The following procedure was used to determined the values for H_c and n.

1. The infinite-width strength was determined for each test data point using the isotropic finite-width correction factor (FWFC).

$$\sigma_N^\infty = \mathrm{FWCF} * \sigma_N \qquad 7.8.4.1.1(b)$$

   where

$$\mathrm{FWCF} = \sqrt{\sec\left(\frac{\pi a}{W}\right)}, \quad a = \text{half notch length}, \quad W = \text{specimen width}$$

   Note that all data was tested using the same width-to-notch-length ($W/2a$) ratio, avoiding problems associated with having data obtained by varying this ratio (see Reference 7.8.1.3(c)).

2. The curve was required to go through the average strength of the largest of the small-notch data (typically 2.5 in. (63 mm)). This requirement determines H_c for any selected value of n.

3. A precise, verified method for determining the appropriate order of singularity, in the absence of large notch data, has not been developed. In the method developed and applied during the Reference 7.8.1.2.4(a) and 7.8.1.3(e) studies, the value of *n* was generally selected as the smallest value that resulted in (a) the actual small-notch data being less than or equal to the resulting Mar-Lin curve, and (b) an increasingly larger difference between the two as notch size decreases. This approach, which is illustrated in Figure 7.8.4.1.1(a), is justified since the small-notch response is typically characterized by increasing fracture toughness with notch size until the "parent" fracture toughness curve is reached.

   Caution should be exercised in selecting exponents for extrapolation, since it is possible to select values that over-predict large-notch capability (i.e., are unconservative). In general, verification tests should be conducted with notch lengths of sufficient size to minimize the extent of extrapolation. In the absence of related large-notch data, a somewhat conservative selection of the exponent is prudent to avoid potential design deficiencies.

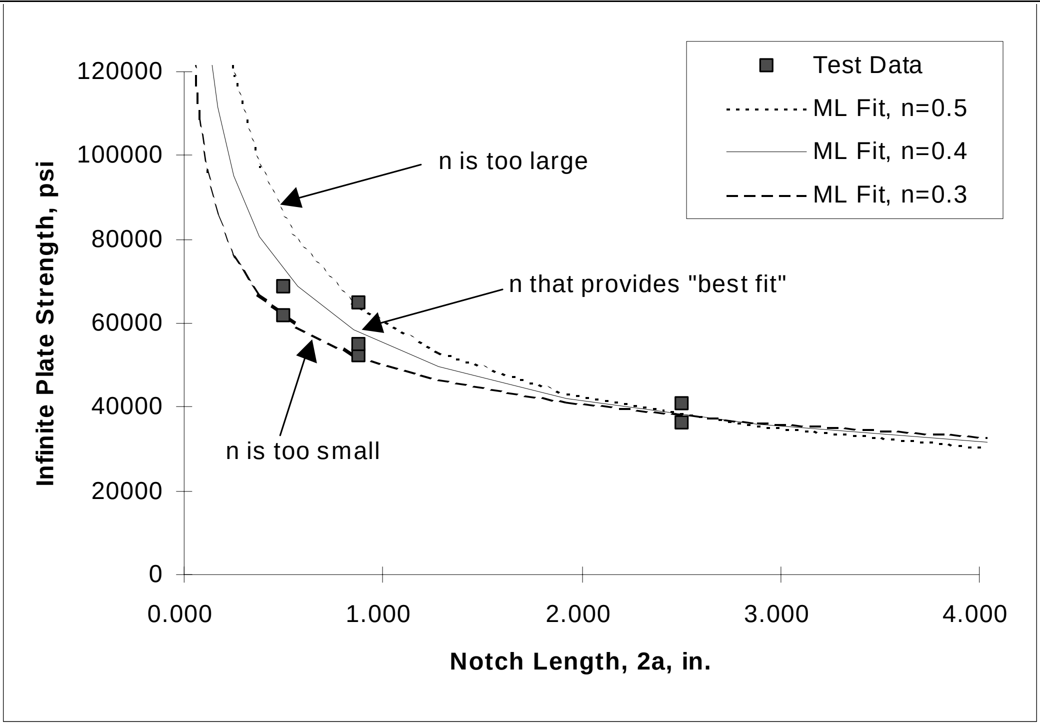

FIGURE 7.8.4.1.1(a) *Selection of singularity from small-notch data.*

This reduced-singularity method described in this section has been successfully used in assessing residual strength of configured structure, as well (References 7.8.1.2.10 and 7.8.1.3(e)). The approach mimicked that often used in metallic analysis, which involves applying empirical or semi-empirical elastic/plastic factors that account for configurational effects to the unconfigured notch strength (e.g., Reference 7.8.4.1.1). Factors developed for metallic configurations were used after modification for directional and part-to-part modulus differences.

Semi-Empirical Mar-Lin Examples

Strength prediction models, including square-root and reduced-singularity approaches, were discussed and compared in Reference 7.8.1.3(c). The four primary models included in the functionality assessment were: linear elastic fracture mechanics (LEFM), Whitney-Nuismer point stress (WN, References 7.8.4.1(b) and (c)), Poe-Sova (PS, References 7.8.4.1(g) and (h)), and Mar-Lin (ML, References 7.8.4.1(e) and 7.8.4.1(n)). When calibrated through a single notch-length/failure-strength point, the WN and PS methods were found to be functionally equivalent. The effect of the characteristic dimensions used in these methods is to reduce the small notch strength predictions from the parent LEFM curve. As crack lengths increase, differences between these characteristic-dimension methods and LEFM converge to a constant value that is small in comparison with the prediction.

The ability of the LEFM, PS, and ML methods to predict residual tensile strength over a wide range of notch sizes were assessed in Reference 7.8.1.3(d). These findings will be summarized here. Additional work on tension and compression of sandwich configurations were reported in References 7.8.1.2.4(a) and 7.8.1.3(e), with similar results.

Three material systems and three lay-ups were included in the evaluation, as described in Figures 7.8.4.1.1(b) and (c), respectively. In each case, the LEFM, PS, and ML methods were calibrated through the average strength with a 2.5 inch (63 mm) notch. The ML exponent, n, was varied to determine the singularity providing the best prediction of the largest-notch strength.

Material	Description
IM7/8551-7	Intermediate modulus carbon fiber in a particulate-toughened resin
AS4/938	Standard modulus carbon fiber in an untoughened resin
S2/AS4/938	Intraply hybrid, with each ply consisting of alternating bands of 1 tow of S-glass fiber and 3 tows of standard modulus carbon fiber, both in an untoughened resin

FIGURE 7.8.4.1.1(b) *Material description for tension tests.*

Laminate	Ply Orientations	Relative Stiff-ness in Load Direction
Crown3-Axial	[45/-45/90/0/60/-60/90/-60/60/0/90/-45/45]	soft
Crown3-Hoop	[-45/45/0/90/-30/30/0/30/-30/90/0/45/-45]	hard
Crown4-Axial	[45/-45/90/0/60/-60/15/90/-15/-60/60/0/90/-45/45]	hard

FIGURE 7.8.4.1.1(c) *Lay-up definition for tension tests.*

Figure 7.8.4.1.1(d) contains the five material/lay-up combinations that were evaluated, as well as the singularity that best fits the 2.5 in. (63 mm) and large-notch (8-12 in. (200-300 mm)) data for each case. Figures 7.8.4.1.1(e) through 7.8.4.1.1(i) compare LEFM, PS, and ML curves with all test data for each configuration. In all but the first case, the square-root-singularity methods provide conservative estimates of the measured large-notch capability. While this conservatism may appear small in absolute magnitude, it can be large as a percentage of the actual capability. This latter relationship defines the required material, assuming that large-notch strength is controlling the design. Note that the Mar-Lin functionality allows excessive conservatisms to be avoided.

Material	Lay-up	Relative Stiffness	“Best” Singularity
IM7/8551-7	Crown3-Hoop	Hard	0.5
	Crown3-Axial	Soft	0.3
AS4/938	Crown3-Hoop	Hard	0.3
	Crown4-Axial	Soft	0.2
S2/AS4/938	Crown4-Axial	Soft	0.1

FIGURE 7.8.4.1.1(d) *Reduced singularity comparisons of material/lay-up combinations in tension.*

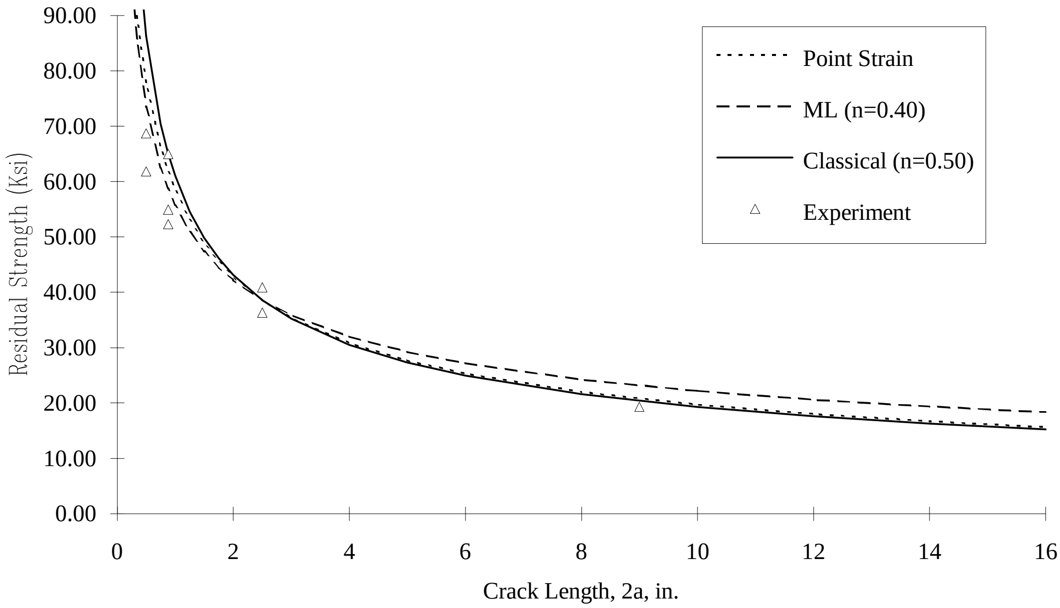

FIGURE 7.8.4.1.1(e) *Comparison of IM7/8551-7, Crown3-Hoop experimental tension results with different failure criteria.*

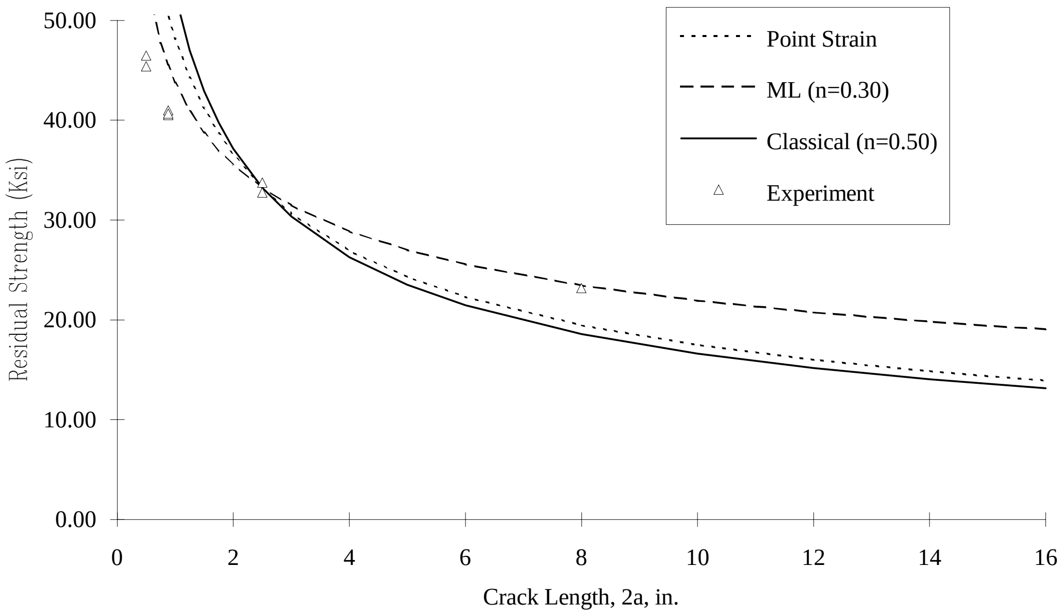

FIGURE 7.8.4.1.1(f) *Comparison of IM7/8551-7, Crown3-Axial experimental tension results with different failure criteria.*

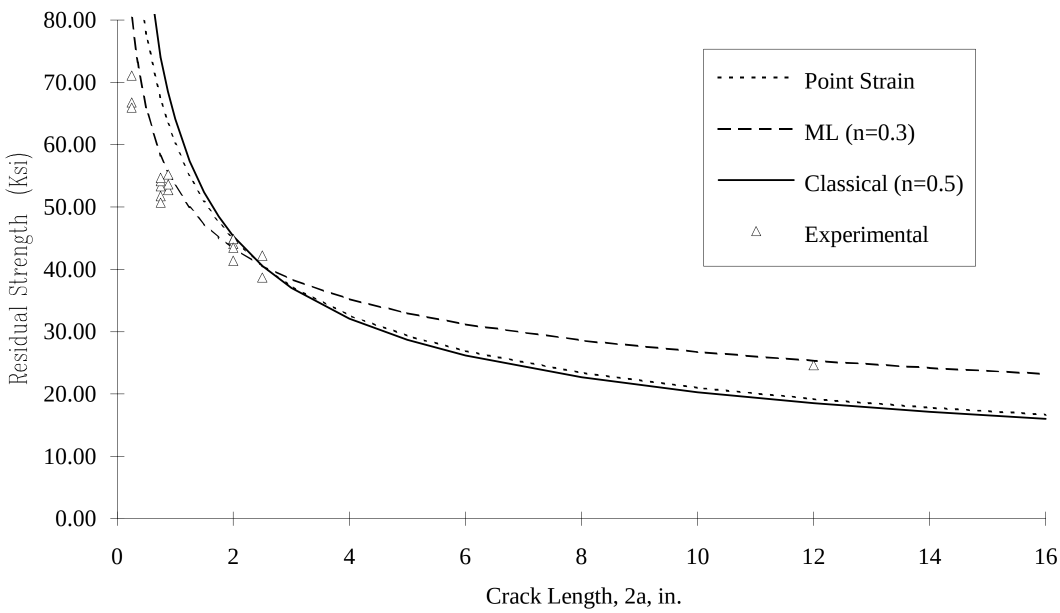

FIGURE 7.8.4.1.1(g) *Comparison of AS4/938, Crown3-Hoop experimental tension results with different failure criteria.*

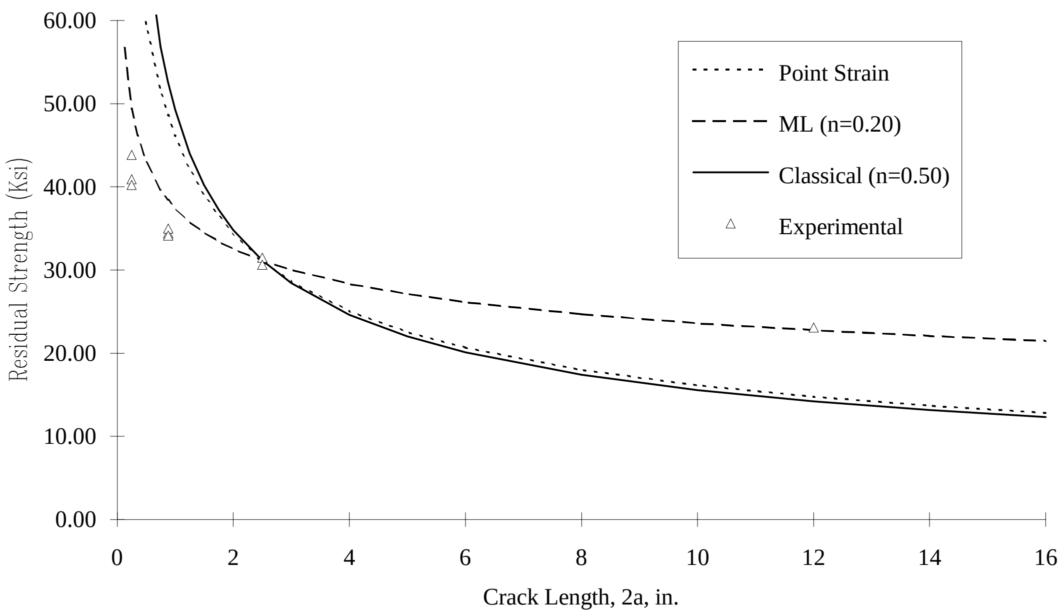

FIGURE 7.8.4.1.1(h) *Comparison of AS4/938, Crown4-Axial experimental tension results with different failure criteria.*

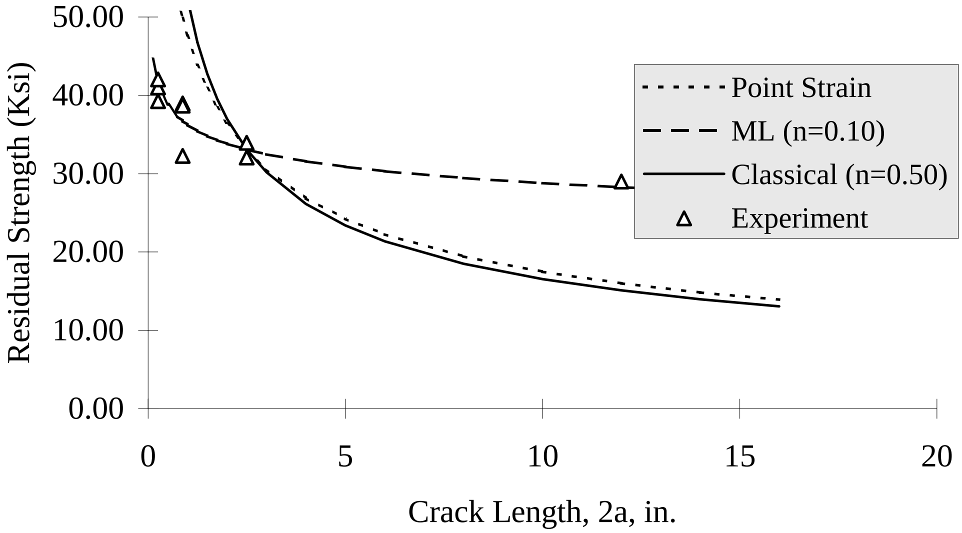

FIGURE 7.8.4.1.1(i) *Comparison of 25%-Glass Hybrid, Crown4-Axial experimental tension results with different failure criteria.*

This approach was also applied to sandwich configurations with facesheets using higher-toughness resins (AS4/8552). Several small-notch (0.875 and 2.5 in. (22.2 and 63.5 mm)) specimens and a single large-notch (9 in. (230 mm)) panel were tested. As shown in Figure 7.8.4.1.1(j), the Mar-Lin extrapolation of the 0.875 and 2.5 in. (22.2 and 63 mm) notch data was significantly more accurate than the LEFM prediction, but it over-predicted the large-notch strength by approximately 10%. The “best” Mar-Lin curve reflects the fit between the two largest notch sizes. This example illustrates the benefit of conservatively selecting the exponent when related large-notch data does not exist.

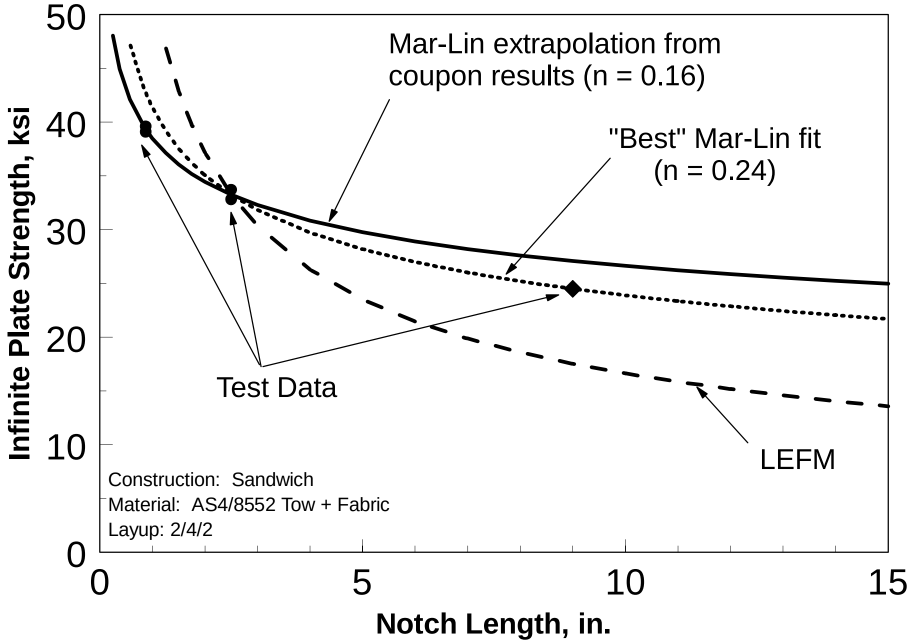

FIGURE 7.8.4.1.1(j) *Extrapolation of small-notch results to large-notch sizes for AS4/8552 sandwich.*

In Reference 7.8.1.2.10, unconfigured notched-strength predictions based on the reduced-singularity method were extended to structural configurations using configuration factors. The response of a 5-stringer panel, shown in Figure 7.8.4.1.1(k), was predicted and compared to experimental measurements. The panel was tow placed from AS4/938, and contained a 14 in. (360 mm) notch that severed a full skin bay and the central stringer.

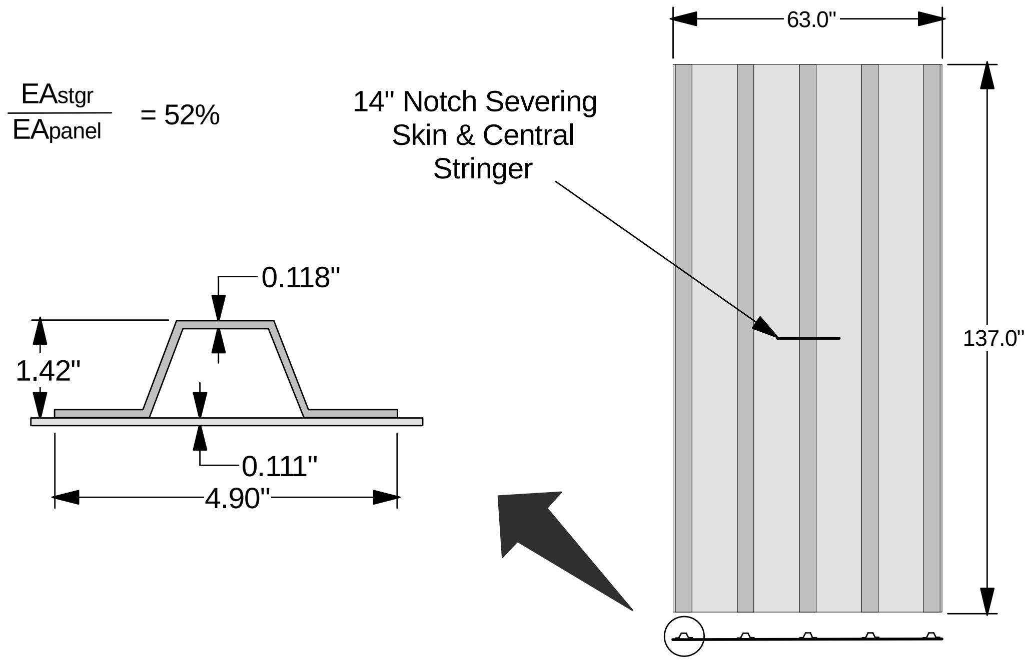

FIGURE 7.8.4.1.1(k) *Flat 5-stringer panel configuration.*

In the test panel, damage grew asymmetrically from the notch tips in a stable manner within the skin to the adjacent stringers, where it arrested. The final failure sequence was caused by extension of the fiber failure beyond the adjacent stringer. Reduction of the skin-to-stringer load transfer, caused by delamination growth that accompanied extension of fiber failure beyond the stringer, provided additional driving force during the failure sequence.

X-rays taken at pre-failure load levels allowed construction of a residual strength curve, shown in Figure 7.8.4.1.1(l). The elastic prediction curve significantly overpredicts the effectivity of the adjacent, unsevered stiffening element in reducing the skin notch tip stresses. A prediction based on elastic/plastic analysis and tests of metallic configurations, similar to those shown in Reference 7.8.4.1.1, provided very good correlation with the observed behavior. This may be coincidental, however, since the metallic configuration included inverted, mechanically-fastened hats while the tested configuration had non-inverted, co-cured hats. The important factor, however, is that consideration of inelastic behavior reduces the effectivity of the unsevered stiffening element, decreasing skin-strength predictions.

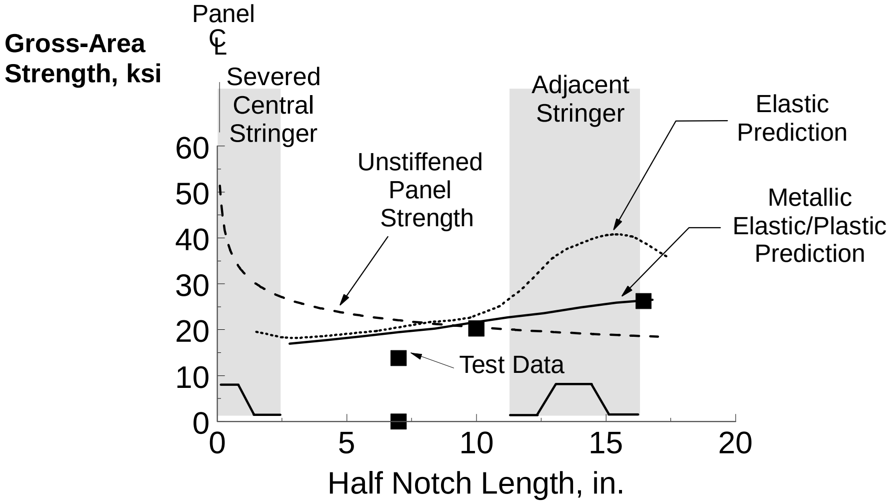

FIGURE 7.8.4.1.1(l) *Comparison of crown 5-stringer tension damage tolerance results with predictions.*

A similar approach was applied to two curved panels tested under biaxial loading in a pressure-box test fixture. The general arrangement of the panels is shown in Figure 7.8.4.1.1(m). These panels, designated Panel 11b and TCAPS-5, each contained a 22 in. (560 mm) longitudinal notch severing skin and the central frame. Differences in design detail are highlighted in Figures 7.8.4.1.1(n) and (o). Panel 11b included all-graphite skins with a relatively high hoop modulus, and bolted frames with mouseholes that extend beyond the full width of the stringers. TCAPS-5 featured a graphite-glass intraply hybrid skin with a relatively low hoop modulus and higher-stiffness bolted frames. Glass-fabric pads beneath the frame allowed a direct bolted attachment between the frame and the stringer flange and the mousehole configuration to be significantly narrower.

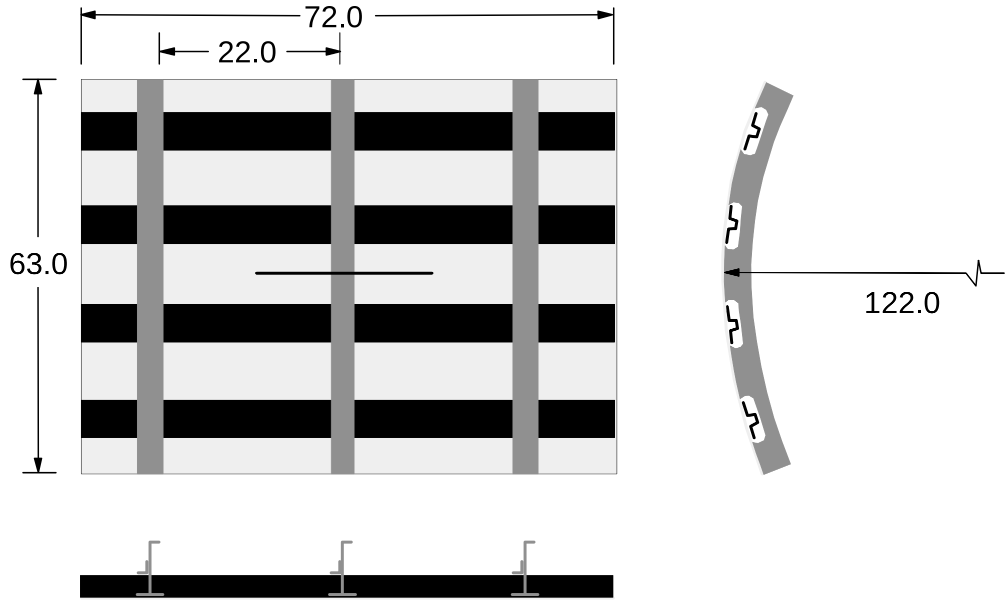

FIGURE 7.8.4.1.1(m) *Pressure-box test panel geometry.*

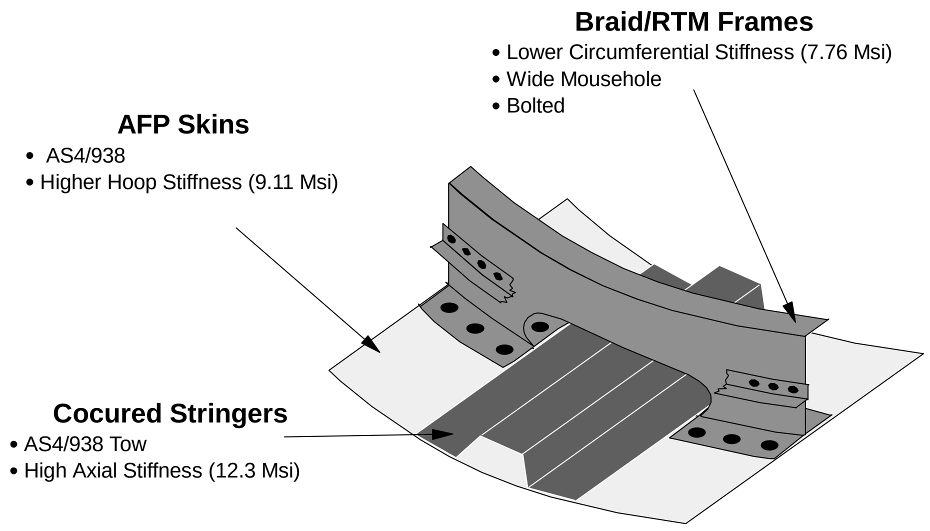

FIGURE 7.8.4.1.1(n) *Panel 11b structural configuration.*

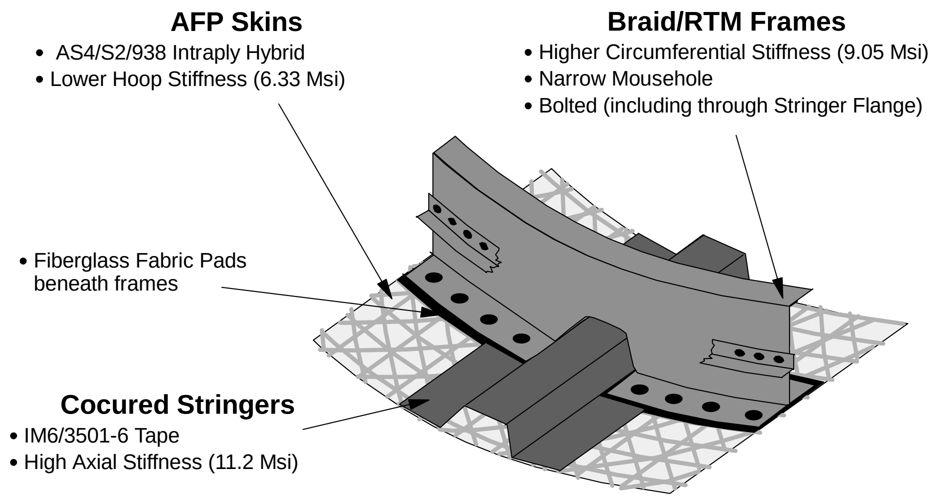

FIGURE 7.8.4.11(o) *TCAPS-5 structural configuration.*

Both panels were subjected to internal pressure only. Figures 7.8.4.1.1(p) and (q) illustrated the damage state in each panel after completion of the tests. The maximum pressure for Panel 11b was 10.0 psi, at which time an explosive decompression occurred. The damage was characterized by extensive delamination and an intense region of fiber failure extending approximately 11 in. (280 mm) from the notch tips to the adjacent frames. TCAPS-5 reached a maximum pressure of 15.5 psi, when air supply limitations precluded further loading. Its final damage state was characterized by delaminations and fiber failure regions on the order of only 3-4 in. (80-100 mm), despite sustaining 55% higher pressure.

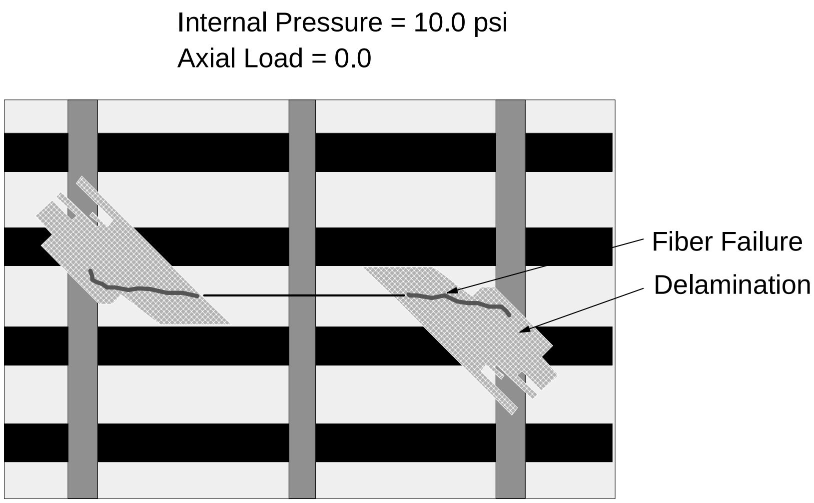

FIGURE 7.8.4.1.1(p) *Panel 11b final damage state.*

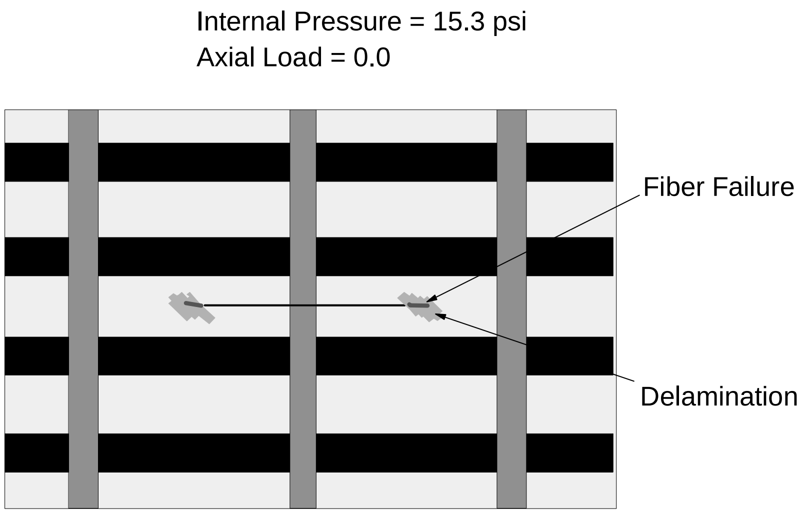

FIGURE 7.8.4.1.1(q) *TCAPS-5 final damage state.*

Residual strength response was predicted for these panels using Mar-Lin extrapolations of notched strength data from flat unstiffened laminates in combination with metallic elastic-plastic configurational correction factors that were modified to account for modulus differences. These predictions are compared with the actual damage growth in Figure 7.8.4.1.1(r). The prediction for Panel 11b was quite accurate for damage growth in the skin, but overpredicted the load transfer to, and hence the beneficial effect of, the undamaged adjacent frames. This reduced load transfer observed in the test is again related to skin delaminations effectively decoupling the frame from the skin. Predictions of TCAPS-5 response were not as accurate. The response, however, exceeded its much higher predicted capability.

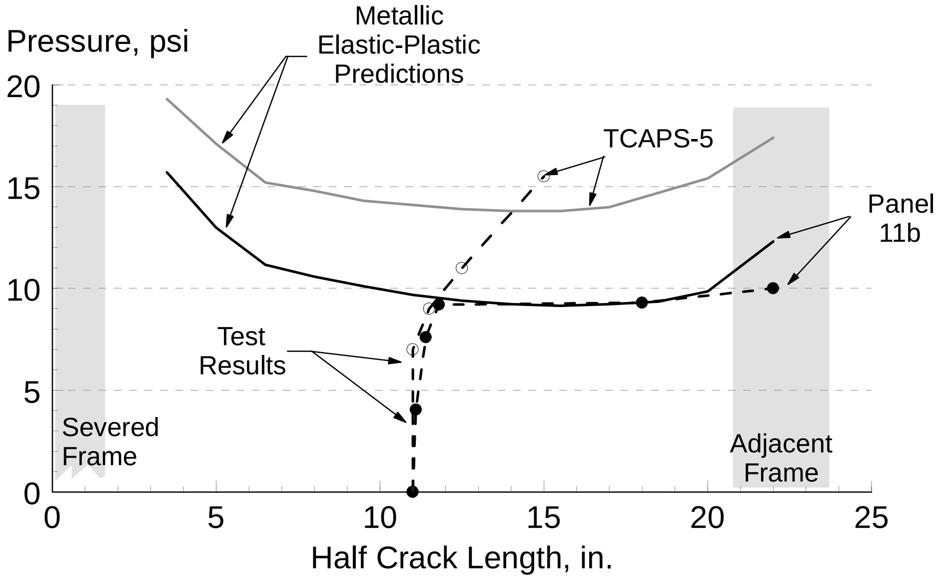

FIGURE 7.8.4.1.1(r) *Comparison of predicted and measured damage growth in crown pressure-box test panels.*

7.8.4.1.2 Strain softening laws

Experimental evidence has demonstrated that composite materials exhibit significant strain capability beyond that associated with the maximum load-carrying capability (Reference 7.8.1.2.8(i)). This strain-softening characteristic, shown in Figure 7.8.4.1.2(a), is not readily apparent in unnotched or small-specimen testing, where failures can appear brittle due to limited load redistribution after localized failures. In notched specimens or in structures capable of load redistribution, however, the strain-softening response is more easily observed.

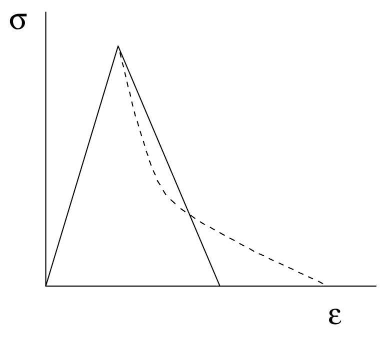

FIGURE 7.8.4.1.2(a) *Strain softening laws.*

To date, most engineering applications using strain-softening approaches have occurred in analyzing inhomogeneous materials used in the building industry (e.g., concrete). References 7.8.4.1.2(a) and (b) extensively document the use of strain-softening methods for analyzing the fracture and collapse of engineering structures. Strain-softening methods have been applied to some laminated composite problems (e.g., References 7.8.4.1.2(c), 7.8.4.1(d) and 7.8.4.1(p)). The most significant application of these methods to large-notch residual strength of composite structure was performed in a series of NASA/Boeing contracts reported in References 7.8.4.2.1(d) and (e), 7.8.1.2(g), 7.8.1.2.4(a), 7.8.1.2.8(h) and (i), and 7.8.1.3(e). The following discussion is based on the findings from that work.

The use of strain softening laws to simulate damage progression has several attractive features. First, it is a generalized continuum approach and is, therefore, more compatible with the complex finite element models required to properly approximate structural configurations than are rigorous progressive damage models (i.e., those with ply-by-ply assessment and tracking of multiple failure mechanisms). The approach also captures the load redistribution caused by local damage formation and growth, and the resulting influence on deformations and other potential failure modes.

Strain-softening laws are typically incorporated into geometrically nonlinear finite element analyses as non-linear, non-monotonic material stress-strain curves. The global analysis becomes a structural collapse problem, as shown in Figure 7.8.4.1.2(b); the damage growth forces load redistribution toward the specimen edges until insufficient material exists to sustain the applied load.

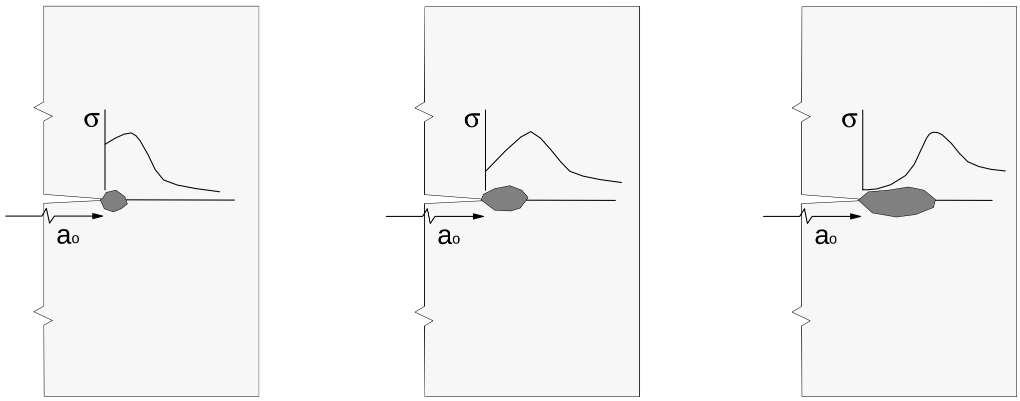

FIGURE 7.8.4.1.2(b) *Modeling of structural collapse due to damage growth.*

Strain-softening laws are strongly dependent on a numerous variables, including material, lay-up, stacking sequence, manufacturing process, environment, and loading. As illustrated in Figure 7.8.4.1.2(c), the shape of the strain-softening curve has a strong influence on the predicted notch-strength response. Material laws with relatively high maximum stresses but low total fracture energy are required to predict high strength, low toughness response. These laws also capture the relatively small notch-tip damage zones and small specimen size effects observed in tests. Conversely, laws with low maximum stresses but high total fracture energies are necessary to capture low strength, high toughness behavior. They also predict the large notch-tip damage zones and the significant specimen size effects observed in tests.

Efficient methods for determining the strain-softening law for a specific combination of these variables are not fully developed for composites. They can be found either by indirectly by matching analysis with small coupon test data (e.g., Reference 7.8.4.1.2(e)) or directly from test measurements (e.g., Reference 7.8.4.1.2(f)). Once determined, these laws are used in finite element models to predict the response of other geometries.

A number of significant difficulties arise in attempting to implement this method, and not all have well-established solutions. The following subsections attempt to summarize the current state-of-the-art for the significant implementation issues.

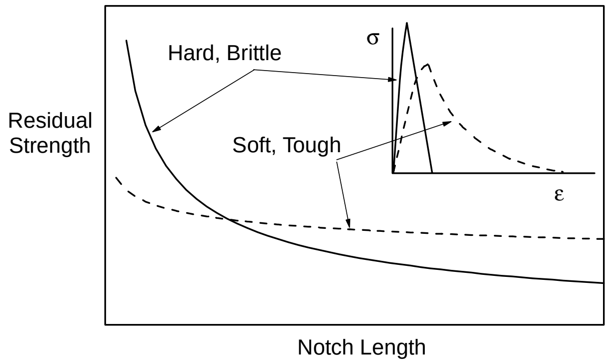

FIGURE 7.8.4.1.2(c) *Effect of strain softening material law on notch-length sensitivity.*

Complexity of Strain-Softening Modeling. Application of the strain-softening law can be accomplished in a variety of ways. The method chosen for a specific problem depends on the loading and damage growth assumptions. For uniaxial in-plane loading, where the assumption of self-similar crack growth is reasonable, a uniaxial implementation can be used. In this case, uniaxial springs, with nonlinear stiffnesses directly related to the strain-softening material law, can be placed between the surfaces of the crack plane, as shown in Figure 7.8.4.1.2(d).

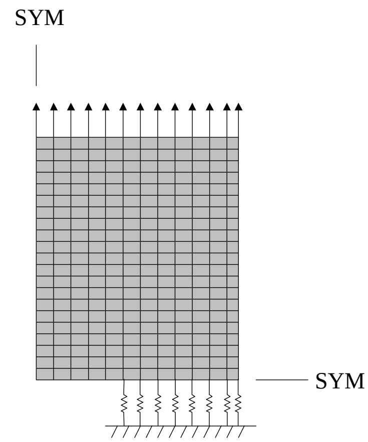

FIGURE 7.8.4.1.2(d) *Spring implementation of strain softening.*

For multi-directional in-plane loading, a multi-directional strain-softening law must be defined, since the direction of damage propagation cannot be assumed. In References 7.8.4.1.2(d) and (e), 7.8.1.2.4(a), 7.8.1.2.8(g) through 7.8.1.2.8(i), and 7.8.1.3(e), the strain-softening laws were defined for the two orthotropic directions of the laminate, and a Hill yield function used for the interaction.

For situations with significant variations of load, geometry, or damage through the thickness of the part, (e.g., bending moments, post-buckled structure, out-of-plane loading, unsymmetrical damage), the modeling approach must also allow variable softening through the thickness. In Reference 7.8.4.1.2(d), this was accomplished by defining several integration points in the thickness direction of the finite element representing the laminate, and applying the strain-softening relationship independently to each of these points. However, it was also noted that a more general formulation is required if the laminate properties vary significantly through the thickness, since the stress-strain relationship is generally developed for the whole laminate assuming homogeneous ply stacking sequences.

Numerical Solution Issues. Finite element solutions of problems involving a strain-softening material laws involve a number of complexities not often associated with static structural analysis. Specifically, singular stiffness matrices are encountered when material failure is occurring in a sufficiently large area and/or when the structure is buckling. In the Reference 7.8.4.1.2(d) studies, ABAQUS® was selected because it has a variety of robust, nonlinear solution algorithms and is capable of modeling strain-softening response for orthotropic materials. Arc length methods, such as Riks (Reference 7.8.4.1.2(g)), have proven useful in dealing with snap-through stability problems, and were useful in initial efforts to model tension loaded strain-softening problems. However, numerical stability problems and very long solution times were frequently encountered, particularly when the unloading portion of the strain-softening curve was very abrupt or steep.

Solving the problem dynamically minimizes a number of numerical difficulties. Similar to real structures, damping and inertial forces smooth out system response and greatly reduce numerical noise in the solution process. As the maximum load is reached, local failure occurs thus accelerating parts of the system. The numerical integration in time can be stopped when a minimum acceleration related to system failure has been achieved. This has proven to be very accurate failure criterion for compression-loaded structural systems (Reference 7.8.4.1.2(d)).

Element Size and Formulation. Strain-softening laws and the finite element size are interrelated, due to the effect of element size on notch-tip strain distribution. Larger elements result in less-severe, but broader, stress concentrations. This is similar to the response of non-classical material models (i.e., Cosserat, non-local) in the presence of a stress concentration (e.g., References 7.8.4.1.2(h) and 7.8.4.1(m)), and also similar to deviations observed in actual strain distributions from classical predictions. Larger element sizes result in strain-softening curves with steeper unloading segments (Reference 7.8.4.1.2(d)).

Element size, therefore, is another degree-of-freedom in the strain-softening approach that must be determined. Fortunately, damage in composite materials typically localizes on a relatively large scale (e.g., relative to plastic yielding at a crack tip in metal). Relatively large elements (i.e., ≥ 0.20 inches (5.0 mm)) are, therefore, found to provide good results. Element sizes required to accurately predict notch-length and finite-width effects in compression are typically larger than those required for tension.

Finite element analyses based on non-local formulations (i.e., the stress at a point is dependent on the strain at that point and the strain in the vicinity of that point) can overcome this element-size dependency. The need to combine strain-softening laws with non-local material models has also been seen in work related to civil engineering structures (e.g., References 7.8.4.1.2(a), 7.8.4.1.2(i), and 7.8.4.1(u)). Several methods (other than element size) have been used to account for non-local responses. The most widely used method to incorporate non-local analysis is based on an integral approach, where a weighted average strain is determined as a material property and is referred to as the characteristic size of the material. Another approach is based on a second order differential method, where the strain used for the stress calculation is based on both the value and second derivative of the point strain. In fact, these two methods are related, and, with selected weighting functions, there is a one-to-one correspondence. A third proposed method involves an imbricated element formulation (Reference 7.8.4.1.2(i)). An approximation of this technique (i.e., overlaid and offset 8-noded elements), shown in Figure 7.8.4.1.2(e), was attempted, but was abandoned due to difficulties associated with modeling at specimen and crack boundaries.

Element formulation and strain softening laws are also interrelated. Limited studies of 4-, 8-, and 9-noded shell elements found that higher order elements lead to higher fracture strengths and large damage zones (Reference 7.8.1.2.8(h)).

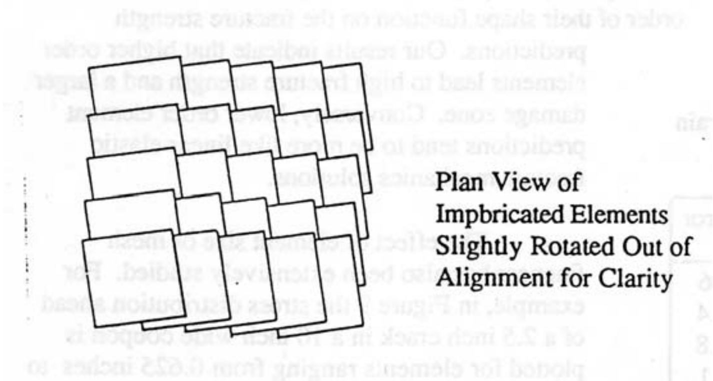

FIGURE 7.8.4.1.2(e) *Staggered layering of 8-node shell elements used to model nonlocal effects of a stress concentration.*

Determination of Strain-Softening Law. Using the indirect method to determine a strain-softening law requires an understanding of the key characteristics of strain-softening curves, and their influence on the structural response. The law is iterated until small-notch data is matched. Test results to support this approach are not well established, but the goal is to have sufficient data to capture notch-size effects and specimen finite-width effects. In the NASA/Boeing research studies, for example, typical test data for determining the tension law consisted of three or four specimen configurations, as shown in Figure 7.8.4.1.2(f). Laws obtained in this manner were typically use to predict the response of configurations with notches in the range of 8 to 20 inches (200 to 500 mm).

Notch Size, in. (mm)	Specimen Width, in. (mm)	Width-to-Notch-Size Ratio
0.88 (22.4)	3.5 (89)	4
1.75 (44.5)	3.5 (89)	2
2.50 (63.5)	10.0 (254)	4
5.00 (127)	10.0 (254)	2

FIGURE 7.8.4.1.2(f) *Typical test for determining strain-softening law in the NASA/Boeing research programs.*

Determination of the strain-softening material laws for both tension and compression through trial and error requires a relatively large number of tests, and is computationally intensive. Approaches have been presented to determine these laws from relatively few tests via energy methods (e.g., Reference 7.8.4.1.2(f)). These require measurement of crack opening displacements (COD) for two specimens of identical geometry and differing notch lengths. Attempts to accomplish this with center-notch specimen configurations were unsuccessful. Two specimens of each of two notch lengths were tested. The resulting strain softening laws for the four specimen combinations are shown in Figure 7.8.4.1.2(g) along with an average response. The scatter was unacceptably large, and is likely a result of the small differences in response of specimens with differing notch lengths relative to experimental error.

Development of improved specimen geometries has also been pursued (e.g., University of British Columbia). In particular the over-height compact tension specimen, shown in Figure 7.8.4.1.2(h), is being evaluated. The greater dependence of specimen compliance on notch length should resolve the problems associated with the center-notch specimens. Test measurements and destructive evaluations are being conducted to provide further insights into the damage growth mechanisms. One unresolved issue with this specimen configuration is the effect of the bending stress distribution on the strain-softening law.

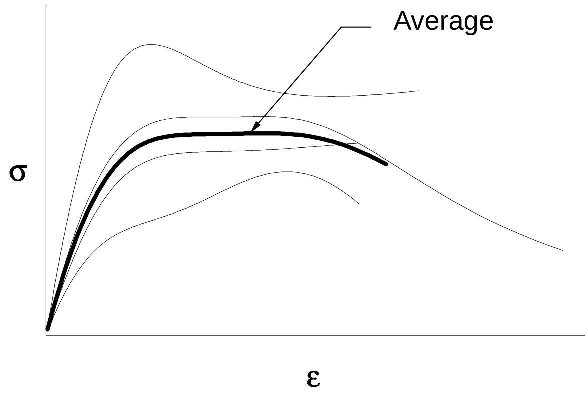

FIGURE 7.8.4.1.2(g) *Strain-softening laws determined from center-notch specimens using energy methods.*

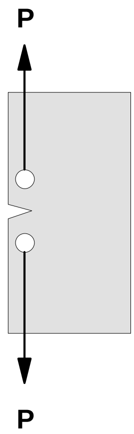

FIGURE 7.8.4.1.2(h) *Over-height compact tension specimen for strain-softening law determination.*

Any approach to determine the material laws directly from test measurements must use tests of sufficient size to capture process-induced performance characteristics.

Load Transfer to Stiffening Elements. In structural configurations with stiffening elements, the ability to model the degradation of the load-transfer capability between the skin and the stiffener is crucial to predict final failure. Physically, this degradation occurs as the damage approaches the stiffener, and can be caused by delamination damage in the skin, or yielding of either the bonded or mechanical attachment. Strain-softening models do not discretely address delamination damage in laminates, and the model fidelity required to predict either yielding for bonded or bolted joints is not compatible with structural-scale models. A practical method to address these issues has not been identified.

Strain-Softening Examples

The described approaches were used to predict unconfigured and configured notched compression strength. The unconfigured results are summarized in Figure 7.8.4.1.2(i). Three test points were used to calibrate the material law, while the other two tests were predicted. The predictions were within 3% of the test results.

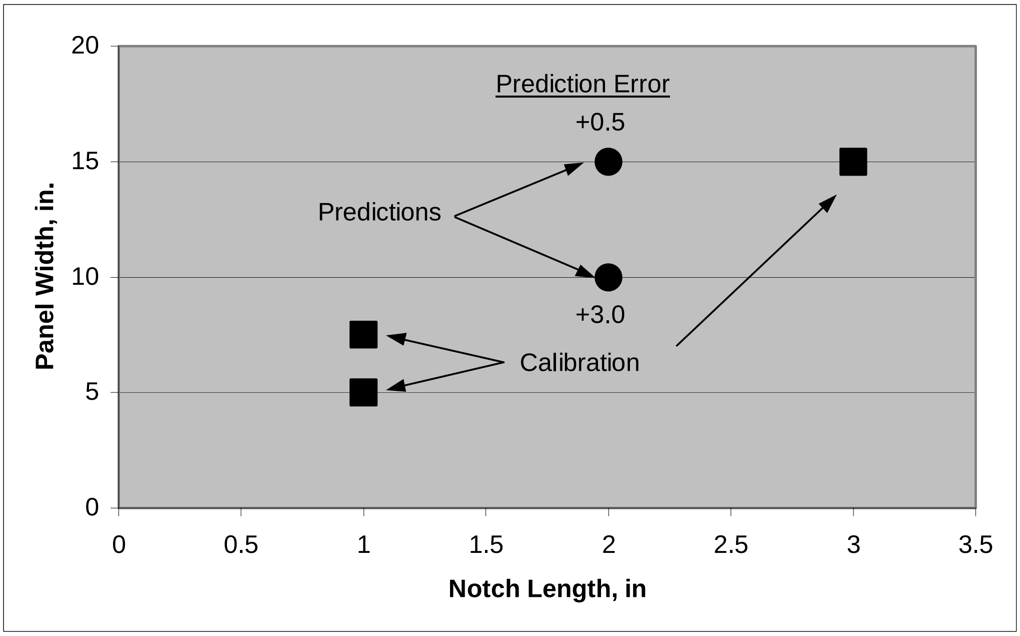

Lay-up: [45/0/-45/90/0/-45/45/0/90/-45/0/45]
Material: AS4/8552
Core: ¾" (19.0 mm) 8 pcf (128 kg/m^3) HRP

Panel Sizes:
1" notch – 5 x 10, (25 mm – 127 x 254 mm), 7.5 x 10 (191 x 254 mm)
2" notch – 10 x 20, (51 mm – 254 x 508 mm), 15 x 20 (381 x 508 mm)
3" notch – 15 x 30 (76 mm – 381 x 762 mm),

FIGURE 7.8.4.1.2(i) *Strain softening prediction on unconfigured notched compression strength.*

Predictions were also made of 30 x 44 in. (80 x 1100 mm) curved panels (122 in. (310 m) radius) with 4 in. (100 mm) notches and a 66 x 88 in. (1.7 x 2.2 m) curved panel with and 8.8 in. (223.5 mm) notch. The predictions are compared with the experimental results in Figure 7.8.4.1.2(j). Predictions were within 7% of the measured values.

7.8.4.1.3 LEFM - based methods

Using classical linear fracture mechanics, the strain in a fiber direction at a distance r directly ahead of a crack tip can be written in the following infinite series (Reference 7.8.4.1(h)).

$$\varepsilon_1 = Q(2\pi r)^{-1/2} + O\left(r^0\right) \qquad 7.8.4.1.3(a)$$

where

$$Q = K\xi / E_x \qquad 7.8.4.1.3(b)$$

$$\xi = \left[1 - \left(\upsilon_{xy}\upsilon_{yx}\right)^{1/2}\right]\left[\left(E_x / E_y\right)^{1/2}\sin^2\alpha + \cos^2\alpha\right] \qquad 7.8.4.1.3(c)$$

r is the distance from the crack tip, K is the usual stress intensity factor, x and y are Cartesian coordinates with x perpendicular to the crack, E is a modulus of elasticity, υ is a Poisson's ratio, α is the angle that the fiber makes to the x axis (perpendicular to the crack), and $O(r^o)$ indicates terms of order r^o and greater. For small r, the terms $O(r^o)$ are negligible.

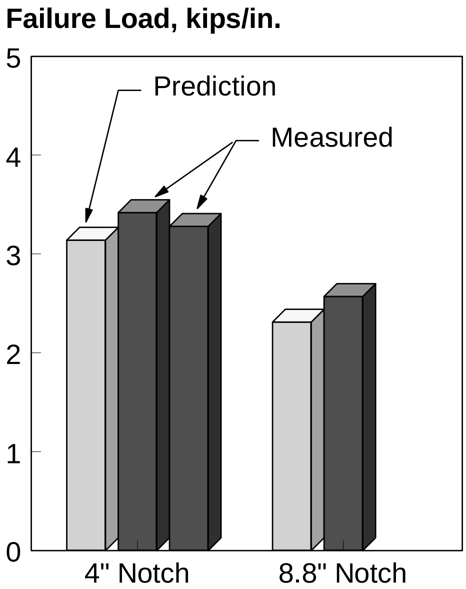

FIGURE 7.8.4.1.2(j) *Comparison of measured notched compression failure loads with strain softening predictions.*

For the point strain failure criterion, $\varepsilon_1 = \varepsilon_{tuf}$ at $r = d_o$, where ε_{tut} is the ultimate tensile failure strain of the fibers. Thus, rearranging equation 7.8.4.1.3(a),

$$(2\pi d_o)^{1/2} = Q_c / \varepsilon_{tuf} \qquad 7.8.4.1.3(d)$$

and

$$K_Q = Q_c E_x / \xi = (2\pi d_o)^{1/2} \varepsilon_{tuf} E_x / \xi \qquad 7.8.4.1.3(e)$$

where the subscript c indicates critical value and K_Q is the laminate fracture toughness.

Equation 7.8.4.1.3(e) can be used to predict fracture toughness without conducting fracture tests. The elastic constants and the failing strain of the fibers can usually be obtained using data from the material supplier and classical lamination theory. Residual strengths can be calculated by equating the fracture toughness and stress intensity factors determined by theory of elasticity or finite element analyses. Approximate stress intensity factors for panels with bonded stiffeners are given in Reference 7.8.1.3.1(a).

7.8.4.1.4 R-curves

For many composites, the value of the normalized characteristic dimension, $(2\pi d_o)^{1/2}$, is not a constant but increases with crack length, especially for thin laminates made with brittle resins. Values of $(2\pi d_o)^{1/2}$ are plotted against damage growth in Figure 7.8.4.1.4(a) for a 13-ply fuselage crown laminate made of prepreg tape using a tow-placement process (Reference 7.8.1.3.1(a)). The damage growth measured in radiographs and calculated from measurements of crack-opening displacements (COD) are in good agreement. (The crack length including damage growth is proportional to the COD, which was measured by a "displacement gage" located midway between the ends of the cut).

The maximum value of $(2\pi d_o)^{1/2}$ in Figure 7.8.4.1.4(a) is about 63% greater than the LEFM value, and the maximum damage growth was one third of the cut length. The values of $(2\pi d_o)^{1/2}$ were calculated using the length of cut plus growth. The curve in Figure 7.8.4.1.4(a) can be used as a crack-growth resistance curve (R-Curve) with failure defined by the tangency of the R-Curve and the crack-driving-force curve (F-Curve) calculated using Equation 7.8.4.1.3(d) and stress intensity factors determined by theory of elasticity or finite element analyses. In the ASTM E561-86 standard (Reference 7.8.4.1.4(a)), the R- and F-Curves are expressed in terms of stress intensity factor. However, for composites, it is convenient to use $(2\pi d_o)^{1/2}$ instead of stress intensity factor to normalize for lay-up and material.

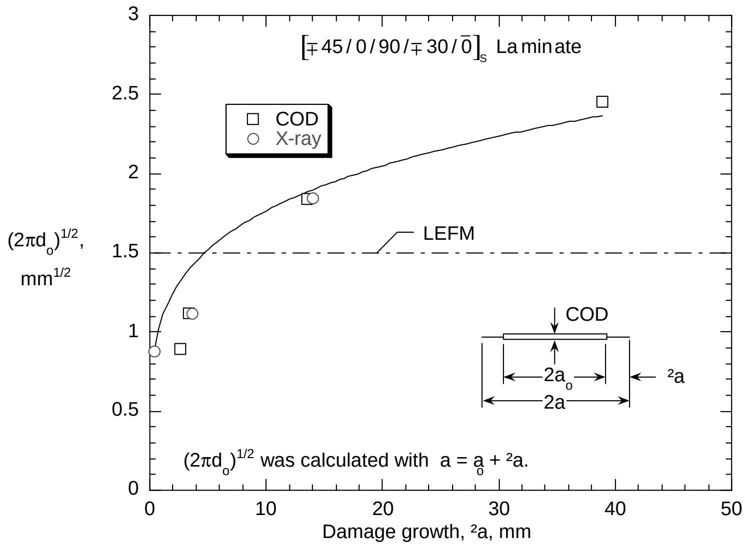

FIGURE 7.8.4.1.4(a) *R-curve for tow-placed AS4/938 fuselage crown laminate (cut length = 9 in. (23 cm) and width = 36 in. (91 cm)) (Reference 7.8.1.3.1(a)).*

R-Curve Examples

Tensile failing strains for large flat fuselage panels with straps and hat-section stiffeners are plotted against cut length in Figures 7.8.4.1.4(b) and (c) (Reference 7.8.1.3.1(a)). The panel with straps contained a 10.0 in. (25.4 cm) cut and that with hat-section stiffeners contained a 14.0 in. (35.6 cm) cut. The central stiffener in both panels was severed, and the skins were [-45/45/0/90/-30/30/0/30/-30/90/0/45/-45] AS4/938 tow placed fuselage crown laminates. The stiffness of the straps was 56% of that of the hat-section stiffeners. The amount of crack growth observed in the test is indicated by the arrow drawn to the right of the "test failure" symbol. The panel with straps in Figure 7.8.4.1.4(b) failed catastrophically at an applied strain of 0.00275 with about 1.0 in. (2.5 cm) of stable tearing at each end of the cut. The cut in the panel with hat-section stiffeners grew stably into the stiffener (about 7 in. (18 cm) at each end of the cut) before catastrophic failure at an applied strain of 0.00274.

Tensile failing strains calculated using LEFM and R-Curve are also plotted against cut length in Figures 7.8.4.1.4(b) and (c). Approximate, closed-form equations in Reference 7.8.1.3.1(a) were used to calculate F-Curves for the various cut lengths. An envelope of F-Curves in Reference 7.8.1.3.1(a) similar to the one in Figure 7.8.4.1.4(a) was used for the R-Curve. The jumps in failing strains occur when the end of the cut (LEFM) or the end of the cut plus stable growth (R-Curve) coincide with the edge of the stiffener. The horizontal dashed lines indicate the region of cut lengths for fracture arrest and give the failing strains with subsequent loading. For cut lengths to the left of the dashed line, failures are catastrophic. The LEFM predictions were 45 and 58% below the test values for the straps and hat-section stiffeners, respectively, and the R-Curve predictions were 14% below and 16% above the test values for the straps and hat-section stiffeners, respectively. The nature of failure, that is catastrophic versus fracture arrest, were predicted correctly by both LEFM and R-Curve.

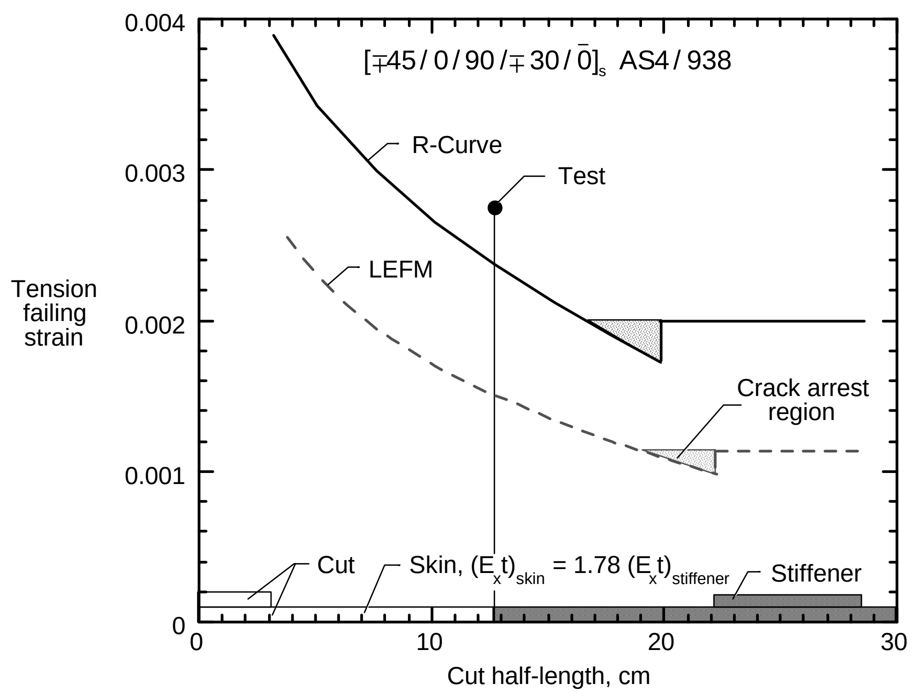

FIGURE 7.8.4.1.4(b) *Measured and predicted failing strains for three-stringer tow-placed fuselage crown panel 30 x 83.9 in. (76 by 213 cm) (Reference 7.8.1.3.1(a)).*

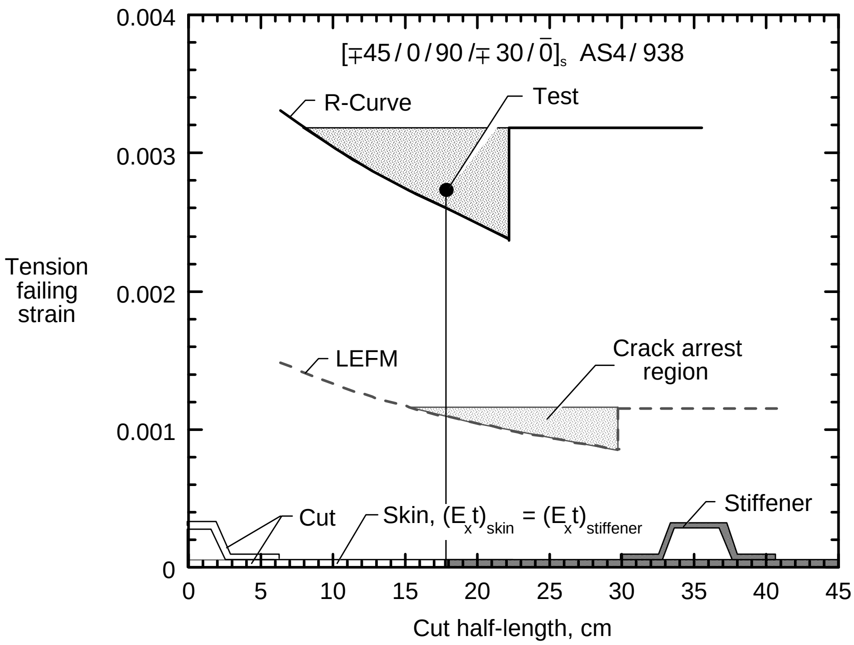

FIGURE 7.8.4.1.4(c) *Measured and predicted failing strains for five-stringer tow-placed AS4/938 fuselage crown panel 63 by 137 in. (160 by 348 cm) (Reference 7.8.1.3.1(a)).*

It should be noted that flat panel results can not be applied directly to shells with longitudinal cracks and internal pressure because stress intensity factors for pressurized shells can be much greater than those for flat plates. (Strengths and burst pressures vary inversely with stress intensity factor.) See Figure 7.8.4.1.4(d), where stress intensity correction factors from Reference 7.8.4.1.4(b) are plotted against $a/\sqrt{Rt}$ for isotropic pressurized cylinders and spheres. For a wide body fuselage with a cut equal to two times the frame spacing, $a/\sqrt{Rt}$ can be as large as five. In that case, the stress intensity factor for an unstiffened cylinder would be more than five times that for a flat unstiffened plate. Analytical results for specially orthotropic cylinders are given in References 7.8.4.1.4(c) and (d). These results were experimentally verified for 12 inch (30 mm) diameter pressurized composite cylinders with longitudinal cuts in Reference 7.8.4.1.4(e). Frames and tear straps can not only reduce the stress intensity factor (Reference 7.8.4.1.4(f)), they can also turn a fracture and limit a failure (see Reference 7.8.4.1.4(g)).

An R-Curve was also successively used to predict residual strength of a curved panel with stiffeners, pressure loading, and discrete source damage in Reference 7.8.4.1.4(h). The F-Curve was calculated by a nonlinear finite element analysis taking into account out-of-plane displacements.

7.8.4.2 Single delaminations and disbonds

The previous section discussed severe accidental and discrete source damage only, represented by crack-like, penetrating cuts. Analysis of laminates containing single plane delaminations or disbonds can also be performed. As discussed earlier, delaminations have little effect on tension strength but delaminations can be critical for compression or shear loading. Analysis methods for damage (including delaminations) resulting from impact damage is contained in Section 7.8.4.3.

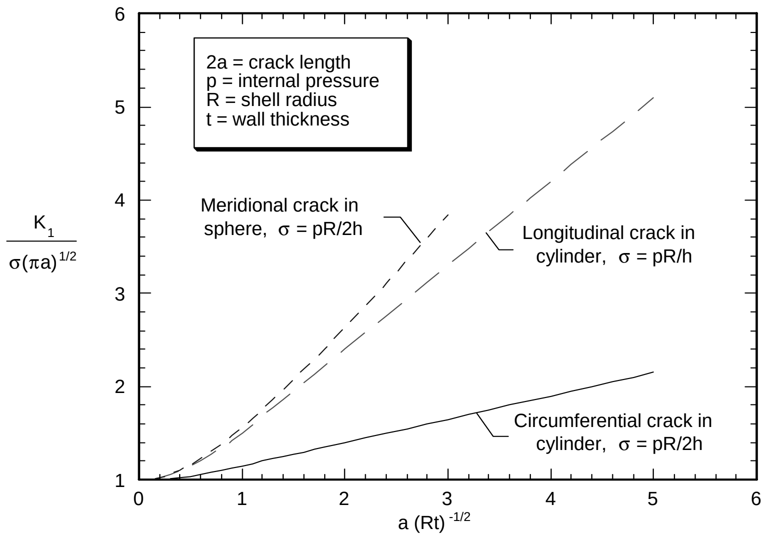

FIGURE 7.8.4.1.4(d) *Stress intensity correction factors for pressurized shells with cuts (Reference 7.8.4.1.4(b)).*

7.8.4.2.1 Fracture mechanics approaches

This section is reserved for future use.

7.8.4.2.2 Sublaminate buckling methods

<u>Method A:</u> Successive Sublaminate Buckling

This method is applicable to solid laminates or facings of sandwich structures. When loaded in compression or shear, the sublaminate adjacent to the delamination may buckle (Reference 7.8.4.2.2(a)). In sandwich structures only the surface sublaminate, not the one bonded to the core, can buckle. In solid laminates both sides can buckle. When the sublaminate buckles, out-of-plane loads develop at the edge of the sublaminate causing a growth of the delamination. A larger delamination will buckle at a lower load. Once a sublaminate buckles it is assumed that it is unable to sustain further loads. This is the basic conservative assumption of the analysis method. The analysis method (References 7.8.4.2.2(b) and (c)) is a step by step application of lamination theory together with first fiber mode failure criteria and buckling analysis of anisotropic plates. The following steps are performed:

1. The laminate is divided into sublaminates according to the through the thickness location of the delamination as obtained from NDE.
2. The external load is distributed between the sublaminates according to their stiffness.
3. The sublaminates are checked for static compression, shear or combined load according to lamination theory.
4. The sublaminates are checked for buckling. Simply supported boundary conditions are assumed for outer sublaminates. Clamped boundary conditions are assumed for inner sublaminates in a case of multiple delaminations.
5. A buckled sublaminate is conservatively assumed to be unable to sustain the buckling load. Additional load is transmitted to the unbuckled sublaminates.

For a single delamination, the strength of the delaminated laminate will equal the strength of the sublaminate with the larger resistance to buckling. For multiple delaminations, as in the case of impact damage (see Section 7.8.1), steps 2-5 are repeated until failure.

This simplified model gives conservative results for sandwich facings, and good results for solid laminates containing delaminations and impact damage.

<u>Method B:</u> In-Plane Stress Concentration Adjacent to Buckled Sublaminates

In Method B, the buckled sublaminates have reduced stiffness, carrying their buckling loads until laminate failure due to an in-plane stress concentration**.**

7.8.4.3 Impact damages

Impact damage has been shown to reduce structural residual strength under tension, compression, shear, and combined load cases. Post-impact residual strength is an important consideration for damage tolerant design and maintenance. Several different approaches to predicting post-impact residual strength have been documented in the literature. A semi-empirical analysis was developed from the large database collected during the U.S. Air Force contract (Reference 7.5.1.1(j)) for stiffened wing structure. This analysis predicted residual strength as a function of key design variables and impact energy. Although such an approach supports design, it has limited benefit to service problems in which little or no data is available on the impact event. Residual strength predictions based on a quantitative measure of the CDS have subsequently emerged.

7.8.4.3.1 Sublaminate buckling methods

When impact damage is dominated by matrix cracks and delaminations, sublaminate stability is crucial to compression or shear stress redistribution and reduction in residual strength (References 7.8.1.2.2(a) through 7.8.1.2.2(d)). The CDS must be known in order to predict sublaminate stability. For example, the CDS shown in Figure 7.8.1.2.7(c) is dominated by 4-ply thick, unsymmetric sublaminates that repeat through the laminate thickness, depending on the number of repeating ply groups in the stacking sequence.

Once buckled, sublaminates may be assumed to carry a constant load and a stress concentration develops in the adjacent undamaged material. The stress concentration is related to the effective reduced stiffness of the buckled sublaminates, which changes as a function of the initial buckling stress and increasing loads. The reduced stiffness at failure can be estimated by matching the buckling stress with the material's local compressive strain at failure. Test measurements of local strains show that these analysis assumptions provide reasonable accuracy in estimating the stress concentration at the edge of buckled damage (Reference 7.5.1.1(m)). Prediction of CAI has also been confirmed by residual strength tests (References 7.8.1.2.2(a) through 7.8.1.2.2(d)). This engineering approach to predicting CAI has been successfully applied to sandwich panels (Reference 7.8.4.3.1(a)). More involved methods, including finite element simulation of the sublaminate buckling and adjacent stress concentration, have also been used to predict failure of laminated composites (Reference 7.8.4.3.1(b)). Such an approach may be required for built-up structure, in which load redistribution occurs.

The basic sublaminate stability analysis (Reference 7.8.4.1(a)) involves four steps. First, the damage state is characterized with the help of NDI and the damage is simulated as a series of sublaminates. Second, sublaminate stability is predicted with a model that includes the effects of unsymmetric LSS. Third, the in-plane load redistribution is calculated with a model that accounts for structural geometry (e.g., finite width effects). Finally, a maximum strain failure criterion is applied to calculate CAI strength. Figure 7.8.4.3.1(a) shows typical results from this analysis procedure.

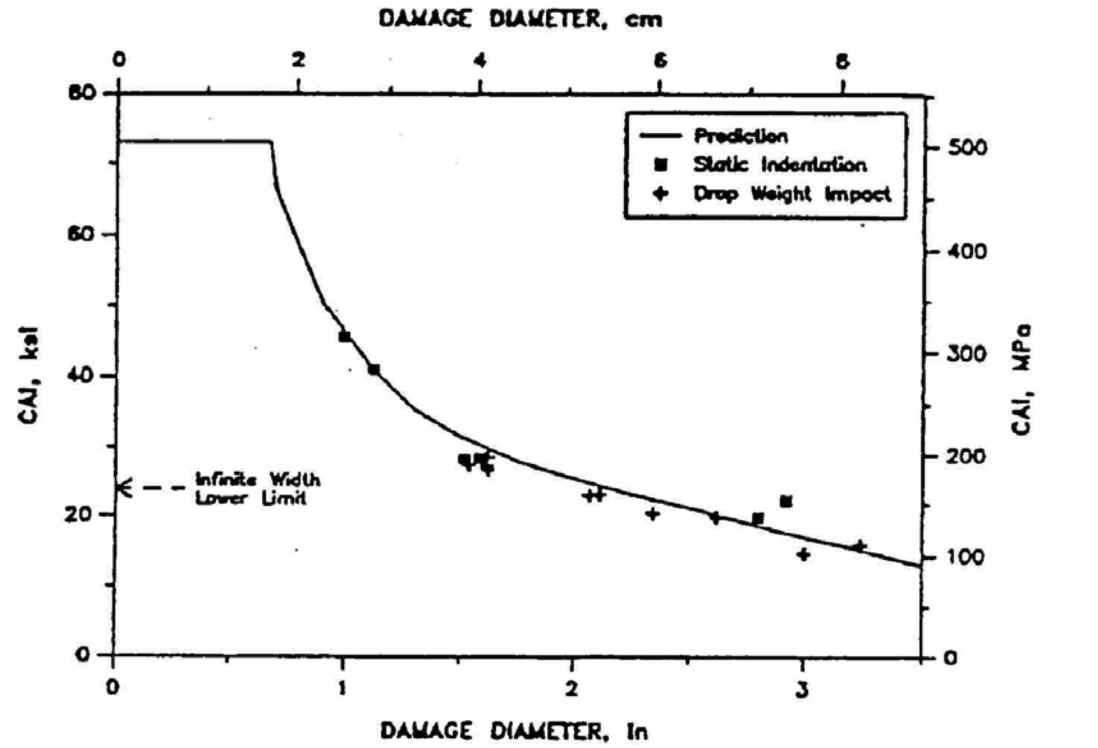

FIGURE 7.8.4.3.1(a) *Analysis and test results for 5 in. (127 mm) wide specimens, AS6/3501-6, [45/0/-45/90]5s and ply thickness = 0.0074 in. (0.1880 mm).*

A similar model with slightly different assumptions has been developed in References 7.8.4.3.1(c) through 7.8.4.3.1(e). The residual strength of an impacted laminate loaded in compression and shear can be estimated by considering the successive buckling of sublaminates and load redistribution among non-buckled sublaminates, until fiber mode failure of the remaining laminate. This model requires input data from NDE to define position, number, and dimensions of the delaminations that divide the laminate into sublaminates. The Damage Model is built from the NDE data and conservative assumptions. The impacted region is simplified to a sequence of sublaminates bonded at the delamination boundaries, Figure 7.8.4.3.1(b). The failure analysis is described schematically in Figure 7.8.4.3.1(c). The applied load is distributed between the various sublaminates according to their relative stiffness. Failure of each sublaminate is checked for compressive strength and buckling. As one sublaminate buckles, it is assumed that it cannot carry additional load, and all the load is redistributed between the remaining sublaminates, until fiber mode failure of the remaining laminate. In spite of the many assumptions made in the interpretation of the NDE results as well as in the construction of the damage and failure model, the results are in very good agreement with compression after impact experimental data for various materials and impact energies (Figures 7.8.4.3.1(d) and (e)). This agreement exists because of the sequential nature of the model. Since the layers are failed one after another, the exact value of a sub-laminate failure is not important, as long as the failure sequence is correct. The overall precision of the calculation is the precision of the fiber mode failure of the last failed sublaminate.

Similar analysis can be applied to compression facings of sandwich structures (Reference 7.8.4.3.1(f)). Sublaminates can only buckle away from the core and the core has a stabilizing effect, so the predictions are more conservative than for thick laminates.

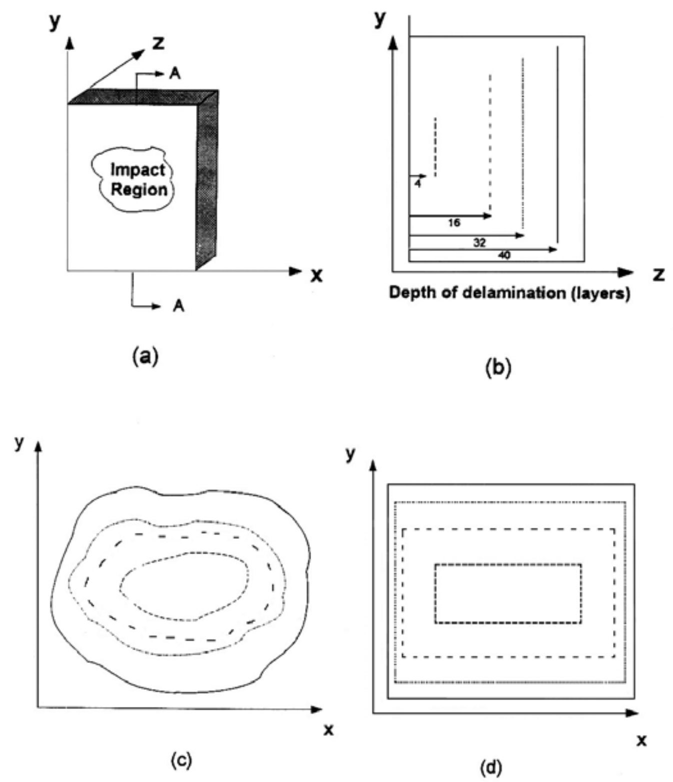

FIGURE 7.8.4.3.1(b) *Construction of damage model (AS4/3502, impact energy of 67.8 ft-lbs (91.9 N-m)) (a) damaged specimen; (b) cross-section through damage region (aa); (c) shape of major delaminations; (d) rectangular delaminations used in the model (References 7.8.4.3.1(c) through 7.8.4.3.1(e)).*

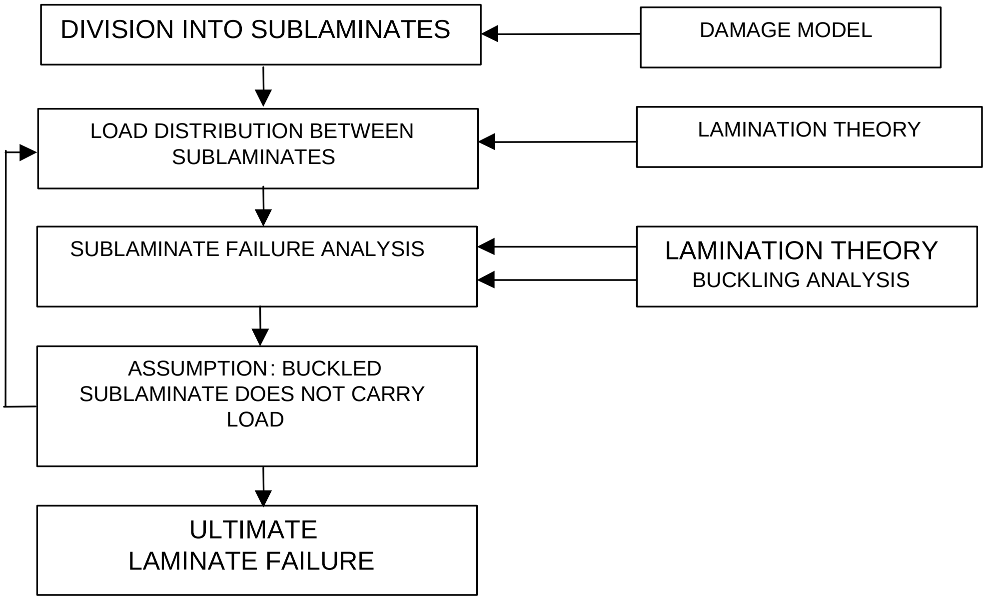

FIGURE 7.8.4.3.1(c) *Schematic description of failure model (References 7.8.4.3.1(c) through 7.8.4.3.1(e)).*

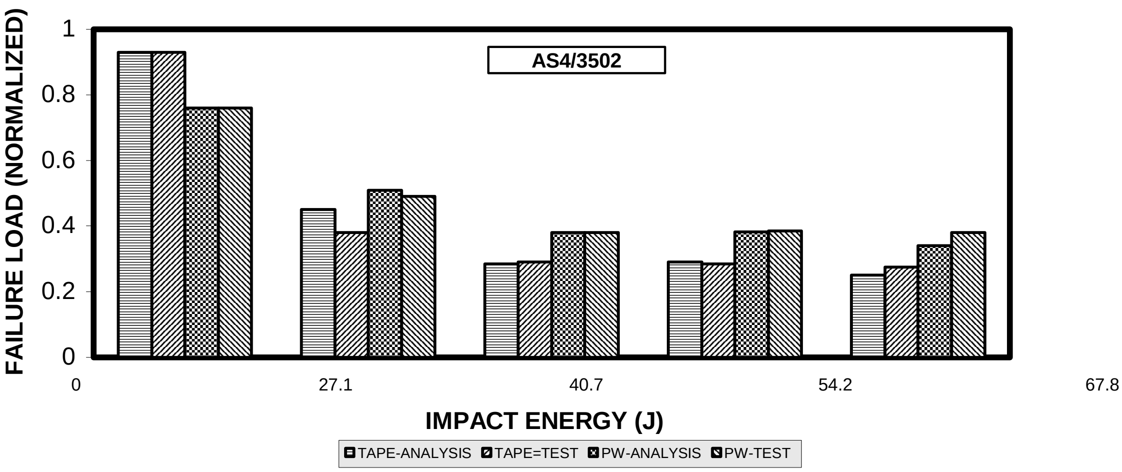

FIGURE 7.8.4.3.1(d) *Failure Load as a function of impact energy (References 7.8.4.3.1(c) through 7.8.4.3.1(e)).*

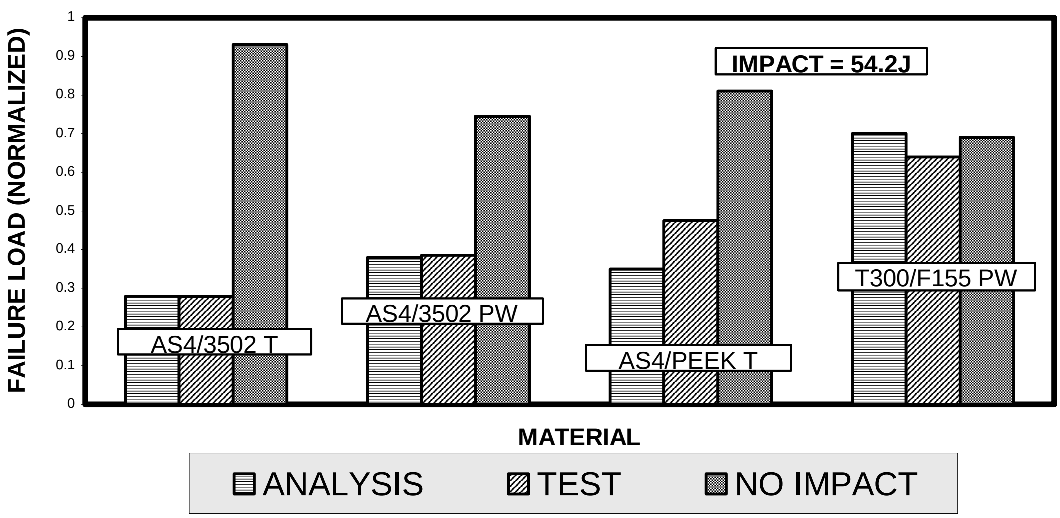

FIGURE 7.8.4.3.1(e) *Failure load as a function of material (References 7.8.4.3.1(c) through 7.8.4.3.1(e)).*

7.8.4.3.2 Strain softening methods

The strain-softening approaches discussed for large through-penetration damage in Section 7.8.4.1.2 can be adapted to address impact damage scenarios. In studies reported in References 7.8.1.2.8(g) and 7.8.1.3(e), material laws for the damaged facesheet material within the impact zone was scaled from the undamaged material law, as shown in Figure 7.8.4.3.2(a). The scaling factors were determined from tests conducted on relatively small specimens containing representative impacts. The indentation resulting from the impact was approximated by reducing the core height at nodes to best represent that measured in the impact trials. Note that the approximations of the perimeter were significantly limited by the fixed mesh size necessary to complement the strain–softening law.

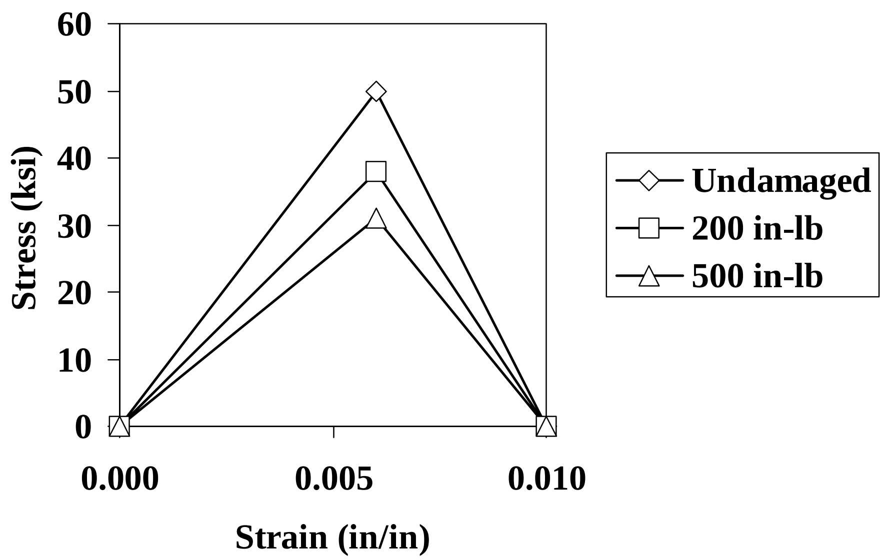

FIGURE 7.8.4.3.2(a) *Strain-softening laws for impact damaged material.*

The described approaches were used to predict unconfigured and configured impacted compressive strength. The unconfigured results are summarized in Figure 7.8.4.3.2(b). Two test points were used to calibrate the material law, while the other two tests were predicted. The predictions were within 10% of the test results.

Predictions were also made of two 30 x 44 in. (762 x 1118 mm) curved panels (122 in. (3.1 m) radius) with two circumferential frames. Both panels were impacted at 200 in-lb (22.6 N-m) impact damage, with one of the panels impacted on the inner (IML) facesheet, while the other was impacted on the outer (OML) facesheet. The predictions are compared with the experimental results in Figure 7.8.4.3.2(c). Predictions were within 7% of the measured values.

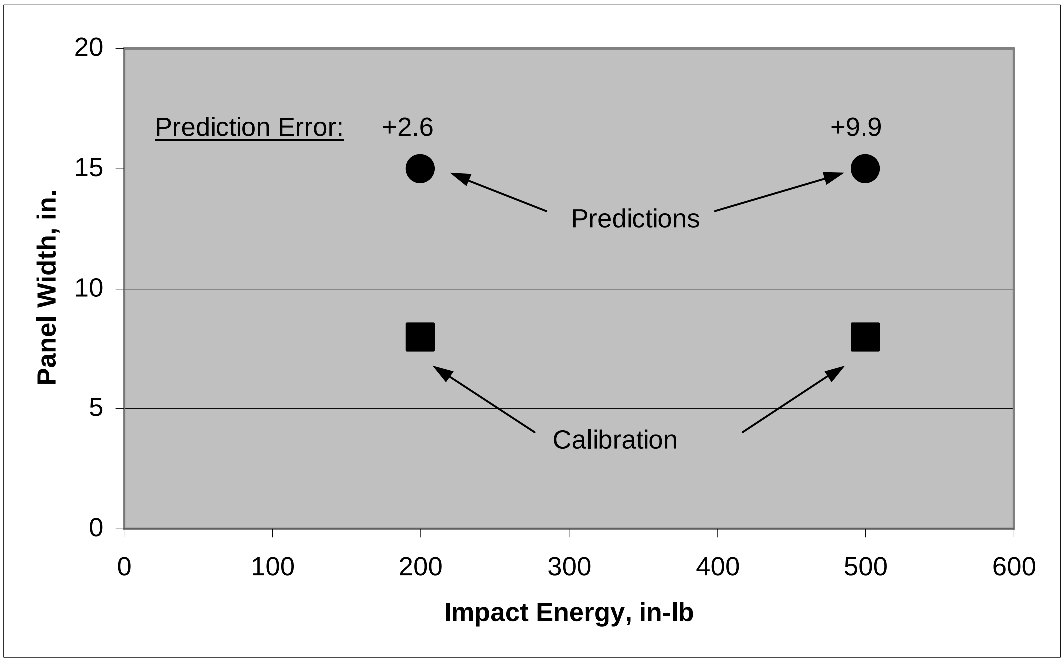

Lay-up: [45/0/-45/90/0/-45/45/0/90/-45/0/45] Panel Sizes: 8 x 15, 15 x 30
Material: AS4/8552
Core: ¾" 8 pcf HRP

FIGURE 7.8.4.3.2(b) *Strain softening predictions of unconfigured impacted compression strength.*

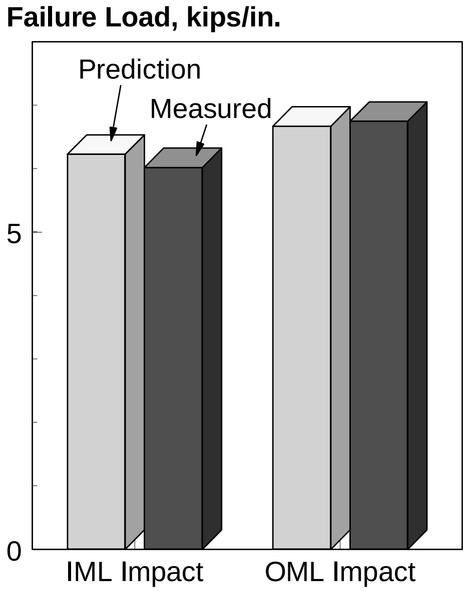

FIGURE 7.8.4.3.2(c) *Comparison of measured impacted compression failure loads with strain softening predictions.*

7.8.4.4 Cuts and gouges

Fortunately, most of the damage that is critical to tensile loading such as cuts and gouges is, to some degree, visible. Tests have shown that for tensile loading, the residual strength of a laminate with a cutout is primarily dependent on the width of the cutout and essentially independent of the cutout shape. Thus ultimate design values reduced to account for the presence of a 0.25 inch (6.4 mm) diameter hole also account for an equivalent length edge cut. Cuts of this type that might be produced during manufacturing are a special problem since they may be filled with paint, and consequently, not detected. Sufficient testing should be done as part of design verification programs to ensure that cuts and gouges that are on the threshold of visibility will not degrade the structural strength below Ultimate Load requirements.

Small cuts and gouges ($\leq$ 0.25 inch (6.4 mm)) can also affect the residual strength for load cases dominated by compression and shear. Such damage has not been a design driver for compression and shear Ultimate Load requirements of composites with first-generation, brittle epoxy matrices because BVID is more critical for such materials. However, small cuts and gouges can be critical for such load requirements when using toughened matrix, textile, or stitched composite materials.

Larger cuts or gouges, which are clearly visible, lower compression, shear, and tensile strengths below Ultimate Load requirements. Methods discussed in Section 7.8.4.1 can be used to evaluate panels with this level of damage.

7.9 APPLICATIONS/EXAMPLES

Composite structure application in the aerospace industry has progressed to the extent that a number of vehicles containing primary composite components have been certified/qualified for use. This section presents a discussion of some representative applications in various categories and types of aircraft. The examples are intended to provide the reader with some insight to how vehicle prime contractors have approached durability and damage tolerance issues and successfully satisfied appropriate requirements.

Requirements are evolving and specific structural applications on various vehicles often contain unique features, hence the examples are not to be construed as the only way to accomplish damage tolerance and durability. Instead, they illustrate the thinking, focus, and scope of the task. It is hoped this will be of help in future programs.

7.9.1 Rotorcraft (Sikorsky)

The damage tolerance approach for composite rotorcraft under cyclic loading combines analysis and building block testing (from coupon to full scale level) to demonstrate the required level of reliability (A or B-basis) of composite parts in the presence of damage. The approach demonstrates no growth of damage under spectrum loading for the required number of cycles at the representative environment(s) and with the appropriate load enhancement factors for statistical reliability. At the end of the lifetime fatigue test, residual strength is demonstrated.

7.9.1.1 Damage

The damage should be representative of the type of damage expected during manufacturing and service. The size of damage is determined as a combination of the maximum damage size allowed by the inspection means selected and a statistical treatment of the expected threats (tool drops, hail, runway debris, etc.). The location of damage is based on statistical analysis of the damage scenarios and the threats to which the most highly loaded areas of the structure may be exposed. Since routine inspections during service are visual inspections, no damage growth of non-visible damage must be demonstrated for the full service life of the aircraft. For visible damage, no growth must be demonstrated for at least three inspection intervals.

7.9.1.2 Environment

The structure should be tested at the worst environment expected in service. For most composite materials used in rotorcraft, this means elevated temperature wet conditions for static and residual strength testing, and room temperature wet conditions for fatigue testing. To avoid increased costs associated with setting up and maintaining environmental chambers, tests can be conducted at room temperature ambient conditions provided the applied loads are adjusted for environment with the use of an appropriate load acceleration factor. This factor is defined by analysis, coupon, and element testing that determine the environmental knockdown factor from room temperature ambient to the service condition for the type of loading and particular failure mode.

7.9.1.3 Test loading conditions related to critical failure modes

The loads applied during testing at the element and component levels should simulate the internal loads in the vicinity of inflicted damage. This is critical in the case of open hole compression and compression after impact tests. Many rotorcraft components such as flexbeams are designed to interlaminar shear or peel loads. Therefore, open hole compression or compression after impact tests are not directly applicable without prior demonstration of equivalence through adjustment of loading and hole size.

7.9.1.4 Test loads - load enhancement factor (LEF)

In addition to the load acceleration factor to account for environmental effects, a load enhancement factor is used to account for material variability. The full scale specimen is tested at a combination of lifetimes (typically one for rotorcraft due to the large number of cycles per lifetime) and applied loads such that at the end of a successful test, the required reliability (A or B-basis) is demonstrated. The LEF depends on the static and fatigue scatter exhibited by the material(s) used. Sufficient tests at the coupon, element, and component level are necessary to quantify the scatter. Weibull statistics and the approach given in Reference 7.9.1.4 are used for the determination of the LEF.

7.9.1.5 Spectrum - truncation

Helicopter dynamic components such as rotor and transmission components as well as airframe or empennage components exposed to rotor wake loading experience a very large number of cycles per lifetime. Typically, a 30000 hour lifetime may include more than a billion cycles. For this reason, a truncation level is established to eliminate loads from the test spectrum which will not propagate damage in the aircraft lifetime.

The truncation level is determined as a ratio of the stress (or strain) corresponding to 10^8 cycles on the S-N curve to the static room temperature wet A basis (or B-basis) strength with damage. This is done for each of the R ratios, loading, and failure modes expected in service. It should be pointed out that the room temperature wet A basis strength value may be significantly higher than the corresponding Limit Load. The truncation level determination is depicted graphically in Figure 7.9.1.5.

The truncation ratio can be shown to depend on R ratio ($\sigma_{min} / \sigma_{max}$) and damage type (hole versus impact or delamination for example). It will also depend on the materials used. For this reason, coupon and element test data covering materials, lay-ups, and representative R-ratios are necessary to establish a conservative truncation level that covers all cases.

As an alternative approach for the determination of the truncation level, the wearout equation proposed by Sendeckyj (Reference 7.9.1.5) and discussed in Reference 7.9.1.4 can be used. This requires sufficient data for each R ratio, material, and damage type which can be an exhaustive series of tests. The wearout equation in Reference 7.9.1.5 can be used to determine the truncation level as the A (or B) basis residual strength at a given number of cycles.

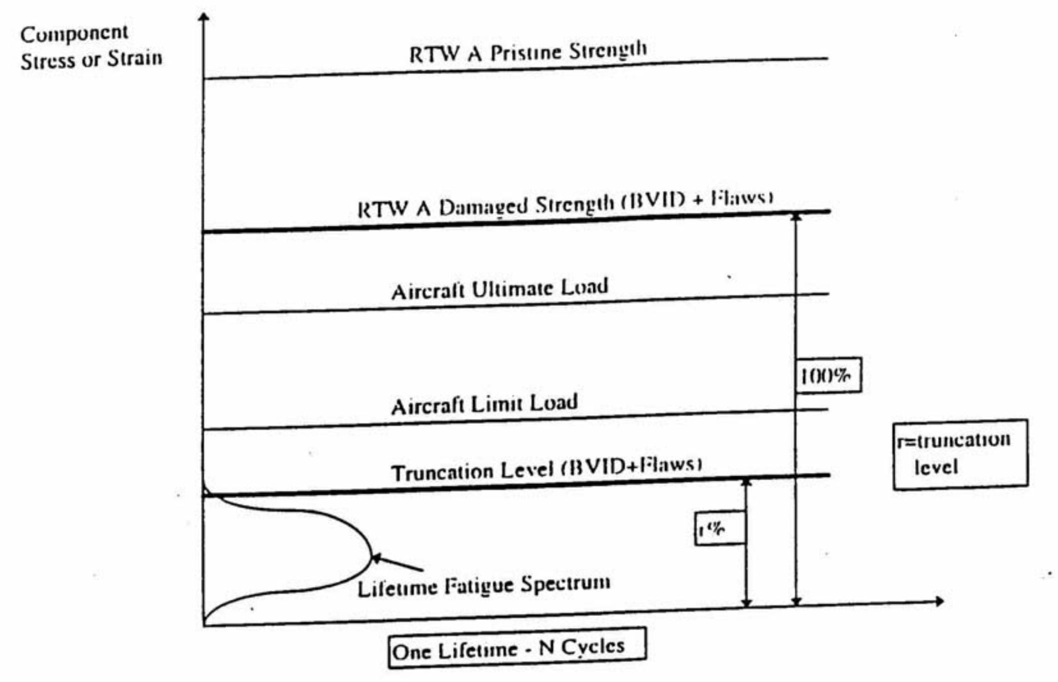

FIGURE 7.9.1.5 *Truncation level determination.*

7.9.1.6 Residual strength test

At the end of a successful fatigue test, residual strength must be demonstrated. Limit Load or Ultimate Load capability must be demonstrated depending on whether the damage present is visible or non-visible, respectively. The environment should be the worst environment for static loading (elevated temperature wet for most materials). Periodic residual strength tests can be incorporated during the fatigue test to protect against early failure or damage growth. In such a case, the last successful residual strength test marks the number of cycles for which the current design is certified.

The damage tolerance certification procedure for rotorcraft composites under fatigue loading is shown in Figure 7.9.1.6.

7.9.2 Commercial aircraft (Boeing 777 empennage torque boxes)

The damage tolerance approach for certification of commercial aircraft composite principal structural elements involves analysis and building block testing from the coupon to the full-scale levels (Reference 7.9.2). The approach demonstrates no growth of damage at the threshold of detectability (BVID) under repeated loading for a minimum of two airframe design service objectives ("lifetimes"). Residual strength for several damage scenarios is demonstrated after application of the repeated loading. The structural inspection plan is developed based on the maintenance program and on environmental deterioration and accidental damage ratings developed in accordance with FAR 25.571.

This section outlines the tests and analyses used to validate the damage tolerance of the Boeing 777 empennage main torque box structure.

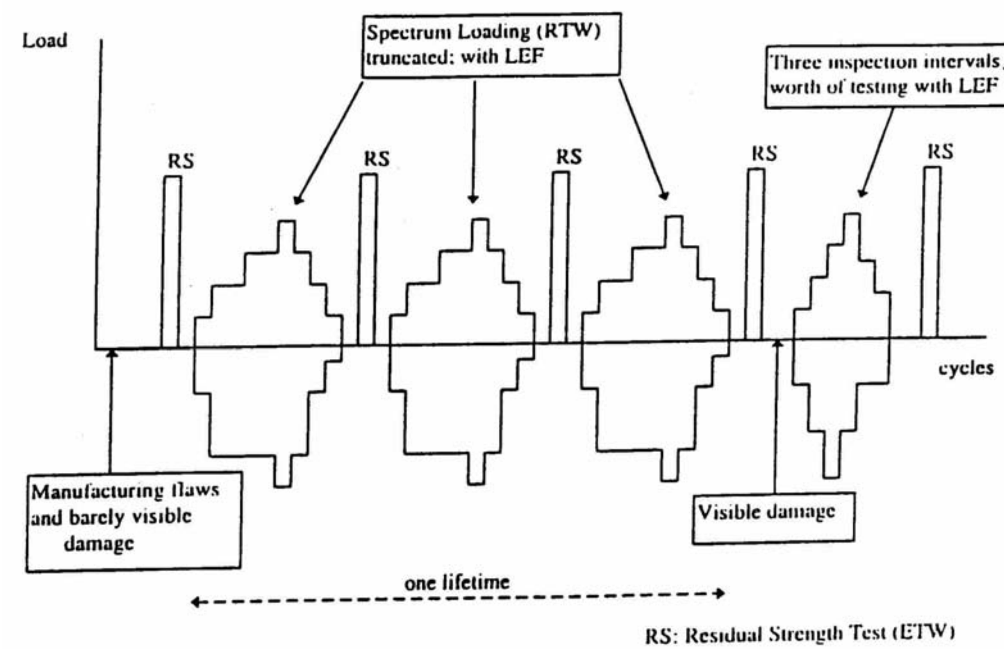

FIGURE 7.9.1.6 *Schematic of fatigue testing for rotorcraft.*

7.9.2.1 Durability - environmental

Environmental durability of the materials and structure was validated by:

- Long term exposure of panels attached to racks in several locations. Periodically the panels are retrieved, specimens machined and tested, and the data compared to baseline data.
- Temperature-moisture cycling of a three (3) stringer skin panel section, bolted joints with moldable plastic shims (MPS), and laminates with resin rich areas.

7.9.2.2 Durability - mechanical loads

A series of coupons, element and sub-component level tests were used to validate that damage from repeated loading does not occur at operational load and strain levels. The following coupon tests were conducted to at least 106 load cycles:

- Unnotched laminates (edge delamination test).
- Laminates with an open hole.
- Laminates with pad-ups.
- Bolted joints (composite-composite, composite-titanium).
- Radius details.

The following sub-component tests were conducted without experiencing damage initiation in the composite structure:

- Five stringer panel with a bonded repair and “barely visible impact damage” (BVID) impacts; tested to 2 lifetimes of repeated loads.
- Horizontal stabilizer skin splice joint panel with BVID impacts; tested to 2 lifetimes of repeated loads + 1 lifetime with enhanced loads.
- Vertical fin-to-body root joint panel; tested to 38 equivalent lifetimes repeated loads.

In addition, a pre-production horizontal stabilizer test box and the 777 horizontal stabilizer and vertical fin were tested to at least two lifetimes of repeated loads without experiencing damage initiation in the composite structure.

7.9.2.3 Damage

The 777 empennage composite structure is designed to be resistant to corrosion, and strain levels are such that damage initiation or growth (of visible and non-visible damages) does not occur with repeated operating loads. Therefore, accidental events are the only realistic damage source for damage tolerance evaluation of the composite structure.

The damages for evaluation are representative of the type and severity expected during manufacturing and service. The size of damage is determined based on the capability of the selected inspection method(s). Structure with damage at the threshold of detectability (BVID) must be capable of Ultimate Loads and demonstrate “no damage growth” under operating loads for the expected service life of the airplane. If detrimental damage growth is indicated, then damage must be shown to be detectable before it reduces the structural strength below Limit Load capability. Damages are generally applied to the most critically loaded areas of the structure.

The main source of discrete source damage for the empennage main torque boxes is from impacting objects. The main torque boxes are located in lightning strike zone 3 (no direct attachment or swept lightning strikes) and, therefore, are not affected by direct lightning. The leading edge structures are of metal construction, and are designed to prevent bird strike damage to the main box.

7.9.2.4 Damage tolerance - "no growth" tests

Since routine inspections of the 777 composite structures during service are visual inspections, and since the characteristic growth of typical damage to composite structure is not visual, the “no growth” approach for damage tolerance certification is used. The “no growth” of damages at the threshold of detectability must be demonstrated for the service life of the aircraft. For visible damages which are readily detectable by scheduled inspections, “no-growth” must be demonstrated for at least two inspection intervals. This is to insure that the damages will not progress beyond the critical damage threshold (CDT) for which the structure must maintain Limit Load capability.

The “no-growth” of small damages was demonstrated with element, sub-component and component level tests tested to a minimum of 2 lifetimes of repeated loads. The following element and sub-component repeated load tests demonstrated no damage growth:

- Laminates with BVID impacts.
- Shear panels with BVID impacts at the edge of cutouts.
- Five stringer panel with a bonded repair and BVID impacts.
- Horizontal stabilizer skin splice joint panel with BVID impacts.
- Spar shear beams with BVID impacts at the edge of web cutouts.

A pre-production horizontal stabilizer test box was subjected to a series of static and repeated spectrum loads to verify the materials, design concepts, manufacturing processes, analysis methods, “no-growth” of damages, and ultimate and residual strength capabilities. Compression has been shown to be the critical mode of loading for impact damaged composite structures. The damage emphasis in the test program was on the highest loaded compression areas.

The specific locations of the individual damages were chosen on the basis of strain patterns developed by FE modeling and previous test results of sub-component panels which indicated critical areas. Various levels of damages were introduced into the test article on three separate locations in the test sequence (see Figure 7.9.2.4).

Apply BVID (small) damages
    60% Design Limit Load (DLL) Conditions - Strain Survey
    Repeated Loads (Fatigue Spectrum) - 1 Lifetime
    60% DLL Conditions - Strain Survey
    Repeated Loads (Fatigue Spectrum) - 1 Lifetime

Apply visible damages
    Repeated Loads (Fatigue Spectrum) - 2 Inspection Intervals
    100% DLL Conditions

Apply element damages   70% DLL Conditions - “Continued Safe Flight” Load Levels

Repair visible and element damages
    Design Ultimate Loads (DUL) Conditions
    Load to Destruction

FIGURE 7.9.2.4 *Testing sequence for pre-production horizontal stabilizer test box.*

The first damages applied were BVID or "small" damages. These were introduced before the start of testing. Small damages are defined as those which are visible at a distance of less than 5 feet (1.5 m) (threshold of detectability or BVID) or are the result of impacts at an energy level less than 1200 in-lb. (135 J), which is the energy level cutoff used for BVID. The small damages were inflicted at critical locations on the skin panels and spars to verify that the structure was capable of sustaining design Ultimate Loads with BVID present. All BVID were assumed to be undetectable and were not repaired during the test program. After application of BVID, the test box was subjected to two lifetimes of repeated loads that included a 1.15 load enhancement factor to account for potential data scatter in CFRP S-N curves. The second damages applied were "visible" damages. These damages were introduced after the end of the two lifetimes of repeated loads. Visible damages were defined as damages readily detectable during the scheduled inspection plan, and included dents and small cuts to the skin panels and spars. The visible damages were then subjected to repeated load testing equivalent to two inspection intervals and then to design Limit Loads.

No significant damage growth was detected at any of the BVID or visible damage locations on the test box. Minor amounts of “rounding” of the damage shape and separation of delaminated surfaces were detected early in the load cycling (delaminations where the ply surfaces are in contact are sometimes not detected by NDI). No damage growth occurred thereafter.

7.9.2.5 Damage tolerance - residual strength

Residual strength tests were conducted on sub-components and the pre-production test box to verify required load levels and validate analytical methods. The following sub-component test types were used to demonstrate limit and discrete source level damage capability.

- Five stringer skin panels with disbonded stringer (Limit Load).
- Five stringer skin panels with visible impact damage (Limit Load).
- Five stringer skin panels with a cut skin bay (Limit Load).
- Five stringer skin panels with a cut center stringer and skin bay (continued safe flight load).

The third set of damages applied to the pre-production test box were "element" damages. These damages were introduced after the completion of the repeated loads testing and Limit Load testing of the visible damages discussed above. Element damages were defined as complete or partial failure of one or more structural units. Three damages were applied: a cut stringer and skin bay, a cut front spar chord and adjacent skin, and a cut rear spar chord and adjacent skin. The test box was then subjected to series of "continued safe flight" static load conditions (approximately 70% of the empennage design Limit Loads). No significant damage growth was detected after application of the load conditions.

Analytical methods were used to demonstrate residual strength capability of the 777 empennage structure for the following damage types. The methods were validated by the sub-component and test box results. Environmental effects were accounted for in the damage tolerance analyses by applying factors derived from coupon tests to material property inputs for the analyses.

- Disbonded stringer - load redistribution and crippling analysis.
- Visible impact damage on skin panel - notch fracture analysis.
- Cut skin - notch fracture analysis.
- Cut skin and stringer - notch fracture analysis.
- Cut spar chord and skin - FE load redistribution analysis.

7.9.2.6 Inspection plan

The inspection plan for the 777 empennage is based on visual inspections. Since the “no-growth” approach was adopted and validated, the inspection intervals are based on environmental deterioration and accidental damage ratings (EDRs/ADRs), rather than on damage growth characteristics. A C-check (a comprehensive inspection of installations with maximum access to components and systems) for the 777 is typically performed at 4000 flight cycles or two years, whichever comes first. Typically, external surveillance inspections for the composite structure are scheduled at 2C intervals. Internal surveillance inspections for the composite structure are scheduled at 4C intervals.

7.9.3 General aviation (Raytheon Starship)

7.9.3.1 Introduction

The first airplanes were built of wood, fabric, and resin. In a way, today’s composite airplanes are returning to those basics, except now, the fibers are carbon and Kevlar and these are set in high temperature curing epoxy resins. The benefits of modern composite construction are obvious: low weight, high bending stiffness, and the ability to fabricate very large structures with compound curvature. These may be cured in a single piece, eliminating parts, joints, sub-assemblies, and associated inspection costs. The civil airplane certification of composite structures involves all the strength, stiffness, and damage tolerance evaluations normally applied to metallic structures; however, in damage tolerance evaluation of composite structures, although the same *principles* apply as those for metallic structures, the application of these principles must take into account the particular properties of composite structures.

7.9.3.2 Damage tolerance evaluation

7.9.3.2.1 Regulatory basis

Damage tolerance evaluation has been the norm for Transport Category Airplane structures (metal or composite) certified under Part 25 of the Federal Aviation Regulations since the late 1970's. The Starship was the first airplane to be certified to damage tolerance requirements under Part 23 Small Airplane regulations. Raytheon engineers worked in cooperation with FAA specialists to establish Special Conditions for Fatigue and Damage Tolerance Evaluation which were first published for application specifically to the Starship in 1986. These conditions have since been codified into the main body of Part 23, Federal Aviation Regulations.

The intent of damage tolerance evaluation is the same regardless of the size of the airplane, even though the regulations may contain different wording. In general terms, the intent is to ensure long term safety based on published inspection procedures considering manufacturing quality intrinsic to the processes used and recognizing that certain damage may occur during service.

7.9.3.2.2 Typical damage scenarios and related requirements

Three different damage scenarios will normally be considered:

Scenario 1, Initial Quality. This covers items intrinsic to the manufacturing process and the inspection standards. Scenario number 1 represents the as-delivered state and, therefore, the structure must be capable of meeting all requirements in terms of strength, stiffness, safety, and longevity.

Scenario 2, Damage During Assembly or Service. Damage from scenario number 2 must exhibit predictable growth, or no growth, during a period of in-service loading (usually expressed in number of inspection intervals) and must be detectable by the specified in-service inspection methods. Also, the residual strength of the structure with such damage must always be at least equal to the applicable residual strength requirements.

Scenario 3, Damage from Discrete Sources. Damage resulting from scenario number 3 will be obvious to the crew during a flight (or be detected during a preflight inspection) and, therefore, a specific set of residual strength criteria apply which are concerned with safely completing a single flight.

7.9.3.2.3 Damage source and modes

Up to this point no details of damage mode, damage magnitude, or structural response have been discussed. It simplifies the evaluation to first recognize the generic scenarios and potential damage sources. Then, from those, identify the possible damage modes and the desired structural response. From the above definitions it is not too difficult to build a matrix such as the one shown in Table 7.9.3.2.3.

The damage modes from scenario 1 are typically not a significant problem from the load capability point of view. However, the potential damage modes from intrinsic manufacturing quality must be identified and controlled by the manufacturing specifications and acceptance criteria. Given this, it is usually easy to demonstrate that these small imperfections will not grow under cyclic loads typical of commercial airplane service.

Scenario 3 imparted damage is at the opposite end of the scale: these modes of damage are easily detectable and will need attention before further flight (except maybe for an authorized ferry flight to a repair facility). Therefore, inspection and longevity are not concerns.

The scenario which creates the most need for investigation is scenario 2, and a typical test program is described in the following section.

7.9.3.2.4 Element testing

To evaluate composite honeycomb structural performance under the various damage modes, element testing is usually performed. It is *possible* to conduct these evaluations on the full scale test articles, but this is a risky approach and the results will be too late to guide the design to a minimum weight and cost configuration.

TABLE 7.9.3.2.3 *Example matrix: damage source and potential modes.*

SCENARIO 1		SCENARIO 2		SCENARIO 3	
Source	**Damage Modes**	**Source**	**Damage Modes**	**Source**	**Damage Modes**
Manufacturing process	Small imperfections within the inspection sensitivity and acceptance criteria: - Porosity - Voids - Disbonds	Tools Baggage Hail Gravel	Resin cracking Delamination Core crush Puncture	Severe lightning	Plies burned Puncture
		Lightning	Resin burn Delamination Loose rivets	Bird strike	Delamination Core crush Puncture
		Water intrusion	Core cell damage	Rotor burst	Puncture Severed elements
		Cyclic loading	Delamination growth Disbond growth	Engine fire	Resin burn Delamination
		Bleed air	Resin burn	Ground equipment Hangar doors	Puncture

Static Tests. Testing to validate tolerance to the damage modes in scenario 2 will include impact tests without puncture, puncture tests of detectable size and larger, water ingression tests with freeze/thaw cycles, and lightning strike tests. Strength testing will be performed for the failure modes shown to be critical based on the internal loads analysis, typically a finite element analysis.

The static strength portion of the element test matrix is shown in Table 7.9.3.2.4(a).

A larger number of undamaged specimens may be tested at a selected loading in order to validate the laminate analyses by comparison of mean and B-basis test results to analytical predictions. This may also be desirable in order to establish that undue variability is not introduced by a particular manufacturing process.

Cyclic Tests. The test matrix for cyclic loading follows the same pattern, except now loading at multiple stress levels is desirable to establish the sensitivity of flaw growth to cyclic stress level. Again an increased number of specimens may be tested at a selected condition to identify variability, in this case as it affects flaw growth. Generally, cyclic testing of undamaged composite panels is not of great interest. Also, composite panels are less sensitive to flaw growth under tensile loading. This insensitivity can be demonstrated by testing at a constant amplitude of 67 percent of the maximum stress test result from similar specimens under static tensile loading, see Table 7.9.3.2.4(b). In addition to constant amplitude stress level testing, spectrum loads representing lifetime varying amplitude loads should be tested as there is, today, no industry-wide acceptance of analytical methods predicting flaw growth rates under lifetime variable amplitude loading.

Pressure Cabin Shell Residual Strength. Honeycomb construction has a particular advantage in maintaining residual strength after incurring large size damage from sources such as those described scenario 3. This is due to the honeycomb shell stiffness imparting great resistance to crack bulging which in thin skin structures is a source of high crack extension forces. Tests to validate residual strength in the presence of large puncture damage are usually conducted on cylinder wall samples loaded to simulate internal pressure or a combination of pressure and shear.

TABLE 7.9.3.2.4(a) *Element test matrix--static loading.*

TEST TYPE/ DAMAGE MODE	TENSION (Fuselage Top)		COMPRESSION (Fuselage Bottom)	SHEAR (Fuselage Side)
	Hoop	Longitudinal		
Undamaged	3	3	12	3
Impact	3	3	3	3
Detectable Puncture	3	3	3	3
Large Puncture	3	3	3	3

NOTE: Numbers in cells indicate number of replicates.

TABLE 7.9.3.2.4(b) *Element test matrix - cyclic loading.*

	TENSION			COMPRESSION				SHEAR		
STRESS LEVEL	**1**	**2**	**3**	**1**	**2**	**3**	**Spectrum Loading**	**1**	**2**	**3**
Impact	3			3	3	3	3	3	3	3
Detectable Puncture	3			3	12	3	3	3	3	3

NOTE: Numbers in cells indicate number of replicates.

7.9.3.2.5 Test results

Selected examples of element test results in typical presentation formats are shown in the following figures. The results shown were obtained from samples representing fuselage shell construction on a business jet. However, scale matters, and different results might be obtained from tests on samples representing large transport airplanes because of different face sheet thicknesses and core densities required to carry the basic pressure and bending loads.

Tension. From Figure 7.9.3.2.5(a), hoop tensile loading from internal pressure, it's clear that designing for damage tolerance need not impose a serious weight penalty. Ultimate design pressure must be carried with the undamaged panel and this means that just a little additional material will enable the panel to meet the required residual strength load with large puncture damage. This is because residual strength required for the pressure case is about 60 percent of the ultimate pressure. In the case of longitudinal tensile loading from fuselage bending, Figure 7.9.3.2.5(b), the residual strength requirement is Limit Load, i.e., about 67 percent of the ultimate pressure, and again to carry that load with a large puncture a small amount of material must be added. In both cases a more robust structure would result if Ultimate Loads were to be carried with impact damaged panels. And this may be required by the regulations unless impact damage is readily detectable.

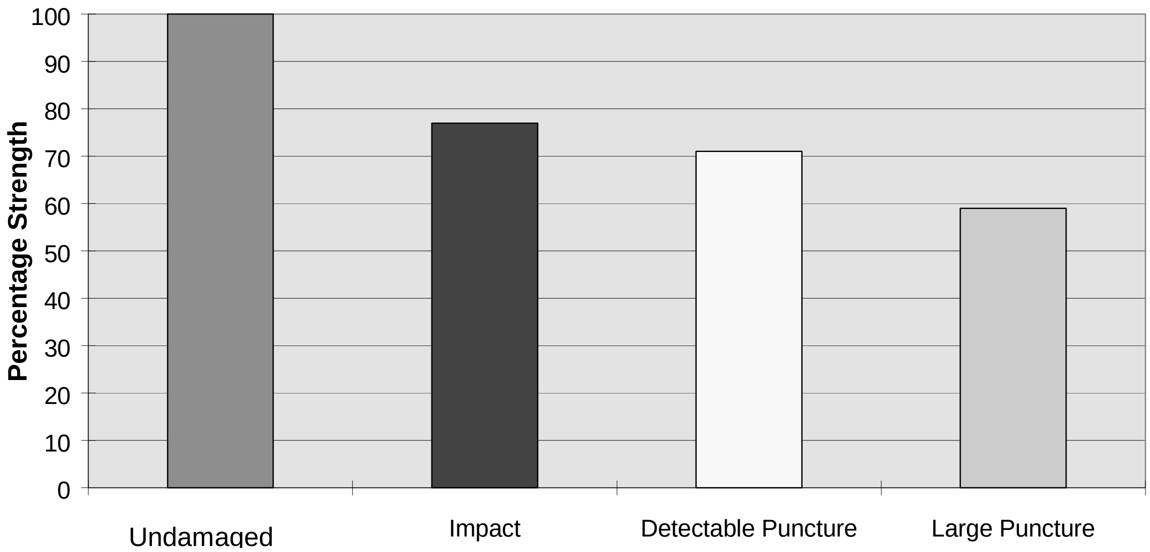

FIGURE 7.9.3.2.5(a) *Tension - hoop.*

Compression. As shown in Figure 7.9.3.2.5(c), a similar situation exists in the case of compressive loading from fuselage bending. Designing to the residual strength requirement with large puncture damage would imply using approximately 85 percent of the allowable undamaged strength; but if impact damage is to be good for Ultimate Load then only 65 percent of the undamaged strength will be used. This may not be a serious penalty as the maximum compressive loads occur in the fuselage bottom from down-bending load cases and the lower fuselage is usually reinforced by cargo or passenger floor structure.

Shear. Maximum shear loading occurs along the side of the fuselage. Again, designing to carry Limit Load (67 percent of Ultimate Load) with large puncture damage is a slight weight penalty, approximately 82 percent of the maximum undamaged strength can be used. But in this case, 82 percent of undamaged strength will accommodate impact damage at Ultimate Load. This is illustrated in Figure 7.9.3.2.5(d).

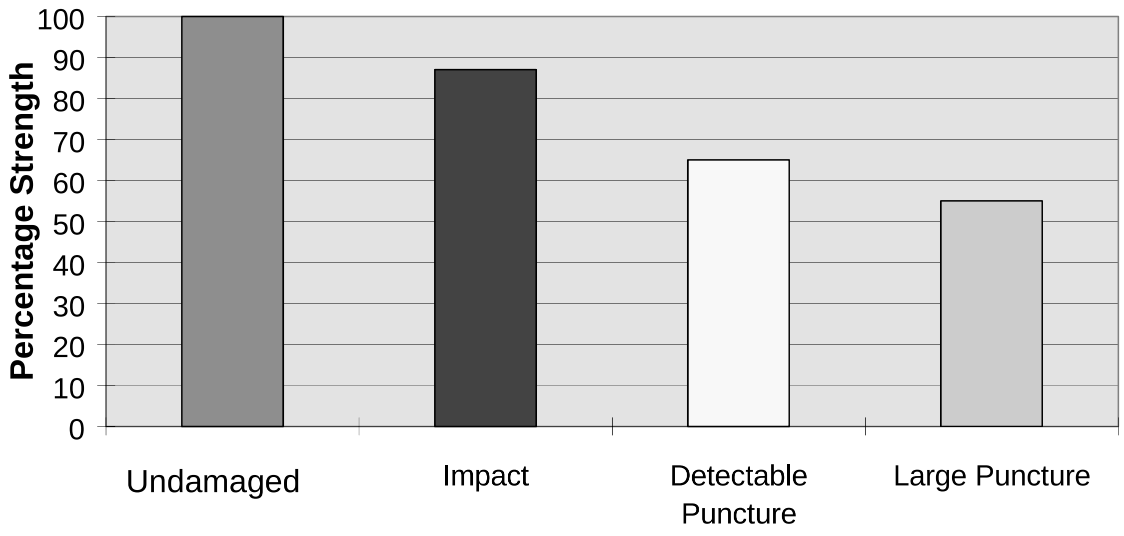

FIGURE 7.9.3.2.5(b) *Tension - longitudinal.*

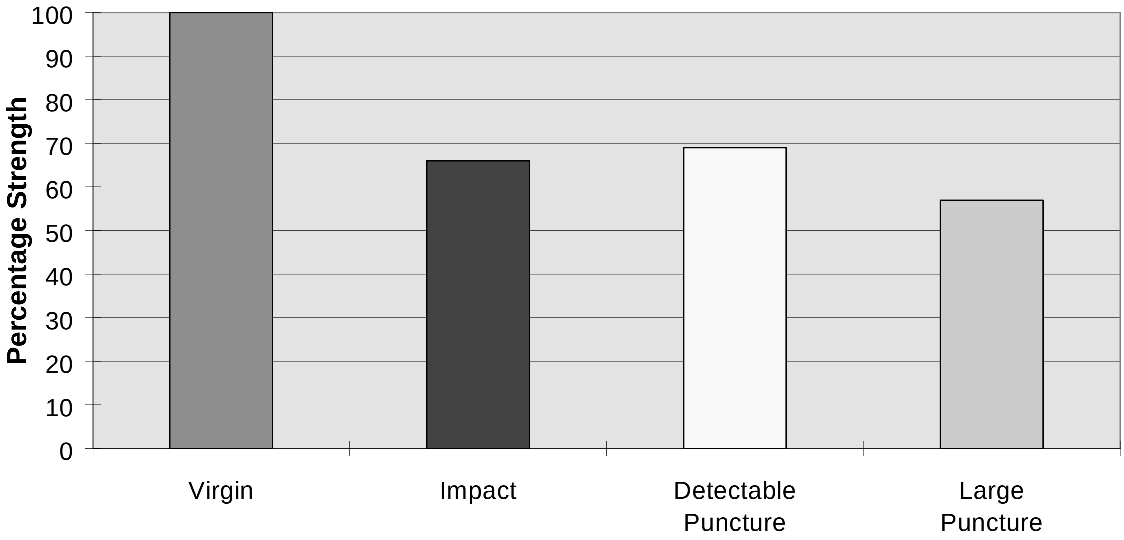

FIGURE 7.9.3.2.5(c) *Compression.*

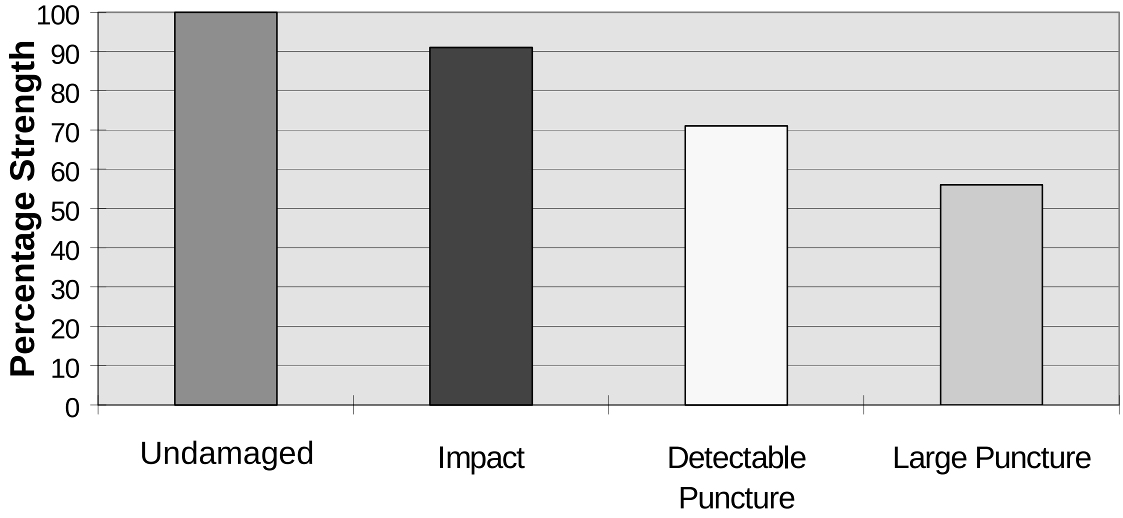

FIGURE 7.9.3.2.5(d) *Shear.*

Pressure Cylinder Results. Figure 7.9.3.2.5(e) presents an assemblage of test results illustrating the trend from no damage to massive damage. Massive damage being the type of wall puncture that could only occur from a serious collision with ground support equipment such as steps, generator carts, refueling equipment, baggage handling equipment, and so on. As mentioned previously, this type of damage should be obvious and should be detected before flight, but, just in case... tests are conducted to determine cylinder wall residual strength with large and obvious damage. The test points indicated as MIT in Figure 7.9.3.2.5(e) are from honeycomb wall cylinders tested at MIT, see Reference 7.9.3.2.5. The trend revealed is typical of test results from big and small airplane pressure containment structure in that with larger and larger damage a residual strength threshold becomes apparent.

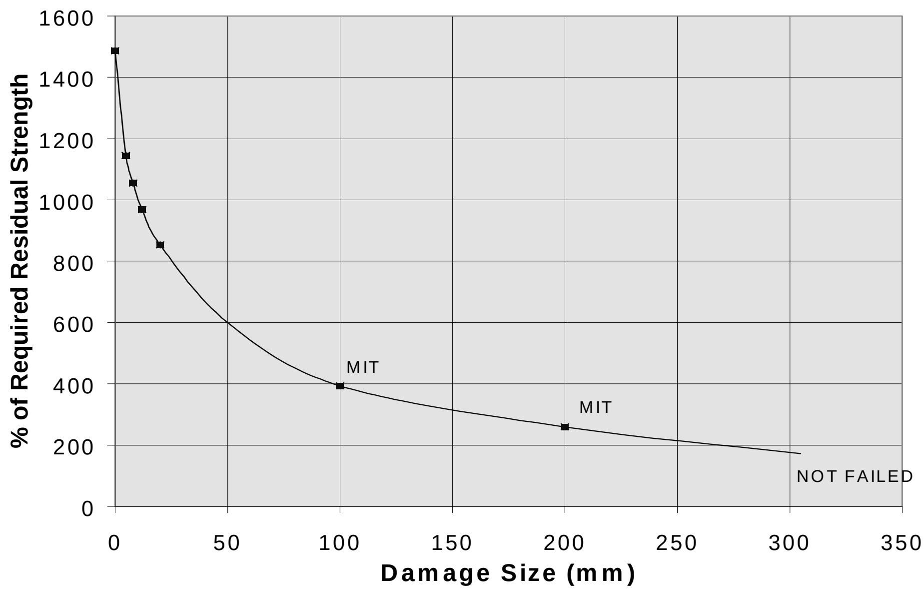

FIGURE 7.9.3.2.5(e) *Cylinder wall test results (internal pressure).*

Cyclic Test Results. An example is presented in Figure 7.9.3.2.5(f) of typical constant amplitude test results for large puncture damage under constant amplitude compressive loading. The most useful presentation for these data is as shown, i.e., a best-fit straight line. This type of plot can be used to assess important damage tolerance characteristics of the materials tested. The significance of scatter in flaw growth life can be assessed by plotting a B-basis stress-life line assumed to be parallel to the mean life plot. The flaw growth threshold may then be determined by extrapolation of the B-basis life line to ten million cycles (100 million in the case of rotating equipment with high cycle loading).

A prime use of these data is to structure the full scale cyclic test to run in an economical, yet rational, manner. All stress cycles below the flaw growth threshold may be eliminated from the full scale test spectrum. Also, scatter in flaw growth life may be accounted for by a factor increasing the applied loads and, therefore, reducing the number of test lifetimes.

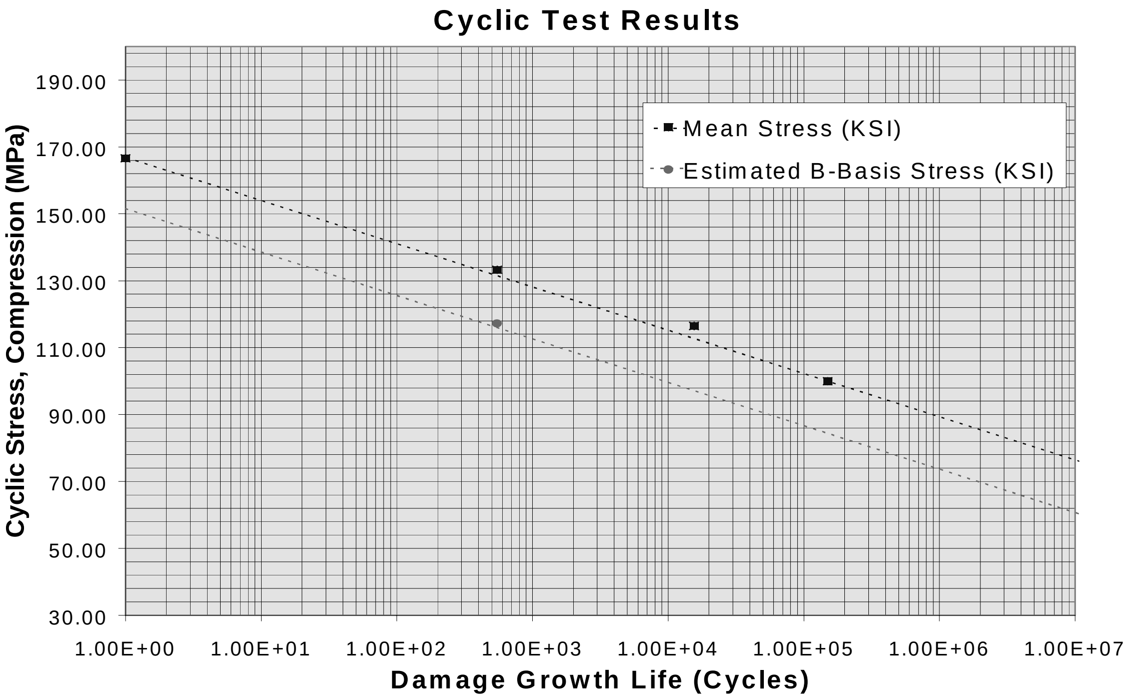

FIGURE 7.9.3.2.5(f) *Constant amplitude cyclic test results - large puncture damage under compression loading.*

7.9.3.2.6 Full scale tests

Full Scale Cyclic Tests. Certification of major load carrying structure requires that components such as wings, fuselages, and tail structures are tested through a sequence of loads representing at least two lifetimes of expected missions. Each lifetime consists of thousands of load cycles, including wing lift, fuselage reactions, tail loads, pressure cycles, and landing loads. During these tests damage will be mechanically inflicted in the structure to simulate in-service damage. These situations include lightning strike, hail damage, runway damage, and tool impacts. These damage modes will be tested through as much as one lifetime of fatigue testing to prove that the structure is, in fact, damage tolerant in the full size articles, i.e., that damage will not grow in an unpredictable manner and will always be detected by the inspections specified.

Larger damage may be inflicted later in the full scale cyclic testing to simulate impacts with ground service equipment, impacts with hangar doors and other aircraft (hangar rash) and poor maintenance practices; all bad things that occasionally happen in the loading, handling, and maintenance of commercial airplanes. The larger damage modes should be detected before the next flight and so the demonstration for these modes may consist of a relatively few flights of cyclic loading and inclusion in the residual strength tests.

Full Scale Residual Strength Tests. After completion of the lifetimes of cyclic testing, the major components of wing, fuselage and tail will be subjected to load tests to verify that, in spite of all the load cycles and inflicted damage, the remaining structure will still carry the required residual strength loads (flight loads and/or pressure loads expected to be encountered during the service life of the aircraft, except for the larger damage modes which are associated with specific residual strength criteria).

7.9.3.2.7 Continued airworthiness inspections

Based on interpretation of the test results obtained, inspection procedures, threshold time, and frequency of inspections will be established and published in the airplane manuals. A factor is usually applied so that allowance is made for the damage to exist over several inspection intervals, depending on the criticality of the structure. A further factor may be needed to account for scatter revealed in the flaw growth test results.

7.9.3.3 Service experience

The service experience with primary composite structures in civil aviation has been excellent. Beech Starships have been flying since the late 80’s and no problems with major structure have been encountered. Composite stabilizer structures have been in use on Beech 1900 commuters flying typically 2500 hours per year since the mid 80’s; again no problems related to the composites have been reported.

Safety in the event of an emergency landing has also proven to be outstanding. A nose landing gear collapsed during a landing of one of the Starship test airplanes; the airplane was flown home and was back in service in 10 days. The repairs were made by procuring blank parts from the factory, cutting out the needed replacement sections, and splicing these into place by bonding and fastening.

An even more spectacular event occurred in Denmark in February, 1994. Starship number 35 ran off the runway into a snow bank at approximately 130 mph (210 km/hr) after an aborted take off. Crew and passengers were shaken but otherwise unhurt. No fuel was spilled, no seats came loose, no windshield or window glass was broken, or even cracked, and the cabin was undistorted enabling the cabin door to open normally. The crew and passengers unbuckled their seat belts and walked away. The right hand main gear collapsed, the other main gear and the nose gear were sheared off (not torn out, but the aluminum forgings severed) from the force of hitting the snow bank at high speed. The right hand wing tip was dragged along the ground and as a result suffered damage to the flaps, tip sail, and rudder. The nose section was damaged by the nose gear being severed and forced upward into the structure. The cabin underbelly was crushed through skidding along without the landing gear but the damage was localized to the area between the seats.

A team was sent to survey the damage and list the replacement parts needed. Later the airplane was repaired on-site by a crew of five technicians plus one engineer, one inspector, and one service manager. Some parts with localized damage were repaired using techniques published in the Starship Structural Repair Manual which allows damage to be repaired on-site by trained service staff. For more extensive damage, blank parts were delivered from the factory and were used as stock from which to cut replacement panels which were then bonded and/or fastened into place. Of course, aircraft systems such as landing gear, hydraulics, antennae, etc., were simply replaced with factory spare parts. The repairs were finished and the airplane rolled out for flight test in July of 1994. This was ahead of schedule and under budget, much to the surprise of the insurance company and the Danish aviation authorities who were both convinced that a metal airplane would have suffered much greater damage and would have been totaled by such an incident.

7.9.3.4 Conclusions

Modern manufacturing methods enable the fabrication of composite primary load carrying structures for commercial aircraft use which are low cost as well as low weight. These structures require a damage tolerance evaluation for certification to Part 23 or Part 25 of the FAA regulations. A rational damage scenario and a supporting element test program will considerably assist the damage tolerance evaluation.

Composite structures can be designed to tolerate large damage with a small weight penalty. It may not be required to design to carry Ultimate Loads after impact damage (it depends on the inspections specified). However, a more robust product will result when composite structures *are* designed to carry Ultimate Load with impact damage. In fact, the FAR 23 regulations are quite specific in this area and require Ultimate Load capability with impact damage at the level of detectability based on the inspection methods.

Composite structures are relatively insensitive to cyclic loading, and a flaw growth threshold may be defined from the test results. Scatter in flaw growth life should be examined in order to establish a relationship between test lifetimes and service lifetimes for full scale cyclic testing. This will also enable the full scale tests to be conducted more economically than on equivalent metal structures.

With the combination of careful analysis, rational testing, and advanced manufacturing techniques, further civil airplane applications of composite primary structures can be expected.

7.9.4 Military aircraft

Reserved for future use.

REFERENCES

7.2 Goranson, U.G, “Damage Tolerance Facts and Fiction,” 14th Plantema Memorial Lecture presented at the 17th Symposium of the International Committee on Aeronautical Fatigue, Stockholm, June, 1993.

7.2.1(a) FAA Advisory Circular 20-107A, “Composite Aircraft Structure,” April 25, 1984.

7.2.1(b) Whitehead, R.S., Kan, H.P., Cordero, R., and Seather, E.S., “Certification Methodology for Composite Structures,” Volumes I and II, Report No. NADC-87042-60, October 1986.

7.2.1(c) Whitehead, R. S., “Certification of Primary Composite Aircraft Structures,” ICAF Conference, Ottawa, Canada, 1987.

7.2.1(d) “Advanced Certification Methodology for Composite Structures,” Report No. DOT/FAA/AR-96/111 or NAWCADPAX-96-262-TR, April 1997.

7.2.2.3(a) Quinlivan, J.T., Kent, J.A., and Wilson, D.R., “NASA-ACEE/Boeing 737 Graphite/Epoxy Horizontal Stabilizer Service,” 9th DoD/NASA Conference on Fibrous Composite in Structural Design, 1991.

7.2.2.3(b) McCarty, J.E., Johnson, R.W., and Wilson, D.R. “737 Graphite/Epoxy Horizontal Stabilizer Certification,” AIAA Paper 82-0745.

7.2.2.3(c) Schreiber, K.H., and Quinlivan, J.T., “The Boeing 777 Empennage,” Presented at ICCM-9 Madrid 1993.

7.2.2.3(d) Takai, J., et.al., “CFRP Horizontal Stabilizer Development Test Program,” Presented at ICCM-9, Madrid 1993.

7.2.2.3(e) Tropis, A., Thomas, M., Bounie, J.L., Lafon, P., “Certification of the Composite Outer Wing of the ATR 72,” I Mech E, 1993.

7.2.2.3(f) Williams, J.G., O’Brien, T.K., and Chapman, A.C., “Comparison of Toughened Composite Laminates Using NASA Standard Damage Tolerance Tests,” NASA CP 2321, Proceedings of the ACEE Composite Structures Technology Conference, Seattle, WA, August, 1984.

7.2.2.3(g) Carlile, D.R., and Leach, D.C., “Damage and Notch Sensitivity of Graphite/PEEK Composite,” Proceedings of the 15th National SAMPE Technical Conference, October, 1983, pp. 82-93.

7.2.2.3(h) Hall, J., and Goranson, U.G., “Principles of Achieving Damage Tolerance With Flexible Maintenance Programs for New and Aging Aircraft,” presented at 13th Congress of the International Council of the Aeronautical Sciences/AIAA Aircraft Systems, Seattle, WA, August 26, 1982.

7.2.2.3(i) ACJ25.571 (a) “Damage Tolerance and Fatigue Evaluation of Structure (Acceptable Means of Compliance),” Dec. 18, 1985.

7.2.2.3(j) Dost, E., Avery, W., Finn, S., Grande, D., Huisken, A., Ilcewicz, L., Murphy, D., Scholz, D., Coxon, B., and Wishart, R., “Impact Damage Resistance of Composite Fuselage Structure,” NASA CR-4658, 1996.

7.2.2.3(k) Walker, T., Scholz, D., Flynn, B., Dopker, B., Bodine, J., Ilcewicz, L., Rouse, M., McGowan, D., and Poe, C., Jr., “Damage Tolerance of Composite Fuselage Structure,” Sixth NASA/DOD/ARPA Advanced Composite Technology Conference, NASA CP-3326, 1996.

7.2.2.3(l) Ilcewicz, L., Smith, P., Olson, J., Backman, B., Walker, T., and Metschan, S., "Advanced Technology Composite Fuselage," Sixth NASA/DOD/ARPA Advanced Composite Technology Conference, NASA CP-3326, 1996.

7.2.2.4(a) Rouchon, J., "Certification of Large Airplane Composite Structures, Recent Progress and New Trends in Compliance Philosophy," 17 ICAS Congress, Stockholm 1990.

7.2.2.4(b) Rouchon, J., "How to Address the Situation of the No-Growth Concept in Fatigue, with a Probabilistic Approach - Application to Low Velocity Impact Damage with Composites," ICAF 97, Edinburgh, Composite Workshop on Certification Issues.

7.2.2.5 "Development of Probabilistic Design Methodology for Composite Structures," Report DOT/FAA/AR-95/17, August 1997.

7.3.2(a) Gottesman, T. and Mickulinski, M., "Influence of Matrix Degradation on Composite Properties in Fiber Direction," Engineering Fracture Mechanics, Vol 20, No. 4, 1984, pp. 667- 674.

7.3.2(b) Horton, R. E. and McCarty, J. E. "Damage Tolerance of Composites," Engineering Materials Handbook, Vol 1, Composites, ASM International, ISBN 0-87170-279-7, 1987.

7.3.2(c) Whitehead, R. S., "Certification of Primary Composite Aircraft Structures," ICAF Conference, Ottawa, Canada, 1987.

7.3.3(a) "Advanced Certification Methodology for Composite Structures," Report No. DOT/FAA/AR-96/111 or NAWCADPAX-96-262-TR, April 1997.

7.3.3(b) Development of Probabilistic Design Methodology for Composite Structures" Report DOT/FAA/AR-95/17, August 1997.

7.3.3(c) Tropis A., Thomas M., Bounie J.L., Lafon P., "Certification of the Composite Outer Wing of the ATR 72," I Mech E, 1993.

7.4.1(a) FAA Advisory Circular 20-107A, "Composite Aircraft Structure," April 25, 1984

7.4.1(b) "Substantiation of Composite Parts - Impact Detectability Criteria," Aerospatiale Report No. 440 225/91.

7.4.1(d) Thomas, M. "Study of the Evolution of the Dent Depth Due to Impact on Carbon/Epoxy Laminates, Consequences on Impact Damage Visibility and on in Service Inspection Requirements for Civil Aircraft Composite Structures," presented at MIL-HDBK 17 meeting, March 1994, Monterey, CA.

7.4.1(d) Komorowski, J.P., Gould, R.W., Simpson, D.L., "Synergy Between Advanced Composites and New NDI Methods," a paper from the Structures, Materials and Propulsion Laboratory, Institute for Aerospace Research, National Research Council of Canada.

7.4.2.2 Dost, E.F., Finn, S.R., Stevens, J.J., Lin, K.Y., and Fitch, C. E., "Experimental Investigations into Composite Fuselage Impact Damage Resistance and Post-Impact Compression Behavior," Proc. of 37th International SAMPE Symposium and Exhibition, Soc. for Adv. of Material and Process Eng., 1992.

7.5.1.1(a) Richardson, M.D.W., Wisheart, M.J., "Review of Low Velocity Impact Properties of Composite Material," Composites, Part A, 27A, 1996, pp. 1123-1131.

7.5.1.1(b) Abrate, S., “Impact on Laminated Composite Materials,” Composites, Vol 24, No. 3, 1991, pp. 77-99.

7.5.1.1(c) Abrate, S., “Impact on Laminated Composites: Recent Advances,” Applied Mechanics Review, Vol 47, No. 11, 1994, pp. 517-544.

7.5.1.1(d) Cantwell, W.J., and Morton, J., “The Impact Resistance of Composite Materials,” Composites, Vol 22, No. 5, 1991, pp. 55-97.

7.5.1.1(e) Rhoades, M.D., Williams, J.G., and Starnes, J.H., Jr., “Effect of Impact Damage on the Compression Strength of Filamentary - Composite Hat -Stiffened Panels,” Society for the Advancement of Material and Process Engineering, Vol 23, May, 1978.

7.5.1.1(f) Rhoades, M.D., Williams, J.G., and Starnes, J. H., Jr., “Low Velocity Impact Damage in Graphite-Fiber Reinforced Epoxy Laminates,” Proceedings of the 34th Annual Technical Conference of the Reinforced Plastics/Composites Institute, The Society of the Plastics Industry, Inc. 1979.

7.5.1.1(g) Byers, B.A., “Behavior of Damaged Graphite/Epoxy Laminates Under Compression Loading,” NASA Contractor Report 159293, 1980.

7.5.1.1(h) Smith, P.J., and Wilson, R.D., “Damage Tolerant Composite Wing Panels for Transport Aircraft,” NASA Contractor Report 3951, 1985.

7.5.1.1(i) Madan, R.C., “Composite Transport Wing Technology Development,” NASA Contractor Report 178409, 1988.

7.5.1.1(j) Horton, R., Whitehead, R., et al, “Damage Tolerance of Composites - Final Report,” AFWAL-TR-87-3030, 1988.

7.5.1.1(k) Horton, R.E., “Damage Tolerance of Composites: Criteria and Evaluation,” NASA Workshop on Impact Damage to Composites, NASA CP 10075, 1991, pp. 421-472.

7.5.1.1(l) Dost, E. F., Avery, W.B., Finn, S.R., Grande, D.H., Huisken, A.B., Ilcewicz, L.B., Murphy, D.P., Scholz, D.B., Coxon, R., and Wishart, R.E., “Impact Damage Resistance of Composite Fuselage Structure,” NASA Contractor Report 4658, 1997.

7.5.1.1(m) Dost, E.F., Finn, S.R., Stevens, J.J., Lin, K.Y., and Fitch, C. E., “Experimental Investigations into Composite Fuselage Impact Damage Resistance and Post-Impact Compression Behavior,” Proc. of 37th International SAMPE Symposium and Exhibition, Soc. for Adv. Of Material and Process Eng., 1992.

7.5.1.1(n) Scholz, D.B., Dost, E.F., Flynn, B.W., Ilcewicz, L.B., Lakes, R.S., Nelson, K.M., Sawicki, A.J., and Walker, T.W., “Advanced Technology Composite Fuselage-Materials and Processes,” NASA Contractor Report 4731, 1997.

7.5.1.2 Walker, T. H., Avery, W. B., Ilcewicz, L. I., Poe, C. C., Jr., and Harris, C. E., "Tension Fracture of Laminates for Transport Fuselage - Part I: Material Screening," *Second NASA Advanced Technology Conference*, NASA CP 3154, pp. 197-238, 1991.

7.5.1.3(a) Dorey, G., Sidey, G.R., and Hutchings, J., “Impact Properties of Carbon Fibre/Kevlar49 Fibre Hybrid Composites,” Composites, January 1978, pp. 25-32. old 5.8.1-a

7.5.1.3(b) Noyes, J.V., et al, “Wing/Fuselage Critical Component Development Program,” Phase I Preliminary Structural Design, Interim Report for the Period 1 Nov. 1977 - 31 Jan. 1978. old 5.8.1-b

7.5.1.3(c) Rhodes, Marvin D., and Williams, Jerry G., "Concepts for Improving the Damage Tolerance of Composite Compression Panels," *5th DOD/NASA Conference on Fibrous Composites in Structural Design,* January 27-29, 1981. old 5.8.1-c

7.5.1.3(d) Nishimura, A., Ueda, N., and Matsuda, H.S., "New Fabric Structures of Carbon Fiber," Proceedings of the 28th National SAMPE Symposium, April 1983, pp. 71-88. old 5.8.1-d

7.5.1.3(e) Masters, J. E., "Characterization of Impact Damage Development in Graphite/Epoxy Laminates," Fractography of Modern Engineering Materials: Composites and Metals, ASTM STP 948, ASTM, Philadelphia, Pa., 1987.

7.5.1.3(f) Evans, R.E., and Masters, J.E., "A New Generation of Epoxy Composites for Primary Structural Applications: Materials and Mechanics," Toughened Composites, ASTM STP 937, ASTM, Philadelphia, Pa., 1987.

7.5.1.3(g) Poe, C.C., Jr., Dexter, H.B., and Raju, I.S., "A Review of the NASA Textile Composites Research," Presented at 38th Structures, Structural Dynamics, and Materials Conference, AIAA paper No. 97-1321, April 7-10, 1997.

7.5.1.3(h) Sharma, Suresh K., and Sankar, Bhavani, V., "Effects of Through-the-Thickness Stitching on Impact and Interlaminar Fracture Properties of Textile Graphite/Epoxy Laminates," NASA Contractor Report 195042, University of Florida, Gainesville, Florida, February, 1995.

7.5.1.3(i) Jackson, W.C., and Poe, C.C., Jr., "The Use of Impact Force as a Scale Parameter for the Impact Response of Composite Laminates," Journal of Composites Technology & Research, Vol 15, No. 4, Winter 1993, pp. 282-289.

7.5.1.4 Poe, C.C., Jr., "Impact Damage and Residual Tension Strength of a Thick Graphite/Epoxy Rocket Motor Case," Journal of Spacecraft and Rockets, Vol 29., No. 3, May-June 1992, pp. 394-404.

7.5.1.6(a) Lloyd, B.A., and Knight, G.K., "Impact Damage Sensitivity of Filament - Wound Composite Pressure Vessels," 1986 JANNAF Propulsion Meeting, CPIA Publication 455, Vol 1, Aug. 1986, pp. 7-15.

7.5.1.6(b) Jackson, Wade C., Portanova, Marc A., and Poe, C. C., Jr., "Effect of Plate Size on Impact Damage," Presented at Fifth ASTM Symposium on Composite Materials in Atlanta, GA., May 4-6, 1993.

7.5.1.7 Smith, P.J., Thomson, L.W., and Wilson, R. D., "Development of Pressure Containment and Damage Tolerance Technology for Composite Fuselage Structures in Large Transport Aircraft," NASA Contractor Report 3996, 1986.

7.5.2 AFGS-87221A (Previously MIL-A-87221) General Specification for Aircraft Structures.

7.6.1 Whitehead, R.S., Kan, H. P., Cordero, R., and Saether, E. S., "Certification Testing Methodology for Composite Structures," Volumes I and II, Report No. NADC-87042-60 (DOT/FAA/CT-86-39), October 1986.

7.6.3 Sendeckyj, G. P., "Fitting Models to Composite Materials Fatigue Data," ASTM STP 734, 1981, pp 245-260.

7.6.4 Sanger, K. B., "Certification Testing Methodology for Composite Structures," Report No. NADC-86132-60, January 1986.

7.6.5(a) Ratwani, M.M. and Kan H.P., "Compression Fatigue Analysis of Fiber Composites," NADC-78049-60, September 1979.

7.6.5(b) Ratwani, M.M. and Kan H.P., "Development of Analytical Techniques for Predicting Compression Fatigue Life and Residual Strength of Composites," NADC-82104-60, March 1982.

7.6.5(c) Jeans, L.L., Grimes, G.C., and Kan, H.P. "Fatigue Spectrum Sensitivity Study for Advanced Composite Materials," AFWAL-TR-80-3130, Volume I-III, November 1980.

7.6.5(d) Whitehead, R. S., et al., "Composite Wing/Fuselage Program," Volume I-IV, AFWAL-TR-88-3098, August 1989.

7.6.5(e) Horton, R. E., Whitehead, R. S., et al., "Damage Tolerance of Composites," Volumes I – III, AFWAL-TR-87-3030, July 1988.

7.7.1(a) Loriot G. Ansart Th., "Fatigue damage behaviour and post-failure analysis in new generation of composite materials" Test Report No. S-93/5676000.

7.7.1(b) Ireman T., Thesken J.C., Greenhalgh E., Sharp R., Gädke M., Maison S., Ousset Y., Roudolff F., La Barbera A., "Damage Propagation in Composite Structural Element-Coupon Experiment and Analyses" - Garteur collaborative programme (1996), *Composite Structures*, v. 36, pp. 209-220, Elsevier Science Ltd.

7.7.4.2.1 Wilkens, D.J., Eisenmann, J.R., Camin, R.A., Margolis, W.S., and Benson, W.A., "Characterizing Delamination Growth in Graphite Epoxy," Damage in Composite Materials, ASTM STP 775, Edited by K.L. Reifsnider, American Society for Testing and Materials, 1982, pp. 168-183.

7.8.1.2.1(a) Dorey, G., Sidey, G.R., and Hutchings, J., "Impact Properties of Carbon Fibre/Kevlar49 Fibre Hybrid Composites," Composites, January 1978, pp. 25-32.

7.8.1.2.1(b) Nishimura, A., Ueda, N., and Matsuda, H.S., "New Fabric Structures of Carbon Fiber," Proceedings of the 28th National SAMPE Symposium, April 1983, pp. 71-88.

7.8.1.2.1(c) Noyes, J.V., et al, "Wing/Fuselage Critical Component Development Program," Phase I Preliminary Structural Design, Interim Report for the Period 1 Nov. 1977 - 31 Jan. 1978.

7.8.1.2.1(d) Rhodes, Marvin D., and Williams, Jerry G., "Concepts for Improving the Damage Tolerance of Composite Compression Panels," 5th DOD/NASA Conference on Fibrous Composites in Structural Design, January 27-29, 1981.

7.8.1.2.2(a) Dost, E.F., Ilcewicz, L.B., Avery, W.B., and Coxon, B.R., "Effects of Stacking Sequence on Impact Damage Resistance and Residual Strength for Quasi-Isotropic Laminates," Composite Materials: Fatigue and Fracture (Third Volume), ASTM STP 1110, T.K. O'Brien, Ed., American Society for Testing and Materials, Phil., 1991, pp. 476-500.

7.8.1.2.2(b) Dost, E.F., Ilcewicz, L.B., and Gosse, J.H., "Sublaminate Stability Based Modeling of Impact Damaged Composite Laminates," in Proc. of 3rd Tech. Conf. of American Society for Composites, Technomic Publ. Co., 1988, pp. 354-363.

7.8.1.2.2(c) Ilcewicz, L.B., Dost, E.F., and Coggeshall, R.L., "A Model for Compression After Impact Strength Evaluation," in Proc. of 21st International SAMPE Tech. Conf., Soc. for Adv. of Material and Process Eng., 1989, pp. 130-140.

7.8.1.2.2(d) Gosse, J.H., and Mori, P.B.Y., “Impact Damage Characterization of Graphite/Epoxy Laminates,” in Proc. of 3rd Tech. Conf. of American Society for Composites, Technomic Publ. Co., 1988, pp. 344-353.

7.8.1.2.3 Horton, R.E., and Whitehead, R.S., “Damage Tolerance of Composites,” Vol I. Development of Requirements and Compliance Demonstration,” AFWAL-TR-87-3030, July 1988.

7.8.1.2.4(a) Scholz, D., et al., "Advanced Technology Composite Fuselage - Materials and Processes," NASA CR-4731, 1997.

7.8.1.2.4(b) Ward, S. H., and H. Razi, “Effect of Thickness on Compression Residual Strength of Notched Carbon Fiber/Epoxy Composites,” 28th International SAMPE Technical Conference, Seattle, WA. November 4-7, 1996.

7.8.1.2.7 Portanova, Marc, “Impact Testing of Textile Composite Materials,” Proceedings of Textile Mechanics Conference, NASA Langley Research Center, Hampton, VA., NASA CP-3311, Dec. 6-8, 1984.

7.8.1.2.8(a) Chai, H., and Babcock, C.D., “Two-Dimensional Modeling of Compressive Failure in Delaminated Laminates,” J. Composite Materials, 19, 1985, pp. 67-98.

7.8.1.2.8(b) Whitcomb, J.D., “Predicted and Observed Effects of Stacking Sequence and Delamination Size on Instability Related Delamination Growth,” J. Composite Technology and Research, 11, 1989, pp. 94-98.

7.8.1.2.8(c) Cairns, Douglas S. “ Impact and Post-Impact Response of Graphite/Epoxy and Kevlar/Epoxy Structures,” Technology Laboratory for Advanced Composites (TELAC), Dept. Of Aeronautics and Astronautics, Massachusetts Institute of Technology, Cambridge, MA, TELAC Report 87-15, August 1987.

7.8.1.2.8(d) Lekhnitskii, S.G., “Anisotropic Plates,” Gordon and Breach Science Publishers, New York, N.Y., 1968, Chapter VI-43.

7.8.1.2.8(e) Awerbuch, J., and Madhukar, M.S., “Notched Strength of Composite Laminates : Predictions and Experiments - A Review,” J. of Reinforced Plastics and Composites, 4, 1985, pp. 1-159.

7.8.1.2.8(f) Poe, C.C., Jr., “A Parametric Study of Fracture Toughness of Fibrous Composite Materials,” J. of Offshore Mechanics and Arctic Eng., Vol III, 1989, pp. 161-169.

7.8.1.2.8(g) Walker, T.H., Minguet, P.J., Flynn, B.W., Carbery, D.J., Swanson, G.D., and Ilcewicz, L.B., “Advanced Technology Composite Fuselage - Structural Performance,” NASA Contractor Report 4732, 1997.

7.8.1.2.8(h) Dopker, B., Murphy, D., Ilcewicz, L.B., and Walker, T., “Damage Tolerance Analysis of Composite Transport Fuselage Structure,” 35th AIAA/ASME/ASCE/AHS/ASC Structures, Structural Dynamics, & Materials Conference, AIAA Paper 94-1406, 1994.

7.8.1.2.8(i) Ilcewicz, L.B., Walker, T.H., Murphy, D.P., Dopker, B., Scholz, D.B., and Cairns, D.S., and Poe, C.C., Jr., “Tension Fracture of Laminates for Transport Fuselage - Part 4: Damage Tolerance Analysis,” Fourth NASA/DoD Advanced Composite Technology Conference, NASA CP-3229, 1993, pp. 265-298.

7.8.1.2.9(a) Lagace, P.A., and Cairns, D.S., “Tensile Response of Laminates to Implanted Delaminations,” Advanced Materials Technology “87, SAMPE, April 1987, pp. 720-729.

7.8.1.2.9(b) Madan, R.C., "The Influence of Low-Velocity Impact on Composite Structures," Composite Materials: Fatigue and Fracture (Third Volume), ASTM STP 1110, T.K. O'Brien, Ed., American Society for Testing and Materials, Phil., pp. 457-475.

7.8.1.2.10 Walker, T., et al., "Tension Fracture of Laminates for Transport Fuselage - Part III: Structural Configurations," Fourth NASA Advanced Technology Conference, NASA CP-3229, pp. 243-264, 1994.

7.8.1.3(a) Ilcewicz, L., et al., "Advanced Technology Composite Fuselage - Program Overview," NASA CR-4734, 1996.

7.8.1.3(b) Walker, T.H.; Ilcewicz, L.B.; Bodine, J.B.; Murphy, D.P.; and Dost, E.F., " Benchmark Panels," NASA CP-194969, August 1994.

7.8.1.3(c) Walker, T., et al., "Tension Fracture of Laminates for Transport Fuselage - Part I: Material Screening," *Second NASA Advanced Technology Conference*, NASA CP-3154, pp. 197-238, 1992.

7.8.1.3(d) Walker, T., et al., "Tension Fracture of Laminates for Transport Fuselage - Part II: Large Notches," *Third NASA Advanced Technology Conference*, NASA CP-3178, pp. 727-758, 1993.

7.8.1.3(e) Walker, T., et al., "Damage Tolerance of Composite Fuselage Structure," *Sixth NASA/DOD/ARPA Advanced Composite Technology Conference*, NASA CP-3326, 1996.

7.8.1.3.1(a) Poe, C.C., Jr., Harris, Charles E., Coats, Timothy W., and Walker, T.H., "Tension Strength with Discrete Source Damage," Fifth NASA/DoD Advanced Composites Technology Conference, Vol I, Part 1, NASA CP-3294, pp. 369-437.

7.8.1.3.1(b) Sutton, J., Kropp, Y., Jegley, D., and Banister-Hendsbee, D., "Design, Analysis, and Tests of Composite Primary Wing Structure Repairs," Fifth NASA/DoD Advanced Composites Technology Conference, Vol I, Part 2, NASA CP-3294, pp. 913-934.

7.8.2.1 Rhodes, Marvin D., Mikulus, Jr., Martin M., and McGowan, Paul E., " Effects of Orthotropy and Width on the Compression Strength of Graphite-Epoxy Panels with Holes," AIAA Journal, Vol 22, No. 9, September 1984, pp. 1283-1292.

7.8.4.1(a) Poe, C. C., Jr., "Fracture Toughness of Fibrous Composite Materials," NASA TP 2370, November 1984.

7.8.4.1(b) Nuismer, R. J. and Whitney, J. M., "Uniaxial Failure of Composite Laminates Containing Stress Concentrations," in Fracture Mechanics of Composites, ASTM STP 593, American Society of Testing and Materials, pp. 117-142 (1975).

7.8.4.1(c) Whitney, J. M. and Nuismer, R. J., "Stress Fracture Criteria for Laminated Composites Containing Stress Concentrations," J. Composite Materials, Vol 8, pp. 253-265, 1974.

7.8.4.1(d) Llorca, J., and Elices, M., "A Cohesive Crack Model to Study the Fracture Behavior of Fiber-Reinforced Brittle-Matrix Composites," Int. J. of Fracture, Vol 54, pp. 251-267, 1992.

7.8.4.1(e) Lin, K. Y. and Mar, J. W., "Finite Element Analysis of Stress Intensity Factors for Cracks at a Bi-Material Interface," Int. J. of Fracture, Vol 12, No. 2, pp. 521-531, 1977.

7.8.4.1(f) Tan, S. C., "Notched Strength Prediction and Design of Laminated Composites Under In-Plane Loadings," J. of Composite Materials, Vol 21, pp. 750-780, 1987.

7.8.4.1(g) Poe, C. C., Jr. and Sova, J. A., "Fracture Toughness of Boron/Aluminum Laminates with Various Proportions of 0° and ±45° Plies," NASA Technical Paper 1707, 1980.

7.8.4.1(h) Poe, C. C., Jr., "A Unifying Strain Criterion for Fracture of Fibrous Composite Laminates," Engineering Fracture Mechanics, Vol 17, No. 2, pp. 153-171, 1983.

7.8.4.1(i) Waddoups, M. E., Eisenmann, J. R., and Kaminski, B. E., "Macroscopic Fracture Mechanics of Advanced Composite Materials," J. Composite Materials, Vol 5, pp. 446-454, 1971.

7.8.4.1(j) Chiang, C. R., "Inhomogeneity Effect on the Stress Intensity Factor," J. Composite Materials, Vol 21, pp. 610-618, 1987.

7.8.4.1.(k) Eringen, A. C., Speziale, C. G., and Kim, B. S., "Crack-Tip Problem in Nonlocal Elasticity," J. Mech. Phys. Solids, Vol 25, pp. 339-355, 1977.

7.8.4.1(l) Ilcewicz, L. B., Shaar, C., Kennedy, T. C., and Wilson, J. B., "Experimental Evidence of a Relationship Between Ultrasonic Wave Dispersion and Fracture," Engineering Fracture Mechanics, Vol 26, pp. 895-908, 1986.

7.8.4.1(m) Nakamura, S., and Lakes, R. S., "Finite Element Analysis of Stress Concentration Around a Blunt Crack in a Cosserat Elastic Solid," Computer Methods in Applied Mechanics and Engineering, Vol 66, pp. 257-266, 1988.

7.8.4.1(n) Mar, J. W. and Lin, K. Y., "Fracture Mechanics Correlation for Tensile Failure of Filamentary Composites with Holes," Journal of Aircraft, Vol 14, No. 7, pp. 703-704, 1977.

7.8.4.1(o) Tsai, H. C., and Arocho, A. M., "A New Approximate Fracture Mechanics Analysis Methodology for Composites with a Crack or Hole," Report NADC-88118-60, 1990.

7.8.4.1(p) Aronsson, D. B., and Backlund, J., “Tension Fracture of Laminates With Cracks,” J. Composite Materials, Vol 20, pp. 287-307, 1986.

7.8.4.1(q) Aronsson, C. G., and Backlund, J., "Damage Mechanics Analysis of Matrix Effects in Notched Laminates," in Composite Materials: Fatigue and Fracture, ASTM STP 907, pp. 134-157, 1986.

7.8.4.1(r) Chamis, C. C., "Computational Simulation of Progressive Fracture in Fiber Composites," NASA TM-87341, 1986.

7.8.4.1(s) Chang, F. K., and Chang, K. Y., "A Progressive Damage Model for Laminated Composites Containing Stress Concentrations," J. of Composite Materials, Vol 32, pp. 834-855, 1987.

7.8.4.1(t) Barenblatt, G. I., "The Mathematical Theory of Equilibrium Cracks in Brittle Fracture," Advances in Applied Mechanics (Edited by Dryden, H.L. and von Karman, T.), Vol 7, pp. 55-129, 1962.

7.8.4.1(u) Mazars, J., and Bazant, Z. P., Eds. “Strain Localization and Size Effects due to Cracking and Damage,” Proceedings of France-U. S. Workshop held at E. N. S de Cachan, University Paris, Sept. 1988, Elsevier, London, U. K.

7.8.4.1.1 Swift, T., "Fracture Analysis of Stiffened Structure," Damage Tolerance of Metallic Structures: Analysis Methods and Application, ASTM STP 842, J. Chang and J. Rudd, eds., ASTM, pp. 69-107, 1984.

7.8.4.1.2(a) Bazant, Z. P., and Cedolin, L., “Stability of Structures: Elastic, Inelastic, Fracture, and Damage Theories,” Oxford University Press, Inc., New York, 1991.

7.8.4.1.2(b) Bazant, Z. P., and Planas, J., Fracture and Size Effect in Concrete and Other Quasibrittle Materials," CRC Press, Boca Raton, 1998.

7.8.4.1.2(c) Sutcliffe, M. P. F., and Fleck, N. A., "Effect of Geometry On Compressive Failure of Notched Composites," Int. J. of Fracture, Vol 59, pp. 115-132, 1993.

7.8.4.1.2(d) Dopker, B., et al., "Composite Structural Analysis Supporting Affordable Manufacturing and Maintenance," Sixth NASA Advanced Technology Conference, NASA CP-3326, 1995.

7.8.4.1.2(e) Walker, T., et al, "Nonlinear and Progressive Failure Aspects of Transport Composite Fuselage Damage Tolerance," Computational Methods for Failure Analysis and Life Prediction, NASA-CP-3230, pp. 11-35, 1993.

7.8.4.1.2(f) Basham, K. D., Chong, K. P., and Boresi, A. P., "A New Method to Compute Size Independent Fracture Toughness Values for Brittle Materials," Engineering Fracture Mechanics, Vol 46, No. 3, pp. 357-363, 1993.

7.8.4.1.2(g) Riks, E., "An Incremental Approach to the Solution of Snapping and Buckling Problems," International Journal of Solid Structures, Vol 15, pp. 529-551, 1979.

7.8.4.1.2(h) Cairns, D.S., Ilcewicz, L.B., Walker, T.H., and Minguet, P.J., "The Consequence of Material Inhomogeneity on Fracture of Automated Tow Placed Structures With Stress Concentrations," Fourth NASA/DoD Advanced Technology Conference, NASA CP-3229, 1993.

7.8.4.1.2(i) Bazant, Z. P., and Chang, T. P., "Nonlocal Finite Element Analysis of Strain-Softening Solids," Journal of Engineering Mechanics, Vol 113, pp. 89-105, No. 1, 1987.

7.8.4.1.4(a) "Standard Practice for R-Curve Determination," ASTM designation: E 561-86, Volume 03.01 of 1988 Annual Book of ASTM Standards, c. 1988, pp. 563-574.

7.8.4.1.4(b) Tada, H., Paris, P.C., and Irwin, G., "The Stress Analysis of Crack Handbook," 2nd Edition, Paris Production Incorporated (and Del Research corp.), 226 Woodbourne Dr., St. Louis, Mi. 63105, 1985.

7.8.4.1.4(c) Erdogan, F., Ratwani, M., and Yuceoglu, U., "On the Effect of Orthotropy in a Cracked Cylindrical Shell," International Journal of Fracture, Vol 10, 1974, pp. 117-60.

7.8.4.1.4(d) Erdogan, F., "Crack Problems in Cylindrical and Spherical Shells," Mechanics of Fracture, Vol 3, Noordhoff International, 1977, pp. 161-99.

7.8.4.1.4(e) Graves, Michael J., and Lagace, Paul A., "Damage Tolerance of Composite Cylinders," Composite Structures, Vol 4, 1985, pp. 75-91.

7.8.4.1.4(f) Yahsi, O. Selcuk, and Erdogan, F., "The Crack Problem in a Reinforced Cylindrical Shell," NASA CP-178140, June 1986.

7.8.4.1.4(g) Ranniger, C.U., Lagace, Paul A., and Graves, Michael J., "Damage Tolerance and Arrest Characteristics of Pressurized Graphite/Epoxy Tape Cylinders," Fifth Symposium on Composite Materials, ASTM STP 1230, 1995.

7.8.4.1.4(h) Wang, J.T., Xue, D.Y., Sleight, D.W., and Housner, J.M., "Computation of Energy Release Rates for Cracked Composite Panels with Nonlinear Deformation," AIAA Paper No. 95-1463, in Proceedings of the 36th AIAA/ASME/ASCE/AHS Structures, Structural Dynamics, and Materials Conference, April 10-14, 1995.

7.8.4.2.2(a) Chai, H., Knauss, W.G., and Babcock, C.D., "Observation of Damage Growth in Compressively Loaded Laminates," Mechanics of Composite Materials, the Winter Annual Meeting of the American Society of Mechanical Engineers, Boston, 1983, pp. 329-337.

7.8.4.2.2(b) Bass, M., Gottesman, T., and Fingerhut, U., "Criticality of Delaminations in Composite Material Structures," Proceedings, 28th Israel Conference on Aviation and Astronautics, 1986, pp. 186-190.

7.8.4.2.2(c) Gottesman, T. and Green, A.K., "Effect of Delaminations on Inplane Shear Mechanical Behaviour of Composites," Proceedings of Mechanics and Mechanisms of Damage in Composites and Multi-Materials, MECAMAT, November 1989, pp. 119-132.

7.8.4.3.1(a) Kassapoglou, C., "Compression Strength of Composite Sandwich Structures After Barely Visible Impact Damage," J. Composite Technology and Research, 18, 1996, pp. 274-284.

7.8.4.3.1(b) Pavier, M.J., and Clarke, M.P., "Finite Element Prediction of the Post-Impact Compressive Strength of Fibre Composites," Composite Structures, 36, 1996, pp. 141-153.

7.8.4.3.1(c) Gerhartz, J.J., Idelberger, H. and Huth, H., "Impact Damage in Fatigue Loaded Composite Structures," 15th ICAF Conference, 1989.

7.8.4.3.1(d) Girshovich, S., Gottesman, T., Rosenthal, H., et al., "Impact Damage Assessment of Composites," Damage Detection in Composite Materials, ASTM STP 1128, J.E. Masters, Ed., American Society for Testing and Materials, Philadelphia, 1992, pp. 183-199.

7.8.4.3.1(e) Gottesman, T., Girshovich, S., Drukker, E., Sela, N. and Loy, J., "Residual Strength of Impacted Composites: Analysis and Tests," Journal of Composites Technology and Research, JCTRER, Vol 16, No. 3, July 1994, pp. 244-255.

7.8.4.3.1(f) Gottesman, T., Bass, M., and Samuel, A., "Criticality of Impact Damage in Composite Sandwich Structures," Proceedings, ICCM6 & ECCM2, Vol 3, Matthews et al., Eds., Elsevier Applied Science, 1987, pp. 3.27 - 3.35.

7.9.1.4 Whitehead, R.S., Kan, H.P., Cordero, R., and Saether, E.S., "Certification Testing Methodology for Composite Structures," Volumes I and II, Report No. NADC-87042-60 (DOT/FAA/CT - 86/39), October, 1986.

7.9.1.5 Sendeckyj, G.P., "Fitting Models to Composite Materials Fatigue Data," ASTM STP 734, 1981, pp 245-260.

7.9.2 A. Fawcett, J. Trostle and S. Ward, "777 Empennage Certification Approach," 11th International Conference on Composite Materials (ICCM-11), Gold Coast, Australia. July 14-18, 1997.

7.9.3.2.5 Trop, David W., "Damage Tolerance of Internally Pressurized Sandwich Walled Graphite/Epoxy Cylinders," MS Thesis, MIT, 1985.